

Inaugural dissertation
for
obtaining the doctoral degree
of the
Combined Faculty of Mathematics, Engineering and Natural Sciences
of the
Ruprecht - Karls - University
Heidelberg

Presented by

M.Sc. Luisa Lübke

born in: Dresden, Germany

Oral examination: 15.06.2022

Deciphering the regulatory network controlling adult neurogenesis in the
telencephalon of *Danio rerio*

Referees: Prof. Dr. Uwe Strähle

Dr. Thomas Dickmeis

Summary

In contrast to mammals, zebrafish display an extensive capacity to generate new neurons and repair injuries of the central nervous system (CNS) at adult stages. During adult neurogenesis, new neurons are formed abundantly from a pool of neural stem cells (NSCs) in order to integrate into existing tissue. Pivotal for the regenerative ability of the zebrafish adult brain is the precise control of NSC behavior and long-term maintenance of the stem cell pool. The balance between quiescent NSCs and activated NSCs is fundamental to the successful functional regeneration of the brain. This balance is controlled by a gene regulatory network (GRN) which is tightly regulated in a spatial and temporal manner through the interplay of different factors including transcription regulators, signaling pathways, key genes and their associated regulatory elements and also small molecules arising from non-coding areas of the genome. Understanding which key players are involved in this regulatory network, how these factors are controlled, how they interact with each other and what their exact function is, will help to comprehend how brain regeneration in the adult zebrafish is facilitated and develop possible strategies for initiating similar regenerative processes in the human brain. Therefore, the overall aim of this thesis was to identify key genes and molecules of this complex GRN and investigate their regulation and function on a molecular level and their expression in the adult zebrafish brain.

The gene *midkine-a* (*mdka*) was previously shown to be involved in the regeneration of the zebrafish retina, heart and fin. In this work, I investigated its expression pattern in the zebrafish adult telencephalon under constitutive and regenerative conditions and found that *mdka* expression is specifically restricted to cells in the ventricular zone of the zebrafish telencephalon, a stem cell niche of the zebrafish brain, and its expression pattern is mainly associated with quiescent NSCs. Furthermore, regulatory elements for *mdka* were identified and can be further investigated regarding their response to signaling pathways and their consequent influence on the cell and time specific expression of *mdka*.

Moreover, micro RNAs (miRNAs), which are small molecules originating from non-coding areas of the genome, that showed an increased expression after injury of the zebrafish brain were investigated for their expression pattern and regulatory role in the GRN. Their increased expression and analysis of targeted genes suggested a role in the control of neuronal genes. However, since miRNAs can regulate a number of different targets, detailed investigation into their role in the GRN is still needed.

Overall, this thesis provides different tools and applications for the investigation of the GRN that regulates NSC behavior in the adult zebrafish brain and identifies *mdka* as one of the key genes in the GRN controlling the proliferative behavior of NSCs and regulating stem cell quiescence.

Zusammenfassung

Der adulte Zebrafisch besitzt im Gegensatz zu Säugetieren die Fähigkeit ständig neue Neuronen zu generieren und Verletzungen des zentralen Nervensystems (ZNS) zu heilen. Während der adulten Neurogenese werden neue Neuronen ausgehend von einem neuralen Stammzellpool produziert um sich in vorhandenes Gewebe zu integrieren. Ausschlaggebend für die Regenerationsfähigkeit des Zebrafischgehirns ist die präzise Kontrolle der Aktivität neuraler Stammzellen (NSZ) und eine langfristige Aufrechterhaltung des Stammzellpools. Die Balance zwischen inaktiven und aktiven NSZ ist die Grundlage für eine erfolgreiche funktionale Wiederherstellung des Gehirns. Diese Balance wird von einem zeitlich und örtlich genau regulierten Gennetzwerk kontrolliert welches Transkriptionsregulatoren, Signalwege, zentrale Schlüsselgene und ihre zugehörigen regulatorischen Elemente, sowie kleine Moleküle die aus nicht-kodierenden Regionen des Genoms entstehen, beinhaltet. Das Wissen darüber welche Schlüsselgene involviert sind und wie die verschiedenen Faktoren kontrolliert werden, zusammenwirken und was ihre exakte Funktion ist, wird helfen Gehirnregeneration im adulten Zebrafisch zu verstehen und die Entwicklung möglicher Strategien um gleichartige Prozesse im menschlichen Gehirn auszulösen, voranzutreiben. Demzufolge war das Ziel dieser Arbeit Schlüsselgene und Moleküle in diesem regulativen Netzwerk zu identifizieren und ihre Regulation und Funktion auf molekularer Ebene, sowie ihre Expression im adulten Zebrafischgehirn zu untersuchen.

Das Gen *midkine-a (mdka)* wurde bereits in der Vergangenheit als ein Gen identifiziert, welches an Regenerationsprozessen in der Retina, dem Herz und der Flosse des Zebrafischs beteiligt ist. In dieser Arbeit wurde das Expressionsmuster von *mdka* im Telencephalon des adulten Zebrafischs während der konstitutiven und regenerativen Neurogenese untersucht und herausgefunden, dass die Expression von *mdka* auf Zellen in der ventrikulären Zone des Telencephalons, eine Stammzellnische des Zebrafischgehirns, begrenzt ist und mit inaktiven NSZ assoziiert werden kann. Außerdem wurden regulatorische Elemente für *mdka* identifiziert, die weiterhin auf ihren Zusammenhang mit verschiedenen Signalwegen und ihren Einfluss auf die zeit- und zellspezifische Expression von *mdka* untersucht werden können. Zusätzlich wurden micro RNAs (miRNAs), welche kleine Moleküle sind die von nicht-kodierenden Abschnitten des Genoms transkribiert werden, auf ihre Expression und regulatorische Rolle im Gennetzwerk untersucht. Ihre erhöhte Expression nach einer Verletzung des Zebrafischgehirns und eine Analyse ihrer Zielgene legen eine Rolle bei der Kontrolle von neuronalen Genen nahe. Jedoch können miRNAs eine große Anzahl verschiedener Gene regulieren, wodurch eine detaillierte Untersuchung ihrer exakten Funktion im regulatorischen Gennetzwerk nötig ist. Insgesamt bietet diese Arbeit verschiedene Werkzeuge um das regulatorische Gennetzwerk welches das Verhalten von NSZ im adulten Zebrafischgehirn reguliert zu untersuchen und ermittelt *mdka* als ein Schlüsselgen, welches die Proliferation und inaktive Form der NSZ kontrolliert.

Table of contents

Summary	1
Zusammenfassung.....	2
Figures	7
Tables	8
Publications	9
1 Introduction	10
1.1 General introduction	10
1.2 Zebrafish as a model organism.....	11
1.3 Development and anatomy of the zebrafish CNS in comparison to the mammalian CNS ...	13
1.3.1 Early neurogenesis and development of the CNS	13
1.3.2 Structural and molecular comparison of the mammalian and zebrafish CNS	15
1.4 Adult neurogenesis.....	17
1.4.1 Stem cell areas in the adult brain.....	18
1.4.2 Stem cell types in the zebrafish and mammalian telencephalon.....	18
1.5 Regenerative neurogenesis	21
1.5.1 Experimental models to study regenerative neurogenesis in zebrafish	21
1.5.2 Acute consequences of brain injury	23
1.6 Signaling pathways implicated in the control of NSC behavior.....	25
1.6.1 The BMP signaling pathway	25
1.6.2 The Notch signaling pathway	27
1.6.3 Interaction between the BMP and Notch pathways in adult neurogenesis	29
1.6.4 The Wnt signaling pathway	29
1.7 Regulation of gene transcription.....	31
1.7.1 Enhancers and promoters (activating CRMs).....	32
1.7.2 Gene regulatory networks.....	32
1.8 The growth factor Midkine-a.....	33
1.8.1 Family and structure.....	33
1.8.2 Regulation and function of <i>mdka</i>	34
1.8.3 Receptors for MK.....	35
1.8.4 <i>mdka</i> in zebrafish adult neurogenesis.....	36
1.9 The role of ncRNAs in the GRN.....	37
1.9.1 miRNA biogenesis and function	37
1.9.2 Tackling the challenge of miRNA detection in the zebrafish adult brain tissue.....	40
1.10 Aim of this thesis	41

2	Material and Methods	42
2.1	Material	42
2.1.1	Bacterial Strains	42
2.1.2	Chemicals.....	42
2.1.3	Enzymes.....	43
2.1.4	Equipment and tools	43
2.1.5	<i>In situ</i> hybridization probes	44
2.1.6	Kits	44
2.1.7	Microscopes	45
2.1.8	Oligonucleotides.....	45
2.1.9	Plasmids.....	46
2.1.10	Primary Antibodies.....	47
2.1.11	Secondary Antibodies.....	47
2.1.12	Software and online sources	47
2.1.13	Solutions and buffers.....	48
2.1.14	Zebrafish lines.....	49
2.2	Methods	50
2.2.1	Zebrafish husbandry.....	50
2.2.2	Genomic DNA extraction from zebrafish embryos	50
2.2.3	Constructs and synthesis of antisense RNA DIG probes	50
2.2.4	Agarose gel electrophoresis	51
2.2.5	ISH/FISH on embryos.....	51
2.2.6	Stab wound assay	52
2.2.7	Preparation of adult zebrafish brains.....	52
2.2.8	ISH on adult brain sections	53
2.2.9	FISH on adult brain sections	54
2.2.10	Double FISH on adult brain sections	54
2.2.11	Immunohistochemistry (IHC) on adult brain sections.....	55
2.2.12	miRNA ISH using LNA probes on adult brain sections.....	56
2.2.13	Imaging	56
2.2.14	Image analysis	56
2.2.15	RT-qPCR	57
2.2.16	Quantification / Statistical analysis	57
2.2.17	Overexpression construct cloning.....	57
2.2.18	Cerebroventricular microinjection	57
2.2.19	Drug treatment.....	58

2.2.20	Identification of putative CRMs and construction of CRM expression plasmids	58
2.2.21	Microinjection into zebrafish embryos	59
2.2.22	FISH using I-FISH, m-FISH and f-FISH probes	59
2.2.23	DAPI staining of adult brain sections.....	60
3	Results.....	61
3.1	Role of the gene <i>mdka</i> in zebrafish adult neurogenesis	61
3.1.1	Expression patterns of <i>mdka</i> and its family members in the zebrafish embryo.....	61
3.1.2	Expression patterns of <i>mdka</i> and its family members in the zebrafish adult brain.....	62
3.1.3	<i>mdka</i> is expressed in quiescent radial glial cells under constitutive conditions	64
3.1.4	<i>mdka</i> is co-expressed with the gene <i>id1</i> , a marker for qRGCs.....	67
3.1.5	<i>mdka</i> is upregulated in a delayed fashion after lesion of the adult telencephalon.....	68
3.1.6	After lesion of the adult telencephalon, <i>mdka</i> expression remains restricted to qRGCs.	70
3.1.7	Influence of <i>mdka</i> overexpression on the proliferative behavior of RGCs	72
3.1.8	Inhibition of <i>Mdka</i> leads to increased proliferation in the zebrafish forebrain.....	73
3.1.9	Identification and validation of regulatory elements for the <i>mdka</i> gene.....	76
3.1.10	Regulation of the gene <i>mdka</i> by major signaling pathways	81
3.2	miRNAs in the GRN controlling NSC behavior	84
3.2.1	Identification of deregulated miRNA candidates in response to telencephalic lesion	84
3.2.2	Visualization of pri-miRNA molecules	87
3.2.3	Visualization of miRNA candidates in the telencephalon via individually synthesized FISH probes.....	89
3.3	Visualization of key genes in the regulatory network with the help of individualized ssDNA FISH probes.....	91
3.3.1	Visualization of <i>sox9a</i> mRNA in the zebrafish telencephalon using m-FISH probes.....	92
3.3.2	Co-expression studies conducted with the m-FISH probes against <i>sox9a</i>	93
3.3.3	Visualization of <i>prdm12b</i> mRNA in the zebrafish telencephalon using m-FISH probes....	94
3.3.4	Visualization of <i>mdka</i> using m-FISH probes	95
4	Discussion.....	97
4.1	The expression of <i>mdka</i> , <i>mdkb</i> and <i>ptn</i> differ in the posterior embryo but overlap in the adult brain.....	97
4.2	In response to telencephalic lesion <i>mdka</i> is upregulated in a delayed fashion.....	98
4.3	<i>mdka</i> expression is restricted to quiescent type I NSCs during constitutive and regenerative neurogenesis	98
4.4	Function of the <i>mdka</i> gene product <i>Mdka</i> is implicated in cell cycle regulation and proliferative pathways.....	100
4.5	Combination of different computational analyses assigned four promising enhancer elements to the gene <i>mdka</i>	102
4.6	Regulation of <i>mdka</i> expression is multifaceted	104

4.7	miRNAs play a pivotal role in the neurogenic regulatory network.....	106
4.8	Development of LNA FISH probes for the detection of mature miRNA candidates in the adult zebrafish telencephalon	108
4.9	Individualized FISH probes against mRNAs are suitable to report expression of endogenous genes	110
5	Conclusion and future perspectives	113
6	Acknowledgements.....	115
7	Literature.....	117

Figures

Figure 1: Scheme representing the different developmental modes of the mammalian and zebrafish telencephalon.....	14
Figure 2: Scheme comparing the anatomy of the zebrafish and mammalian telencephalon with annotation of important regions or nuclei.....	17
Figure 3: Schematic simplified representation of NSC types and localization in the adult zebrafish telencephalon.....	19
Figure 4: The canonical BMP signaling pathway	27
Figure 5: The canonical Notch signaling pathway.....	28
Figure 6: The canonical Wnt pathway is dependent on β -catenin and GSK-3 β	31
Figure 7: Biogenesis and function of miRNAs	39
Figure 8: Graphic representation of the stab wound assay on adult zebrafish.....	52
Figure 9: Schematic depiction of the ventricle injection into adult zebrafish	58
Figure 10: The expression patterns of <i>mdka</i> , <i>mdkb</i> and <i>ptn</i> overlap in the embryo.....	62
Figure 11: The expression patterns of <i>mdka</i> , <i>mdkb</i> and <i>ptn</i> are overlapping but distinct in the adult zebrafish brain.....	64
Figure 12: In the adult telencephalon, <i>mdka</i> is mainly expressed by quiescent radial glia cells.....	66
Figure 13: <i>mdka</i> is highly co-expressed with the gene <i>id1</i> in the adult zebrafish telencephalon	68
Figure 14: Upregulation of <i>mdka</i> expression levels after lesion is dependent on the time elapsed ...	70
Figure 15: <i>mdka</i> expression is associated with qRGCs and <i>id1</i> expression after telencephalic lesion.	71
Figure 16: Overexpression of <i>mdka</i> leads to reduced PCNA expression in RGCs.....	73
Figure 17: iMDK treatment leads to increased cell proliferation in the zebrafish telencephalon.....	75
Figure 18: Identification of putative regulatory elements for <i>mdka</i> using ATAC sequencing data and the DANIO CODE track hub in the UCSC genome browser	79
Figure 19: Creation of transgenic zebrafish lines for putative enhancers of <i>mdka</i> and comparison of transgene expression in 24 hpf zebrafish embryos.....	81
Figure 20: <i>mdka</i> expression is not controlled by the BMP pathway	82
Figure 21: <i>mdka</i> expression is not influenced by any of the major signaling pathways.....	83
Figure 22: <i>dre-miR-146a</i> is broadly expressed in the zebrafish telencephalon.....	87
Figure 23: Primary miRNAs of all six miRNA candidates are mainly expressed in the Vz.....	88
Figure 24: LNA modified I-FISH probe reliably reports expression pattern of the endogenous <i>dre-miR-9</i> gene	90
Figure 25: I-FISH probes against miRNA candidates are useful for detection of mature miRNA molecules	91

Figure 26: m-FISH probes against <i>sox9a</i> mRNA report the expression pattern of the endogenous gene and its upregulation in response to telencephalic lesion	93
Figure 27: m-FISH probes can be used in combination with IHC to report cellular expression of <i>sox9a</i> in the adult zebrafish telencephalon.....	94
Figure 28: m-FISH probes against <i>prdm12b</i> mRNA fail to fully resemble the endogenous expression pattern of the <i>prdm12b</i> gene.....	94
Figure 29: m-FISH probes against <i>mdka</i> mRNA report expression and upregulation of the <i>mdka</i> gene in response to lesion of the zebrafish telencephalon	96

Tables

Table 1: List of chemicals used in this thesis.....	42
Table 2: List of enzymes used in this thesis	43
Table 3: List of equipment and tools used in this thesis	43
Table 4: Gene names and references for ISH probes used in this thesis.....	44
Table 5: List of kits used in this thesis	44
Table 6: Types of microscopes used for imaging in this thesis	45
Table 7: List of oligonucleotides used in this thesis.....	45
Table 8: List of plasmids used in this thesis, including antibiotic resistance and references	46
Table 9: Primary antibodies used in this thesis.....	47
Table 10: Secondary antibodies used in this thesis	47
Table 11: List of software and online tools used in this thesis	47
Table 12: List of solutions and buffers used in this thesis	48
Table 13: Zebrafish lines used in this study	49
Table 14: miRNA candidates in descending order of log ₂ fold change of expression.....	84

Publications

Lübke, L.; Zhang, G.; Strähle, U.; Rastegar, S. *mdka* Expression Is Associated with Quiescent Neural Stem Cells during Constitutive and Reactive Neurogenesis in the Adult Zebrafish Telencephalon. *Brain Sci.* **2022**, *12*, 284.

Zhang, G.; **Lübke, L.**; Chen, F.; Beil, T.; Takamiya, M.; Diotel, N.; Strähle, U.; Rastegar, S. Neuron-Radial Glial Cell Communication via BMP/Id1 Signaling Is Key to Long-Term Maintenance of the Regenerative Capacity of the Adult Zebrafish Telencephalon. *Cells* **2021**, *10*, 2794.

Gourain, V.; Armant, O.; **Lübke, L.**; Diotel, N.; Rastegar, S.; Strähle, U. Multi-Dimensional Transcriptome Analysis Reveals Modulation of Cholesterol Metabolism as Highly Integrated Response to Brain Injury. *Front. Neurosci.* **2021**, *15*, 671249.

Ghaddar, B.; **Lübke, L.**; Couret, D.; Rastegar, S.; Diotel, N. Cellular Mechanisms Participating in Brain Repair of Adult Zebrafish and Mammals after Injury. *Cells* **2021**, *10*, 391.

Diotel, N.; **Lübke, L.**; Strähle, U.; Rastegar, S. Common and Distinct Features of Adult Neurogenesis and Regeneration in the Telencephalon of Zebrafish and Mammals. *Front. Neurosci.* **2020**, *14*, 568930.

Zhang, G.; Ferg, M.; **Lübke, L.**; Takamiya, M.; Beil, T.; Gourain, V.; Diotel, N.; Strähle, U.; Rastegar, S. Bone morphogenetic protein signaling regulates Id1-mediated neural stem cell quiescence in the adult zebrafish brain via a phylogenetically conserved enhancer module. *Stem Cells* **2020**, *38*, 875–889.

1 Introduction

1.1 General introduction

Neurons are highly specialized cells which provide the basic building blocks of the nervous system. They receive and transmit signals in physical and electrical ways from and to different parts of the body and communicate with other neurons. Unfortunately, in humans, neurons lack the ability to reproduce, repair or replace themselves which consequently leads to neuronal loss in an event of neuronal damage (Steward, Sridhar, and Meyer 2013; Yiu and He 2006b). Long lasting consequences from neuronal loss are becoming an increasing problem in modern human society. Medical conditions or traumatic brain injury (TBI) can cause processes such as oxidative stress, inflammation and consequently apoptosis which all contribute to the loss of cells in the central nervous system (CNS) (Carron, Alwis, and Rajan 2016). The inflammatory processes can also lead to long-term effects including neurodegenerative diseases such as Alzheimer's and Parkinson's disease leading to an accumulating population living with significant deficits related to their brain injury which does not only pose a great burden on the patients but also on their family members, care-takers and loved ones (Galvano et al. 2017). Although several therapeutic approaches aim to alleviate some of the physical and psychological symptoms, no effective treatment to slow or inhibit progression of those pathologies has been developed to date as there is no known way to reverse neuronal death. Therefore, there is a critical need and socioeconomic pressure to understand the basis of neural regeneration and develop effective approaches for treatment of neuronal loss and the resulting symptoms in humans.

One approach is to characterize key molecules and cellular pathways which influence the formation of new neurons, called neurogenesis, and the survival of neurons in the adult nervous system and based on that develop approaches to re-establish functioning neuronal networks in the human CNS. To this end, several animal models have been used including non-regenerative models such as mammals, largely represented by murine models and models capable of regeneration such as axolotl and zebrafish (Zambusi and Ninkovic 2020).

In contrast to mammals, the adult zebrafish displays great regenerative potential and can effectively recover tissue structure and function of many organs including the heart, fin and spinal cord. Nevertheless, of particular interest is their extensive ability to regenerate parts of the central CNS at adult stages by replacing neurons which have been lost due to an injury or disease (Zambusi and Ninkovic 2020; Kizil, Kaslin, et al. 2012; Gemberling et al. 2013). This process is called adult neurogenesis and relies on the availability of neural stem cells (NSCs) which will proliferate and give rise to neural precursors (Grandel et al. 2006; Diotel et al. 2020; Ghaddar et al. 2021).

1.2 Zebrafish as a model organism

The zebrafish (*Danio rerio*) is an extensively studied and broadly used vertebrate model which has proven significance in different scientific research fields including oncology, embryonic development, behavior and regeneration. Lately, zebrafish have also been widely recognized as an effective model organism to study adult neurogenesis, due to its vast regenerative potential, and help in the search for effective treatments against neuronal loss in humans (Lieschke and Currie 2007). Although fish and human diverged millions of years ago they share about 70% of conserved genes providing the possibility to study common molecular pathways and a number of additional advantages suitable for the comparison to the situation in humans (Howe et al. 2013).

One of the obvious advantages is the fact that they are vertebrates and therefore share many biological properties with humans including anatomical and biochemical aspects. Hence, despite major physiological differences, they are useful for the study of vascular diseases, inflammation or bone diseases which cannot be provided by invertebrate models like *Drosophila melanogaster* or *Caenorabditis elegans* (Lieschke and Currie 2007).

As the zebrafish is rather small in comparison to other more closely related models like *Mus musculus* (mouse) or *Rattus norvegicus* (rat), with only 2-3 cm adult size, its maintenance and care is relatively easy and considerably cheap (Dahm, Geisler, and Nüsslein-Volhard 2006). They can be maintained in large numbers in specialized aquarium systems requiring less space in relation to larger rodent models. Additionally, they display a high fecundity as one female can lay between 300-600 eggs in one mating event (Dahm, Geisler, and Nüsslein-Volhard 2006). Their rapid generation time of only three months and fast development exhibiting complex behavior like food seeking already at 5 dpf (days post fertilization) pose the chance to execute a variety of complex analyses, including behavioral studies already at early stages while keeping ethical concerns low.

Early on, the optical transparency of the embryos and larvae and the fact that fertilization and development of the embryos takes place externally, made the zebrafish a highly appreciated model for researchers studying development. The unique features of *in vivo* visualization of embryonic stages and developmental events as well as easy manipulation of the embryo quickly increased the popularity of the zebrafish as a model organism (Laale 1977; Lieschke and Currie 2007).

In recent years, the availability of genetic tools has increased the use of zebrafish as a mainstream animal model not limited to the field of development. These tools included novel techniques for mutagenesis and the establishment of transgenic zebrafish lines and was surpassed by broad genetic screens establishing thousands of zebrafish mutants and unraveling the molecular basics of cellular pathways and genetic diseases (Haffter et al. 1996; Amsterdam et al. 1999; Amsterdam and Hopkins 2006; Stuart, McMurray, and Westerfield 1988; Driever et al. 1996).

However, an important foundation of continuing and more established genetic studies of the zebrafish is the fully sequenced zebrafish genome including detailed annotation of genes and proteins (Howe et al. 2013). This major advantage drives the improvement of genetic tools and establishment of zebrafish mutants analogous to human genetic diseases through forward genetics (Kettleborough et al. 2013). The relative optical transparency that is maintained by the zebrafish into adulthood allows fluorescent cell-tracing and *in vivo* studies of processes like inflammation and infection while keeping the complex environment of a living organism intact. Through transgenesis, modelling of acquired diseases in humans has also improved (Nolan et al. 2000). Based on this, reverse genetic approaches like knockouts have recently risen in popularity and availability and propelled the study of human diseases in the zebrafish model. A collection of transgenic and gene knockout lines that is readily available further supports the continuing studies and insights into human diseases and the interchange between researchers of different fields. However, one disadvantage that the zebrafish holds is the duplicated genome resulting in the presence of two copies of several genes which are unique in the mammalian genome. This complicates the study of gene function by reverse genetics as orthologous genes frequently overtake redundant functions (Holland et al. 1994; Meyer and Schartl 1999).

After the discovery of a disease, the treatment is also a considerable step. Correspondingly, in the field of pharmaceutical drug discovery and testing, zebrafish is used as an established model organism. The small size of the embryos, its permeability to small compounds and the high abundance of embryos are ideal factors for high-throughput chemical screens in a 96-well format on whole animals (Lieschke and Currie 2007).

Taken together, with the availability of a vast genetic tool box to manipulate zebrafish genetics, its high amount of orthologous human genes and a number of other advantages, zebrafish are a suitable model to study human diseases. One pivotal factor is also the remarkable regenerative capacity of the zebrafish which is displayed in several organs and structures and has been extensively studied in the brain in connection with neural regeneration (Gemberling et al. 2013; Alunni and Bally-Cuif 2016; Kizil, Kaslin, et al. 2012). Due to this regenerative potential, its similar neural structural organization and even a similar neurotransmitter pool, studies of neurodegenerative diseases in zebrafish in recent years have increased (Wang and Cao 2021; Matsui and Takahashi 2018; Panula et al. 2010; Zhang et al. 2020; Zhang et al. 2021; Diotel et al. 2020; Ghaddar et al. 2021; Rodriguez Viales et al. 2015). Intensified research already lead to the establishment of several zebrafish disease models for Parkinson's, Alzheimer's and other neurodegenerative diseases (Wang and Cao 2021; Matsui and Takahashi 2018). A zebrafish Alzheimer's disease model exhibiting accumulation of amyloid- β 42 which is implicated in many symptoms of Alzheimer's disease, established a significant association between aging, neuroinflammation, regenerative neurogenesis and neural stem cell plasticity (Bhattarai, Thomas, Cosacak, et al. 2017; Bhattarai, Thomas, Zhang, et al. 2017). In summary, zebrafish provide a

powerful tool for the study of the molecular background of neurogenesis and prevalent neurodegenerative diseases which holds the promise of developing drugs and potential therapies in humans.

1.3 Development and anatomy of the zebrafish CNS in comparison to the mammalian CNS

1.3.1 Early neurogenesis and development of the CNS

The nervous system is composed of two parts: the central nervous system (CNS), including the brain and spinal cord and the peripheral nervous system (PNS) which encompasses neurons outside of the CNS. The development of the CNS in zebrafish starts early at around 6 hours post fertilization (hpf) (Woo and Fraser 1995). As a first step for the development of the nervous system in all vertebrates, specification of the neural ectoderm is facilitated by neural induction, a process during which the mesodermal layer is brought in contact with the overlying ectoderm (Lumsden and Krumlauf 1996; Spemann and Mangold 2001; Doniach and Musci 1995). The process of neural induction is dependent on a combination of extrinsic signaling factors including members of the bone morphogenetic protein (BMP), wntless-integrated (Wnt) and fibroblast growth factor (Fgf) families and intrinsic factors, most prominently the members of the SRY- box containing transcription factor family B1 (SoxB1) (Wilson et al. 2001; Streit et al. 2000; Streit et al. 1997; Sasai 1998). All these factors and a combination of them are also important for later neurogenesis at adult stages. After specification, the neural ectoderm gives rise to the neural plate which is again relying on a tight control of the interplay between the different extrinsic and intrinsic signaling factors (Rentzsch et al. 2004; Okuda et al. 2010). Especially important for patterning of the neural plate is the sonic hedgehog (Shh) pathway, another signaling factor. Shh acts as the main signal of the mid-diencephalic organizer (MDO) which facilitates the patterning of the zebrafish diencephalon (Hagemann and Scholpp 2012; Scholpp et al. 2006).

In the next developmental step, the zebrafish displays a major difference to other vertebrates in that it develops a neural keel before developing the neural tube. In other vertebrates, the neural plate folds up into the neural tube encompassing a lumen, called the ventricle. Instead, in zebrafish, first a solid neural keel is formed which is afterwards inflated and forms a neural tube, adding one additional step to the process (Papan and Campos-Ortega 1994). However, in both cases the result of the neurulation process is the neural tube which will give rise to different parts of the CNS based on positional fate decisions (Papan and Campos-Ortega 1999; Clarke 2009; Tawk et al. 2007). An important signaling pathway involved in fate decisions of progenitor cells during CNS maturation is the Notch pathway. After the formation of the lumen, cells in the neural tube will mainly undergo asymmetric cell division in order to maintain the critical balance between the production of new neurons and replenishing the population of neural progenitors. Here the asymmetric inheritance of a subcellular membrane domain of the dividing progenitors is associated with the asymmetric fate of the daughter cells (Alexandre et

al. 2010). The more apically derived daughter cells display low Notch activity and differentiate into neurons while basal daughter cells are self-renewing and display high Notch activity (Alexandre et al. 2010; Dong et al. 2012).

The most studied part of the zebrafish brain with regard to the investigation of neurogenesis is the telencephalon, which is part of the forebrain (Grandel et al. 2006; Lam, Marz, and Strahle 2009). One reason for that is that it shares numerous homologies with the mammalian forebrain (Diotel et al. 2020). Another important reason for focusing on the telencephalon is that it harbors numerous stem cell niches at adult stages and is therefore implicated to show a high regenerative potential, important for studying the survival and regeneration of neurons (Diotel et al. 2020). During the final formation of the CNS, a significant difference between the development in zebrafish and other vertebrates like mammals is the mode of development of the telencephalon. They both arise from the neural tube but in contrast to mammals, the zebrafish telencephalon is formed by eversion as opposed to evagination in the mammalian brain (figure 1) (Folgueira et al. 2012; Mueller and Wullimann 2005). Due to this specific mode of development, the zebrafish telencephalon contains one medial ventricle between the two telencephalic hemispheres as opposed to two telencephalic ventricles of the mammalian telencephalon (figure 1) (Diotel et al. 2020). This leads to differences in the ability of tissue manipulation which is pivotal for the investigation of regenerative programs in the adult telencephalon.

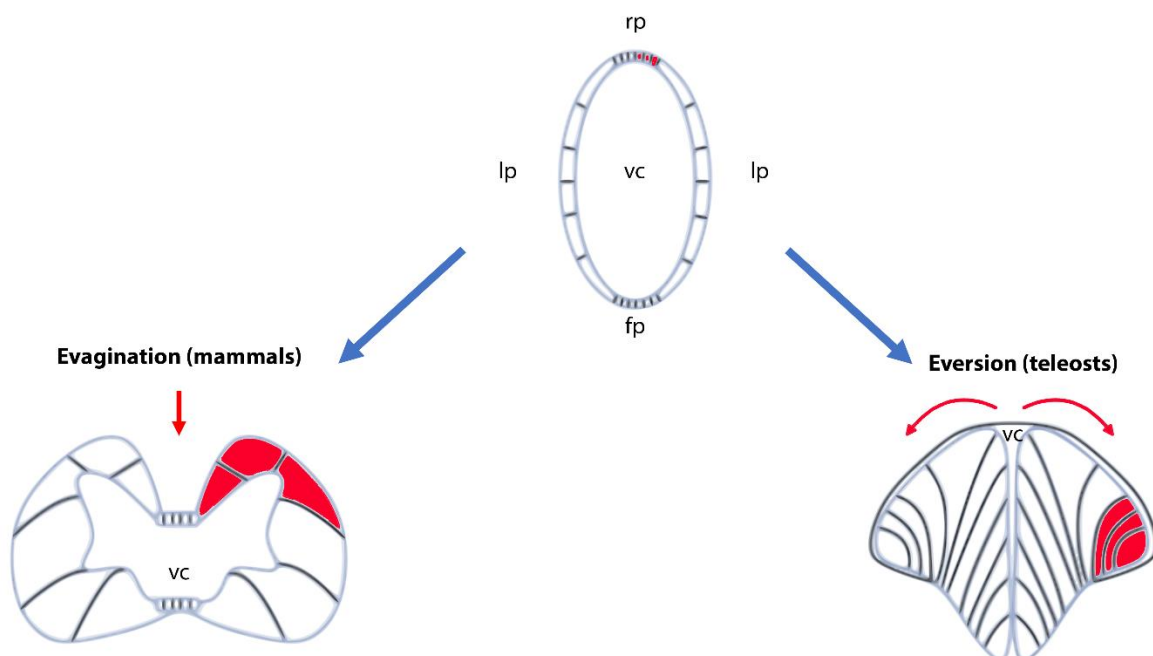


Figure 1: Scheme representing the different developmental modes of the mammalian and zebrafish telencephalon. Adapted from (Diotel et al. 2020). The neural tube (top) develops into the telencephalon by evagination, in the case of mammals (left) and by eversion in the case of zebrafish (right). This results in two telencephalic hemispheres encompassing two internal ventricles in the mammalian telencephalon. In the zebrafish, the neural tube grows laterally and folds ventrally (red arrows) giving rise to two hemispheres flanking one ventricle. The different movements ultimately

result in different positioning of distinct parts of the neural tube (marked in red). Abbreviations: fp, floor plate; lp, lateral plate; rp, roof plate; vc, ventricular cavity.

1.3.2 Structural and molecular comparison of the mammalian and zebrafish CNS

As already mentioned, the zebrafish CNS displays an array of highly similar anatomical structures to the human CNS which is why neurogenesis in comparison to the human situation is extensively studied in the zebrafish as a model organism. Obviously, the most significant difference between the zebrafish CNS and human CNS is the scale. However, key areas which are implicated in human diseases show a high degree of conservation with the corresponding structure in the human or mammalian CNS (Sager, Bai, and Burton 2010).

Similarly to the organization in the mammalian CNS, the zebrafish CNS can be divided into spinal cord, hindbrain, midbrain and forebrain (Sager, Bai, and Burton 2010). All of these parts are divided into subdivisions with different functionalities and show high structural homology to mammalian counterparts. This includes parts of the hindbrain like the medulla and hypothalamus, the dorsal portion of the midbrain which is the tectum and other structures like the olfactory system and the spinal cord (Sager, Bai, and Burton 2010). One region displaying high compositional homology also on a cellular level is for example the zebrafish cerebellum. It contains different cell layers including the molecular, Purkinje and granule cell layers which are all cell types that are present in the human cerebellar cortex as well. Additionally, the different cell types receive analogous information inputs, display similar synaptic connections and express comparable sets of genes and specialized markers (Bae et al. 2009; Sager, Bai, and Burton 2010). However, one major difference between mammalian and zebrafish cerebellar structures can also be noted: cell bodies of eurydendroid cells, which are output projection neurons, reside in the cortex of the zebrafish cerebellum and not in the deep nuclei as in mammals (Sager, Bai, and Burton 2010; Ikenaga, Yoshida, and Uematsu 2005).

When focusing on the vastly studied telencephalon, its different parts include the olfactory bulbs, the ventral telencephalon and the dorsal telencephalon (pallium). The ventral telencephalon is composed of two nuclei, called the ventral (Vv) and dorsal (Vd) nuclei of the ventral telencephalon (figure 2 and figure 11) (Wullimann, Rupp, and Reichert 1996). Accordingly, the dorsal telencephalon can also be divided into several substructures including the central (Dc), dorsomedial (Dm), lateral (Dl) and posterior (Dp) zone of the dorsal telencephalon (figure 2 and figure 11) (Wullimann, Rupp, and Reichert 1996). The different modes of development of the zebrafish and mammalian telencephalon complicate the comparison of anatomical structures. Nevertheless, many zebrafish structures can be assigned to mammalian counterparts: The Vv is considered to be homologous to the subventricular zone (SVZ) of the lateral ventricles and the Dl and the Dp are considered to be equivalent of the subgranular zone (SGZ) of the mammalian dentate gyrus (DG) (Broglio et al. 2005; Grandel and Brand 2013; Ganz et al.

2014; März et al. 2010). Strikingly, these two regions in the mammalian brain correspond to regions displaying high levels of proliferation (Kozareva, Cryan, and Nolan 2019; Doetsch, García-Verdugo, and Alvarez-Buylla 1997). The SVZ gives rise to cycling cells that migrate towards the olfactory bulbs and therefore resembles the RMS-like structure in the zebrafish telencephalon where cycling progenitors, called neuroblasts are accumulated (figure 3) (Adolf et al. 2006; März et al. 2010; Kishimoto et al. 2011). Therefore, these structures do not only show anatomical but also functional similarities between the zebrafish and the mammalian telencephalon which are important for the formation of new neurons during neurogenesis.

Further structurally similar regions include the Dm which is considered to correspond to the amygdala in the mammalian telencephalon, an area which was shown to be involved in motivation and emotion (figure 2) (Ganz et al. 2014). Additionally, the Dc is found to be homologous to the cortex and the Dl to resemble the hippocampus (figure 2) (Ganz et al. 2014). The mouse hippocampus contains the SGZ, an area which also harbors proliferative neural stem cells (NSCs) and progenitor cells (Kozareva, Cryan, and Nolan 2019).

On a molecular level, considering the genetic markup of the different telencephalic regions, a screen for transcription regulators (TRs) in the telencephalon of adult zebrafish suggested crucial genetic similarities between the zebrafish and the mammalian telencephalon (Diotel et al. 2015). In a similar way, homologies with the mammalian telencephalon were revealed by analysis of the spatial expression of neurotransmitters and their synthesizing enzymes which lead to conclusions about the distribution of inhibitory and excitatory neurons (Kaslin and Panula 2001; Mueller, Vernier, and Wullimann 2004). Additionally, it was reported that the location of serotonergic neurons innervating the telencephalon are located in a similar manner to what was observed in the rodent telencephalon (Parker et al. 2013).

In summary, although mammals and zebrafish, as part of the teleost family, diverged a long time ago the process of early neurogenesis during embryonic stages is highly comparable and only displays few differences. Accordingly, the CNS of both phylogenetic groups shares many structural and functional similarities which once more validates the zebrafish as a suitable model organism to study neurogenesis with respect to the human CNS.

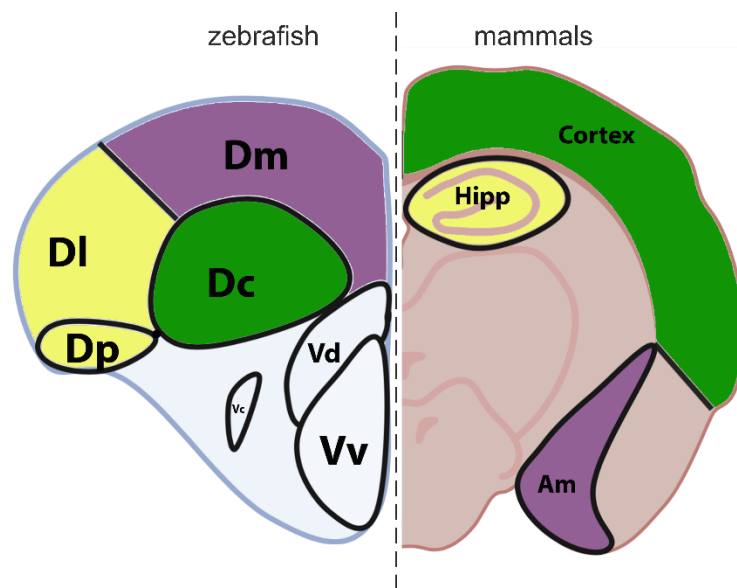


Figure 2: Scheme comparing the anatomy of the zebrafish (left) and mammalian (right) telencephalon with annotation of important regions or nuclei. Adapted from (Diotel et al. 2020). Only one hemisphere each is displayed. Homologous structures are depicted in the same color. The Dm (purple), the Dl/Dp (yellow) and Dc (green) have been implicated to be equivalents of the Amygdala (purple), hippocampus (yellow) and cortex (green) in the rodent telencephalon, respectively. Abbreviations: Am, amygdala; Dc, central zone of the dorsal telencephalon; Dl, lateral zone of the dorsal telencephalon; Dm, dorsomedial zone of the dorsal telencephalon; Dp, posterior zone of the dorsal telencephalon; Hipp, hippocampus; Vc, central nucleus of the ventral telencephalon; Vd, dorsal nucleus of the ventral telencephalon; Vv, ventral nucleus of the ventral telencephalon

1.4 Adult neurogenesis

The process of neurogenesis, was for many years believed to only occur at embryonic stages in order to shape the nervous system during early development (Oppenheim 2019). In contrast, studies in the 1960s and 1980s demonstrated that the formation of new neurons also takes place in the brains of adult rodents and monkeys, establishing the concept of adult neurogenesis (Altman 1969; Altman and Das 1965; Kaplan 1985). In these mammalian species, adult neurogenesis was observed in the cerebellum, the SVZ and in the DG of the hippocampus (Altman 1969; Altman and Das 1965; Uzman 1960; Miale and Sidman 1961). Since this discovery, an increasing number of studies demonstrated that adult neurogenesis can also occur in the human brain although its precise function remains elusive (Boldrini et al. 2018; Eriksson et al. 1998; Sorrells et al. 2018; Oppenheim 2019). The continuous generation of new neurons during adulthood is pivotal to maintain brain plasticity during processes like learning and support cognitive functions. The discovery of adult neurogenesis in mammals was the starting point for in depth investigation into the repair of neuronal damage caused by injury or neurodegenerative diseases (Ghaddar et al. 2021; Diotel et al. 2020). Also in zebrafish, it is nowadays well established that neurogenesis is occurring abundantly at adult stages because the animal is continuously growing and increasing in size (Zupanc, Hinsch, and Gage 2005; Zupanc and Sîrbulescu 2011).

1.4.1 Stem cell areas in the adult brain

The foundation for the continuous supply of new neurons are NSCs which are organized in discrete stem cell niches distributed throughout different brain areas (Ghaddar et al. 2021). In mammals, radial glial cells (RGCs) deriving from neuroepithelial cells (NECs) are considered NSCs because they can give rise to almost all neurons of the brain (Noctor et al. 2002; Pinto and Gotz 2007; Kriegstein and Götz 2003; Spassky et al. 2005). However, not all of these NSCs retain their neurogenic properties throughout adulthood. Indeed, in adult mammals only two main neurogenic niches, the SVZ of the lateral ventricles and the SGZ of the DG in the hippocampus, harboring RGC-like cells with neurogenic potential, were identified (Dennis et al. 2016; Fares et al. 2019).

In sharp contrast, RGCs which are also considered NSCs in the zebrafish brain, maintain their neurogenic properties and are localized in a high number of distinct stem cell niches located throughout the entire brain, supporting an increased neurogenic potential of the zebrafish brain at adult stages (Zupanc, Hinsch, and Gage 2005; Zupanc and Sîrbulescu 2011; Pellegrini et al. 2007; März et al. 2010; Lindsey and Tropepe 2006; Edelmann et al. 2013; Kaslin et al. 2009; Diotel et al. 2020). The different neurogenic niches are distributed along the rostrocaudal axis of the zebrafish brain with the most prominent ones being located on the ventricular layers of the telencephalon, diencephalon and rhombencephalon (Pellegrini et al. 2007; Lindsey and Tropepe 2006; Zupanc, Hinsch, and Gage 2005). The most extensively studied neurogenic niche is the subpallial zone of the dorsal zebrafish telencephalon, also for its ease of experimental manipulation due to the development of the telencephalon by eversion (figure 1) (Folgueira et al. 2012; Grandel et al. 2006; Lam, Marz, and Strahle 2009; Adolf et al. 2006). This area is usually called the ventricular zone (Vz) of the telencephalon because of its contact with the ventricle.

1.4.2 Stem cell types in the zebrafish and mammalian telencephalon

The NSCs located in the Vz of the zebrafish telencephalon display heterogeneity regarding their morphology and proliferative potential (März et al. 2010; Schmidt, Strahle, and Scholpp 2013). They can be divided into type I, type II and type III NSCs which are distinguished by the expression of numerous markers and have distinct properties (März et al. 2010). Type I cells are considered non-proliferative or quiescent NSCs (qNSCs) and are therefore negative for the proliferation marker proliferating cell nuclear antigen (PCNA). They instead express a variety of RGC markers, including the calcium binding protein β (S100 β), glial fibrillary acidic protein (GFAP), brain lipid binding protein (BLBP), Aromatase B and Vimentin, labeling them as RGCs (Diotel et al. 2016; Pellegrini et al. 2007; Diotel et al. 2020; März et al. 2010). Furthermore, they exhibit a distinct morphology attributed to RGCs including a triangular shaped soma and long processes spanning the parenchyma towards the pial surface (figure 3) (Diotel et al. 2020). Type II cells also show the distinct RGC morphology and

express the whole set of RGC markers but the major difference to the type I cells is that they are actively proliferating and therefore positive for PCNA (figure 3). Consequently, type II cells are considered proliferating RGCs (Diotel et al. 2020; Schmidt, Strahle, and Scholpp 2013). Type III NSCs can be divided into two subpopulations which are called type IIIa and type IIIb. Both of them are positive for the proliferation marker PCNA and therefore in a proliferative state. Additionally, they both express PSA-NCAM which is a marker for early neuronal differentiation. The major difference between the two subtypes is that type IIIa cells express the progenitor marker Nestin which is not the case for type IIIb cells. Furthermore, in most incidences they both lost the expression of RGC markers, although type IIIa cells can express them weakly (Diotel et al. 2020; März et al. 2010). Morphologically, both type III subtypes can be distinguished from type I and type II cells because they do not show the typical triangular cell morphology anymore and lose their process (figure 3) (Schmidt, Strahle, and Scholpp 2013). Type III cells are consequently considered neural precursors, called neuroblasts (Diotel et al. 2020).

There is a confirmed lineage between type I, type II and type III NSCs (Rothenaigner et al. 2011; Lange et al. 2020). Type II cells can either undergo symmetric divisions giving rise to either two new type II cells, thereby self-renewing and displaying stem cell features or asymmetric division, giving rise to one type II and one type III cell (figure 3B) (Rothenaigner et al. 2011). In the case of an injury, it was observed that NSCs occasionally undergo symmetric division giving rise to two new type III cells, thereby not conserving the type II NSC. This mode of division is however uncommon under constitutive conditions. Additionally, there is evidence that RGCs can undergo direct conversion into neurons (Barbosa et al. 2015; Diotel et al. 2020). Both of the latter conversions lead ultimately to a reduction of the stem pool. Type III cells mainly undergo symmetric neurogenic divisions and consequently leave the Vz to integrate into existing tissue (Rothenaigner et al. 2011; Ghaddar et al. 2021).

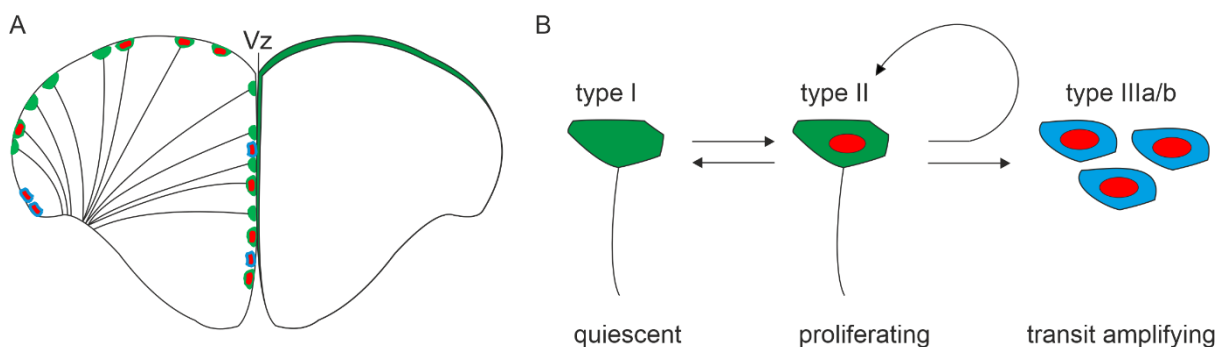


Figure 3: Schematic simplified representation of NSC types and localization in the adult zebrafish telencephalon. Adapted from (Schmidt, Strahle, and Scholpp 2013). (A) Cell bodies of NSCs reside in the ventricular zone (Vz) of the telencephalon (green) and reach their processes towards the pial surface. (B) Most of the NSCs in the Vz are in a quiescent state (type I), characterized by a triangular shaped cell body and long processes. Type II cells are proliferating (red nucleus) and can self-renew or give rise to type III cells, corresponding to neuroblasts (blue) which are characterized by a missing process and missing typical RGC morphology. Abbreviations: Vz, ventricular zone of the telencephalon

In the two neurogenic areas of the adult rodent brain, similar stem cell heterogeneity is observed and characterized by the expression of evolutionary conserved markers. In the SVZ, so called B cells are considered NSCs. They display astrocytic characteristics and are quiescent and therefore negative for the proliferation marker PCNA. They express GFAP, like zebrafish type I cells while being negative for the neuroblast marker doublecortin (DCX). B-cells supply transit amplifying cells, called C cells, which in turn can give rise to neuroblasts, called A cells. C-cells are also negative for DCX but only weakly express GFAP. However, as they are amplifying cells, they strongly express PCNA. A-cells are consequently positive for the neuroblast marker DCX and negative for GFAP while showing strong PCNA expression (Cavaliere, Benito-Muñoz, and Matute 2016).

The SGZ of the hippocampus is considered to be highly similar to the zebrafish Vz regarding proliferative behavior and lineage features of the progenitor cells. Here the existence of quiescent (called type 1) and proliferative (type 2) progenitors which express GFAP, Nestin and BLBP resembles type I and type II NSCs in the zebrafish Vz. The proliferative progenitors in the mouse SGZ are positive for PCNA and give rise to neuroblasts (type 3) which are positive for DCX and PSA-NCAM reminding strongly of the type III cells in the zebrafish Vz and again displaying a close link between zebrafish and mammalian brain composition (Kozareva, Cryan, and Nolan 2019; Knoth et al. 2010). Additionally, the type 1 in the SGZ are radial glial-like cells and also display a triangular shaped cell body and a long cytoplasmic process extending to the pial surface (Diotel et al. 2020).

Additional markers which have been recently identified and further defined the genetic character of adult NSCs in both species include inhibitor of DNA binding 1 (*Id1*) and the chemokine receptor *Cxcr4* (Diotel, Vaillant, et al. 2010; Rodriguez Viales et al. 2015; Nam and Benezra 2009; Tran et al. 2007; Mithal, Ren, and Miller 2013). In the zebrafish telencephalon, the gene *id1* is considered to be a marker for qNSCs because it is mainly expressed by type I cells and only by a few type II cells and functions by conferring quiescence to NSCs (Rodriguez Viales et al. 2015; Zhang et al. 2020; Zhang et al. 2021). In the mammalian telencephalon, *Id1* is expressed by B1 cells, the quiescent NSCs of the SVZ and modulates the self-renewal of stem cells (Nam and Benezra 2009; Diotel et al. 2020). Further important markers include downstream targets of Notch signaling, the *her* genes in zebrafish and their mammalian orthologues, the *Hes* genes. Both of which are important factors in influencing the cell fate of adult NSCs (Chapouton et al. 2011; Alunni et al. 2013; Kageyama, Ohtsuka, and Kobayashi 2007). Taken together, the entirety of these genetic markers demonstrate a remarkable resemblance also on the molecular level of the zebrafish and mammalian telencephalon. Moreover, they are valuable for the distinction of different cell-types under experimental conditions.

However, one striking difference between the cellular composition of the zebrafish and mammalian telencephalon that needs to be highlighted is the occurrence of astrocytes. In mouse, the majority of RGCs transform into astrocytes after embryonic development is concluded. Except for cells located in

the previously described neurogenic niches, the greater part of cells in the adult mouse telencephalon is consequently non-neurogenic which leads to an overall reduced neurogenic potential. (Diotel et al. 2020; Ventura and Goldman 2007; Gaiano, Nye, and Fishell 2000). In contrast to that, the zebrafish telencephalon is lacking astrocytes but retains neurogenic RGCs acting as NSCs, explaining the high regenerative potential (Than-Trong and Bally-Cuif 2015; Kaslin et al. 2009). Astrocytes are mainly responsible for the formation of a glial scar after injury to the brain which has been shown to inhibit neural regeneration in the mammalian brain (Yiu and He 2006a; Burda, Bernstein, and Sofroniew 2016; Wang et al. 2018). This scar formation contributes to the reduced restorative ability of the mammalian brain. Already under constitutive or homeostatic conditions, the zebrafish adult telencephalon displays a higher regenerative potential than the mammalian telencephalon. However, the importance of the zebrafish model in studying the effects of neuronal loss in humans is escalated by the extensive analysis of regenerative neurogenesis in the adult CNS.

1.5 Regenerative neurogenesis

Due to the high regenerative potential of the adult zebrafish brain which is based on the prevalence of neurogenic cells and the absence of scar formation, zebrafish are a widely accepted model to study the effects of traumatic brain injury and neuronal loss in the adult brain and the mechanisms of regenerative neurogenesis (Diotel et al. 2020). Knowledge from these studies can be applied to the development of treatments for the long term effect caused by neuronal loss in humans.

1.5.1 Experimental models to study regenerative neurogenesis in zebrafish

In order to study regenerative neurogenesis in the adult zebrafish brain, there are different techniques to induce neuronal loss and trigger the process of regeneration or to particularly mimic diseases affecting the brain (Zambusi and Ninkovic 2020). On a genetic level, specific alteration of gene expression by using morpholinos, zinc finger nucleases, transcription activator-like effector nucleases or clustered regularly interspaced short palindromic repeats were mainly used to establish models for neurodegenerative diseases. However, these models are largely confined to juvenile stages and assume that the targeted gene is already identified (Doyon et al. 2008; Huang et al. 2011; Nasevicius and Ekker 2000; Hruscha et al. 2013). A comprehensive paradigm for neurodegeneration at adult stages was established by the cerebroventricular microinjection of amyloid β 42 (A β 42) derivatives, causing symptoms comparable to the phenotype of Alzheimer's disease including apoptosis and consequent neuronal loss (Bhattarai et al. 2016; Bhattarai, Thomas, Cosacak, et al. 2017; Bhattarai, Thomas, Zhang, et al. 2017). The deposition of A β 42 leads through the initiation of the interleukin-4 (IL4)/Stat6 pathway to the activation of NSCs (Bhattarai et al. 2016).

In order to model the effects of traumatic brain injury and study the behavior of NSCs in response to neuronal loss multiple paradigms inducing acute damage have been established (Zambusi and Ninkovic 2020). Widely used is a stab wound assay in which a syringe needle is inserted through the skull into one telencephalic hemisphere of the zebrafish. Due to the everted form of the zebrafish telencephalon, during this assay, the Vz containing NSCs is acutely damaged (Schmidt et al. 2014; März et al. 2011). In contrast to that is a method where the needle is inserted through the nostrils of the fish, damaging the parenchyma of the telencephalon but keeping the Vz intact (Baumgart et al. 2012; Barbosa et al. 2015; Kyritsis et al. 2012a; Kishimoto, Shimizu, and Sawamoto 2012). Both of these assays only lesion one hemisphere while the contralateral hemisphere remains unlesioned and can serve as control. The consequent activation of regenerative programs in these two models can be used to study cellular and molecular mechanisms regulating adult brain regeneration (Zupanc and Sîrbulescu 2011; März et al. 2011; Schmidt et al. 2014; Kishimoto, Shimizu, and Sawamoto 2012; Baumgart et al. 2012).

In addition to inflicting mechanical injuries, neuronal damage assays based on chemical compounds have also been used to target specific cell types in the zebrafish brain. The exposure to cadmium chloride, quinolinic acid or titanium nanoparticles (TiO₂) all lead to neurotoxicity and therefore cause brain damage without mechanical injury (Zambusi and Ninkovic 2020; Monaco, Grimaldi, and Ferrandino 2016; Sheng et al. 2016; Skaggs, Goldman, and Parent 2014). An assay partially modelling the phenotypes of Parkinson's disease has been established by exposure to the chemical Paraquat which leads to modulation of redox levels and activity of mitochondria (Nunes et al. 2017). These chemical induced models promote the activation of neurogenesis without the simultaneous initiation of inflammatory or repair programs which makes it easier to decipher core mechanisms of regeneration in the adult zebrafish brain. Overall, a combination and comparison of the different paradigms should be employed when analyzing adult neurogenesis as each of them is only able to mimic a subset of symptoms or consequences of neuronal loss (Zambusi and Ninkovic 2020). However, this work will be focused on the molecular mechanisms involved in the regenerative response after telencephalic injury as described in the first injury paradigm (März et al. 2011; Schmidt et al. 2014).

In rodents, traumatic brain injury models are not as well established as in zebrafish. Therefore, investigation of cellular events occurring after damage to the mammalian CNS are often also based on rodent stroke models. Nevertheless, according to multiple studies, both result in similar regenerative processes and lead to a similar recovery outcome (Ghaddar et al. 2021; Castor and El Massioui 2018).

1.5.2 Acute consequences of brain injury

After mechanical injury of the zebrafish telencephalon, the first initiated process is cell death which can be observed already at 4 hours after the lesion (hours post lesion, hpl) but is quickly decreased and returns to control levels at 3 days post lesion (dpl) (Kroehne et al. 2011). In contrast to that, in rodents, cell death also appears shortly after the damage but persists much longer until 28 days in stroke models (Zhang et al. 2010). Due to the prolonged occurrence of cell death, recruitment and activation of microglia to the injury site is also more persistent in mammals than in zebrafish (Ghaddar et al. 2021).

Following cell death is the immune response in which microglia cells and peripheral immune cells are recruited to the lesion site (Kroehne et al. 2011; Baumgart et al. 2012; Kyritsis et al. 2012b). Furthermore, elevated expression levels of inflammatory cytokines like interleukin 1 β (IL1 β) and interleukin 8 (IL8) and the tumor necrosis factor α (NF α) released by activated microglia have been observed, revealing that shortly after traumatic brain injury an acute inflammatory response is initiated (Kizil, Kyritsis, and Brand 2015; Kizil, Kyritsis, et al. 2012; Kyritsis et al. 2012b; Ghaddar et al. 2021; Kanagaraj et al. 2022). The process of neuroinflammation is a pivotal consequence of traumatic brain injury because it acts as an activator of reactive neurogenesis in the zebrafish (Diotel et al. 2020; Kyritsis et al. 2012b). As a response to inflammation there is an upregulation of expression of the transcription factor *gata3* in RGCs in the Vz which leads to increased proliferation and consequent differentiation of RGCs into neurons (Kizil, Kyritsis, et al. 2012). Inflammation in the brain can also be modeled by sterile cerebroventricular microinjection of Zymosan A, a compound which is derived from *Saccharomyces cerevisiae*. Similarly to injury, it leads to the expression of the pro-inflammatory cytokines IL1 β and IL8 and increased proliferation of RGCs (Kyritsis et al. 2012a). On the opposite, treatment of adult zebrafish with the anti-inflammatory drug Dexamethasone can be used to investigate the effects of immunosuppression in injured telencephala. Past studies observed a significantly reduced reactive neurogenesis after treatment with Dexamethasone in lesioned adult zebrafish, supporting the notion that inflammation is a molecular process which is highly important for the regenerative response following telencephalic injury in the zebrafish (Kyritsis et al. 2012a).

In sharp contrast to that stands the finding in mammals, where acute neuroinflammation is considered to be a negative regulator of neurogenesis and regeneration as it leads to the formation of a glial scar and inhibits the proliferation of precursor cells (Monje, Toda, and Palmer 2003; Ekdahl et al. 2003; Popovich et al. 2002; Fitch and Silver 2008). However, there are also reports suggesting that pro-inflammatory cytokines and chemokines which are released during brain injury in mammals cause NSC proliferation, neuronal migration and promote cell survival (Carpentier and Palmer 2009; Whitney et al. 2009; Covacu and Brundin 2017). The role of neuroinflammation in the mammalian CNS is highly complex as there also needs to be a distinction between short and long-lasting effects as persisting

inflammation in the mammalian CNS is believed to be the main cause of neurodegenerative diseases (Amor et al. 2010; Glushakova, Johnson, and Hayes 2014; Kinney et al. 2018).

In zebrafish, from 48 hpl onwards an increased proliferation can be observed especially in the neurogenic niche along the subpallial zone of the telencephalon which harbors RGCs (März et al. 2011; Kishimoto, Shimizu, and Sawamoto 2012). The proliferation rate in the Vz peaks between 5 dpl and 8 dpl and reaches baseline levels at around 35 dpl (Diotel, Page, et al. 2010; März et al. 2011; Baumgart et al. 2012). This reactive neurogenesis is surprisingly confined to the lesioned hemisphere of the telencephalon and is suggested to be mainly taking place by symmetric division of type II stem cells which consequently gives rise to newborn neurons (Barbosa et al. 2015; Baumgart et al. 2012; Kroehne et al. 2011; März et al. 2011). Since this mode of division does not allow the self-renewal of stem cells it slowly leads to a depletion of the stem cell pool. In the rodent brain injury model, NSCs from the SVZ give rise to neuroblasts that will migrate toward the lesion site mediated by attractive factors (Chang et al. 2016).

Additionally, in the zebrafish telencephalon there is an accumulation of *oligodendrocyte lineage transcription factor 2 (olig2)* expressing mature oligodendrocytes and oligodendrocyte precursor cells (OPCs) in the injured region which is observed over a longer time period between 1 and 14 dpl (März et al. 2011). However, only a small amount of OPCs show a strong proliferative response in the lesioned hemisphere and the accumulation at the lesion site does not persist and is already resolved at 35 dpl (März et al. 2011). This is again a striking difference to the situation in the mammalian brain. After injury to the mouse brain, OPCs are also accumulating at the lesion site and show strongly increased proliferation which leads to the formation of a glial scar, inhibiting neural regeneration (Hampton et al. 2004; Burns et al. 2009; Magnus et al. 2007; Dimou et al. 2008). Therefore, although the initiated process of OPC recruitment to the lesion site is similar in mammals and zebrafish, the result is fundamentally different, adding another key factor contributing to the enhanced regenerative potential of the zebrafish brain in comparison to the mammalian brain (März et al. 2011).

As already mentioned, astrocytes play a pivotal role in the formation of a glial scar after injury of the mammalian brain. The glial scar is a conglomerate of extracellular matrix (ECM) components and processes from activated astrocytes which surround the lesion site and react to the injury by undergoing morphological changes (Sims and Yew 2017; Sofroniew 2009; Ghaddar et al. 2021). In zebrafish, no astrogliosis occurs in response to brain injury due to the lack of astrocytic cell-like structures in the adult zebrafish brain. Nevertheless, multiple studies suggest that RGCs take over astrocytic roles and neurogenic properties including gliosis considering there is an increased expression of glial markers, increased proliferation and hypertrophy and increased ECM deposition which is however not persistent (Jurisch-Yaksi, Yaksi, and Kizil 2020; Diotel et al. 2018; Kroehne et al. 2011). Initially, the role of the glial scar is beneficial for the regeneration process as it forms a physical

barrier to isolate the injury site and restrict the diffusion of inflammatory signals (Rolls, Shechter, and Schwartz 2009). However, this physical barrier consequently prevents newborn neurons to migrate to the lesion site and replace neurons which have been lost due to injury, resulting in failed regeneration of the injured tissue (Muramatsu et al. 2012).

Finally, on a morphological level at one month after brain injury, the lesioned hemisphere in the zebrafish telencephalon is observed to be entirely repaired and after one year, it displays no traces of traumatic injury in the telencephalic tissue anymore (Kroehne et al. 2011).

1.6 Signaling pathways implicated in the control of NSC behavior

The replacement of lost neurons by newborn neurons as part of the regenerative response to injury is dependent on the shift of NSCs from a quiescent to an activated state. However, there needs to be a fine-tuned balance between these two states as an over-proliferation can lead to a loss of NSCs and to the development of cancer (Diotel et al. 2020). Simultaneously, under constitutive conditions, the control between these two states is highly important to maintain brain homeostasis. In both species, zebrafish and mouse, multiple signaling pathways are implicated in controlling the behavior of NSCs under homeostatic and under regenerative conditions, including the Shh, Notch, BMP and Wnt pathways, which already play important roles during neurogenesis at embryonic stages (Urban and Guillemot 2014; Choe, Pleasure, and Mira 2015; Horgusluoglu et al. 2017; Schmidt, Strahle, and Scholpp 2013). Interestingly, after optic tectum injury, the Shh and Notch signaling pathways were shown to regulate RGC behavior in opposing ways and influence the decision of RGCs between proliferation versus differentiation. While Shh signaling is activated in RGCs after injury and promotes RGC proliferation, Notch signaling is downregulated which influences the generation of newborn neurons (Ueda et al. 2018).

1.6.1 The BMP signaling pathway

BMP proteins are secreted molecules which belong to the family of transforming growth factor β (TGF- β) proteins (Miyazono, Kamiya, and Morikawa 2010). They play important roles during many key processes including developmental and homeostatic processes at adult stages (Wang et al. 2014). Interestingly, they often act in a dose-dependent manner which has special impact during patterning events at embryonic stages (Bier and De Robertis 2015). The correct local concentration of BMPs is due to a balance between BMPs and their secreted antagonistic molecules including Noggin, Chordin and Follistatin (figure 4). During the canonical BMP signaling pathway, secreted BMP proteins form hetero- or homodimers which can bind to a heterotetrameric complex of transmembrane serine/threonine receptors (BMPRI and BMPRII). Interaction of BMP dimers with their receptor complex initiates a series of phosphorylation events leading to the phosphorylation of BMP specific

Smad proteins (Smad1/5/8) in the cell. Consequently, the specific Smad1/5/8 protein interacts with the downstream mediator Smad4 and forms a heteromeric complex which can translocate to the nucleus. In the nucleus, the complex interacts with cell and tissue specific cofactors and binds to the regulatory sequences of BMP responsive genes to regulate their transcription (figure 4) (Shi and Massague 2003).

Well characterized target genes of the BMP pathway in mouse and zebrafish are *Id* genes which contain an evolutionary conserved BMP-responsive element (BRE) (figure 4) (Korchynskiy and ten Dijke 2002; Lopez-Rovira et al. 2002; Zhang et al. 2020; Nakahiro et al. 2010; Javier et al. 2012). Indeed, the role of BMP signaling during adult neurogenesis in zebrafish was mainly investigated through the BMP responsive gene *id1* which is important in maintaining the balance between activated and quiescent NSCs in the Vz of the zebrafish telencephalon (Rodriguez Viales et al. 2015). An evolutionary conserved cis-regulatory module (CRM) of *id1* which is important for its specific expression pattern during constitutive and regenerative neurogenesis, was found to harbor a BRE, leading to the conclusion that the BMP pathway plays a crucial role in controlling the quiescence of RGCs in the adult telencephalon through mediating the expression of *id1* (Zhang et al. 2020).

Similarly, *Id1* in the adult mouse SVZ was described to be highly expressed in B1 cells (quiescent NSCs) and control their capacity to self-renew (Nam and Benezra 2009). Moreover, an interplay between BMPs and the antagonist Noggin was found to be necessary for keeping adult NSCs quiescent in the SGZ (Lim et al. 2000; Mira et al. 2010; Bond, Bhalala, and Kessler 2012). Similarly, under regenerative conditions, an upregulation of BMP and its downstream activated gene *Id3* in the SVZ were shown to lead to the differentiation of neural stem/precursor cells (NSPCs) into astrocytes compromising regeneration (Bohrer et al. 2015).

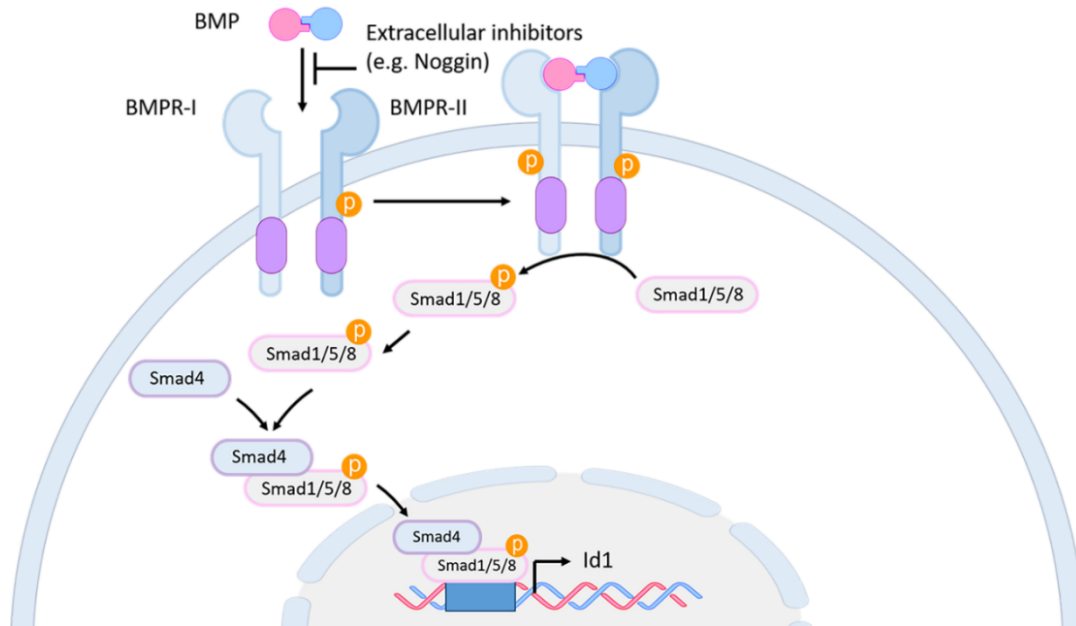


Figure 4: The canonical BMP signaling pathway. Adapted from (Diotel et al. 2020). A dimer of BMP proteins binds to the transmembrane receptor complex which leads to a phosphorylation cascade, activating the Smad1/5/8 proteins. Activated Smad1/5/8 interacts with Smad4 to form a complex that translocates to the nucleus and modulates the expression of downstream target genes, such as *Id1*. Abbreviations: BMP, bone morphogenetic protein; BMPR, BMP receptor; *Id1*, inhibitor of DNA binding 1.

1.6.2 The Notch signaling pathway

In the canonical Notch signaling pathway (figure 5), the transmembrane ligands Delta and Jagged interact extracellularly with the Notch receptor of a neighboring cell leading to multiple cleavage steps (Andersson, Sandberg, and Lendahl 2011). During these steps, the Notch extracellular truncation (NEXT) undergoes proteolytic cleavage by a multi-protein complex called γ -secretase, leading to the release of the Notch intracellular domain (NICD) (Artavanis-Tsakonas, Matsuno, and Fortini 1995; van Tetering and Vooijs 2011). NICD is then translocated to the nucleus where it forms a complex with the Notch signaling mediator Rbpj (Artavanis-Tsakonas, Rand, and Lake 1999). This complex facilitates the activation of downstream target genes, including members of the hairy/enhancer of split (*Hes*) transcription factor family (figure 5). The mammalian *Hes* genes and their zebrafish orthologues, the *her* (human epidermal growth factor receptor) genes, belong to the family of basic helix-loop-helix (bHLH) transcription factors (Ohtsuka et al. 1999; Takke and Campos-Ortega 1999; Takke et al. 1999; Yeo et al. 2007; Davis and Turner 2001). These transcription factors consist of two main domains where the basic domain binds the target DNA sequence and the HLH domain forms homo- or heterodimers with other HLH proteins. These targets can include proneural genes such as *Achaete-scute like* (*Ascl*) which act as activators of gene transcription, inducing neuronal fate. By binding to the regulatory sequences of bHLH proneural genes, the *Hes/Her* proteins inhibit the transcription of those genes and act as repressors of neuronal fate (figure 5) (Bertrand, Castro, and Guillemot 2002; Imayoshi and

Kageyama 2014; Kageyama, Ohtsuka, and Kobayashi 2007; Castro et al. 2011; Fischer and Gessler 2007).

During constitutive adult neurogenesis in the zebrafish telencephalon, studies showed that *notch3* is expressed in quiescent, as well as in activated RGCs, suggesting a dual role of Notch3 signaling depending on the specific bHLH downstream mediator (Than-Trong et al. 2018). Notch signaling through Notch3 and the effector Her4 leads to repression of proneural genes and therefore quiescence, while signaling through Notch3 and Hey1 drives proliferation (Than-Trong et al. 2018; Alunni et al. 2013). In contrast, *notch1b* expression can only be found in activated progenitors and Notch1b has been implicated to function by keeping the progenitor cells in an undifferentiated and proliferative state (Chapouton et al. 2010). Strikingly, the dual expression of *Notch3*, as well as the different functions of Notch3 and Notch1 are conserved between species during constitutive neurogenesis of the adult brain (Diotel et al. 2020).

Similarly, to zebrafish *notch3*, *Notch3* in mouse is also expressed in qNSCs and aNSCs and is implicated in maintaining the quiescent state of NSCs in the SVZ while *Notch1* is expressed in aNSCs and promotes a proliferative state in the SVZ (Kawai et al. 2017; Ables et al. 2010; Basak et al. 2012). After injury to the adult mouse brain, *Notch* expression is induced and promotes astrogenesis in the SVZ, thereby repressing neurogenesis and leading to reduced neurogenic capacity (Tatsumi et al. 2010; Benner et al. 2013).

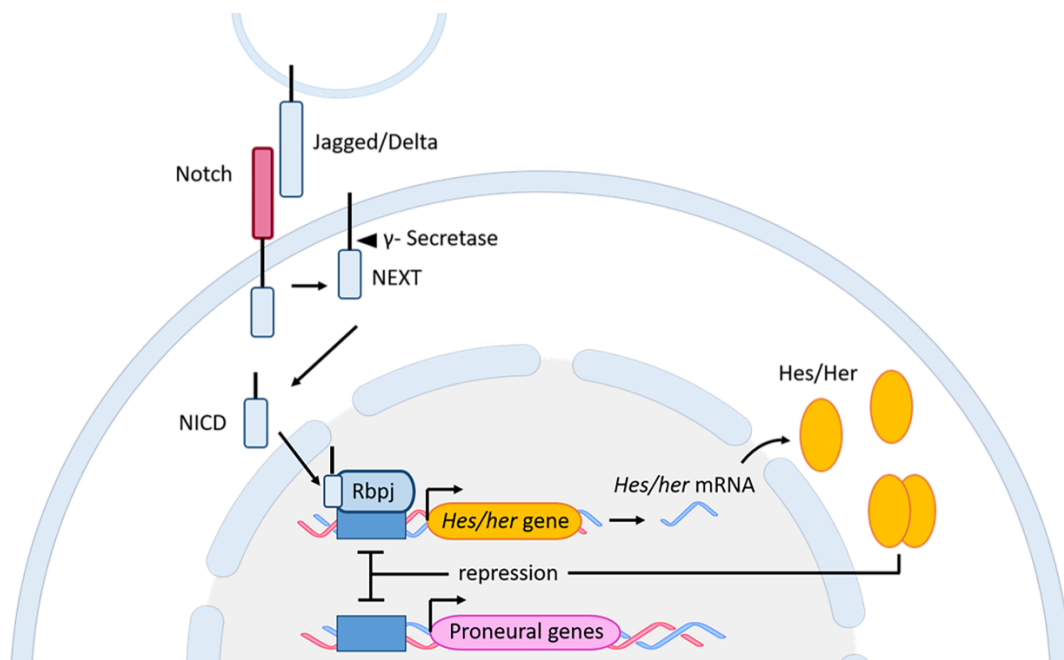


Figure 5: The canonical Notch signaling pathway. Adapted from (Diotel et al. 2020). The ligands of one cell interact with the Notch receptor of a neighboring cell leading to cleavage events which result in a translocation of the NICD to the nucleus. In the nucleus, the NICD interact with the Rbpj to activate the expression of Notch regulated genes such as *Hes/her* genes. The gene products of the *Hes/her* genes can repress the transcription of proneural genes by binding as homodimers to their promoter. Binding of the dimer to its own promoter leads to a negative auto-regulation. Abbreviations: bHLH, basic helix-

loop-helix; Her, human epidermal growth factor receptor; Hes, Hairy/enhancer of split; NEXT, Notch extracellular truncation; NICD, Notch intracellular domain; Rbpj, Recombining binding protein suppressor of hairless

1.6.3 Interaction between the BMP and Notch pathways in adult neurogenesis

An interesting interaction between the Notch and BMP pathways in relation with the gene *id1/Id1* has been demonstrated in the zebrafish and mouse telencephalon (Zhang et al. 2021; Rodriguez Viales et al. 2015; Sueda and Kageyama 2020; Bai et al. 2007; Diotel et al. 2020).

Id1 is proven to interact with members of the Hes/Her protein family by forming a dominant negative complex with those proteins through the HLH domain. This complex can act as a competitor, preventing the binding of Hes/Her dimers to their target DNA (Diotel et al. 2020). An example for this mechanism in the mouse telencephalon is the interaction between ID1 with HES which competes with the negative auto-regulation of the *Hes* promoter. Therefore, *Hes* is constantly expressed at a high level in NSCs, conferring quiescence to the cells (Bai et al. 2007; Sueda and Kageyama 2020). The observation that many molecular key players of both pathways and their interaction seem to be conserved between mouse and zebrafish, lead to the speculation that also in the zebrafish CNS an interplay between both pathways could contribute to the control of NSC behavior. In fact, in the zebrafish telencephalon Id1 was shown to bind to Her4.1 which is related to the mouse HES1 protein suggesting an interaction (Rodriguez Viales et al. 2015). Supposing the same mechanism of disrupting the negative auto-regulatory feedback loop was in place due to the interaction of Id1 with Her4.1, *her4.1* expression would be highly increased in the zebrafish. Blocking of the BMP signaling pathway or knocking-out *id1* was observed to decrease *her4.1* expression in the zebrafish telencephalon, suggesting that an interaction between the Notch and BMP pathways, acting through the BMP effector gene *id1* is in place also in the zebrafish telencephalon (Zhang et al. 2021).

1.6.4 The Wnt signaling pathway

The Wnt pathway is a conserved pathway which is highly complex owing to a great variety of different Wnt genes, a high number of Frizzled (Fzd) receptors and multiple co-receptors. It is therefore involved in several processes during nervous system development and numerous processes in the adult CNS (Choe, Pleasure, and Mira 2015).

In the canonical Wnt pathway (figure 6), which is dependent on the downstream transcription factor β -catenin while the non-canonical pathway is β -catenin independent, the first pivotal step is the interaction between the extracellular Wnt ligand and the transmembrane receptor Fzd (Zhang et al. 2011; Choe, Pleasure, and Mira 2015). An important regulator of this interaction is the low-density lipoprotein receptor-related protein 5/6 (LRP5/6) (Tamai et al. 2000; Zhang et al. 2011). In the cell, Wnt-Fzd interaction leads to the phosphorylation and consequent activation of Dishevelled (Dvl) which

in turn inactivates glycogen-synthase-kinase-3 β (GSK-3 β), an important modulator of the pathway (figure 6). Wnt signaling regulates the activity of GSK-3 β by displacing it from its interaction partners (figure 6). In the absence of Wnt, β -catenin is targeted for ubiquitination by the so called destruction complex and then degraded by the proteasome. In this way the amount of β -catenin is constantly kept at a low level (Dale 1998; Logan and Nusse 2004). The destruction complex consists of the serine/threonine kinases casein kinase 1 (Ck1), Axin, adenomatous polyposis coli (APC) and GSK-3 β and phosphorylates β -catenin which leads to its ubiquitination. If Wnt is present, activated Dvl prevents GSK-3 β from interacting with the destruction complex, stabilizing β -catenin which can then relocate to the nucleus to initiate the activation of Wnt target genes (figure 6) (Toledo, Colombres, and Inestrosa 2008). Tankyrases also play an important role in the process of destabilization of the destruction complex because they label Axin for ubiquitination and lead to its degradation (figure 6) (Huang et al. 2009).

Despite the implication of the role of Wnt/ β -catenin signaling in the regeneration of different parts of the zebrafish CNS at adult stages, such as the tectum and spinal cord, to date the function of the signaling pathway in adult neurogenesis especially in the telencephalon, has not been extensively studied (Strand et al. 2016; Wehner et al. 2017; Shimizu, Ueda, and Ohshima 2018; Lindsey et al. 2019). One recent report by Demirci et al. (2020) observed a strong activation of Wnt/ β -catenin signaling early after lesion of the zebrafish telencephalon (Demirci et al. 2020). Furthermore, they identified a set of 119 positively regulated target genes after lesion and concluded that the activation of the Wnt pathway is pivotal for molecular events occurring during the early wound healing stage and that Wnt modulated activation of downstream pathways like the mTOR and FoxO pathways might contribute to the regenerative response in the telencephalon (Demirci et al. 2020).

In the mammalian SVZ and SGZ stem cell niches, Wnt/ β -catenin responsive cells are present and the canonical Wnt pathway was shown to be required for maintenance of the stem cell pool on the one hand and to have a role in the differentiation of newborn neurons on the other hand (Varela-Nallar and Inestrosa 2013; Wexler et al. 2009; Qu et al. 2010).

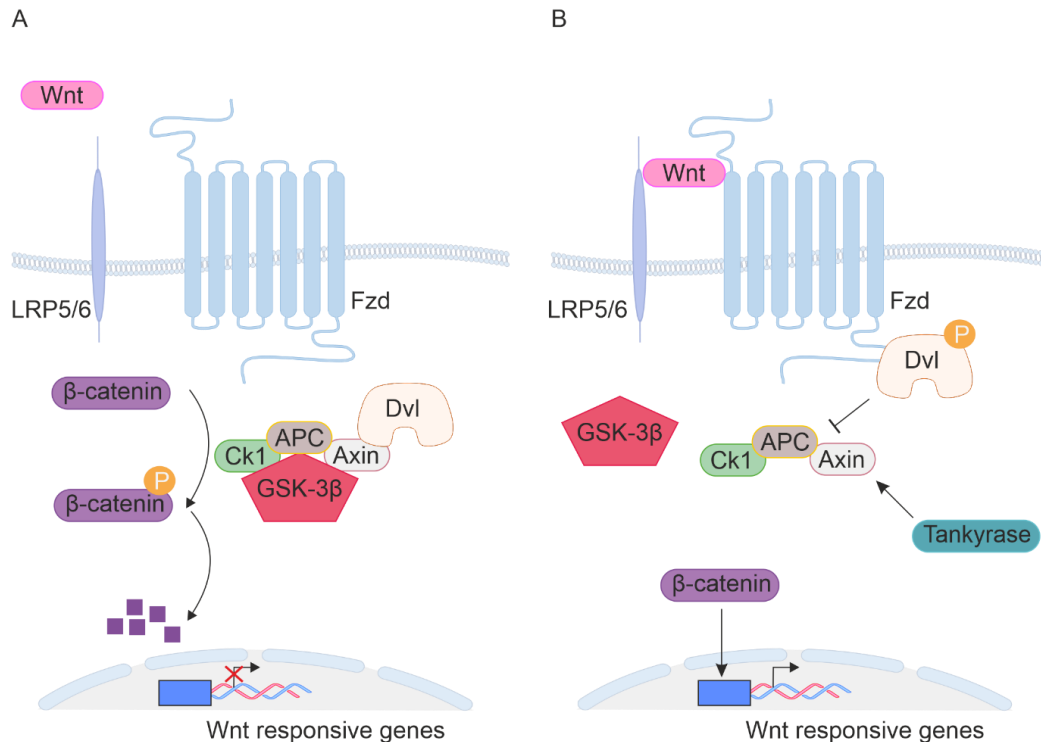


Figure 6: The canonical Wnt pathway is dependent on β -catenin and GSK-3 β . (A) No interaction between Wnt and its receptor Fzd leads to degradation of β -catenin which is mediated by the destruction complex. In this case, β -catenin is not available to initiate the transcription of Wnt target genes. The central component of the destruction complex is GSK-3 β . (B) After binding of Wnt to Fzd, Dvl is activated by phosphorylation and inhibits the destruction complex by detaching GSK-3 β . β -catenin is consequently stabilized and can relocate to the nucleus to facilitate transcription of Wnt responsive genes. Tankyrases help in the degradation of Axin, another part of the destruction complex by labeling it for ubiquitination. Abbreviations: APC, adenomatous polyposis coli; Ck1, casein kinase 1; Dvl, Dishevelled; Fzd, Frizzled; GSK-3 β , glycogen-synthase-kinase-3 β ; LRP, lipoprotein receptor-related protein; Wnt, wingless-integrated

In conclusion, the major signaling pathways BMP, Notch and Wnt all display pivotal and distinct functions not only during early neurogenesis but also during adult neurogenesis, most of which are conserved between zebrafish and mammals. Their influence on downstream transcription factors and with this the consequent influence on signaling molecules including Midkine will be investigated in this thesis using specific inhibitors.

1.7 Regulation of gene transcription

The different kinds of neurons and glial cells which originate from distinct progenitors during embryonic and adult neurogenesis need particular cues to define their cell type identity. As already mentioned, the major signaling pathways BMP, Notch and Wnt constitute external signals which in turn activate the expression of specific genes in progenitor cells. The differential expression and unique combination of genes leads consequently to the particular cell identity adapted by a progenitor cell (Diotel et al. 2015). Genes are generally transcribed by RNA polymerases, in the case of protein-coding genes this is usually RNA polymerase II (Kornberg 1999). During the process of transcription, gene

expression is controlled by multiple transcription regulators (TRs) that can be divided into chromatin-remodeling factors which modulate the accessibility of CRMs through alteration of chromatin state, proteins of the basic transcription machinery and transcription factors (TFs). A varying expression, combination and interaction of these TRs leads to a differential expression of affected genes which is a pivotal control mechanism in a number of processes like differentiation and proliferation of cells (Diotel et al. 2015; Ferg et al. 2014; Norton 2000). TFs contain one or several DNA binding domains with which they recognize a specific DNA sequence, the binding site motif (Ptashne and Gann 1997). Upon binding to the CRMs of target genes they repress or activate the transcription of those genes. CRMs are characterized by a high occurrence of conserved sequences across species and can be divided into activating modules which includes promoters, enhancers and locus control regions (LCR) and repressing elements which includes silencers and insulators (Ferg et al. 2014).

1.7.1 Enhancers and promoters (activating CRMs)

Enhancers are a class of activating CRMs which can be located up- or downstream of a regulated gene and in some cases also in the introns of that gene. Additionally, there are also cases where the enhancers overlap with the coding exons or the 5' untranslated region (UTR) (Tümpel et al. 2008; McLellan, Kealey, and Langlands 2006; Ferg et al. 2014). However, they may also be located at a certain distance from the regulated gene, which can be up to 1 megabase (Lettice et al. 2003). Therefore, the regulation of enhancers is thought to be independent of location and orientation in regard to their associated gene. Their mode of action is characterized by providing an open chromatin region which is recognized and bound by TFs (Li, Barkess, and Qian 2006). Here again, a specific combination of TFs leads to a unique output, namely the regulation of transcription of the corresponding gene.

Promoters can be divided into proximal, located closely to the transcription start site (TSS) of their regulated gene, and core promoters which encompass the TSS. Proximal promoters contain binding sites which are recognized by TRs, similar to enhancers, while core promoters show a different motif organization (Ferg et al. 2014; Thomas and Chiang 2006; Juven-Gershon and Kadonaga 2010).

The interaction between enhancer elements and their associated promoters is possible through a DNA loop which is facilitated via the de-condensation of chromatin (Carter et al. 2002; Chambeyron and Bickmore 2004). However, not every type of core promoter can interact with enhancers (Li, Barkess, and Qian 2006).

1.7.2 Gene regulatory networks

The specific combination of TRs interacting with CRMs of various genes results in complex species and tissue specific gene regulatory networks (GRNs) which are the basis of cell differentiation during processes like development and regeneration of multicellular organisms (Davidson 2010; Ettensohn

2013; Peter and Davidson 2011). Theoretically, the DNA of CRMs encodes regulatory information for a specific gene, which is then realized by their interaction with a specific combination of TRs. As GRNs are the foundation of highly complex processes, the tight spatial and temporal control of the interaction between the different factors is crucial for the normal function of these processes. The knowledge of which signaling pathways, downstream TFs, other interacting TRs and affected genes are involved, provides the possibility to manipulate these GRNs on multiple levels. The notion that many TRs are expressed ubiquitously in the zebrafish but their role is context dependent, substantiate the fact that specific combinations and control of expression lead to differing outcomes, indicating the high complexity of GRNs (Ferg et al. 2014).

1.8 The growth factor Midkine-a

The complex process of neurogenesis constitutes its very own GRN with specific genes, TRs, signaling molecules and other factors which are interacting to regulate the differentiation of neural progenitors into mature neurons dependent on the timing and location. Already, in early neurogenesis, it is evident that a tight spatial and temporal control of expression is pivotal to control this developmental process. During adult neurogenesis, under homeostatic but especially under regenerative conditions, the balance between quiescent and activated stem cells is especially interesting as a regulatory point. In an effort to decipher the GRN which constitutes the basis for adult neurogenesis, I aimed to identify genes which regulate NSC behavior in the adult zebrafish telencephalon.

As a starting point, an RNA sequencing experiment comparing the expression levels of genes in lesioned vs. unlesioned telencephalic tissue from adult zebrafish was conducted. Via this experiment, hundreds of genes were identified with either upregulated or downregulated expression levels in response to telencephalic lesion, among them the gene *midkine-a (mdka)* (Gourain et al. 2021).

1.8.1 Family and structure

The zebrafish *mdka* is a homologue of the human *midkine (MK)* gene which is a heparin binding growth factor that was firstly discovered by Muramatsu and Kadomatsu as a retinoic acid (RA) inducible gene in embryonic carcinoma cells (Kadomatsu, Tomomura, and Muramatsu 1988). Later it was found to be expressed during mid-gestation periods of mammalian embryos. Hence, the name “midkine” (Tsutsui et al. 1991).

The *MK* gene belongs to a small family which is highly conserved among vertebrates and only contains one more member called pleiotrophin (*PTN*) (Matsumoto et al. 1994; Muramatsu 2014). However, in the zebrafish, this family contains a third member: the *mdka* paralogue *mdkb*, which arose due to genome duplication during teleost evolution and cannot be found in mammals (Matsumoto et al. 1994; Muramatsu 2002, 2014; Muramatsu and Kadomatsu 2014; Holland et al. 1994; Winkler et al. 2003).

mdka is located on chromosome 7 of the zebrafish genome and consists of five exons. Only exon two, three, four and a part of exon five contribute to the *mdka* coding region (figure 18A). There is a 65% sequence identity between the two paralogues *mdka* and *mdkb* and *mdka* shares about 62.3% of amino acids with the human *MK* gene (Svensson et al. 2010).

Structurally, the MK protein consists of an N-domain and a more complex C-domain, located N-terminally and C-terminally, respectively. They both contain heparin binding sites and different functions. The two domains both extend a short tail (N-tail and C-tail) and are connected by a few amino acids forming the hinge region (Muramatsu 2014). Strikingly, the highest degree of conservation among species was observed in the hinge region which is responsible for the flexibility of the protein but has also been proposed to harbor its own heparin binding domain (Muramatsu 2014; Lim et al. 2013).

1.8.2 Regulation and function of *mdka*

The promoter region of the human *MK* gene exhibits various binding sites, for example for RA and Nuclear Factor kappa-light-chain-enhancer of activated B cells (NF- κ B) which is suggested to play a role in the induction of *MK* upon inflammation and tumorigenesis (Uehara et al. 1992). There is also evidence of a hypoxia inducible element in the promoter region which is thought to be involved in the upregulation of *MK* upon ischemia and in different kinds of tumors (Reynolds et al. 2004a).

The MK protein is known to be pleiotropic, meaning it is involved in the regulation of a variety of different processes including development, tumorigenesis, inflammation and regeneration (Weckbach, Muramatsu, and Walzog 2011; Muramatsu 2010). Its initial function was discovered as a key player during early development but its role has especially been implicated during the development of the nervous system (Muramatsu 2014; Winkler et al. 2003). During early zebrafish development the two paralogues *mdka* and *mdkb* show overlapping expression patterns in the embryo CNS: *mdka* is expressed throughout the neural tube while *mdkb* expression is restricted to the dorsal neural tube (Winkler et al. 2003). However, they display quite differential functions at this stage: while *mdka* is pivotal for the formation of neural crest cells, *mdkb* is responsible for the establishment of the neural plate border (Winkler and Moon 2001; Liedtke and Winkler 2008). Additionally, it was recently found that in the adult zebrafish retina, the constitutive expression patterns of the two homologues differ but align during retinal regeneration (Calinescu et al. 2009). Here, several recent and interesting studies have developed a comprehensive idea of the function of *mdka* in retinal regeneration. *mdka* has been shown to regulate the cell-cycle during the neurogenesis of photoreceptors. In more detail, it regulates the progression from the S- to the M-phase of the cell cycle which is facilitated through its downstream effector *id2a* (Luo et al. 2012). Furthermore, *mdka* was proven to be regulated by the circadian clock in the zebrafish retina. *mdka* and *mdkb* both show a circular asynchronous expression in

the Müller-glia, implying different biological functions with distinct timing (Calinescu, Raymond, and Hitchcock 2009).

In mammals, MK appearance in various tumors has for years been an interest as it correlates with poor prognosis and resistance to chemotherapy (Kadomatsu, Kishida, and Tsubota 2013). Therefore, the investigation of MK for the purpose of drug development in connection with cancer is exhaustive (Muramatsu 2011).

Interestingly, there are already proven connections between *Mk* and neurodegenerative diseases as *Mk*-deficient mice display Parkinson's-like symptoms, suggesting a role of *Mk* in the development of dopaminergic neurons (Prediger et al. 2010; Ohgake et al. 2009). One very interesting aspect of MK function is its implication in neuroprotection which has been proposed firstly in relation with drug-induced neurodegeneration and later also in mouse-models for Parkinson's and Alzheimer's disease (Gramage and Herradón 2011; Muramatsu 2011). Additionally, the role of MK in inflammation has been studied in different environments and many reports concluded a pro-inflammatory role of MK increasing the incidences of chronic inflammatory diseases (Weckbach, Muramatsu, and Walzog 2011; Sorrelle, Dominguez, and Brekken 2017). However, a recent study in axolotls rather reported an anti-inflammatory role of the salamander orthologue *mk*, functioning to resolve injury-induced inflammation after limb amputation (Tsai, Baselga-Garriga, and Melton 2020).

1.8.3 Receptors for MK

In the mammalian system, interaction of MK with multiple receptors has been demonstrated exhibiting regulation of a high number of distinct downstream pathways (Muramatsu 2014; Weckbach, Muramatsu, and Walzog 2011). The most established interaction of MK is with the receptor Protein tyrosine phosphatase ζ (PTP ζ), an interaction which regulates processes such as migration of embryonic neurons and survival of B cells (Maeda et al. 1999; Cohen et al. 2012). Multiple kinases, including phosphatidylinositol 3-kinase (PI3K) and Mitogen-activated protein kinase (MAPK) are involved in signaling downstream of PTP ζ . In mammals, MK has been reported by several studies to enhance the survival of neurons by modulation of the MAPK pathway, effectively inhibiting apoptosis (Owada et al. 1999; Satoh et al. 1993; Hida et al. 2003). Further proven MK-receptor interactions include low-density lipoprotein related receptor-1 (LRP-1), integrins, Neuroglycan C, Notch-2 and anaplastic lymphoma kinase (ALK) with which MK was shown to regulate proliferation in immature sympathetic neurons (Reiff 2011; Muramatsu 2014). ALK is considered to be a basic regulator of neurogenesis in the CNS and PNS in vertebrates and therefore interaction of MK or any of its species-specific orthologues with ALK is an interesting aspect to be investigated (Reiff 2011; Yao et al. 2013). During the regeneration of the zebrafish retina, it has already been shown that activation of a *Mk*-ALK

complex is required for proliferation of Müller-glia which act as retinal stem cells (Nagashima et al. 2020).

Not all of these receptors have a similar affinity to MK and several of them also bind PTN. Additionally, in many cases, an interaction between the different pathways can be observed, although the PI3K/AKT and MAPK signaling axes seem to be the most preferred. However, the function of MK is multifaceted and it is also likely that the MK receptor is a complex of several proteins including ALK, LRP6 and others (Sakaguchi et al. 2003).

Elucidating the exact role of *mdka* in the zebrafish is therefore difficult and can additionally not be easily facilitated by a knockdown or knock-out of the gene, since the paralogue *mdkb* would initiate a compensatory mechanism. Furthermore, a deficiency in both *mdka* and *mdkb* would probably be compensated by *ptn*, complicating the study of the exact function.

1.8.4 *mdka* in zebrafish adult neurogenesis

Adult neurogenesis in the zebrafish brain is based on a complex GRN which regulates the balance between NSCs that are quiescent and NSCs which are activated to give rise to new neurons. The implication of *mdka* in the regulation of NSC behavior is an interesting aspect to be investigated for multiple reasons: (1) the mammalian and salamander orthologues of *mdka*, *Mk* and *mk* respectively, have already been shown to play an important role during regeneration in those organisms, including regenerative processes in the muscle and liver of mice or in the limb of Axolotl (Tsai, Baselga-Garriga, and Melton 2020; Ikutomo et al. 2014; Ochiai et al. 2004). (2) *Mk* has also been shown to be expressed in the rat cerebral cortex and in neural precursor cells at later stages in mice (Matsumoto et al. 1994; Zou et al. 2006). (3) In multiple zebrafish organs, *mdka* demonstrates an upregulation in response to lesion. This includes the retina, the fin and the zebrafish heart (Calinescu et al. 2009; Grivas, González-Rajal, and de la Pompa 2021; Thompson et al. 2020). (4) Members of the *midkine* family in salamander (*mk*) and also the zebrafish *mdka* were shown to play a pivotal role during the inflammatory process that follows an injury and is a key process during regeneration of the nervous system (Tsai, Baselga-Garriga, and Melton 2020; Kyritsis et al. 2012a; Weckbach, Muramatsu, and Walzog 2011). However, *mdka* or any of its orthologues have never been investigated regarding its role during regeneration in the forebrain of any organism. (5) Also in the zebrafish brain, *mdka* showed an increased expression in response to telencephalic lesion (Gourain et al. 2021). Hence, the investigation of its expression pattern, regulation and function and therefore its specific place in the GRN during constitutive and regenerative neurogenesis is intriguing.

1.9 The role of ncRNAs in the GRN

In recent years another layer of complexity was added to GRNs by the discovery of the regulatory influence of non-coding RNAs (ncRNAs). Only 2% of the human genome actually encodes for proteins while the rest was historically regarded as junk DNA (Djebali et al. 2012; Doolittle 2013). However, about 90% of the human genome is actively transcribed, suggesting that the non-coding parts also play more important roles in cellular development, physiology or pathologies than what was historically regarded to them (Sana et al. 2012).

NcRNAs can be grouped into two major classes which is based on the size of the transcript: small ncRNAs which are usually up to 25 nucleotides (nt) in length and long ncRNAs which can be larger than 200 nt. Each of these groups contain a number of different subclasses which exhibit diverse characters and functions (Sana et al. 2012). Many of these subclasses are historically known and have an accepted function, such as ribosomal RNA (rRNA) and transfer RNA (tRNA) which have long been proven to play an essential role during translation of mRNA to a protein. Recently, the regulatory role of enhancer RNAs (eRNAs) and micro RNAs (miRNAs), both subclasses of small ncRNAs, has also shifted into focus. Enhancer RNAs arise when active enhancers are bi-directionally transcribed by RNA Polymerase II, therefore eRNAs are regarded as tissue-specific markers of enhancer activity (De Santa et al. 2010; Cheng et al. 2015). However, not all active enhancers are transcribed into eRNAs (Ding et al. 2018). eRNAs are capped at their 5' which makes them detectable by Cap Analysis of Gene Expression (CAGE) sequencing but are not polyadenylated or undergo splicing events (Murakawa et al. 2016). Recent evidence suggests that eRNAs function by regulating the expression levels of target genes and with that are involved in the development of multiple diseases (Melo et al. 2013; Murakawa et al. 2016; Ding et al. 2018). They are proposed to influence gene expression on multiple levels, including strengthening of enhancer-promoter looping to promote transcription, abolishment of transcriptional repression, activation of positive transcription elongation factors to regulate gene transcription or modification of histones to modulate accessibility of a DNA region (Ding et al. 2018). Which genes eRNAs target exactly remains elusive because enhancers can be located at any distance from the target gene. Therefore, linking eRNAs and their target genes is usually facilitated by correlating eRNA expression with expression levels of putative targets (Melo et al. 2013; Kim et al. 2010). Since eRNAs are unstable, expressed at very low levels and also usually short molecules, detection and deciphering their exact function is challenging.

1.9.1 miRNA biogenesis and function

MiRNAs are the most extensively studied class of small ncRNAs. They are short single-stranded RNA molecules with a length of only 18-25 nt which are generally low abundant (Sana et al. 2012). MiRNAs are evolutionary conserved and it is predicted in the human genome that miRNAs make up 1-2% of the

whole genome and control an estimated 50% of protein coding genes (Krol, Loedige, and Filipowicz 2010; Griffiths-Jones 2006). Most miRNAs originate from genomic regions located distantly from annotated genes which implies that they are transcribed independently (Lau et al. 2001; Lagos-Quintana et al. 2001). Nonetheless, a small amount of miRNAs was also found in the intronic regions of annotated genes where they appeared in a sense, as well as in an antisense orientation (Krol, Loedige, and Filipowicz 2010; Bartel 2004). MiRNA genes can be arranged as clusters in the genome which leads to the transcription as a multi-cistronic primary transcript. These miRNAs are often related to each other but related miRNAs do not necessarily have to be clustered (Lagos-Quintana et al. 2001; Lau et al. 2001).

MiRNA genes can be transcribed from their own promoter by RNA Polymerase II (figure 7A). Afterwards, miRNA biogenesis can either happen through a dominant canonical or non-canonical, Drosha independent pathway which will both result in a functional miRISC complex (O'Brien et al. 2018). During the canonical pathway (figure 7A), transcription results in a primary transcript, the primary miRNA (pri-miRNA) which is a double-stranded molecule with a 5' cap. These pri-miRNAs are longer than the mature miRNA as they can be up to 1 kilobase (kb). After transcription, the pri-miRNA is cleaved by Drosha, an RNase III endonuclease, resulting in a 70 nt long stem-loop structure, called the preliminary miRNA (pre-miRNA) (Lee et al. 2003). Consequently, the pre-miRNA is relocated to the cytoplasm which is facilitated by exportin 5, a RAN GTP dependent transporter (Lund et al. 2004; Yi et al. 2003). Dicer, another RNase III endonuclease then recognizes the double-stranded part of the pre-miRNA and removes the loop structure resulting in a short-lived duplex composed of the mature miRNA and a complementary fragment of the pre-miRNA called miRNA* (Lee et al. 2003). The guide strand of the duplex, which represents the 18-25 nt long mature miRNA gets loaded onto the miRNA-induced silencing complex (miRISC) while the miRNA* is released and degraded (figure 7A). The miRISC complex is similar to that used for the RNA interference (RNAi) pathway. It contains a member of the Argonaute protein family at the core and serves by identifying target sequences based on near-perfect complementarity between the miRNA and targeted mRNA (Bartel 2004; Hutvagner and Zamore 2002; Hammond et al. 2001).

With the RISC, miRNAs exert their function on target genes which is facilitated by one of two mechanisms on a post-transcriptional level (figure 7B). They can either lead to cleavage of the targeted mRNA or lead to the repression of mRNA translation. Interestingly, the choice of which mechanism is applied is dependent on the complementarity to the target: translation is repressed if the complementarity is not sufficient for cleavage but a suitable constellation of complementary sequences is recognized (Hutvagner and Zamore 2002; Zeng, Yi, and Cullen 2003). Consequently, protein levels of targeted genes are significantly decreased while mRNA levels remain unchanged. MiRNAs primarily bind to sequences in the 3' UTR of their target genes (Lim et al. 2005; Huntzinger

and Izaurralde 2011). This binding and consequent cleavage or translational repression is facilitated by the so-called seed region of the miRNA which incorporates nucleotides 2-8 at the 5' of the miRNA (figure 7B) (Ellwanger et al. 2011). This seed region needs to fit perfectly to the targeted sequence whereas mismatches in the rest of the miRNA-mRNA duplex are tolerated and probably determine the mechanism of action, as described (Hutvagner and Zamore 2002; Zeng, Yi, and Cullen 2003).

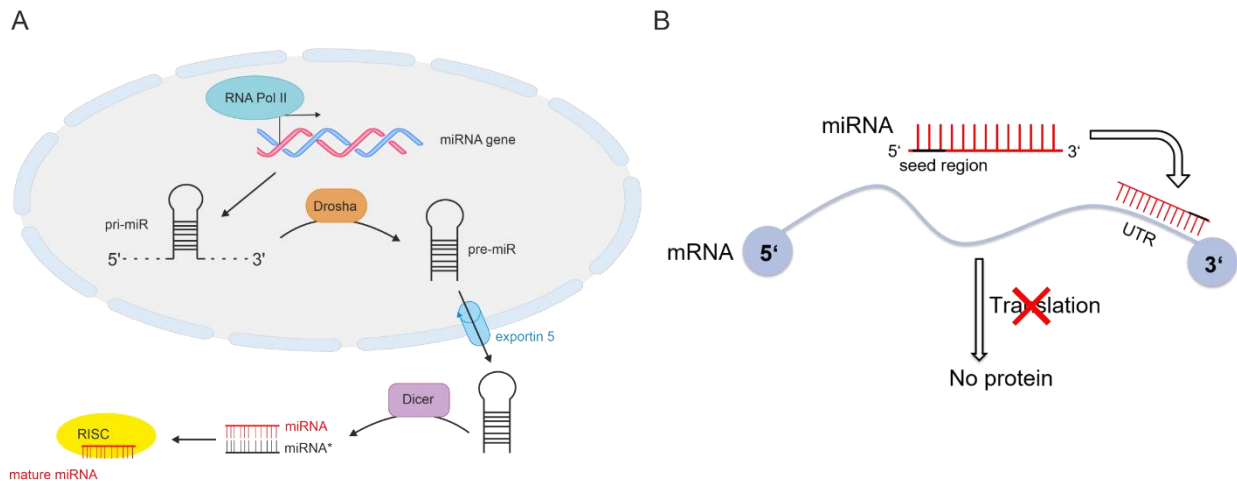


Figure 7: Biogenesis and function of miRNAs. (A) The miRNA gene is transcribed by RNA Polymerase II and then undergoes several maturation steps and one export step before the mature miRNA is loaded onto the RISC complex exerting the function. (B) Scheme of miRNA function. MiRNAs attach with their short seed region to the 3' UTR of the targeted mRNA and lead either to degradation of the mRNA or to repression of translation. In both cases, no protein results from the targeted gene. Abbreviations: miRNA, micro RNA; mRNA, messenger RNA; RISC, RNA induced silencing complex; RNA Pol II, RNA Polymerase II; pri-miR, primary miRNA; pre-miR, preliminary miRNA; UTR, untranslated region

MiRNAs can be differentially expressed at different stages of development or in different regions, which was for example shown for the mammalian brain (Krichevsky et al. 2003). Furthermore, due to the shortness of the seed region, one miRNA can recognize multiple sequences and therefore regulate multiple target genes. Conversely, one target gene can be regulated by different miRNAs which may in some cases compensate for the low abundance of miRNAs as opposed to targeted mRNA. Indeed, the synergistic effect of miRNAs has been shown to be implicated in different processes including human embryonic stem cell differentiation and murine adult neurogenesis (Sahu and Mallick 2018; Lemus-Diaz et al. 2017; Pons-Espinal et al. 2017). In the latter study, they did not only demonstrate that miRNAs are essential for favoring the generation of new neurons over the generation of astrocytes but could also identify eleven distinct miRNAs that influence this fate choice by aNSCs (Pons-Espinal et al. 2017). An intriguing hypothesis about general miRNA function on a cellular level is the idea that they might not be primarily target-specific regulators but rather buffer out transcription fluctuations and in this way maintain a stable gene expression (Ebert and Sharp 2012; O'Brien et al. 2018).

One example of an extensively studied miRNA in neurogenesis is miR-9 which is expressed at high levels in the developing and adult brain in vertebrates (Coolen, Katz, and Bally-Cuif 2013). In embryonic

mice, overexpression of *miR-9* resulted in reduced NSC proliferation while a knockdown increased proliferation (Zhao et al. 2009; Lang and Shi 2012). Also in the developing fish it was shown that *dre-miR-9* drives progenitor commitment but also inhibits antagonistic factors leading to the opposite effect. This shows that *dre-miR-9* has a context-dependent function in the developing zebrafish brain which can probably be extrapolated to the function of all miRNAs (Coolen et al. 2012; Coolen, Katz, and Bally-Cuif 2013).

Therefore, miRNA mediated gene regulation is highly complex and the specific pathways by which they regulate adult neurogenesis in the zebrafish are not well studied yet. In an effort to characterize the role of miRNAs in zebrafish adult neurogenesis, sequencing of small RNAs and their expression changes in response to injury, based on lesioned and unlesioned telencephalic tissue was conducted. During this small RNA sequencing experiment, 184 miRNAs were detected in the transcriptome of the adult zebrafish telencephalon, 31 of which were deregulated after injury (Gourain et al. 2021). The resulting question is which role these miRNAs play in the GRN controlling adult NSC behavior.

1.9.2 Tackling the challenge of miRNA detection in the zebrafish adult brain tissue

The knowledge of exact miRNA localization, together with their concentration and the level of the targeted mRNA is important. However, visualization of those short and low abundant molecules in zebrafish adult brain tissue is challenging. Advanced imaging techniques would greatly impact the field as tracing the origin and movement of single miRNAs and/or miRNA-mRNA interaction with high temporal resolution as its offered by single molecule detection, would help to understand these complex dynamics (O'Brien et al. 2018). Using fluorescent *in situ* hybridization (FISH), a method where RNA molecules are recognized by a specific complementary probe and then visualized via fluorescence is one method to tackle the challenge of miRNA detection in the adult zebrafish brain.

The development and employment of fluorescent highly specific probes constitutes a substantial proportion of this thesis and was considered a promising approach to decipher the role of the identified deregulated miRNAs in adult neurogenesis. These probes were developed in collaboration with organic chemists from the group of Prof. Dr. Hans-Achim Wagenknecht at the Institute of organic chemistry at the KIT in the so called "FISH in fish project". The specific synthesis and functionality of these probes will be explained in detail in a later chapter but for miRNA detection, firstly a set of ssDNA probes (f-FISH probes) and then a set of locked nucleic acid (LNA) (l-FISH probes) were developed. Furthermore, with the goal of single molecule detection, another set of probes, based on a different method was developed and resulted in m-FISH probes, which are ssDNA probes against specific mRNAs.

The FISH probes offer a set of advantages compared to classically used RNA probes: (1) they are time-saving as there is no need to apply and incubate primary and secondary antibodies. In all the developed

FISH probes, the fluorophore is directly attached to the probe. (2) The probes are specifically synthesized against the miRNAs or mRNAs of interest and can be tailored to all needs also by exchanging fluorophores. (3) The ssDNA probes and especially the LNA probes are more stable than classical RNA probes and therefore easier to handle and to transport between facilities. This stability, especially with respect to temperature makes them also suitable for detection of low-abundant and short molecules like miRNAs or eRNAs. (4) Synthesis of all the probes is faster and leads to less waste of chemicals and materials as the need to clone a cDNA sequence into a vector to consequently make RNA is erased. Therefore, the probes are also cost-effective. (5) Additionally, reports about more intense fluorescent signals generated by ssDNA probes in contrast to RNA probes make them promising probes for the detection of low abundant molecules (Hannon et al. 1993).

A combination of those FISH probes was envisioned to aid with decoding miRNA-mRNA interactions in the adult zebrafish brain which are a substantial part of the GRN that regulates adult neurogenesis.

1.10 Aim of this thesis

The balance between quiescent and activated NSCs is crucial during adult brain homeostasis but also in response to neuronal loss due to injury or disease where the need to form new neurons is acutely given. In the zebrafish brain, with its remarkable regenerative ability, a shift from quiescent to activated states is just as important as a shift back to the quiescent state in order to maintain the NSC pool. A complex gene regulatory network is the basis for the balance between the two states and needs to be precisely controlled in a temporal and spatial manner. Therefore, the aim of this thesis was to identify key molecules and pathways embedded in this GRN which is controlling the balance between the two NSC states.

The gene *mdka* was characterized regarding its cellular expression pattern in the zebrafish adult brain and investigated for its regulation and function during zebrafish adult neurogenesis. Furthermore, imaging techniques for the identification of short miRNA molecules and mRNA molecules of genes implied in regulating neurogenesis have been developed and tested for their functionality in the adult brain tissue.

Hopefully, my thesis can be a reference for further studies of the GRN controlling NSC behavior in the adult zebrafish telencephalon and can provide tools and new approaches to decipher the regulation, function and identity of key regulators in the GRN. The identification of key molecules and pathways could provide groundwork to develop specific drugs and in order to effectively impact the symptoms following neuronal loss in the humans CNS.

2 Material and Methods

2.1 Material

2.1.1 Bacterial Strains

The chemically competent *E. coli* strains XL-1 Blue from Promega and TOP10 from ThermoFisher were used for all cloning in this work.

2.1.2 Chemicals

Table 1: List of chemicals used in this thesis

Name	Supplier
1-phenyl-2Tricaine	Sigma-Aldrich, Taufkirchen, Germany
4',6-diamidino-2-phenylindole (DAPI)	Sigma-Aldrich, Taufkirchen, Germany
Agarose	Peqlab, Erlangen, Germany
Ampicillin	Carl Roth GmbH + Co. KG; Karlsruhe, Germany
Anti-Digoxigenin-POD (poly), Fab fragments	Roche, Mannheim, Germany
Anti-DNP-HRP	Perkin Elmer, Waltham, USA
BCIP	Perkin Elmer, Waltham, USA
Bovine Serum Albumin (BSA)	Sigma-Aldrich, Taufkirchen, Germany
Calcium chloride (CaCl ₂)	Sigma-Aldrich, Taufkirchen, Germany
Citric Acid	Carl Roth GmbH + Co. KG; Karlsruhe, Germany
Chloroform	VWR International GmbH, Darmstadt, Germany
Dextran sulfate sodium salt	Sigma-Aldrich, Taufkirchen, Germany
Dimethylformamide	Carl Roth GmbH + Co. KG; Karlsruhe, Germany
Dimethylsulfoxide (DMSO)	Carl Roth GmbH + Co. KG; Karlsruhe, Germany
DMH1	Tocris, Bristol, UK)
DNA- Ladder GeneRuler (mix)	ThermoFisher Scientific, Schwerte, Germany
dnTPs	Promega, Mannheim, Germany
Ethanol (EtOH)	Carl Roth GmbH + Co. KG; Karlsruhe, Germany
Ethylene diaminetetra acetic acid (EDTA)	Carl Roth GmbH + Co. KG; Karlsruhe, Germany
Ethidiumbromide	Carl Roth GmbH + Co. KG; Karlsruhe, Germany
Fast Green FCF	Sigma-Aldrich, Taufkirchen, Germany
Formamide	VWR International GmbH, Darmstadt, Germany
Gylogen	ThermoFisher Scientific, Schwerte, Germany
Heparin	Sigma-Aldrich, Taufkirchen, Germany
HEPES	Carl Roth GmbH + Co. KG; Karlsruhe, Germany
Hydrogen peroxide (H ₂ O ₂)	VWR International GmbH, Darmstadt, Germany
iMDK	Tocris, Bio-Techne GmbH, Wiesbaden, Germany
Isopropanol	Carl Roth GmbH + Co. KG; Karlsruhe, Germany
IWR-1	Sigma-Aldrich, Taufkirchen, Germany
Kanamycin	Sigma-Aldrich, Taufkirchen, Germany
Kaliumchloride (KCl)	Sigma-Aldrich, Taufkirchen, Germany
Kaliumhydroxide (KOH)	Carl Roth GmbH + Co. KG; Karlsruhe, Germany
LY411575	Sigma-Aldrich, Taufkirchen, Germany
Magnesium chloride (MgCl ₂)	Carl Roth GmbH + Co. KG; Karlsruhe, Germany
Magnesium sulphate (MgSO ₄)	Sigma-Aldrich, Taufkirchen, Germany
Methanol (MeOH)	Carl Roth GmbH + Co. KG; Karlsruhe, Germany

NBT	Perkin Elmer, Waltham, USA
Paraformaldehyde	Merck, Darmstadt, Germany
Phosphate buffered saline (PBS)	Life Technologies GmbH, Darmstadt, Germany
Phenol red	Carl Roth GmbH + Co. KG; Karlsruhe, Germany
Sheep Serum	Merck, Darmstadt, Germany
Sodium Chloride (NaCl)	Carl Roth GmbH + Co. KG; Karlsruhe, Germany
Spectinomycin	Sigma-Aldrich, Taufkirchen, Germany
Sucrose	VWR International GmbH, Darmstadt, Germany
Tris-base	Carl Roth GmbH + Co. KG; Karlsruhe, Germany
Tris-HCl	Carl Roth GmbH + Co. KG; Karlsruhe, Germany
Trizol	ThermoFisher Scientific, Schwerte, Germany
Tween-20	Carl Roth GmbH + Co. KG; Karlsruhe, Germany

2.1.3 Enzymes

Table 2: List of enzymes used in this thesis

Name	Manufacturer
BamHI	New England Biolabs, Frankfurt am Main, Germany
GoTaq™ DNA Polymerase	Promega, Mannheim, Germany
LR Clonase II	Gateway™ LR Clonase™ II Enzyme mix
NcoI	New England Biolabs, Frankfurt am Main, Germany
Proteinase K	Carl Roth GmbH + Co. KG; Karlsruhe, Germany
Ribonuclease RNasin® RNase Inhibitor	Promega, Mannheim, Germany
RNase free DNase	Promega, Mannheim, Germany
Shrimp Alkaline Phosphatase (SAP)	New England Biolabs, Frankfurt am Main, Germany
SP6 RNA Polymerase	Promega, Mannheim, Germany
T4 DNA Ligase	Promega, Mannheim, Germany
T7 RNA Polymerase	Promega, Mannheim, Germany
XbaI	New England Biolabs, Frankfurt am Main, Germany
XhoI	New England Biolabs, Frankfurt am Main, Germany

2.1.4 Equipment and tools

Table 3: List of equipment and tools used in this thesis

	Name	Manufacturer
Bacteria Incubator	Shaker Innova® 44	Heraeus, Hanau, Germany
Centrifuge	5810 R	Eppendorf, Hamburg, Germany
Coverslips	Precision cover glasses Menzel Gläser	Paul Marienfeld GmbH & Co KG, Lauda- Königshofen, Germany ThermoFisher Scientific, Schwerte, Germany
Forceps for dissection	Fine Tip No. 5	Dumont, Switzerland
Glass slides for microscopy		Lab Nord, France
Gel Chamber	Easycast B2	ThermoFisher Scientific, Schwerte, Germany
Falcon tubes		Greiner, Nürtingen, Germany
Microinjector	FemtoJet	Eppendorf, Hamburg, Germany
Gas microinjector	MINJ-1	Tritech research, California, USA
Heating Block	SBH200D/3	Stuart, Chelmsford, UK
Incubator for fish embryos	Kendro UB6760	Heraeus, Hanau, Germany

Microloader tips		Eppendorf, Hamburg, Germany
Microcentrifuge	5430 R	Eppendorf, Hamburg, Germany
Microcentrifuge tubes	Safe Lock tubes	Eppendorf, Hamburg, Germany
Microtome	Vibratome VT1000	Leica AG, Wetzlar, Germany
Mounting Medium	Aqua Polymount	Polysciences, Pennsylvania, USA
Multitank recirculation system for fish		Schwarz Ltd., Germany
NanoDrop	ND-1000	Peqlab, Erlangen, Germany
Needle puller	Flaming/ Brown Needle Puller Model P-97	Sutter Instruments, USA
Parafilm		Sigma-Aldrich, Taufkirchen, Germany
PCR Thermocycler	Mastercycler Nexus Gradient	Eppendorf, Hamburg, Germany
Petri dishes		Greiner, Nürtingen, Germany
Pipettes	Pipetman	Gilson, USA
Pipette tips		Corning, Corning, UK
Pipettor	PipetBoy Acu 2	INTEGRA Biosciences Inc., Biebertal, Germany
RT-qPCR system	ABI StepOnePlus	ThermoFisher, Scientific, Schwerte, Germany
Syringe Needles	Omnican® 40	Braun, Melsungen, Germany
Vortex Shaker	Top- Mix 11118	ThermoFisher Scientific, Schwerte, Germany

2.1.5 *In situ* hybridization probes

Table 4: Gene names and references for ISH probes used in this thesis

Name	reference
<i>id1</i>	(Diotel et al. 2015)
<i>mdka</i>	this thesis
<i>mdkb</i>	(Winkler and Moon 2001)
<i>ptn</i>	this thesis
<i>pri-miR-9</i>	this thesis
<i>pri-miR-31</i>	this thesis
<i>pri-miR-96</i>	this thesis
<i>pri-miR-146a</i>	this thesis
<i>pri-miR-182</i>	this thesis
<i>pri-miR-183</i>	this thesis
<i>pri-miR-726</i>	this thesis
<i>sox9a</i>	(Diotel et al. 2015)
miRCURY miRNA detection probes: <i>dre-miR-9</i>	QUIAGEN, Hilden, Germany
miRCURY miRNA detection probes: <i>dre-miR-146a</i>	QUIAGEN, Hilden, Germany

2.1.6 Kits

Table 5: List of kits used in this thesis

Name	Supplier
Gateway™ LR Clonase™ II Enzyme mix	ThermoFisher Scientific, Schwerte, Germany
GoTaq qPCR Master	Promega, Mannheim, Germany

Illustra ProbeQuant G-50 Micro Columns	GE Healthcare, Buckinghamshire, UK
Maxima first strand cDNA synthesis kit	ThermoFisher Scientific, Schwerte, Germany
pCR [®] 8/GW/TOPO [®] TA Cloning [®] Kit	ThermoFisher Scientific, Schwerte, Germany
pGEM [®] -T Easy Vector System	Promega, Mannheim, Germany
Quiagen Plasmid Midi Kit	QUIAGEN, Hilden, Germany
Tol2kit	Chien lab, Utah

2.1.7 Microscopes

Table 6: Types of microscopes used for imaging in this thesis

	Name	Manufacturer
Confocal microscope	TCS SP5	Leica AG, Wetzlar, Germany
Compound microscope	DM5000B	Leica AG, Wetzlar, Germany
Fluorescent Stereo Microscope	MZ16 F	Leica AG, Wetzlar, Germany
Stereo Microscope	SMZ645	Nikon, Düsseldorf, Germany
Cameras	DFC320 DFC 300FX	Leica AG, Wetzlar, Germany

2.1.8 Oligonucleotides

All oligonucleotides utilized in this thesis, were purchased from Metabion International AG and designed using ApE or Primer3 web version 4.1.0.

Table 7: List of oligonucleotides used in this thesis

Primer name	Sequence (5'-3')	Notes
<i>β-actin</i> fw	GCCTGACGGACAGGTCAT	Primers for the <i>β-actin</i> housekeeping gene, used for RT-qPCR
<i>β-actin</i> rev	ACCGCA AGATTCCATACCC	
CRM2 fw	ACCTCCGTCACCTGTGCTA	Primers encompassing the putative enhancer region CRM2, used for amplification from gDNA
CRM2 rev	ACGTGATCAGGCCCAACTTA	
CRM3 fw	TCCTGAAGAACCCAAGACCC	Primers encompassing the putative enhancer region CRM3, used for PCR amplification from gDNA
CRM3 rev	ACACACACACATGCGCTTAA	
CRM5 fw	AAAGCCTACCCGTCTTTGGA	Primers encompassing the putative enhancer region CRM5, used for PCR amplification from gDNA
CRM5 rev	TTCGACGTTGAAGAGAGCCT	
CRM6 fw	CTAGTGCAGGGTTTCGCAACC	Primers encompassing the putative enhancer region CRM6, used for PCR amplification from gDNA
CRM6 rev	CCTGTTTGAAGCCACTCAAGTCT	
<i>mdka</i> fw	CGACACAGAAAACAAAATGCGGG	Primers for the <i>mdka</i> gene, used for RT-qPCR
<i>mdka</i> rev	TAGAGCCACTCCGCACAGTC	
<i>mdka</i> fw XhoI	GCGCTCGAGGCCACCATGCGGGG CCTGTTTTCCACCTC	Primers to amplify the <i>mdka</i> coding sequence from the pCS2 plasmid, used for subsequent restriction enzyme digest with XhoI and NcoI
<i>mdka</i> rev NcoI	GCGCCATGGCAGGGCCGGGATTCT CCTCCACGTCACCGC	
<i>pri-miR-9</i> fw	CTGGTTGGATGGAAATGGAC	Primers encompassing the genetic region of <i>dre-miR-9</i> , used for PCR amplification from gDNA
<i>pri-miR-9</i> rev	ACTTGGGAGGGAAAAGAGGA	

<i>pri-miR-31</i> <i>fw</i>	AAAACCAATAGCGGGTTTGA	Primers encompassing the genetic region of <i>dre-miR-31</i> , used for PCR amplification from gDNA
<i>pri-miR-31</i> <i>rev</i>	GGCTCCAGACTGAAGGTTTG	
<i>pri-miR-96</i> <i>fw</i>	CATTGCTATTGCCGGAGTCT	Primers encompassing the genetic region of <i>dre-miR-96</i> , used for PCR amplification from gDNA
<i>pri-miR-96</i> <i>rev</i>	CAAAGGTGCAGTTGCTTTCA	
<i>pri-miR-146a</i> <i>fw</i>	TGCGGAGAAACACCTATGAA	Primers encompassing the genetic region of <i>dre-miR-146a</i> , used for PCR amplification from gDNA
<i>pri-miR-146a</i> <i>rev</i>	CTCAAACGAGTCATGGCAAA	
<i>pri-miR-182</i> <i>fw</i>	TTGCCCAAAAATACGTTGCT	Primers encompassing the genetic region of <i>dre-miR-182</i> , used for PCR amplification from gDNA
<i>pri-miR-182</i> <i>rev</i>	CGGAGCTTGTGACATCATTG	
<i>pri-miR-183</i> <i>fw</i>	TGCGTTTCCTTCTCACTCTC	Primers encompassing the genetic region of <i>dre-miR-183</i> , used for PCR amplification from gDNA
<i>pri-miR-183</i> <i>rev</i>	TGTGCTAGTGCCAAAACAGG	
<i>pri-miR-726</i> <i>fw</i>	AGTGGAGCAGGAGGAAGTGA	Primers encompassing the genetic region of <i>dre-miR-726</i> , used for PCR amplification from gDNA
<i>pri-miR-726</i> <i>rev</i>	CAAAGGTGCAGTTGCTTTCA	

2.1.9 Plasmids

Table 8: List of plasmids used in this thesis, including antibiotic resistance and references

Name	Resistance	Reference
pCS2P-mdk1	Ampicillin	Christoph Winkler, National University of Singapore
pCS2Zmk-2	Ampicillin	(Winkler and Moon 2001)
p3E-polyA	Kanamycin	Tol2 kit Chien lab, Utah
p5E-CMVSP6	Kanamycin	Adapted from Tol2 kit Chien lab, Utah
pDESTTol2pA2	Ampicillin	Tol2 kit Chien lab, Utah
pGEM®-T Easy Vector	Ampicillin	Promega, Mannheim, Germany
pME-eGFP	Kanamycin	Tol2 kit Chien lab, Utah
pME-MCS	Kanamycin	Tol2 kit Chien lab, Utah
pME-mdkaT2AeGFP	Kanamycin	this thesis
TOPO® Vector	Spectinomycin	pCR®8/GW/TOPO® TA Cloning® kit, ThermoFisher

T2KHGpzGATA2 C1 destination vector	Ampicillin	(Navratilova et al. 2009)
------------------------------------	------------	---------------------------

2.1.10 Primary Antibodies

Table 9: Names, host species and applied dilutions for primary antibodies used in this thesis

Name	Host species	Supplier	Dilution
Anti- GFP	chicken	Aves labs, Davis, USA	1:1000
Anti- PCNA	mouse	Agilent, Santa Clara, USA	1:500
Anti- S100 β	rabbit	Agilent, Santa Clara, USA	1:400
Anti- HuC/D	rabbit	Abcam, Cambridge, UK	1:400

2.1.11 Secondary Antibodies

Table 10: Specification, host species and employed dilutions for Alexa conjugated secondary antibodies used in this thesis

Name	Host species	Supplier	Dilution
Anti-chicken A488	goat	Invitrogen, Carlsbad, USA	1:1000
Anti-rabbit A488	goat	Invitrogen, Carlsbad, USA	1:800
Anti-rabbit A633	goat	Invitrogen, Carlsbad, USA	1:1000
Anti-mouse A546	donkey	Invitrogen, Carlsbad, USA	1:1000

2.1.12 Software and online sources

Table 11: List of software and online tools used in this thesis

Name	Description	Source
ApE	Plasmid editor	Wayne Davis from the University of Utah
CorelDRAW® Graphics Suite 2021	Used for figure configuration	Corel Corporation, Ottawa, Canada
Fiji	Imaging Software	Open Source Software
Graph Pad Prism 5	Used for quantifications and statistical analysis	GraphPad Software Inc., La Jolla, USA
Primer3 version 4.1.0	Online tool to design PCR primers	http://primer3.ut.ee/
miRBase	Online database of published miRNA sequences and annotations	https://mirbase.org/
TargetScanFish 6.2	Online tool to identify putative targets of miRNAs in zebrafish, based on sequence comparison	http://www.targetscan.org/fish_62/
UCSC Genome Browser	Online tool offering genome sequence data and annotation of genes	https://genome.ucsc.edu/
DANIO-CODE Track Hub	Track hub for UCSC genome browser, integrated under “public hubs”	DANIO-CODE: Central repository for zebrafish genomic datasets
ATAC seq	ATAC seq track hub of lesioned and unlesioned telencephala,	https://raw.githubusercontent.com/arvincfs/KIT_Regeneration/main/Regeneration_ATAC_CyVerse/hub.txt ,

	integrated in the UCSC genome browser under “my hubs”	unpublished data from collaborative work of the Rastegar and Müller labs
--	---	--

2.1.13 Solutions and buffers

If not specified otherwise, all solutions were prepared with deionized water and stored at room temperature (RT).

Table 12: List of solutions and buffers used in this thesis

	Recipe (final concentration)
20x SSC-Buffer	3 M NaCl, 0.3 M sodium citrate
3% H ₂ O ₂ in PBS	4.5 ml 1x PBS; 500 µl 30% H ₂ O ₂
4% Paraformaldehyde	4 g in 100 ml
0.2x SSCT	500 µl 20x SSC, 500 µl 10% Tween-20, 49 ml H ₂ O
1x SSCT	2.5 ml 20x SSC, 500 µl 10% Tween-20, 47 ml H ₂ O
5x SSCT	12.5 ml 20x SSC, 500 µl 10% Tween-20, 37 ml H ₂ O
10% Tween-20	5 ml Tween-20, 45 ml H ₂ O
0.002% H ₂ O ₂ in PTW	15 ml PTW, 1 µl 30% H ₂ O ₂
Antibody Blocking solution, 16 ml	300 µl Sheep Serum, 1 ml 10% BSA, 15 ml PTW
BCIP stock solution	50 mg/ml in Dimethylformamide, stored at -20°C
Blocking Buffer, 50ml	5 ml 10x PBS, 0.5 ml 10% Tween- 20, 1 ml 10% BSA, 0.5 ml DMSO, filled up to 50 ml with H ₂ O, stored at 4°C
CellTracker™ CMTPX Dye stock solution	10 mM stock, Thermo Fisher Scientific, stored at -20°C
CutSmart buffer	10x, New England Biolabs, stored at -20°C
DMH1 stock solution	10 mM in DMSO, stored at -20°C
E3 medium (60x)	5 mM NaCl, 0.17 mM KCl, 10 mM HEPES, 0.33 mM MgSO ₄ , 0.33 mM CaCl ₂
GoTaq™ Reaction Buffer	10x, Promega, stored at -20°C
Hybridization (HYB) Buffer, 50 ml	25 ml Formamide, 12.5 ml 20x SSC, 2.5 ml Yeast t-RNA (100 mg/ml), 50 µl Heparin (50 mg/ml), 0.5 ml 10% Tween- 20, filled up to 50 ml with H ₂ O , stored at -20°C
Hybridization solution for FISH, 10 ml	1 ml Formamide, 1 g Dextran sulfate, 20 µl 10% BSA, 50 µl yeast tRNA, 1 ml 20x SSC, filled up to 10 ml with H ₂ O, stored at -20°C
iMDK stock solution	10 mM in DMSO, stored at -20°C
IWR-1 stock solution	10 mM in DMSO, stored at -20°C
KOH solution (50x)	1.25 M KOH, 10 mM EDTA; stored at 4°C
LB Medium with Antibiotics, 500ml	50 ml 10x LB stock, 450 ml water, 500 µl Ampicillin/ Spectinomycin/ Kanamycin
LY411575 stock solution	10 mM in DMSO, stored at -20°C
NBT stock solution	50 mg/ml in Dimethylformamide, stored at -20°C
Neutralization buffer (50x)	315.2 g/l; stored at 4°C
Pronase solution	0.01 g/ml Pronase in E3 medium; stored at -20°C
Proteinase K stock solution	10 mg/ml Proteinase K in PTW, stored at -20°C
Proteinase K solution	10 µg/ml Proteinase K in PTW
PTW, 1 l	1 l 1x PBS, 1ml 10% Tween-20

Perkin blocking buffer	0.1 M Tris-HCl pH 7.5, 0.15 M NaCl, 0.5% v/v Tween20, 0.5% Blocking Powder (PerkinElmer tyramide Kit), stored at -20°C
RNase free water	Invitrogen, Carlsbad, USA
Staining buffer, 25 ml	2.5 ml Tris (pH 9,5, 1 M), 1.25 ml MgCl ₂ (1 M), 0.5 ml NaCl (5 M), 0.25 ml 10% Tween- 20, filled up to 25 ml with H ₂ O
Staining solution	3.5 µl NBT, 3.5 µl BCIP, 1 ml staining buffer
T4 Ligase buffer	New England Biolabs, Frankfurt am Main, Germany, stored at -20°C
TAE buffer pH 7.8	40 mM TRIS- Base, 1 mM EDTA, 5 mM Acetic Acid
TE buffer	10 mM Tris-HCl pH 8.0, 1 mM EDTA
Tricaine	0,4%, stored at -20°C
Tyramide Cy3 solution	300 µl 0.002% H ₂ O ₂ PTW, 1.2 µl tyramide Cy3
Tyramide Cy5 solution	300 µl 0.002% H ₂ O ₂ PTW, 1.2 µl tyramide Cy5
Washbuffer 1	50% formamide/ 50% 2x SSC, 0.1% Tween- 20
Washbuffer 2	2x SSC, 0.1% Tween- 20
Washbuffer 3	0.2x SSC, 0.1% Tween- 20
Washbuffer 4	0.2x SSC, 0.1% Tween- 20, 50% PTW
Washing solution for FISH, 50 ml	5 ml Formamide, 5 ml 20x SSC, 500 µl 10% Tween- 20, 39.5 ml H ₂ O

2.1.14 Zebrafish lines

Table 13: Zebrafish lines used in this study

Name	Allele	Description	Reference
<i>Tg(id1-CRM2:GFP)</i>	ka713	labels qRGCs in the telencephalon with GFP	(Zhang et al. 2020)

2.2 Methods

2.2.1 Zebrafish husbandry

All zebrafish stocks were maintained in the European Zebrafish Research Center (EZRC) in an aquarium system equipped with recirculation (system by Aqua Schwarz, Germany). The system works as follows: 5%-20% fresh fish water per day flows continuously into the fish tanks and is collected by an overflow system. Impurities like feces, ammonia and nitrite are removed by filtering the water through a biological filter system and pumping it back into the water reservoir, which is exposed to UV light to reduce pathogens. Water conditions are assessed every day and the optimal conditions include a temperature of 26°C to 29°C, a pH of 6.9-8.5, conductivity of 250-600 µs, nitrate at less than 2.5 mg/l and nitrite at less than 0.025 mg/l. Approximately 5 fish are kept per 1 l of water but higher densities are usually tolerated without imposing stress on the animals. The fish are kept under a 14 hour light-10 hour dark cycle.

The crossing was performed in 1 l laying cages, filled with system water, containing one couple or more per cage. The cages contained an insert with a grid at the bottom through which the eggs will fall into a compartment below that cannot be reached by the parents to prevent cannibalism. The laying starts with the onset of light in the facility the morning after the crossing. The eggs were then collected, transferred into petri dishes, cleaned and used for experiments.

Experiments were performed on 8-12 month old AB wild-type (WT) or *Tg(id1-CRM2:GFP)* zebrafish. All animal experiments were carried out in accordance with the German protection standards and were approved by the Government of Baden-Württemberg, Regierungspräsidium Karlsruhe, Germany.

2.2.2 Genomic DNA extraction from zebrafish embryos

Genomic DNA (gDNA) was obtained from 5 dpf old embryos as follows: Embryos were individually placed into PCR tubes and 75 µl of KOH solution was added. Afterwards the tubes were incubated for 20 minutes in the Thermocycler at 94°C and subsequently cooled to RT. 75 µl of Neutralization buffer was added and mixed thoroughly. The extracted gDNA was stored at 4°C.

2.2.3 Constructs and synthesis of antisense RNA DIG probes

The following antisense digoxigenin (DIG) or dinitrophenyl (DNP)-labeled probes were used: *id1*, *mdka*, *mdkb*, *ptn*, *pri-miR-9*, *pri-miR-31*, *pri-miR-146a*, *pri-miR-182*, *pri-miR-183* and *pri-miR-726*. The *pcs2+* plasmids containing either *mdka* or *mdkb* cDNA were kindly provided by Christoph Winkler, National University of Singapore. For *ptn* a sequence of about 600 nucleotides (nt) located in the 3'UTR of the gene was PCR amplified from cDNA using a specifically designed primer pair and GoTaq DNA Polymerase (primer sequences see table 7). For all pri-miRNA probes a stretch of 200-300 nt

encompassing the mature sequence was PCR amplified from gDNA using GoTaq DNA Polymerase (primer sequences see table 7). Consequently, the PCR product was cloned into the pGEM-Teasy vector system and used for probe synthesis.

For probe synthesis, 1 µg of the plasmid was linearized for 30 minutes at 37 °C using the appropriate restriction enzyme. After deactivation of the restriction enzyme for 5 minutes at 80 °C, the linearized plasmid was used for in vitro transcription with the DIG/DNP labeling mix and RNA polymerase. The mixture was incubated for 3 h at 37 °C. Afterwards, the reaction was stopped by adding 0.2 M EDTA (pH8) and purified using the ProbeQuant G50 Micro column kit. The probe was then diluted 1:1 using hybridization buffer and stored at -20 °C (Schmidt et al. 2014).

2.2.4 Agarose gel electrophoresis

For size and quality check, as well as the separation of DNA fragments, agarose gel electrophoresis was performed with 1% to 3% agarose gels. For visualization of the DNA on a UV-transilluminator, 1-3 µl of a 100% ethidium bromide solution was added in 100 ml dissolved agarose. Before loading, the samples were supplemented with loading buffer and the electrophoresis carried out in TAE electrophoretic buffer with about 120 V. An appropriate DNA marker (DNA ladder) was loaded in parallel for determining the size of the DNA samples.

2.2.5 ISH/FISH on embryos

Fixation of embryos

Zebrafish embryos at the desired stage were fixed overnight at 4°C in 4% PFA. After removal of the PFA, the embryos were washed 2 times with PTW before dehydration an ascending Methanol series by incubation in 25%, 50% and 25% methanol in 1 time PBS for 5 minutes each. 100% Methanol was added as a last step before storage at -20°C.

Hybridization of probe

Embryos were re-hydrated in a descending methanol series, by incubation in 75%, 50% and 25% methanol in 1 time PBS for 5 minutes each. Afterwards, embryos were digested with Proteinase K in PTW buffer for 5 minutes for 24 hpf old embryos and immediately re-fixed in 4% PFA for 20 minutes at 4°C. Then embryos were washed 3 times for 5 minutes in PTW. In the case of FISH, embryos were treated with 1% H₂O₂ in PTW for 1 hour before being washed again 3 times for 5 minutes in PTW. After pre-incubation in Hyb buffer for 3 hours at 70°C, embryos were incubated with probes diluted 1:200 in Hybridization buffer overnight at 70°C. The next day the embryos were washed 2 times for 30 minutes in washbuffer 1, once for 15 minutes in washbuffer 2, 2 times for 30 minutes in washbuffer 3 and once for 5 minutes in washbuffer 4 at 70°C to remove not hybridized probes. The embryos were then washed 5 minutes in PTW at RT.

Blocking of unspecific binding sites and anti-DIG incubation

Embryos were washed, incubated for 2 hours at RT in blocking buffer and afterwards treated overnight at 4°C with an anti- DIG-alkaline phosphatase (AP) dilution of 1:4000 in blocking buffer for ISH or an anti-DIG-peroxidase (POD) 1:200 dilution in blocking buffer for FISH.

Staining

The next day embryos were washed 5 times for 15 minutes in PTW. In the case of ISH the embryos were afterwards washed 2 times for 10 minutes in staining buffer. Next, the embryos were stained with NBT/BCIP in staining buffer. At the desired staining intensity, the embryos were repeatedly washed with PTW at RT to stop staining. In the case of FISH, the embryos were rinsed 2 times for 10 minutes in 0.002% H₂O₂ in PTW. Afterwards, 150 µl of tyramide-Cy3 staining solution was added and incubated for 1 hour at RT in the dark. After staining, embryos were washed 3 times for 5 minutes in PTW at RT and the signal checked under the microscope.

2.2.6 Stab wound assay

The procedure was performed as described in (März et al. 2011; Schmidt et al. 2014). In brief, to inflict an injury to the telencephalon, fish were first anesthetized with tricaine. Then a syringe needle was inserted vertically through the skull into the left hemisphere of the telencephalon, so the right hemisphere would serve as an unlesioned control hemisphere (figure 8). For recovery fish were kept in tanks with fresh fish water and taken out for dissection at significant time points after the lesion.

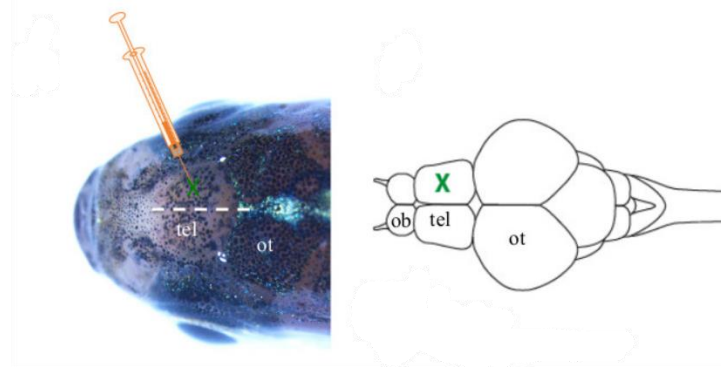


Figure 8: Graphic representation of the stab wound assay on adult zebrafish. Adapted from (Schmidt et al. 2014). A syringe needle is inserted through the skull of the adult zebrafish (left) into one hemisphere of the telencephalon. This creates a lesion in one hemisphere while the other hemisphere can serve as an unlesioned control (right).

2.2.7 Preparation of adult zebrafish brains

Dissection and Fixation of brains

Before dissection, fish were anesthetized with tricaine and then euthanized in ice water. Afterwards the heads were removed and fixed overnight in 4% Paraformaldehyde in PTW at 4°C. The next day the brains were dissected from the skull and stored in 100% methanol overnight at -20°C.

Embedding of brains in Agarose

Brains were rehydrated through a descending methanol series, by incubation in 75%, 50% and 25% methanol in 1 time PBS for 5 minutes each. Afterwards, they were washed with PTW and embedded in 2% agarose in 1 time PBS so that the dorsal side was oriented upwards. For *in situ* hybridization, brains were hybridized with corresponding DIG or DNP probes before sectioning.

Sectioning

Embedded brains were cut transversally with a vibratome into sections of 50 µm thickness. The resulting sections were collected into the wells of 24- well plate, filled with 1 ml of blocking buffer.

Mounting

Adult brain sections treated with ISH, FISH or LNA ISH were mounted on glass slides using Aqua- Poly/ Mount. Fluorescently labeled brain sections were covered with glass coverslips of 0.17 mm thickness and ISH brain sections with glass coverslips of 0.13-0.16 mm thickness. Mounted sections were stored at 4°C.

2.2.8 ISH on adult brain sections

Hybridization of DIG labeled RNA probes

Brains were prepared as described under 2.2.7 before hybridization. Before embedding, the brains were washed 5 times in PTW for 5 minutes and digested with Proteinase K for 30 minutes before being re- fixed in 4% PFA for 20 minutes. In the next step the brains were washed 5 times for 5 minutes in PTW. Then the brains were rinsed with hybridization (HYB) buffer and incubated in fresh HYB buffer for 4 hours at 70°C. The DIG probes were diluted 1:200 in HYB buffer and 500 µl of that mixture was added to the brains and incubated overnight at 70°C. The next day the brains were washed 2 times for 30 minutes in washbuffer 1, once for 15 minutes in washbuffer 2, 2 times for 30 minutes in washbuffer 3 and once for 5 minutes in washbuffer 4 at 70°C to remove not hybridized probes. The brains were washed 5 minutes in PTW at RT and afterwards embedded and sectioned, as described under 2.2.7.

Blocking of unspecific binding sites and anti-DIG incubation

Brain sections were washed, incubated for 1 hour at RT in blocking buffer and afterwards treated overnight at 4°C with an anti- DIG-alkaline phosphatase (AP) dilution of 1:4000 in blocking buffer.

Staining

The next day sections were washed 5 times for 15 minutes in PTW and afterwards 2 times for 10 minutes in staining buffer. Next, the brains were stained with NBT/BCIP in staining buffer. At the desired staining intensity, the brains were repeatedly washed with PTW at RT to stop staining.

Brain sections were mounted as described under 2.2.7.

2.2.9 FISH on adult brain sections

Hybridization of DIG labeled RNA probes

Brains were prepared as described under 2.2.7 before hybridization. Before embedding, the brains were washed 4 times in PTW for 5 minutes and incubated in 1 ml of 3% H₂O₂ in PBS. Afterwards, they were washed once in PTW for 5 minutes and digested with Proteinase K for 30 minutes before being re-fixed in BT-Fix for 20 minutes. In the next step the brains were washed 5 times for 5 minutes in PTW. Then the brains were rinsed with hybridization (HYB) buffer and incubated in fresh HYB buffer for 4 hours at 70°C. The DIG probes were diluted 1:200 in HYB buffer and 500 µl of that mixture was added to the brains and incubated overnight at 70°C. The next day the brains were washed 2 times for 30 minutes in washbuffer 1, once for 15 minutes in washbuffer 2, 2 times for 30 minutes in washbuffer 3 and once for 5 minutes in washbuffer 4 at 70°C to remove not hybridized probes. The brains were washed 5 minutes in PTW at room temperature and afterwards embedded and sectioned, as described under 2.2.7.

Blocking of unspecific binding sites and anti-DIG incubation

Brain sections were washed, incubated for 1 hour at room temperature in blocking buffer and afterwards treated overnight at 4°C with an anti- DIG Peroxidase (POD) dilution of 1:400 in blocking buffer.

Staining

The next day sections were washed 5 times for 15 minutes in PTW and afterwards 2 times for 10 minutes in 0.002% H₂O₂ PTW solution. In the next step 300 µl of tyramide- Cy3 solution was added to the sections and incubated for 60 minutes at room temperature in the dark. Then the sections were washed 3 times for 5 minutes in PTW and checked for signal under the Stereo Microscope. In the case of co- staining with Immunohistochemistry, brains were further treated as described under 2.2.11.

2.2.10 Double FISH on adult brain sections

Hybridization of DIG and DNP labeled RNA probes

Brains were prepared and washed as described under 2.2.7. After pre-incubation 500 µl of a 1:200 dilution of each DNP and DIG probe was incubated simultaneously overnight at 70°C with the brains.

Blocking of unspecific binding sites and anti-DNP incubation

The next day, brain sections were washed, incubated for 1 hour at room temperature in Perkin blocking buffer and afterwards treated overnight at 4°C with an anti-DNP-horseradish peroxidase (HRP) dilution of 1:200 in Perkin blocking buffer.

1st staining

Sections were washed 5 times for 15 minutes in PTW and afterwards 2 times for 10 minutes in 0.002% H₂O₂ PTW solution. In the next step, 300 µl of tyramide- Cy3 solution was added to the sections and incubated for 60 minutes at room temperature in the dark. Then the sections were washed 3 times for 5 minutes in PTW and checked for signal under the Stereo Microscope.

Inactivation of the 1st peroxidase and anti-DIG incubation

Sections were washed in 3% H₂O₂ for 2 hours at RT to inactivate HRP. Afterwards sections were washed 5 times for 10 min in PTW and blocked in Perkin blocking buffer for 1 hour. Then a 1:400 dilution of anti-DIG-POD Perkin in blocking buffer was incubated with the brain sections at 4°C overnight.

2nd staining

Sections were washed 5 times for 15 minutes in PTW and afterwards 2 times for 10 minutes in 0.002% H₂O₂ PTW solution. In the next step, 300 µl of tyramide- Cy5 solution was added to the sections and incubated for 60 minutes at room temperature in the dark. Then the sections were washed 3 times for 5 minutes in PTW and checked for signal under the Stereo Microscope.

In the case of co-staining with IHC, brains were further treated as described under 2.2.11.

2.2.11 Immunohistochemistry (IHC) on adult brain sections

Blocking of unspecific binding sites

To prepare for IHC treatment, the sections were incubated in 1 ml of blocking buffer per well, for 1 hour at room temperature.

Addition of primary antibodies

After the blocking buffer was removed, the sections were incubated in 300 µl of blocking buffer containing different primary antibodies overnight at 4°C. Primary antibodies and dilutions are listed in table 9.

Addition of secondary antibodies

The next day, the primary antibody solution was removed and sections were washed 3 times in PTW for 10 minutes each. Afterwards, the sections were incubated with the secondary antibodies in PTW for 2 hours at room temperature and kept in the dark. The secondary antibodies were conjugated with Alexafluor dyes and are listed in table 10. Afterwards, brains were mounted as described under 2.2.7.

2.2.12 miRNA ISH using LNA probes on adult brain sections

Hybridization of LNA probes

Adult brains were prepared as described under 2.2.7. After pre-hybridization, the brains were incubated with 40 nM of the LNA probe diluted in hybridization buffer overnight at the desired temperature. The hybridization temperature was calculated by subtracting 30°C from the manufacturers declared RNA T_m.

Blocking of unspecific binding sites and anti-DIG incubation

The next day, brains were washed in SSCT washing solutions at the hybridization temperature before being washed in PTW for 5 minutes at RT. After embedding and sectioning as described under 2.2.7, sections were blocked for 1 hour at room temperature in antibody blocking solution and afterwards treated overnight at 4°C with an anti-DIG reagent mix.

Staining

Sections were washed and stained as described under 2.2.8.

2.2.13 Imaging

To obtain single-cell resolution images, an HCX PL APO CS x63/1.2NA objective was used with the pinhole size set to 1-airy unit. Fluorescent images for green (GFP), red (PCNA, Cy3), and infrared channels (S100β, HuC/D, Cy5) were acquired sequentially in 16-bit color depth with excitation/emission wavelength combinations of 488 nm/492–550 nm, 561 nm/565–605 nm, and 633 nm/650–740 nm, respectively. Pixel resolution for XY and Z planes are 0.24 μm and 0.50 μm, respectively. For individual brain samples, at least three transverse sections at different anterior-posterior levels representing anterior, posterior and intermediate telencephalic regions were imaged. ISH stained sections were imaged with a stereo microscope.

Transgenic or ISH stained embryos were imaged using a 2% Agarose plate for embedding and a Stereo microscope.

2.2.14 Image analysis

Confocal brain images were opened with Fiji/ImageJ software as composite hyperstack to manually evaluate co-localization of proteins (overexpression experiment) or proteins and expression of the mRNA (FISH with IHC). Cells expressing individual markers or marker combinations were counted in the dorsomedial and the dorsolateral ventricular zones in three transverse sections prepared at different anteroposterior levels of the telencephalon.

2.2.15 RT-qPCR

Total RNA was isolated from adult telencephala using Trizol. First-strand cDNA was synthesized from 1 µg of total RNA with the Maxima First-Strand cDNA synthesis kit according to the manufacturer's protocol. A StepOnePlus Real-Time PCR system and SYBR Green fluorescent dye were used. Expression levels were normalized using *β-actin*. The relative levels of mRNA were calculated using the $2^{-\Delta\Delta CT}$ method. The primer sequences are listed in table 7. Experiments were performed with at least 3 technical replicates, each time with RNA pooled from 3 WT brains.

2.2.16 Quantification / Statistical analysis

For the quantification of proliferating NSCs, the number of type I and type II cells expressing *mdka* or the number of cells expressing the *Tg(id1-CRM2:gfp)* transgene and *mdka* was counted in 1 µm steps of 50 µm-thick z-stacks (imaged with a 63x objective). Three sections per brain from at least three individuals were analyzed. Comparisons between two data sets, from quantification of proliferating NSCs or RT-qPCR, were performed by Welch two-sample *t*-test.

2.2.17 Overexpression construct cloning

For the overexpression construct, *mdka* was PCR amplified from the *pcs2+ mdka* plasmid with specific primers adding a T2A and a restriction site for XhoI at the 5' and a restriction site for NcoI at the 3'. Afterwards the PCR product was digested with these enzymes. Simultaneously, eGFP was digested from the pMEEGfp (#383, Tol2 kit from the Chien lab) with NcoI and XbaI. pME-MCS (#237) was digested with XhoI and XbaI and afterwards incubated with Shrimp Alkaline Phosphatase (SAP) for 1 hour at 37°C to avoid self-ligation. The *mdka* and EGFP fragments were then ligated into the pME-MCS using T4 ligase overnight at 4°C. The plasmid was partly sequenced to verify correct integration of the inserts. Via Gateway recombination using LR clonase II and 20 fmol of the constructed pME-mdkaT2AEgfp, 20 fmol of p5E-CMVSP6 (#382) and 20 fmol of p3E-polyA (#302), all parts were cloned into the destination vector containing Tol2 sites for integration into the genome pDESTTol2pA2 (#394). The ligation was performed overnight at RT.

2.2.18 Cerebroventricular microinjection

The procedure was performed as described in (Kizil and Brand 2011; Kizil et al. 2013). Injection solutions were prepared by diluting the plasmid DNA to 1 µg/µl with distilled water. Additionally, 1 µl Fast Green was added for better visibility and tracing of the solution in the skull and filled up with water to a final volume of 10 µl. After fish were anesthetized with Ethyl-3-aminobenzoate methanesulfonate (tricaine) a syringe needle (30G) was inserted into the skull to create a hole at the

telencephalic-diencephalic junction (figure 9). The injection solution was injected into the ventricle with a glass capillary using a Microinjector and stereo microscope.

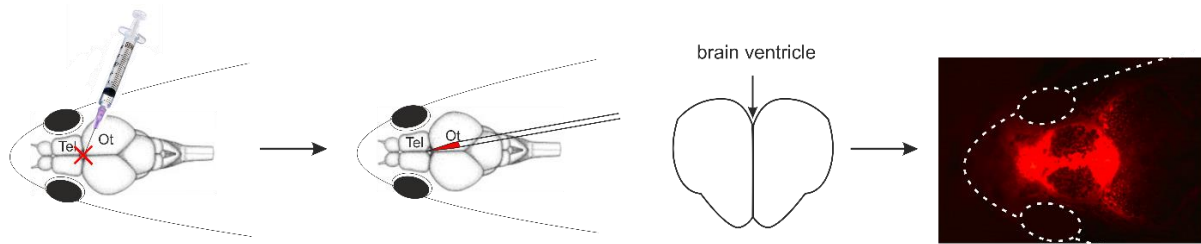


Figure 9: Schematic depiction of the ventricle injection into adult zebrafish. After creating a hole in the skull, a glass capillary containing the injection solution is inserted into the ventricle. After successful injection, the liquid disperses throughout the ventricle reaching all cells covering the surface of the telencephalon as depicted here with CellTracker™ (red).

2.2.19 Drug treatment

For treatment with the inhibitors DMH1, LY411575, IWR-1, iMDK and the control compound DMSO, WT fish were separated into couples. A 600 ml beaker was filled with 300 ml of fresh fish water and 300 μ l of a 10 mM stock solution of DMH1 (final concentration 10 μ M), 300 μ l of a 10 μ M stock solution of LY411575 (final concentration 10 μ M), 300 μ l of a 10 μ M stock solution of IWR-1 (final concentration 10 μ M) or 300 μ l of a 10 mM iMDK stock solution (final concentration 10 μ M) was added. For the control with DMSO 300 μ l of DMSO was added to 300 ml of fresh fish water. A pair of fish was added and the beaker sealed with perforated Parafilm to provide oxygen flow. Every morning the fish were fed with regular adult fish food and the inhibitor or DMSO solution was changed every two days. For analysis of telencephalic lesion, fish removed from the solution for a stab wound assay on the third day of treatment as described under 2.2.6 and then transferred back to freshly prepared solution. After 5 days after the injury, fish were sacrificed.

2.2.20 Identification of putative CRMs and construction of CRM expression plasmids

Identification of putative CRMs for the gene *mdka* was based on ATAC sequencing from lesioned and unlesioned telencephalic hemispheres (sources in table 11). Genomic coordinates of putative CRMs chosen to test for regulatory potential were PCR-amplified using Taq-Polymerase from zebrafish genomic DNA. Amplicons were subcloned into pCR8/GW/TOPO to create entry vectors for subsequent cloning into the Tol2-eGFPdestination vector pT2KHGpzGATA2C1 as described in (Navratilova et al. 2009). All plasmids were partly sequenced to verify the correct integration of the insert. These constructs were used to generate stable zebrafish transgenic lines.

2.2.21 Microinjection into zebrafish embryos

For the generation of transgenic fish 50 ng/μl plasmid DNA was used to assay reporter gene activity. The injection solution was prepared by diluting the plasmid DNA to the desired concentration in distilled water. Additionally, 1% of phenol red and 30 ng/μl *Tol2* mRNA was added and filled up with water to a final volume of 10 μl. Phenol red served as a color marker to distinguish injected from uninjected embryos. The *tol2* mRNA is translated to a Tol2 transposase element in the embryo, mediating the insertion of DNA into the genome. If the DNA insertion occurs early enough, resulting germ cells will have the insertions and are transmitted with higher probability to the F1-generation (Kawakami 2007).

DNA Microinjection experiments were performed using a gas- driven Microinjector system and Stereo Microscopes. Microinjection needles were prepared from borosilicate glass capillaries (0.85 mm inner and 1.0 mm outer diameter) on a Flaming- Brown needle puller. Needles were filled with 5 μl of injection solution. After injection the embryos were incubated at 28°C until they reached the desired stage.

Injected embryos were examined under a fluorescent stereo Microscope and pictures were taken at 24 hpf. Injected embryos expressing EGFP were selected and raised to adulthood. At about 3 mpf (months post fertilization) they were crossed to wild- type fish. F1 embryos were again observed under a fluorescent stereo microscope at 24 hpf and selected for a unique expression pattern.

2.2.22 FISH using I-FISH, m-FISH and f-FISH probes

Probes were synthesized according to the methods described in the dissertations of Larissa Doll, Fabian Lang and Julian Gebhard, IOC, KIT.

For FISH, sections were immediately after sectioning washed with hybridization solution for m-FISH probes and Hyb+ buffer for f- and I- FISH probes. After pre-hybridization for 3-4 hours, the probe was added in a 1:6 dilution in hybridization solution and incubated overnight at 72°C in the case of m-FISH probes. F- and I-FISH probes were hybridized overnight at 43°C using 5-50 ng of probe in Hyb+ buffer. On the second day, I- and f-FISH treated sections were washed with a descending SSCT series (5x SSCT, 1x SSCT, 0,2x SSCT) and stained with DAPI (5 μg/ml). m-FISH conjugated brain sections were washed with washing solution at the hybridization temperature and, if needed, treated with IHC. For IHC, the primary antibody was rabbit anti-S100β and the secondary antibody was anti-rabbit Alexa 488.

Brain sections were mounted as described under 2.2.7.

2.2.23 DAPI staining of adult brain sections

DAPI staining was performed by adding 300 μ l of a 1:2000 dilution of DAPI in PTW to free floating brain sections in a well plate. After 20 minutes of shaking in the dark at RT, the sections were washed 3 times for 5 minutes with PTW and mounted as described under 2.2.7.

3 Results

3.1 Role of the gene *mdka* in zebrafish adult neurogenesis

The highly complex GRN underlying neural regeneration in the zebrafish adult telencephalon is dependent on a tight control of gene expression and regulatory elements in order to maintain the balance between activated and quiescent NSCs. The implication of *mdka* in the regulation of regenerative processes in other tissues and organisms and its response to injury by upregulating expression make it an important key factor to be examined regarding its role in this GRN. This is especially supported by the fact that its expression, regulation and function has to date not been investigated in the context of regeneration of the adult telencephalon in zebrafish.

3.1.1 Expression patterns of *mdka* and its family members in the zebrafish embryo

My first aim was to investigate and compare the expression patterns of *mdka*, its zebrafish paralogue *mdkb* and the third family member *ptn* in the embryo. I performed chromogenic *in situ* hybridization (ISH) on 24 hpf embryos using probes against the mRNA of all three genes (figure 10). For *mdka*, strong expression was detected in all major brain regions including the surface of the forebrain, the midbrain and the hindbrain (figure 10A). More specifically, in the midbrain, *mdka* expression was clear in the optic tectum and the cerebellum (figure 10A'). Furthermore, prominent *mdka* expression was observed along the entire length of the neural tube but was absent from the floor plate (figure 10A). For *mdkb*, the expression was detected also mainly in the brain regions but with some differences: *mdkb* was expressed throughout the forebrain, not only on the surface and was missing the strong expression in the cerebellum (figure 10B, B'). Additionally, there was obvious expression in the neural tube which was confined to the dorsal part (figure 10B), confirming the descriptions of expression by (Winkler et al. 2003). Interestingly, *mdka* was also slightly expressed in the eye, where *mdkb* was completely absent (Figure 10A, B). The expression pattern of *ptn* was more different and highly restricted to the anterior part of the fish with no trunk expression (figure 10C). Expression was very strong throughout all brain regions and included also the otic vesicle, which is the future ear, and the eye (figure 10C, C'). In contrast, most of these areas were not stained by chromogenic ISH against *mdka* or *mdkb* (compare figure 10C with 10A and 10B) demonstrating that the expression patterns of all three family members in the embryo overlap in distinct regions but are not entirely similar.

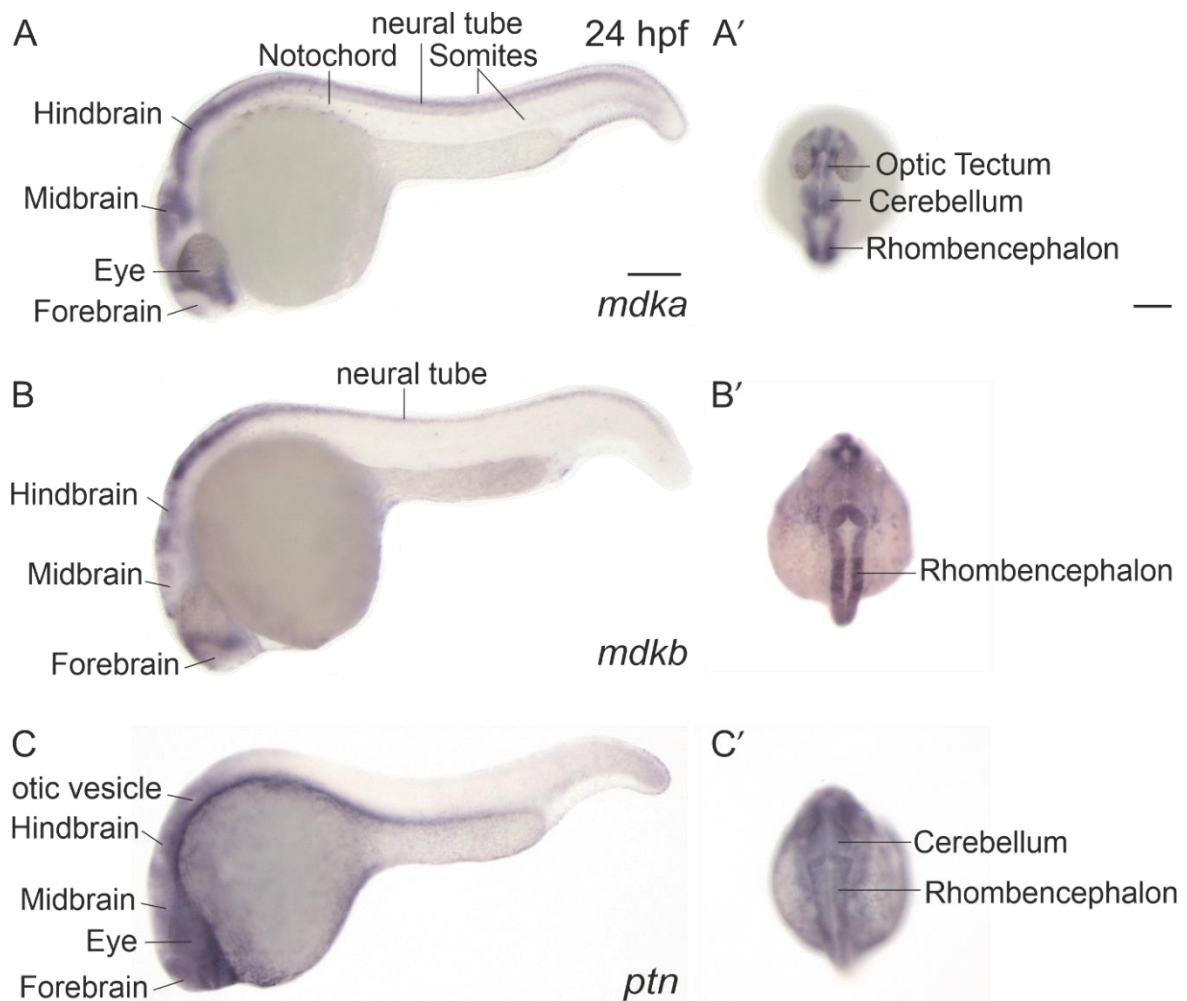


Figure 10: The expression patterns of *mdka*, *mdkb* and *ptn* overlap in the embryo. *In situ* hybridization (ISH) against *mdka* (A), *mdkb* (A) and *ptn* (C) mRNA on 24 hpf embryos. (A, A') Expression of *mdka* was mainly detected in the forebrain, the optic tectum, cerebellum and the hindbrain of the embryo. Additional strong expression was visible in the embryo trunk along the neural tube (A). (B, B') For *mdkb*, expression was also strong throughout all brain areas but very weak in parts of the midbrain. Expression in the neural tube could only be detected in the dorsal part. (C, C') *ptn* expression was observed in the posterior part of the embryo, throughout the brain areas including the eye and otic vesicle. Scale bar = 200 μm in (A, B, C), 100 μm in (A', B', C'). Abbreviations: hpf, hours post fertilization; *mdka*, *midkine a*; *mdkb*, *midkine b*; *ptn*, *pleiotrophin*

3.1.2 Expression patterns of *mdka* and its family members in the zebrafish adult brain

Since the expression patterns of all three family members demonstrated to be overlapping but distinct in the zebrafish embryo, the next question was if this was also the case in the adult zebrafish brain. Subsequently, the next task was to identify the brain regions in which these genes are expressed and explore if the individual expression pattern hints to an involvement with neural regeneration. I again performed chromogenic ISH against the mRNA of *mdka*, *mdkb* and *ptn* but this time on cross-sections of different levels of the zebrafish brain, including one forebrain (telencephalon) section and one anterior and posterior midbrain (diencephalon) section each (figure 11).

In the telencephalon, expression of all three family members was detected along the ventricle of the dorsomedial telencephalon (Dm), between the two telencephalic hemispheres (ventricular zone [Vz]), along the dorsolateral telencephalon (Dl) and in the ventricular layer of the dorsal and ventral nuclei of the ventral telencephalon (Vd and Vv) (black arrows figure 11A, D, G). However, *mdka* was the only one where expression was restricted to the above mentioned areas (figure 11A). *mdkb* and *ptn* additionally showed expression in cells outside of the ventricular layer of the dorsal and ventral telencephalon, inside the dorsal and ventral nuclei of the ventral telencephalon (Vd and Vv) and prominent expression in the central nucleus of the ventral telencephalon (Vc) (black arrows figure 11D, G).

In the anterior part of the diencephalon, strong *mdka* and *mdkb* expression was observed in the periventricular grey zone (PGZ) of the optic tectum (TeO) and the lateral division of the valvula cerebelli (Val) (black arrows figure 11B, E). Additional expression was detected in the caudal zone of the periventricular hypothalamus (Hc) (figure 11B, E). The preglomerular nucleus (PG) and cells surrounding the lateral recess of the diencephalic ventricle (LR) in the periventricular hypothalamus (Hd) also exhibited strong *mdka* expression, which was not as prominent for *mdkb* (figure 11B, E). Instead, *mdkb* expression was detectable in the torus lateralis (TLa) (Figure 11E). Here, the expression pattern of *ptn* was different from the other two family members, exhibiting distinct expression in the superficial and central zone of the TeO and only very weak expression in the PGZ (black arrows figure 11H). However, there was a prominent expression in the diffuse nuclei of the inferior lobe (DIL) (black arrow figure 11H).

Going further through the brain, to the posterior part of the diencephalon, *mdka* expression remained strong in the PGZ and the LR and was also perceived at the periphery of the torus longitudinalis (TL) and at the periphery of the lateral and medial divisions of the valvula cerebelli (Val and Vam) (black arrows figure 11C). In the posterior diencephalon, *mdkb* and *ptn* exhibited similar expression patterns as *mdka* (figure 11F and 11I).

Overall, the expression patterns of all three family members strongly coincided also in the brain but exhibited some differences. Especially *ptn* displayed an expression pattern which was more diverse than those of *mdka* and *mdkb* which is probably due to the fact that *mdka* and *mdkb* are evolutionary closer related to each other than to *ptn* (Winkler et al. 2003). However, the fact that all three are expressed in the Vz, a stem cell niche of the forebrain, suggests an involvement with the regulation of NSC behavior. Nevertheless, since *mdka* was the only family member which showed a higher expression in response to telencephalic lesion in the RNA sequencing experiment, my further investigation was mainly focused on this gene (Gourain et al. 2021).

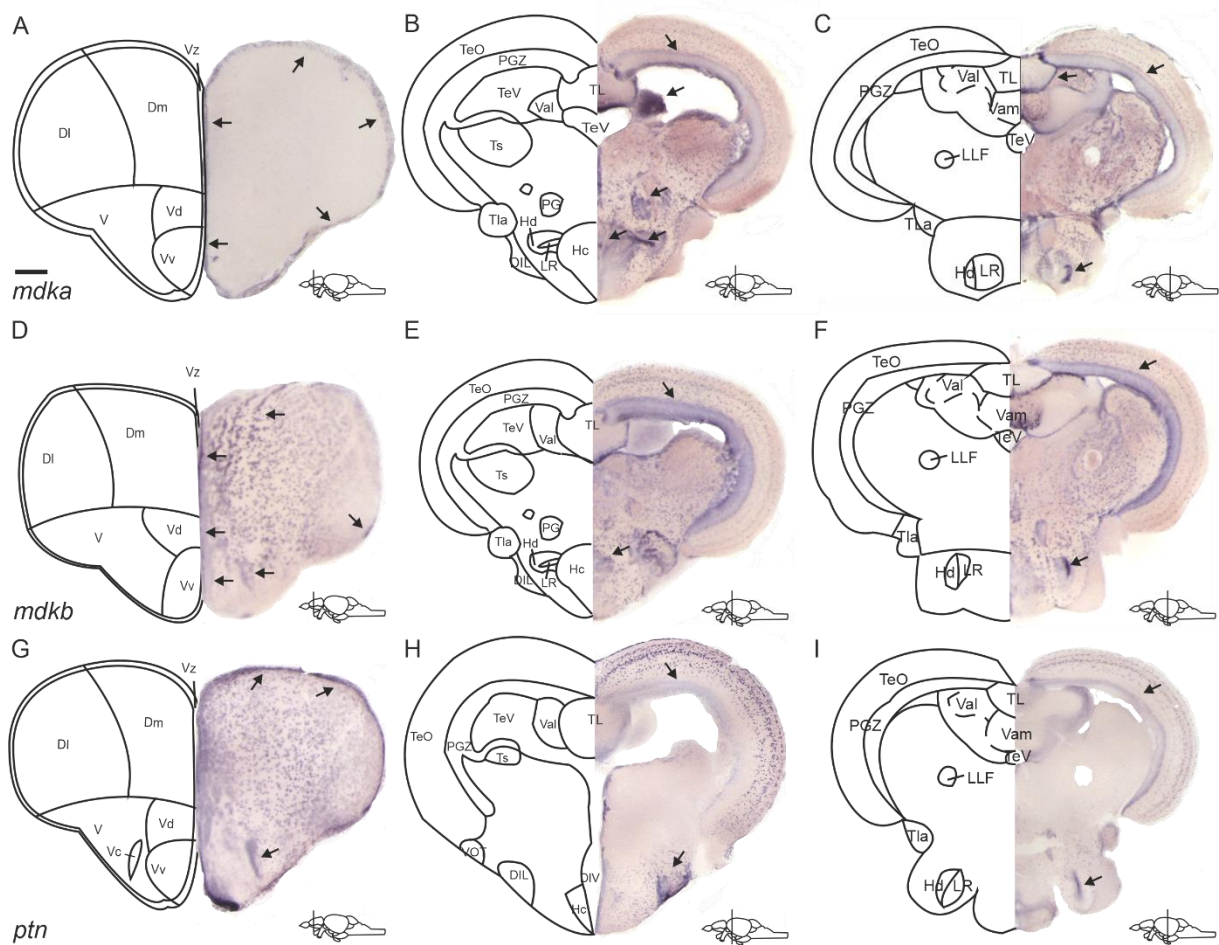


Figure 11: The expression patterns of *mdka*, *mdkb* and *ptn* are overlapping but distinct in the adult zebrafish brain. (A-I) ISH against *mdka* (A-C), *mdkb* (D-F) and *ptn* (G-I) mRNA on cross-sections through the zebrafish adult brain. *mdka* and *mdkb* staining was detected along the ventricle of the dorsal and ventral telencephalic areas (A, D), in the periventricular grey zone of the optic tectum in the posterior diencephalon and in the valvula cerebelli (B, E). In the telencephalon, both *mdkb* and *ptn* showed additional expression outside of the ventricular layers and strong expression in the central nucleus of the ventral telencephalic area (D, G). In the posterior diencephalon, *ptn* expression was strong in the diffuse nuclei of the inferior lobe and distinctively labeling cells in the optic tectum (H) while expression in the periventricular grey zone was weak. Scheme in the lower right-hand corner of (A-I) indicates level of respective cross-section. Scale bar = 100 μ m. Abbreviations: D, dorsal telencephalic area; DI, lateral zone of D; DIL, diffuse nuclei of the inferior lobe; Dm, medial zone of D; Hc, caudal zone of the periventricular hypothalamus; Hd, dorsal zone of the periventricular hypothalamus; LLF, lateral longitudinal fascicle; LR, lateral recess of the diencephalic ventricle; PG, preglomerular nucleus; PGZ, periventricular grey zone of TeO; TeO, optic tectum; TeV, telencephalic ventricle; TL, torus longitudinalis; TLa, torus lateralis; Ts, torus semicircularis; V, ventral telencephalic area; Val, lateral division of the valvula cerebelli; Vam, medial division of the valvula cerebelli; Vc, central nucleus of V; Vd, dorsal nucleus of V; Vv, ventral nucleus of V; Vz, ventricular zone of the telencephalon

3.1.3 *mdka* is expressed in quiescent radial glial cells under constitutive conditions

In order to understand the role of *mdka* during adult neurogenesis in the zebrafish telencephalon, the next step was to identify the cell type in which *mdka* is mainly expressed. For that purpose, I combined fluorescent *in situ* hybridization (FISH) against *mdka* mRNA with Immunohistochemistry (IHC) using

antibodies against the RGC marker S100 β on cross-sections of the zebrafish adult telencephalon (figure 12). Along the ventricle of the dorsomedial telencephalon between the two telencephalic hemispheres and along the dorsolateral telencephalon, *mdka* expression was again prominent (figure 12A, A''', 12B, B'''). Interestingly, it was mainly expressed in S100 β + RGCs (white arrows, figure 12A''', B''', quantification figure 12F) which are type I NSCs. Along the Vz, the signal of the *mdka* mRNA was obviously detected to form a triangle, corresponding to the characteristic triangular shaped cell bodies of the RGCs (figure 12C). Remarkably, along the ventricular layer of the dorsal nucleus of the ventral telencephalic area there was a region lacking *mdka* expression (white arrowheads figure 12A-A'''). This region, called the rostral migratory stream (RMS) is an area with a high amount of committed progenitor cells, called neuroblasts, which have high proliferative potential (März et al. 2010). This suggests that *mdka* is not expressed in proliferative cells. To further confirm that notion, the telencephalic cross-sections were additionally co-stained with an antibody against the proliferation marker PCNA (figure 12A'', B''). As implied, PCNA+ type II cells mainly lacked *mdka* expression (yellow arrows figure 12B-B''', quantification figure 12F). Therefore, the prominent expression of *mdka* in S100 β +/PCNA- cells suggested that this gene is primarily expressed in non-proliferating RGCs which are type I NSCs.

In another approach, I used an anti-HuC/D (Hu) antibody to label post-mitotic neurons and demonstrate the restricted expression of *mdka* to RGCs. There was no co-expression between *mdka* mRNA and the marker HuC/D (white arrows figure 12D-E) confirming the finding that *mdka* is predominantly expressed in RGCs.

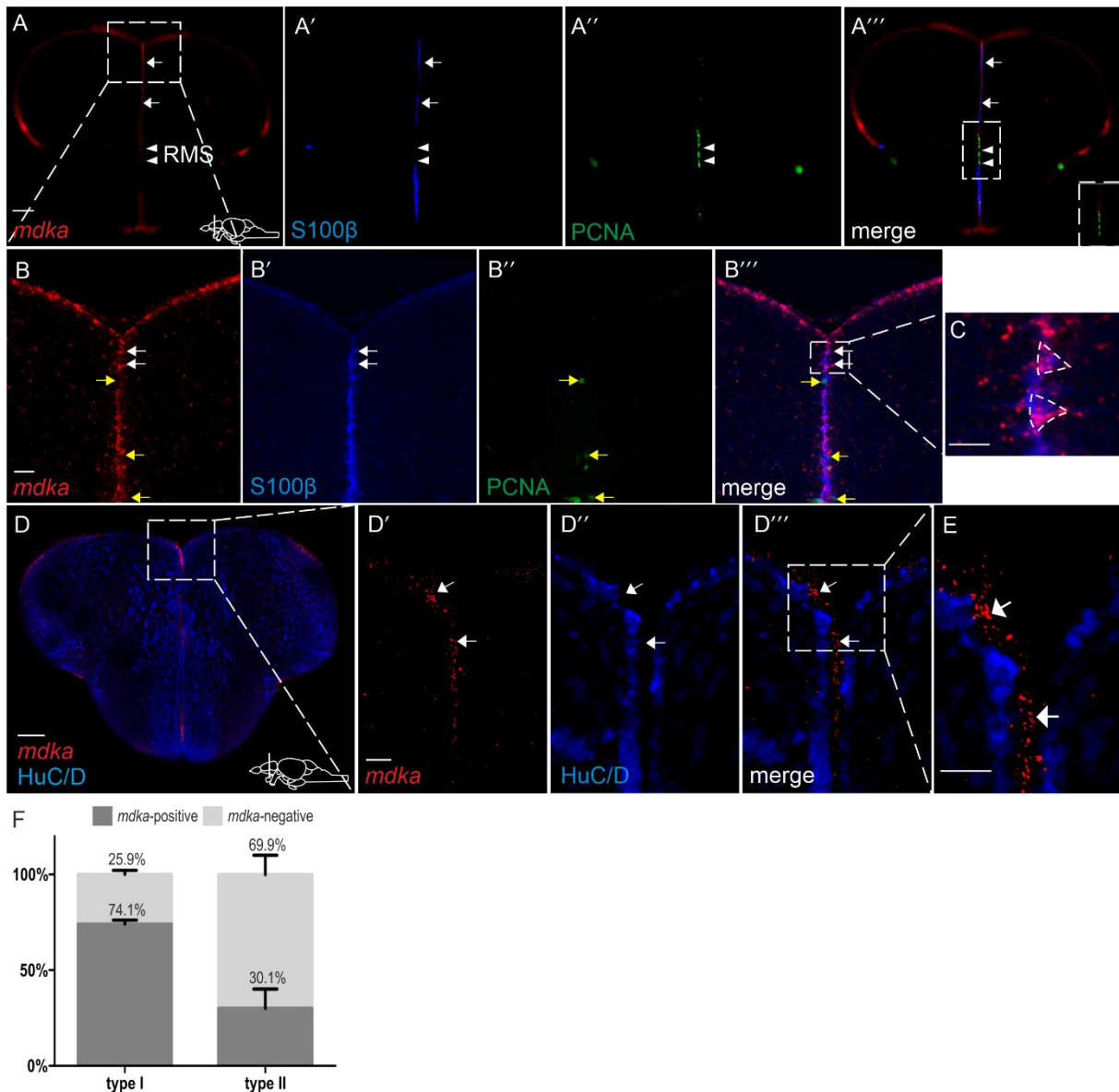


Figure 12: In the adult telencephalon, *mdka* is mainly expressed by quiescent radial glia cells (qRGCs). (A-A''', B-C) Fluorescent *in situ* hybridization (FISH) against *mdka* mRNA (red) combined with Immunohistochemistry (IHC) using antibodies against S100 β (blue) and PCNA (green) on cross-sections of WT telencephala. Expression of *mdka* mRNA was mainly detected in S100 β ⁺/PCNA⁻ cells. White arrows point to *mdka*⁺/S100 β ⁺ cells, yellow arrows indicate *mdka*⁻/PCNA⁺ cells. White arrowheads point to RMS. (A''') inset: magnified view of the RMS demonstrating a lack of *mdka* expression in this area. Boxed-in area in (A) represents area of magnification in (B-B'''). Boxed-in area in (B''') represent area of magnification in (C). Note the characteristic triangular shaped cell body of the RGCs with high expression of *mdka* mRNA. (D-E) FISH against *mdka* mRNA combined with IHC for the neuronal marker HuC/D (blue) indicating no co-localization between the two signals. Boxed-in area in (D) represents area of magnification in (D'-D'''). Boxed in area in (D''') represents area of magnification in (E). White arrows point to *mdka*⁺/HuC/D⁻ cells. (F) Quantification of S100 β ⁺/PCNA⁻ type I cells and S100 β ⁺/PCNA⁺ type II cells expressing *mdka*. Significance is indicated by asterisks: ****p* < 0.001. *n* = 3 brains, 3 sections/brain for quantification. Scheme in the lower right-hand corner of (A, D) indicates level of respective cross-section. Scale bar = 100 μ m (A-A''', D), 20 μ m (B-C, D'-E). Abbreviations: Hu, human neuronal protein; PCNA, proliferating cell nuclear antigen; RMS, rostral migratory stream

3.1.4 *mdka* is co-expressed with the gene *id1*, a marker for qRGCs

In an effort to further prove the previously observed restricted expression of *mdka* to quiescent (qRGCs), single cell sequencing data from Lange et al. (2020) was mined for genes with a high correlation of expression with *id1*, a gene which was previously identified as being a marker specifically for qRGCs (Zhang et al. 2020; Zhang et al. 2021). *mdka* stood out for showing a high correlation with *id1*, with a positive Spearman correlation coefficient, assessing the monotonic relationship between two variables, of 0.28 (p-value =0.07) (Lange et al. 2020). I evaluated this bioinformatics analysis by performing a double FISH against the mRNA of *mdka* and *id1* on adult telencephalon sections (figure 13A-B''). Both genes were highly detectable in the telencephalic ventricle (figure 13A) and showed a high degree of co-expression in individual cells (white arrows figure 13B-B''). Additionally, I used the transgenic zebrafish line *Tg(id1-CRM2:gfp)* which contains a CRM of the *id1* gene (*id1*-CRM2) driving expression of GFP and faithfully reports expression of the endogenous *id1* gene. Therefore, this line can be used to mark qRGCs and further assess the cellular location of *mdka* (Zhang et al. 2020). I again combined FISH against *mdka* mRNA with IHC against GFP and S100 β (figure 13C-E) and found that there is indeed a high expression of *mdka* mRNA in GFP+ cells (white arrows figure 13D-D''). When quantifying these results, co-expression of *mdka* and *id1*-CRM2 was noted for 72.7% of cells (figure 13E), again allocating *mdka* expression to qRGCs. Additionally, in the single cell sequencing experiment, *mdka* was identified as being a marker for the radial glia cell population, confirming the reported observations (Lange et al. 2020). Taken together, these data associate *mdka* expression with qRGCs in two ways: firstly, its mRNA is expressed in S100 β + /PCNA- non-proliferating RGCs and secondly it is highly co-expressed with the qRGC marker *id1*.

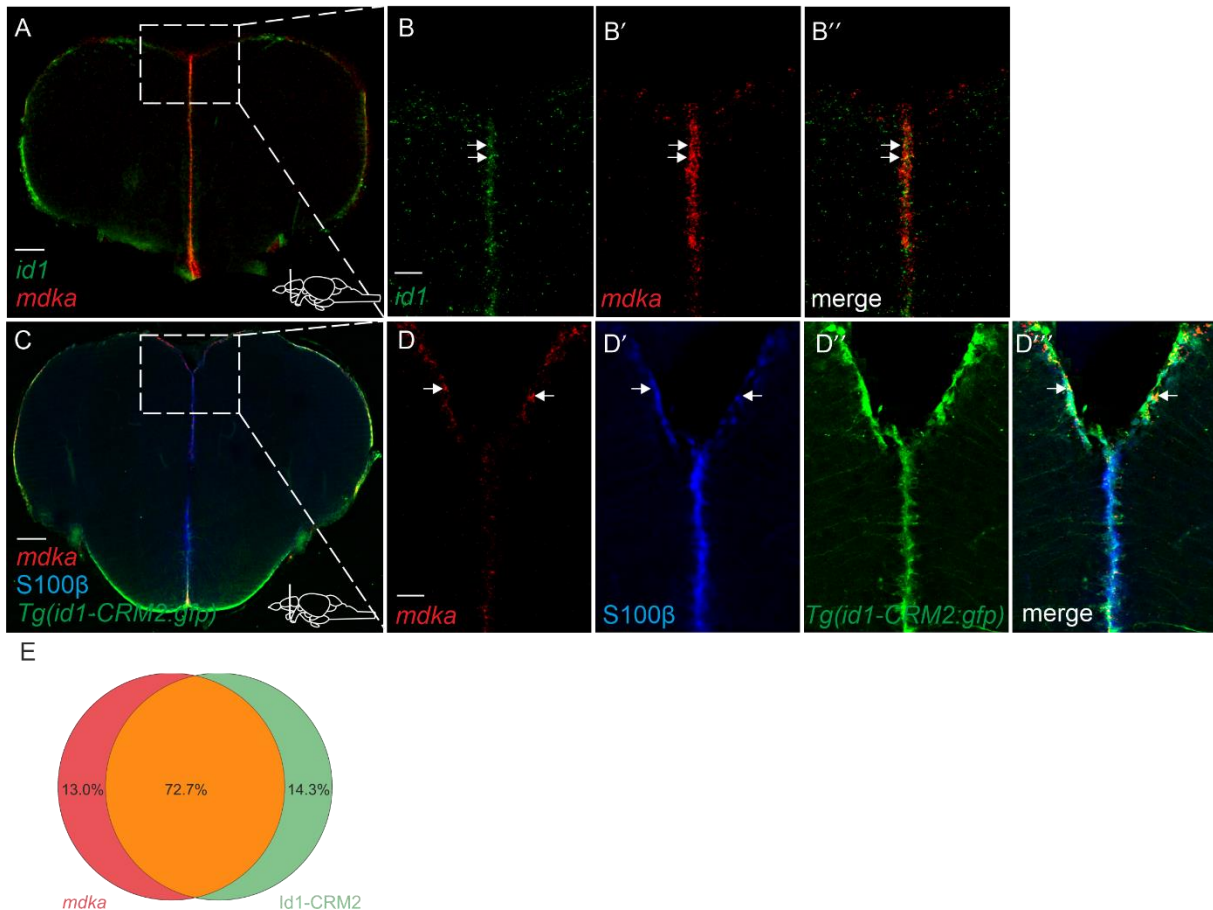


Figure 13: *mdka* is highly co-expressed with the gene *id1* in the adult zebrafish telencephalon. (A-B'') Double FISH with probes directed against the mRNAs of *id1* (green) and *mdka* (red) on cross-sections of WT telencephala. (A) mRNA expression of *id1* and *mdka* was detected in the Vz between the two hemispheres. (B-B'') Both genes are highly co-expressed in the region and in individual cells. White arrows indicate cells co-expressing *id1* and *mdka* mRNA. Boxed-in area in (A) represents area of magnification in (B-B''). (C-D''') FISH with a probe against *mdka* mRNA (red) in combination with IHC against S100β (blue) on cross-sections of telencephala of the *Tg(id1-CRM2:gfp)* transgenic line (GFP, green). There was a high co-localization of *mdka* mRNA with the signal for the *id1-CRM2:gfp* reporter and the marker S100β. White arrows point to *mdka*+/*id1-CRM2*+ cells. Boxed-in area in (C) represents area of magnification in (D-D'''). (E) Quantification of cells expressing *mdka* and the *id1-CRM2* transgene in telencephala of *Tg(id1-CRM2:gfp)* fish. n = 3 brains, 3 sections/brain for quantification. Scheme in the lower right-hand corner of (A, C) indicates level of respective cross-section. Scale bar = 100 μm in (A, C), 20 μm in (B-B'', D-D'''). Abbreviations: CRM, cis-regulatory module; GFP, green fluorescent protein; *id1*, inhibitor of DNA binding 1

3.1.5 *mdka* is upregulated in a delayed fashion after lesion of the adult telencephalon

In order to better understand the role *mdka* plays during neural regeneration in the zebrafish adult telencephalon, a telencephalic lesion was induced by utilizing a stab-wound assay. During this, I inserted a syringe needle through the zebrafish skull into the left telencephalic hemisphere while the fish was under anesthesia in order to trigger regeneration. By keeping the right hemisphere unlesioned, it served as an internal control (Schmidt et al. 2014; März et al. 2011). In a past RNA sequencing experiment comparing the expression levels of different genes between lesioned and

unlesioned telencephalic hemispheres at 5 dpl, *mdka* showed a 1.37-fold increase of expression in the lesioned tissue compared to unlesioned ($p\text{-value} = 2.68^{-9}$) (Gourain et al. 2021). With the intention of confirming and visualizing these findings, I carried out a chromogenic ISH for *mdka* mRNA on telencephalic cross-sections at 5 dpl (figure 14D). Indeed, *mdka* displayed a higher expression in the telencephalic ventricle of the lesioned left hemisphere compared to the unlesioned right hemisphere (black arrows figure 14D) which confirmed the results from the RNA sequencing experiment.

In order to evaluate expression changes at different time points after lesion, as well as identifying a temporal peak of expression, I additionally conducted ISH at 1 dpl, 3 dpl, and 10 dpl. Immediately after inflicting the lesion, at 1 dpl, there was no noticeable difference in the level of *mdka* expression between the lesioned and the unlesioned hemispheres (figure 14B). Also, in comparison to an entirely unlesioned telencephalon, there was no obvious change in expression (compare Figure 14A with figure 14B). At 3 dpl, the change in the *mdka* expression level was already obvious, as it displayed a stronger expression in the Vz of the left lesioned hemisphere (black arrows figure 14C). Nevertheless, the difference between the expression levels in lesioned and unlesioned hemispheres was more significant at 5 dpl (black arrows, compare figure 14C with 14D). A few days after the lesion of the telencephalon, at 10 dpl, the expression level in the lesioned hemisphere reached baseline levels and was not obviously different to the expression level in the unlesioned hemisphere anymore (black arrows figure 14E). For confirmation of these observations, I performed a quantitative reverse transcription PCR (RT-qPCR) experiment where I compared the expression level of *mdka* in lesioned and unlesioned hemispheres at the different time points after lesion (figure 14F). This quantification confirmed that there is a temporal change in the expression level of *mdka* in regard to the days after lesion with a peak of deregulation between 3 and 5 dpl (figure 14F). This observation demonstrated another similarity with the gene *id1*, which also showed a delayed upregulation of expression in response to lesion at 5 dpl (Rodriguez Viales et al. 2015).

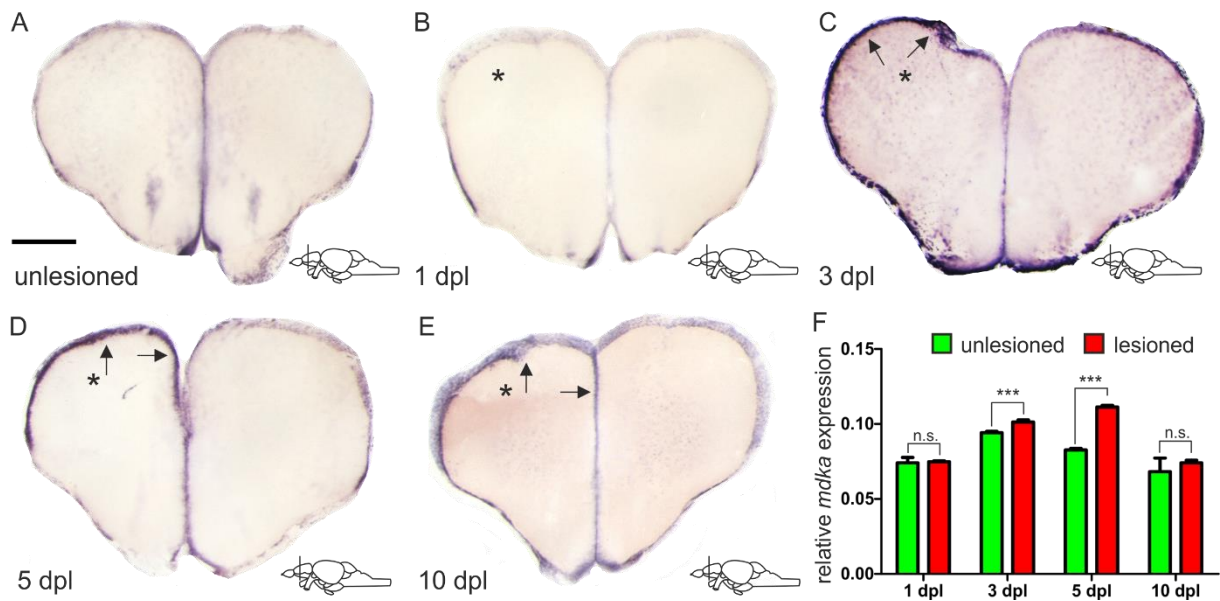


Figure 14: Upregulation of *mdka* expression levels after lesion is dependent on the time elapsed. (A-E) ISH with a probe against *mdka* mRNA on cross-sections of the adult telencephalon in an unlesioned telencephalon (A) and at different time points after the lesion (B-E). (B) Shortly after the lesion, there was no obvious upregulation of *mdka* expression in the lesioned hemisphere. (C-E) Expression of *mdka* in the lesioned hemisphere was increased in comparison to the unlesioned hemisphere at later time points after lesion, displaying a peak of deregulation at 5 dpl (D). (E) At 10 dpl, the expression in the lesioned hemisphere was back to baseline levels. Black arrows point to areas of expression of *mdka* in the Vz of the left lesioned hemisphere. The lesioned hemisphere is marked by an asterisk. (F) RT-qPCR of relative *mdka* expression levels normalized to β -actin expression at different time points after the lesion. Significance is indicated by asterisks: n.s. = not significant, *** $p < 0.001$. $n = 3$ brains/time point for RT-qPCR. Scheme in the lower right-hand corner of (A-E) indicates level of respective cross-section. Scale bar = 100 μ m. Abbreviations: dpl, days post lesion

3.1.6 After lesion of the adult telencephalon, *mdka* expression remains restricted to qRGCs

The next question to be asked was whether there would be change in the cellular location of *mdka* expression after lesion of the adult zebrafish telencephalon. As established earlier, under constitutive conditions *mdka* was predominantly expressed by qRGCs in the zebrafish telencephalon. However, reports in the zebrafish adult retina state that after lesion, under regenerative conditions, *mdka* expression is associated with proliferating stem cells (Calinescu et al. 2009).

To explore the cellular expression pattern of *mdka* in a lesioned telencephalon, I again employed FISH in combination with IHC using antibodies against S100 β and PCNA on telencephalic cross-sections of lesioned WT brains (figure 15). The previously confirmed upregulation of expression of *mdka* in the lesioned hemisphere was also visible in this staining (figure 15A, B). Co-expression of *mdka* occurred mainly with the S100 β staining against RGCs (white arrows figure 15B-B', B'', quantification figure 15G). Cells positive for the proliferation marker PCNA, in large part did not exhibit co-staining for *mdka* mRNA (yellow arrows figure 15B, B''-B''', quantification figure 15G). Additionally when again conducting the FISH experiment on cross-sections of telencephala from the transgenic line *Tg(id1-*

CRM2:gfp) and co-staining with antibodies against GFP and S100 β , I observed a high co-localization of the signal for *mdka* mRNA and the signal for GFP, marking *id1*+ cells (figure 15C-D'''). Indeed, 76.6% of *mdka*+ cells were also expressing the *id1*-CRM2 transgene (figure 15H). Likewise, when conducting a double FISH using probes against *id1* and *mdka* mRNA (figure 15E-F''), I could observe a strong upregulation not only for the *mdka* mRNA (white arrowhead figure 15E and 15F') but also for the *id1* mRNA (white arrowhead figure 15E and 15F) in the lesioned hemisphere and a strong co-localization of the signals for both transcription products in the Vz (white arrows figure 15F-F''). These observations attest that even after lesion of the zebrafish telencephalon, *mdka* expression is primarily associated with qRGCs and highly co-expressed with the qRGC marker *id1* (Zhang et al. 2020; Zhang et al. 2021).

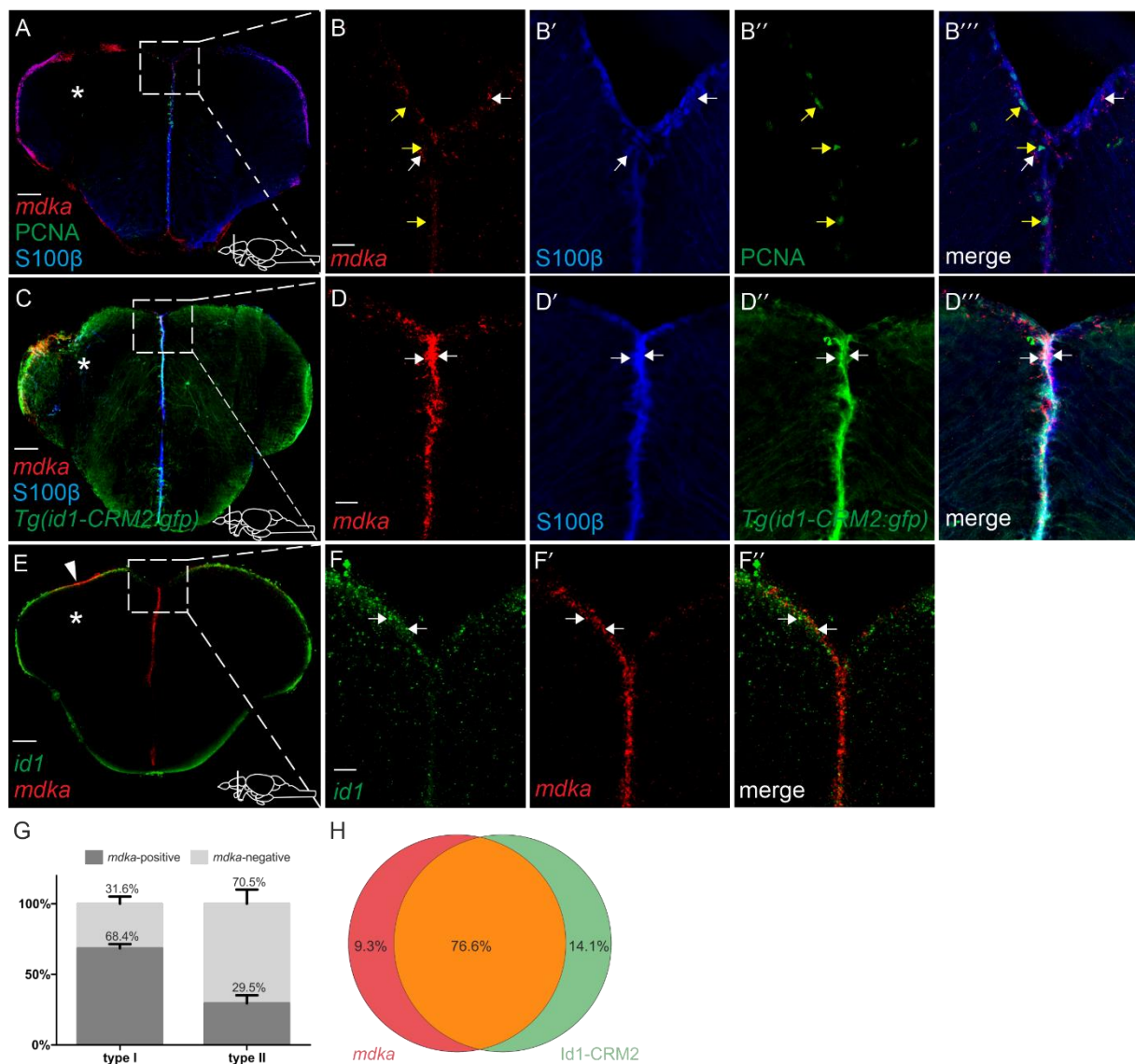


Figure 15: *mdka* expression is associated with qRGCs and *id1* expression after telencephalic lesion. (A-B''') FISH against *mdka* mRNA (red) combined with IHC against S100 β (blue) and PCNA (green) on cross-sections of lesioned WT telencephala at 5 dpl. *mdka* expression is mainly co-localized with the signal for S100 β and remains absent from PCNA+ cells. Boxed-in area in (A) represents area of magnification in (B-B'''). White arrows indicate *mdka*+/S100 β + cells and yellow arrows point to *mdka*-/PCNA+ cells in the Vz. (C-D''') FISH against *mdka* mRNA (red) with IHC using antibodies against S100 β (blue) on

telencephalic cross-sections of the *Tg(id1-CRM2:gfp)* line (GFP, green) at 5 dpl. There was a strong co-localization of *mdka* expression and the signal for the *id1-CRM2* transgene. Note again the characteristically triangular shaped cell bodies of the RGCs expressing S100 β , *mdka* and GFP (D'''). Boxed-in area in (C) represents area of magnification in (D-D'''). White arrows point to *mdka*+/S100 β +/GFP+ cells. (E-F'') Double FISH with probes against *id1* (green) and *mdka* mRNA (red) on cross-sections of WT telencephala at 5 dpl. Both genes displayed an upregulation of expression in the lesioned left hemisphere and a high co-expression in cells located in the Vz (white arrows). The lesioned hemisphere is indicated with an asterisk. (G) Quantification of S100 β +/PCNA- type I and S100 β +/PCNA+ type II cells expressing *mdka* mRNA at 5 dpl. (H) Quantification of cells expressing *mdka* mRNA in telencephala of the *Tg(id1-CRM2:gfp)* transgenic line at 5 dpl. n= 3 brains, 3 sections/brain for quantification. Significance is indicated by asterisks: *** p< 0.001. Scheme in the lower right-hand corner of (A, C, E) indicates level of respective cross-section. Scale bar = 100 μ m (A, C, E), 20 μ m (B-B''', D-D''', F-F'')

3.1.7 Influence of *mdka* overexpression on the proliferative behavior of RGCs

After investigating the cellular expression of *mdka* in the adult zebrafish telencephalon, the next step was to have a closer insight on the function of the gene. The previously observed restricted expression of *mdka* to qRGCs under constitutive and regenerative conditions suggests that it may confer quiescence to RGCs. For the purpose of testing this hypothesis, an *mdka* overexpression construct was created (*CMV:mdka-T2A-EGFP*) which contained the *mdka* coding sequence fused to a self-cleaving peptide T2A and EGFP under the control of a CMV minimal promoter (Hans et al. 2011; Provost, Rhee, and Leach 2007). The functionality of the construct was first validated via injection into zebrafish embryos which were analyzed for EGFP expression. At 24 hpf EGFP expression was visible in a mosaic pattern in the brain and trunk region (data not shown).

Following this validation, the expression construct was injected into the ventricle of the zebrafish brain via cerebroventricular microinjection and transfected into cells lining the telencephalic ventricle. Control brains were transfected with a construct containing EGFP alone (*CMV:EGFP*). At 24 hours post injection (hpi) the fish were euthanized and the proliferative behavior of cells was analyzed via IHC using antibodies against EGFP, S100 β and PCNA (figure 16). In both cases, the transfection of RGCs was successful, indicated by the co-expression of S100 β and EGFP in the cells lining the telencephalic ventricle (figure 16A-F). After injection of the control construct, a number of transfected RGCs also expressed the proliferation marker PCNA in the Vz between the two hemispheres (white arrows figure 16B-B'') and additionally in the Vz of the individual hemisphere (white arrow figure 16C). The same observation was true for the brains transfected with the *mdka* overexpression construct (white arrows figure 16E-F). However, after quantification of cells that co-expressed EGFP, PCNA, S100 β and therefore represented successfully transfected and proliferating RGCs, there was a significant difference in the number of proliferating cells between telencephala transfected with the *mdka* overexpression construct and the control construct (figure 16G). While 47.8% of RGCs transfected with the control construct were also PCNA+, in RGCs transfected with the *mdka* overexpression construct,

the proportion of cells expressing PCNA was reduced to 32.4% (figure 16G). Therefore, overexpression of *mdka* correlated with decreased proliferation of RGCs.

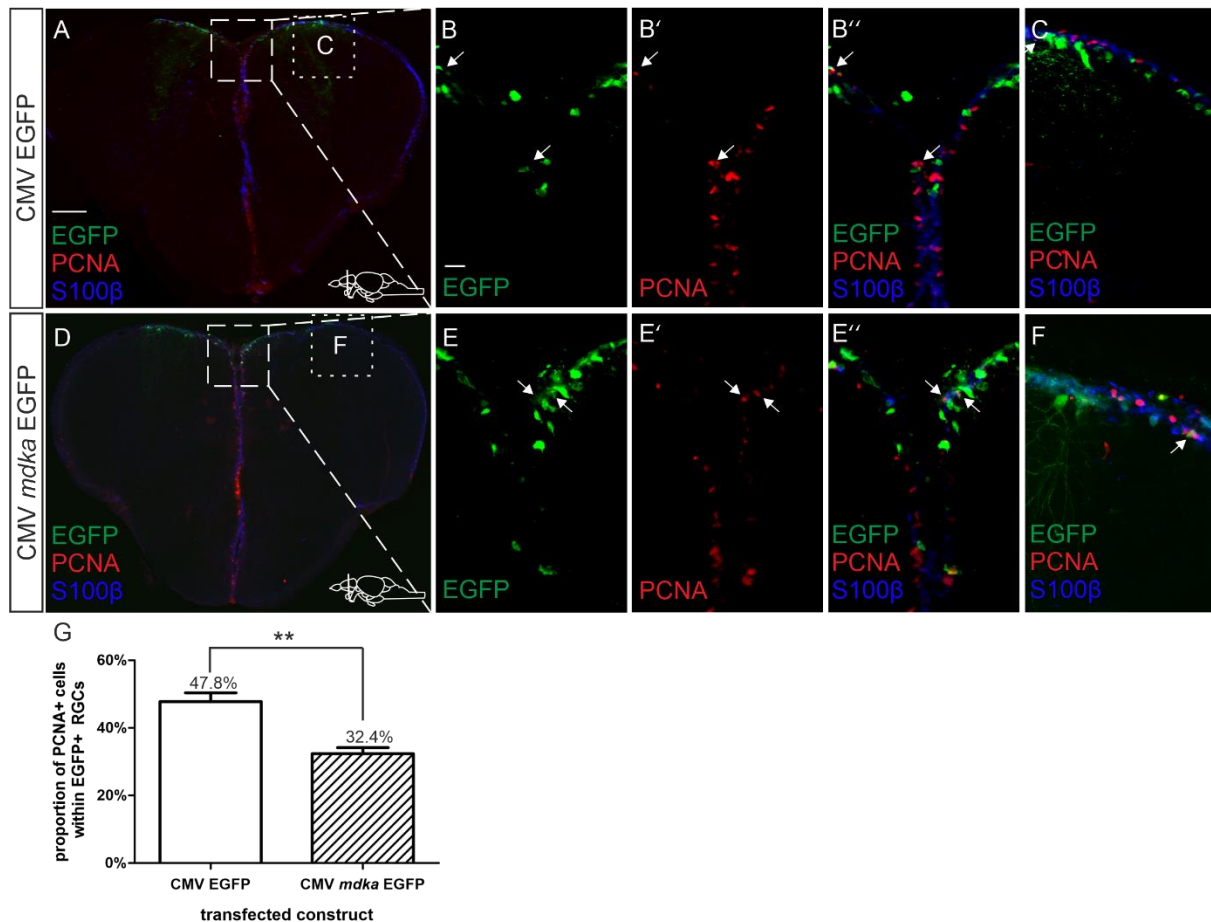


Figure 16: Overexpression of *mdka* leads to reduced PCNA expression in RGCs. IHC against EGFP (green), PCNA (red) and S100β (blue) on WT brains which were transfected either with a control construct containing EGFP under the control of a CMV promoter (A-C) or a *mdka* overexpression construct where *mdka* and EGFP expression are under the control of a CMV promoter (D-F). In both cases RGCs lining the telencephalic ventricle, that were successfully transfected with the injected construct and therefore EGFP+, also occasionally displayed PCNA expression. Dashed line boxed-in area in (A) and (D) represents area of magnification between two hemispheres in (B-B'') and (E-E'') respectively. Dotted line boxed-in area in (A) and (D) represents area of magnification on the right hemisphere in (C) and (F), respectively. White arrows indicate cells positive for the markers EGFP, S100β and PCNA in the Vz. (G) Quantification of the proportion of cells expressing PCNA within successfully transfected RGCs (EGFP+/S100β+) indicating a significant reduction of the number of PCNA+ RGCs transfected with the *mdka* overexpression construct in comparison with the control construct. Significance is indicated by asterisks: ** 0.001<p<0.01. n= 3 brains/construct, 3 sections/brain. Scheme in the lower right-hand corner of (A, D) indicates level of respective cross-section. Scale bar = 100 μm in (A, D), 20 μm in (B-C, E-F). Abbreviations: CMV promoter, cytomegalovirus promoter

3.1.8 Inhibition of MdkA leads to increased proliferation in the zebrafish forebrain

In order to further decipher the function of *mdka* in the context of NSC behavior, I next investigated the influence of the *mdka* gene product, the protein MdkA, on the proliferative behavior of RGCs in

the zebrafish telencephalon. After the previous experiment, indicating reduced proliferation of RGCs in the case of *mdka* overexpression, inhibition of the *mdka* gene product could lead to the opposite effect.

To this end, an inhibitor for the Mdk protein, iMDK (inhibitor of MDK) was administered to adult WT fish via the fish water (Hao et al. 2013). Control fish were treated for the same amount of time with DMSO. After seven consecutive days of treatment the telencephala of iMDK treated fish and control fish were analyzed using IHC with antibodies against S100 β and PCNA (figure 17). Additionally, the influence of Mdk inhibition on RGC behavior under regenerative conditions was studied by treating a proportion of the fish to a stab wound assay on the 2nd day of drug treatment (figure 17C-D'). Under homeostatic conditions, there was no obvious increase in the number of PCNA+ cells in the Vz in brains treated with the Mdk inhibitor (compare figure 17A-A' to figure 17B-B'). However, after quantification of three individual telencephala for each condition, there was no significant statistical difference in the number of PCNA+ RGCs detected (figure 17E). After the lesion, the number of PCNA+ cells was increased in the lesioned hemispheres of both the telencephala treated with iMDK and DMSO (figure 17C-C' and figure 17D-D'). Remarkably, In the telencephalon treated with iMDK, the signal for the antibody against PCNA was highly detectable around the lesion site and also in the parenchyma of the lesioned hemisphere (white arrows figure 17D-D') which was not as prominent for the DMSO treated telencephalon (figure 17C-C') or the unlesioned telencephala (figure 17A-B'). However, quantification of three individual lesioned telencephala for each condition showed no significant difference in the number of PCNA+ RGCs (figure 17E). The obvious increase in the green signal for PCNA was therefore due to an increase in the number of proliferating cells which were not RGCs and were therefore not considered in the quantification. This is also substantiated by the fact that in the lesioned brain, the increase in PCNA signal was mainly observed around the lesion and not in the stem cell niche (white arrows figure 17D-D').

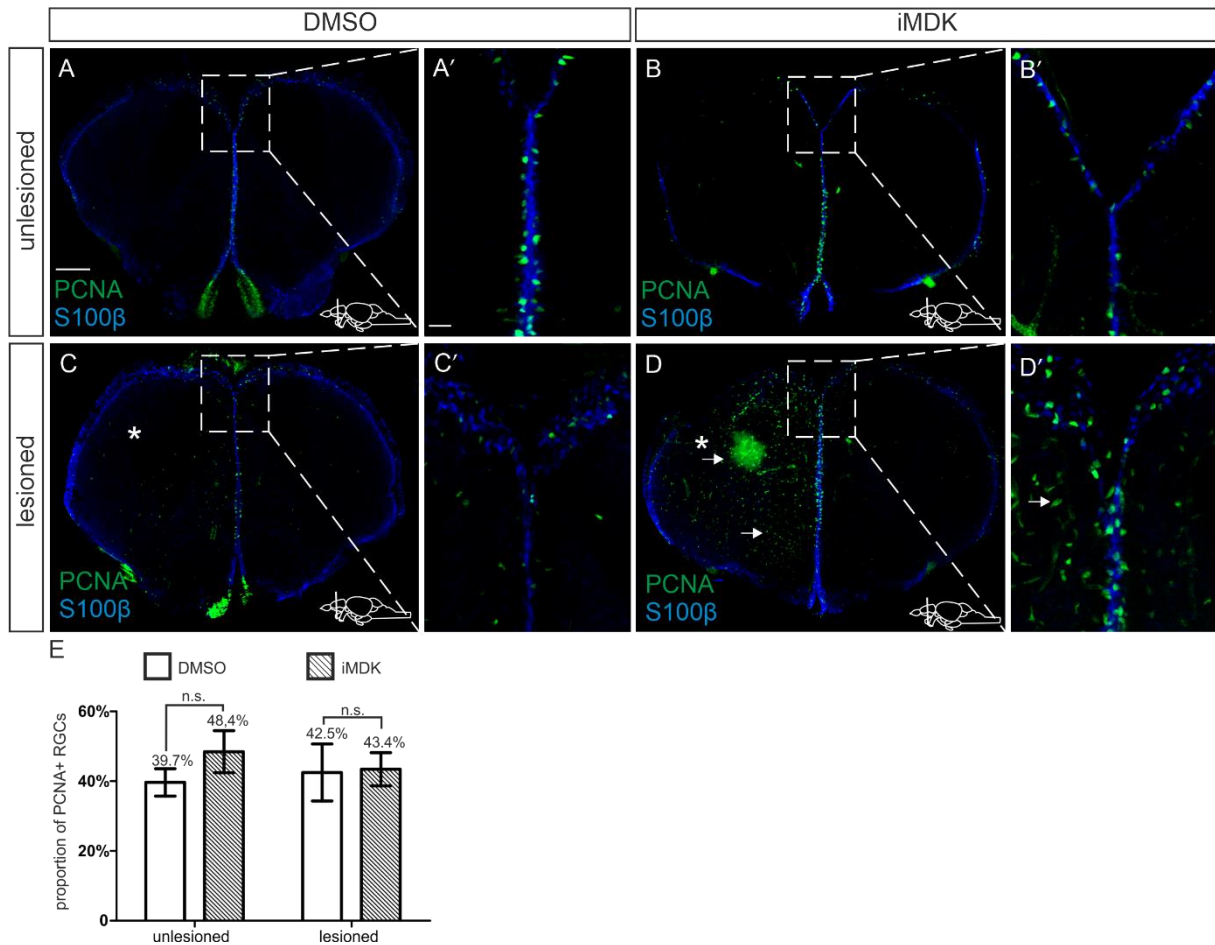


Figure 17: iMDK treatment leads to increased cell proliferation in the zebrafish telencephalon. (A-D') IHC using antibodies against PCNA (green) and S100 β (blue) on cross-sections of DMSO treated unlesioned (A-A'), iMDK treated unlesioned (B-B'), DMSO treated lesioned (C-C') and iMDK treated lesioned (D-D') WT telencephala. Under homeostatic conditions, the number of PCNA+ cells seemed increased in brains treated with iMDK (B, B'). After the lesion, the signal for PCNA was increased in the lesioned hemisphere for both iMDK and DMSO treated brains (C-C' and D-D'). In the iMDK treated brain there was also a high number of PCNA+ cells around the lesion site and in the parenchyma of the lesioned left hemisphere. White arrows indicate cells expressing PCNA in the parenchyma and at the lesion site. The lesioned hemisphere is marked with an asterisk. Boxed-in area in (A, B, C and D) represents area of magnification in (A', B', C' and D') respectively. (E) Quantification of the proportion of PCNA+ RGCs in DMSO or iMDK treated unlesioned or lesioned brains showed no significant difference in DMSO vs. iMDK brains under unlesioned or lesioned conditions. $n = 3$ brains, 3 sections/brain for quantification. Significance is indicated by n.s. = not significant. Scheme in the lower right-hand corner of (A, B, C, D) indicates level of respective cross-section. Scale bar = 100 μm in (A, B, C, D), 20 μm in (A', B', C', D'). Abbreviations: iMDK, inhibitor of MDK

3.1.9 Identification and validation of regulatory elements for the *mdka* gene

In order to embed the gene *mdka* in the regulatory network controlling NSC behavior and therefore adult neurogenesis in the zebrafish, it is pivotal to not only identify the function of the gene product but also the regulation of the gene. The identification of upstream signaling pathways and regulators is crucial to gain knowledge about the spatial and temporal control of gene expression which will also allow conclusions about the different functions.

One approach to investigate *mdka* regulation is the identification of enhancer sequences for *mdka* as they generally control the on/off state of genes and the level of expression (Rastegar et al. 2008; Strähle and Rastegar 2008). Additionally, these regulatory elements or CRMs can harbor binding sites for different transcriptional regulators TRs which influence expression of their target genes positively or negatively (Strähle and Rastegar 2008; Davidson 2001). Through the identification of the CRMs and investigation of their binding sites it would be possible to gain knowledge about the regulation of *mdka* and the factors which are responsible for the specific expression of *mdka* in qRGCs under homeostatic and regenerative conditions.

There are different ways to identify putative enhancer elements for a gene of interest including comparative genomic approaches to predict regulatory elements based on conservation, genomic features such as epigenetic marks or the opening of DNA through Assay for transposase accessible chromatin (ATAC) sequencing. These methods can be used in combination and the identified elements can consequently be tested for their in-vivo activity by zebrafish transgenesis (Ahituv, Rubin, and Nobrega 2004; Nobrega and Pennacchio 2004; Doganli et al. 2017; Kikuta et al. 2007; Catarino and Stark 2018).

Here, ATAC analysis was performed on lesioned WT telencephalic tissue in comparison to unlesioned tissue and the resulting peaks, indicating opening of chromatin, were matched with nearby differentially transcribed genes from RNA sequencing (black peaks figure 18B-C). Through this, five peaks in the vicinity of the *mdka* gene were identified and called CRM1-CRM5 according to their relative order on the DNA region (light blue, figure 18A, B). Additionally, Thompson et al. (2020) identified a different putative CRM for *mdka* when performing ATAC sequencing on WT zebrafish fin regenerates (Thompson et al. 2020). This element was also used for my experiment and consequently called CRM6 (light blue, figure 18A, C). When analyzing the spatial distribution of the different putative CRMs in relation to the *mdka* gene which is located on chromosome 7 in the zebrafish genome, it was obvious that the majority of the CRMs were situated outside of the coding region of *mdka* (figure 18A). Indeed, CRM1 and CRM2 were localized upstream of the TSS and the 5' UTR of the *mdka* gene while CRM3, CRM4 and CRM5 were located inside of the gene. More specifically, CRM3 and CRM4 were positioned in an intronic region between the first and second exon of *mdka*. CRM5 displayed a special location as it was also located in the intronic region between exon 1 and 2 but also fully overlapped

with exon 2 which is part of the *mdka* coding region (figure 18A). CRM6 was the only one located downstream of the *mdka* coding sequence (figure 18A).

For validation of those identified elements I matched the known chromosomal locations of the putative CRMs with the DANIO-CODE data coordination centre (DCC) track in the UCSC genome browser (Figure 18B-C, chromosomal locations of CRMs highlighted in light blue) (Baranasic et al. 2021). These tracks provide confirmation of regulatory elements via different methods: (1) ATAC seq data from the Skarmeta lab for different developmental stages of the zebrafish displaying peaks at accessible chromatin regions (green, figure 18B-C). Here, I only utilized Prim-5 (24 hpf) and Long-pec (48 hpf) stages because the comparison is supposed to be done with ATAC sequencing from adult brain tissue. (2) ATAC seq supported Developmental Regulatory Elements (PADREs) at the previously chosen stages which are predicted regulatory elements in the area based on the reproducibility of ATAC seq peaks and histone modification marks using ChromHMM (black, figure 18B-C) (Baranasic et al. 2021). ChromHMM is a software which integrates different datasets like chipSeq in order to identify and characterize genomic regions based on chromatin marks (Ernst and Kellis 2012, 2017). (3) Annotation of regulatory elements including EnhA1 which are active enhancers (red, figure 18B-C) and TssA1 and TssA2 (blue, figure 18B-C) specifying active transcription start sites. (4) Analysis of conservation using the cyprinid phastCons score, indicating conservation scores between cyprinid and zebrafish by black boxes (figure 18B-C) (Chen et al. 2019). The putative CRMs are marked in light blue and the ATAC seq peaks from lesioned and unlesioned telencephala are shown in black (figure 18B-C). Interestingly, the ATAC seq peaks corresponding to CRM1 and CRM2 are significantly smaller than for CRM3-5, while in the area of the putative CRM6, no peak could be observed. Surprisingly, there is one prominent peak located after CRM5, which is still in the coding region of the *mdka* gene, but not annotated as a CRM. When comparing the annotated chromosomal locations of putative CRMs identified by ATAC sequencing of lesioned and unlesioned telencephalic hemispheres with the DANIO CODE track hub in the UCSC genome browser, it was obvious that the putative CRM1 did not correlate with any annotated enhancer elements, ATAC seq peaks from the Skarmeta lab or a high conservation score. However, it showed an overlap with the coding region of another zebrafish gene called *diacylglycerol kinase, zeta a (dgkza)* (figure 18B). The putative element CRM2 matched with ATAC seq peaks at 24 hpf and 48 hpf stages and regions with a high conservation score, as well as an annotated active enhancer region (figure 18B). The elements CRM3 and CRM4 were very closely located which is the reason that the light blue highlighted regions merge in the depiction (figure 18B). Nevertheless, they could both be matched with ATAC seq peaks from the Skarmeta lab, active enhancer regions and a region displaying a high conservation score (figure 18B). Interestingly, both putative enhancer regions matched an active transcription start site in the 24 hpf ATAC seq from the Skarmeta lab, but at the later stage, at 48hpf, the same region was annotated as an enhancer (figure 18B). Additionally, the CRM4 was located in a

region where the ATAC seq peak from 24 hpf and 48 hpf was very prominent (figure 18B). The chromosomal location of CRM5 fully overlapped with the exon 2 of the *mdka* coding region and also matched ATAC seq peaks, active enhancers and a region with a high conservation score between zebrafish and the cyprinid family (figure 18B).

About 280 kilobases (kb) downstream of the *mdka* coding region, the element CRM6 was identified (figure 18C). Like CRM1, it did not match regions with annotated ATAC seq peaks or enhancer regions. In contrast, it was located in the coding region of another zebrafish gene, *troponin T type 3b (tnnt3b)* (figure 18C). Based on this evaluation, CRM2, CRM3, CRM4 and CRM5 should be considered the most reliable putative enhancer regions because they matched with active chromatin regions annotated by different methods and based on a variety of datasets and were located in regions with a high conservation score (figure 18B).



Figure 18: Identification of putative regulatory elements for *mdka* using ATAC sequencing data and the DANIO CODE track hub in the UCSC genome browser. (A) Schematic depiction of the *mdka* gene including its five exons and relative location of the putative CRM regions. The gene, as well as the CRMs are localized on chromosome 7 of the zebrafish genome. The chromosomal coordinates for the identified CRMs (light blue) as well as for the *mdka* transcribed region (orange) are given. All putative

CRMs laid either outside of the *mdka* transcribed region or were located in the intron between the first and second exon. Only CRM5 fully overlapped with exon 2 of the *mdka* gene. (B-C) UCSC genome browser track hub comparing ATAC seq data from unlesioned telencephala and lesioned telencephala at 5 dpl (black peaks) with DANIO-CODE tracks marking ATAC seq peaks at Prim-5 and Long-Pec developmental stages (green), PADREs (black), annotation of regulatory elements including EnhA1 (red) and TSSs (blue) and phastCons conservation scores between the cyprinid family and zebrafish (black boxes). Putative CRMs identified through ATAC seq of lesioned and unlesioned adult zebrafish telencephala are indicated by light blue highlights. CRM1 did not match with any peaks from the ATAC seq of the Skarmeta lab, nor with any other annotated regulatory element from the DANIO-CODE track and overlapped with the coding region of the gene *dgkza*. CRM2-5 matched with annotated ATAC peaks, putative enhancers and a high conservation score in the DANIO-CODE track (B). (C) Zoomed out region downstream of the *mdka* coding region. CRM6 was located about 280 kb downstream of the *mdka* coding region and did not match any annotated regulatory elements. It overlapped with the coding region of the gene *tnnt3b*. Abbreviations: ATAC, Assay for transposase accessible chromatin; *dgkza*, diacylglycerol kinase, zeta *a*; EnhA1, active enhancer; PADREs, ATAC seq supported Developmental Regulatory Elements; *tnnt3b*, troponin T type 3b; TSS, transcription start site; UTR, untranslated region

In order to identify individual CRMs which faithfully mimic the endogenous expression of the *mdka* gene under homeostatic but also under regenerative conditions, I attempted to create zebrafish transgenic lines for each CRM. The expression plasmid contained the region of the individual putative CRM (primer sequences used for cloning in table 7) with a *gata2a* promoter driving expression of EGFP (figure 19A) (Navratilova et al. 2009). This construct was flanked by Tol2 transposase sites which facilitate integration into the zebrafish genome (figure 19A) (Kawakami 2007). After injection, the F0 generation embryos which displayed mosaic EGFP expression were selected, raised and crossed out with WT fish once sexually matured. The F1 generation embryos which contained a stably integrated transgene were then analyzed for EGFP expression in comparison to endogenous *mdka* expression at 24 hpf (compare figure 19B with figure 19C-F). The elements CRM1 and CRM4 were not integrated into the subsequent analysis, since cloning of these chromogenic regions was unsuccessful. The embryo carrying the *mdka-CRM2-gata2a:EGFP* transgene displayed EGFP expression in the cerebellum and the hindbrain, as well as in the notochord and somites (white arrows figure 19C). All other transgenic lines showed prominent expression of the CRM transgene in the forebrain, cerebellum, optic tectum and hindbrain (white arrows figure 19D-F). However, while embryos of the *Tg(mdka-CRM3-gata2a:EGFP)* and *Tg(mdka-CRM6-gata2a:EGFP)* lines additionally exhibited expression of EGFP in the spinal cord and weak expression in the somites (figure 19D, F), the embryo of the *Tg(mdka-CRM5-gata2a:EGFP)* transgenic line displayed trunk expression only in the neural tube (white arrow figure 19E). Therefore, out of the analyzed putative CRMs, the CRM5 transgene best resembled expression of the endogenous *mdka* gene in the 24 hpf embryo (compare figure 19E to figure 19B and figure 10A).

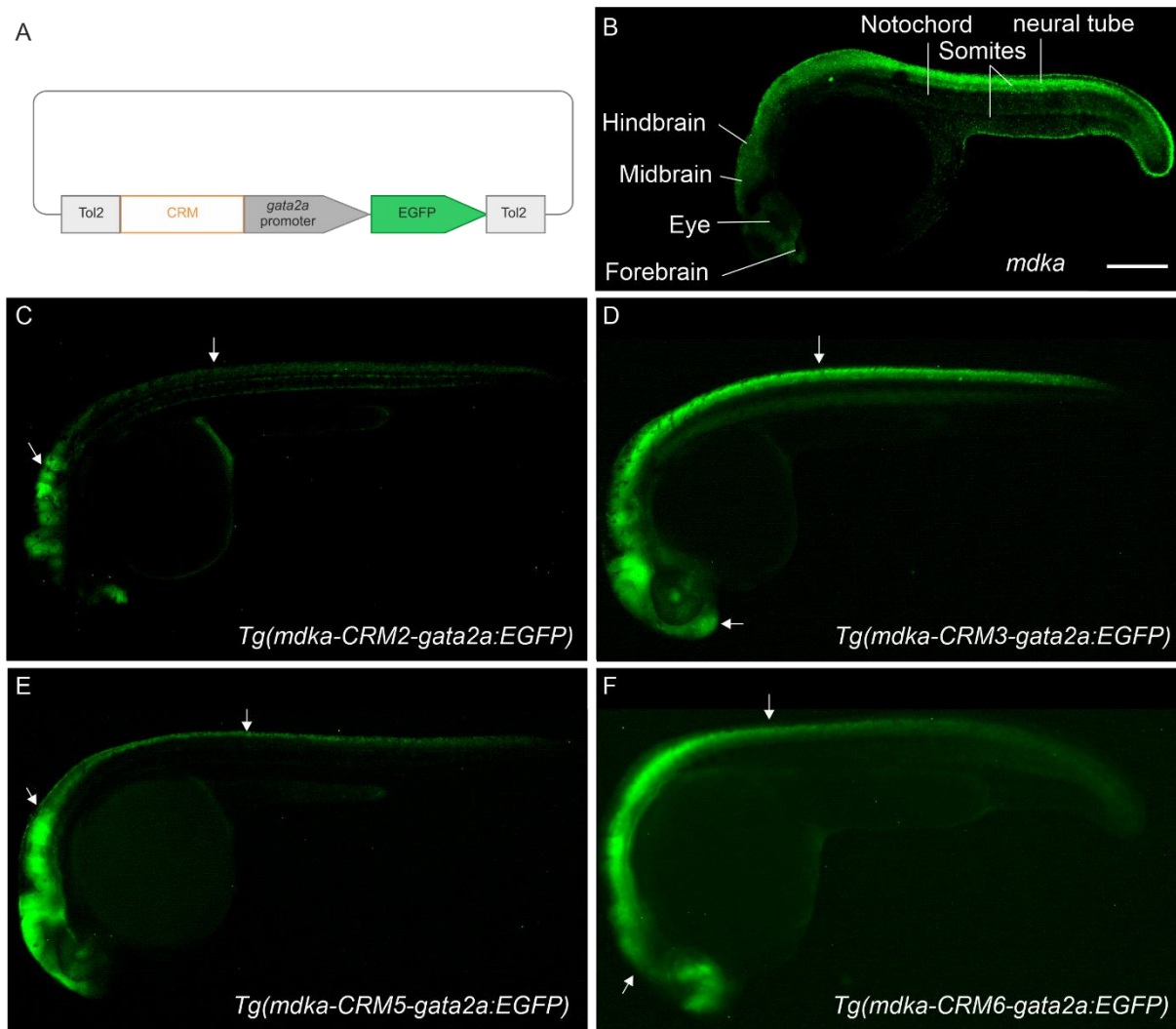


Figure 19: Creation of transgenic zebrafish lines for putative enhancers of *mdka* and comparison of transgene expression in 24 hpf zebrafish embryos. (A) Schematic representation of the expression plasmid injected into zebrafish embryos to establish transgenic lines for individual CRMs. The CRMs were cloned in front of a *gata2a* promoter driving expression of EGFP. This construct was flanked by Tol2 sites for integration into the zebrafish genome. (B) FISH using a probe against *mdka* mRNA on a 24 hpf zebrafish embryo labeling the regions where the endogenous *mdka* gene is expressed in green. (C-F) Expression patterns of the CRM transgenes (green) in zebrafish embryos of the F1 generation at 24 hpf. The expression patterns were mostly similar in the head region, displaying expression in the fore-, mid- and hindbrain areas. Only the embryo of the *Tg(mdka-CRM2-gata2a:EGFP)* line was missing forebrain expression. The embryo of the *Tg(mdka-CRM5-gata2a:EGFP)* line best resembled endogenous expression of the *mdka* gene as it showed restricted EGFP expression in the brain areas and the neural tube (E). Scale bar = 200 μ m. Abbreviations: EGFP, enhanced green fluorescent protein

3.1.10 Regulation of the gene *mdka* by major signaling pathways

As previously mentioned, CRMs harbor binding sites for transcription factors which regulate the activity of a gene to control the gene expression at the right time and correct cellular location. Since I could previously show strong evidence of a spatial and temporal co-expression between the genes *mdka* and *id1* (see sections 3.1.4 and 3.1.6), it is tempting to speculate that both genes are regulated by the same pathways. In preceding work it was shown that the CRM2 of *id1* harbors a Smad binding

site which are transcription factors transducing the signal from bone morphogenetic protein (BMP) pathways (Sánchez-Duffhues et al. 2015; Zhang et al. 2020). Therefore, the next question was if *mdka* is also regulated by the BMP pathway.

In order to manipulate BMP signaling in the forebrain, I treated adult zebrafish with dorsomorphine homologue-1 (DMH1), a small molecule inhibitor for the BMP pathway which blocks the phosphorylation of Smad1/5/8, for five consecutive days before analyzing *mdka* expression via ISH (figure 20) (Hao et al. 2010; Hao et al. 2014). Control fish were treated with dimethylsulfoxide (DMSO) for the same amount of time. To ensure the functionality of the inhibition experiment, I also performed ISH against *id1* mRNA which is known to be downregulated in the forebrain after treatment with DMH1 (figure 20D-E) (Zhang et al. 2020). When comparing the expression pattern of *mdka* between the DMSO treated and DMH1 treated telencephala, there was no obvious difference in the level of expression (compare figure 20A to 20B). However, the level of expression of *id1* was significantly lower in treated telencephala than in the control telencephala, proving the functionality of the treatment (figure 20D-E). It is still probable that the BMP pathway has an influence on *mdka* expression that is however limited to controlling its upregulation in response to telencephalic lesion. Therefore, I performed a stab wound on the 2nd day of DMH1 or DMSO treatment on selected fish and tested for *mdka* expression via ISH (figure 20C). Also in the case of lesion, the inhibition of the BMP pathway had no influence on *mdka* expression, suggesting that *mdka* in contrast to *id1*, is not regulated by the BMP pathway (figure 20C).

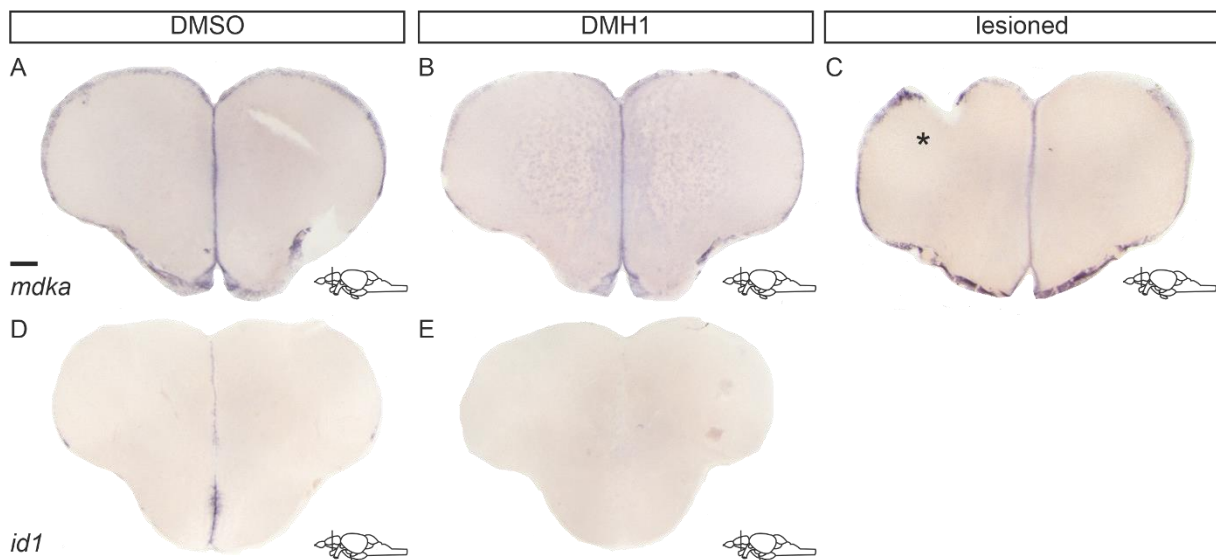


Figure 20: *mdka* expression is not controlled by the BMP pathway. (A, B) ISH against *mdka* mRNA on cross-sections of WT telencephala treated with DMSO control (A) or DMH1 (B). There was no difference in the expression level of *mdka* between treated and control telencephala. (C) ISH using probes against *mdka* mRNA on cross-sections of lesioned WT telencephala treated with DMH1 at 5 dpl. Also under regenerative conditions, inhibition of the BMP pathway had no influence on *mdka* expression in the telencephalon. The lesioned hemisphere is marked with an asterisk. (D, E) ISH against the gene *id1* on cross-sections of DMSO control telencephala (D) and DMH1 treated telencephala (E).

The expression level of *id1* was significantly downregulated after DMH1 treatment proving the functionality of the inhibition method. Scheme in the lower right-hand corner of (A-E) indicates level of respective cross-section. Scale bar = 100 μ m. Abbreviations: DMSO, dimethylsulfoxide; DMH1, dorsomorphine homologue -1

I next wanted to know if *mdka* is a downstream effector of any of the other major signaling pathways that are important during development, besides BMP. I decided to investigate the Notch pathway because of its implication in controlling the balance between quiescence and activation of adult NSCs and the Wnt pathway which has been suggested to control pivotal cellular events during the early wound healing stage after telencephalic lesion (Chapouton et al. 2010; Diotel et al. 2020; Demirci et al. 2020). For that purpose, I employed the same regimen of treatment using LY411575, an inhibitor of the γ -secretase in the Notch pathway which blocks the release of the NICD and consequently the transcription of Notch target genes (figure 21B). Similarly, I used IWR-1, a tankyrase inhibitor which blocks the degradation of axin in the β -catenin destruction complex of the Wnt pathway (figure 21C). This inhibition leads to degradation of β -catenin and inhibition of gene transcription of Wnt target genes (Fauq et al. 2007; Chen et al. 2009). Control fish were again treated with DMSO (figure 21A). When analyzing *mdka* expression in all treated brains, I noticed no difference in the level of *mdka* expression between LY411575 treated and DMSO control telencephala or between IWR-1 treated and DMSO control telencephala (compare figure 21A with figure 21B and figure 21C). In all cases, the expression pattern restricted to the Vz of the telencephalon remained the same (figure 21A-C). Therefore, *mdka* is a gene which expression seems to be independent of the tested major signaling pathways.

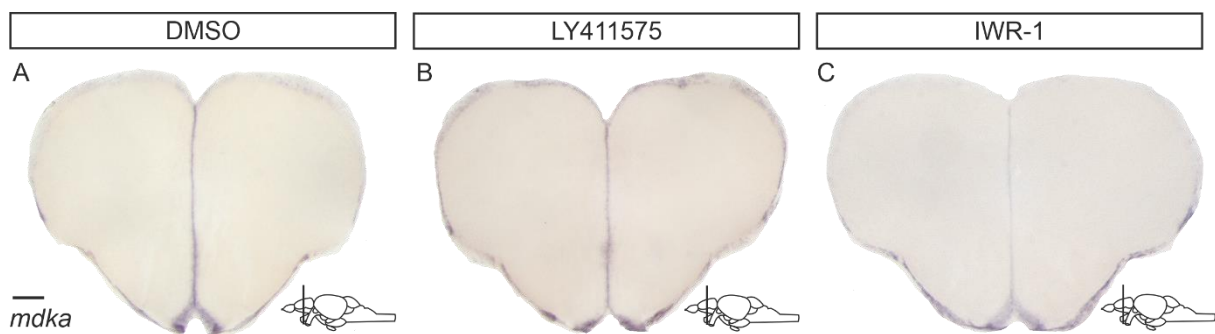


Figure 21: *mdka* expression is not influenced by any of the major signaling pathways. (A-C) ISH against *mdka* mRNA on cross-sections of WT telencephala, treated with DMSO control (A), the Notch pathway inhibitor LY411575 (B) and the Wnt pathway inhibitor IWR-1 (C). In all cases there is no obvious difference between the expression levels with and without treatment, indicating that *mdka* is not regulated by the Notch or the Wnt pathway. Scheme in the lower right-hand corner of (A-C) indicates level of respective cross-section. Scale bar = 100 μ m

3.2 miRNAs in the GRN controlling NSC behavior

Recently, evidence about the role of non-coding RNA molecules in brain regeneration has been emerging (Yang et al. 2021; Gourain et al. 2021). Among them, miRNAs, which are capable of inhibiting the translation of their target gene, are a fairly new field of research but their importance in gene regulation has been proven in the zebrafish brain (Giraldez et al. 2005; Lang and Shi 2012). In order to know their position in the regulatory network, it is again pivotal to decipher their cellular location and temporal expression. Since miRNAs are rather short, about 20-22 nt long, the visualization in tissue using classical methods is difficult (Lang and Shi 2012). Here, three different approaches to investigate miRNAs and especially visualize their cellular expression pattern in the zebrafish adult telencephalon have been utilized.

3.2.1 Identification of deregulated miRNA candidates in response to telencephalic lesion

In an effort to first identify individual miRNA candidates which are involved with neural regeneration, RNA sequencing data comparing the expression of genes between unlesioned and lesioned telencephalic hemispheres at 5 dpl was mined for miRNA genes. This resulted in a candidate portfolio containing six different miRNA genes with a substantial log₂ fold change of expression after telencephalic lesion with a significant p-value (table 14). In order to identify in which functions these miRNAs are involved, the RNA seq data was again mined for genes downregulated after telencephalic lesion since miRNAs are capable of downregulating their targets. Among them, potential targets of the miRNA candidates were identified by the presence of the miRNA seed region in the 3'UTR of mRNAs downregulated in the lesioned telencephalic hemisphere and matched with a target gene search from TargetScanFish6.2 (table 14).

The miRNA *dre-miR-146a* showed the highest log₂ fold change in response to lesion (log₂ fold change = 2.1067) with a highly significant p-value while the miRNA *dre-miR-183* displayed the least significant log₂ fold change (table 14). From the selection of target genes, it becomes obvious that several miRNAs can regulate one target gene (e.g. *nrn1* [*neurtin 1a*] is targeted by *dre-miR-31*, *dre-miR-726* and *dre-miR-183*) and that there is a high abundance of target genes involved in a variety of different functions (table 14). Furthermore, a number of transcription factors could also be identified among the target genes.

Table 14: miRNA candidates in descending order of log₂ fold change of expression. The table indicates the name of the miRNA, the ENSEMBL ID, sequence of the miRNA, log₂ fold change and p-value, as well as a selection of known targets of the miRNAs which are downregulated at 5 dpl and a selection of their corresponding GO term names. Abbreviations: *bhlhe*, basic helix-loop-helix family, member 22; *camk2b1*, calcium/calmodulin-dependent protein kinase (CaM kinase) II beta 1; *chga*, chromogranin A; *clstn3*, calyntenin 3; *dre-miR*, *danio rerio* micro RNA; *diras1a*, DIRAS family, GTP binding RAS-like 1a; *dre*, *danio rerio*; *fosl2*, FOS like 2, AP-1 transcription factor subunit; *gpm6ab*, glycoprotein M6Ab; *miRNA*, micro RNA; *mllt11*, MLLT11 transcription factor 7 cofactor; *nggf*, neuronal guanine nucleotide

exchange factor; nrn1a, neuritin 1a; prdm8b, PR domain containing 8b; sipa111, signal-induced proliferation-associated 1 like 1; shank3b, SH3 and multiple ankyrin repeat domains 3b; sptbn2, spectrin, beta, non-erythrocytic 2; stmn2a, stathmin 2a; sypb; synaptophysin b

Candidate name	ENSEMBL ID	Sequence 5'-3'	log ₂ fold change	adjusted p-value	predicted downregulated target genes (selection)	GO term names of predicted targets
<i>dre-miR-146a</i>	ENSDARG00000083310	UGAGAAC UGAAUU CCAUAGA UGG	2.1067	3.61E-67	<i>chga, sptbn2, mltt11</i>	Cytoplasm, cytoskeleton, synapse
<i>dre-miR-31</i>	ENSDARG00000080961	UGGCAA GAUGUU GGCAUA GCUG	2.0972	2.52E-36	<i>prdm8b, nrn1a, ngef, gpm6ab</i>	oligodendrocyte development, nervous system development
<i>dre-miR-96</i>	ENSDARG00000083126	UUUGGC ACUAGCA CAUUUU UGCU	1.8761	2.07E-11	<i>clstn3, gpm6ab, stmn2a, sipa111</i>	Neuron projection, nervous system development
<i>dre-miR-726</i>	ENSDARG00000082495	UUCACUA CUAGCAG AACUCGG	1.3764	6.59E-07	<i>nrn1a, camk2b1, sypb</i>	Nervous system development, regulation of neuronal synaptic plasticity
<i>dre-miR-182</i>	ENSDARG00000081095	UUUGGC AAUGGU AGAACUC ACA	1.1471	6.66E-05	<i>sipa111, fosl2, bhlhe22, stmn2a</i>	Regulation of dendrite morphogenesis, regulation of transcription by RNA polymerase II
<i>dre-miR-183</i>	ENSDARG00000080467	UAUGGC ACUGGU AGAAUU CACUG	1.1376	0.1E-03	<i>nrn1a, shank3b, sipa111</i>	Nervous system development, neuron projection, neuron development

After identification of the different miRNA candidates I focused further on visualizing the expression patterns of those candidates in the zebrafish telencephalon. To this end, I first made use of commercially available locked nucleic acid (LNA, Quiagen) probes which carry a digoxigenin (DIG) modification at the 5' end and attach to the mature miRNA sequence. This modification can be recognized by either anti-DIG-AP or anti-DIG-POD antibodies and therefore be used in a regular chromogenic or fluorescent ISH. LNAs are modified RNA nucleotides containing an extra bridge that

connects the 2' oxygen with the 4' carbon leading to a locked state of the ribose in the 3' conformation (Frieden et al. 2003; Frieden, Hansen, and Koch 2003; Kurreck et al. 2002). Through this locked conformation, LNA probes are more stable than usually used RNA probes and therefore allow a higher specificity of detection even for small molecules like miRNAs.

I first performed the ISH using LNA probes against *dre-miR-146a*, as it was the most significantly upregulated miRNA in the RNA sequencing and therefore demonstrated the highest chances of detecting a change in expression level using ISH (table 14 and figure 22). As a control for the method, I used a LNA probe against *dre-miR-9*, an already thoroughly investigated miRNA where the expression pattern in the zebrafish brain is known (figure 22A-B) (Leucht et al. 2008; Coolen et al. 2012). In the unlesioned, as well as in the lesioned telencephalon, expression of *dre-miR-9* was associated with the Vz which matches previous reports (black arrows figure 22A, B) (Coolen et al. 2012). Additionally, the ISH also showed additional staining outside of the Vz in the dorsal telencephalic area (figure 22A, B). *dre-miR-9* was never reported to be up- or downregulated in response to telencephalic lesion and also not picked up in the RNA sequencing which was confirmed by the ISH (figure 22B).

In contrast, *dre-miR-146a* expression was detected in what appears to be a layer left and right of the Vz but spares the cells in the Vz (black arrows figure 22C, D). Furthermore, some expression was detected on the edge of the ventral and dorsal telencephalic areas (black arrows figure 22D). After lesion there was a higher expression in the lesioned left hemisphere, but the expression could not be allocated to a certain area of the telencephalon except the periphery of the ventral telencephalic area (black arrows figure 22D).

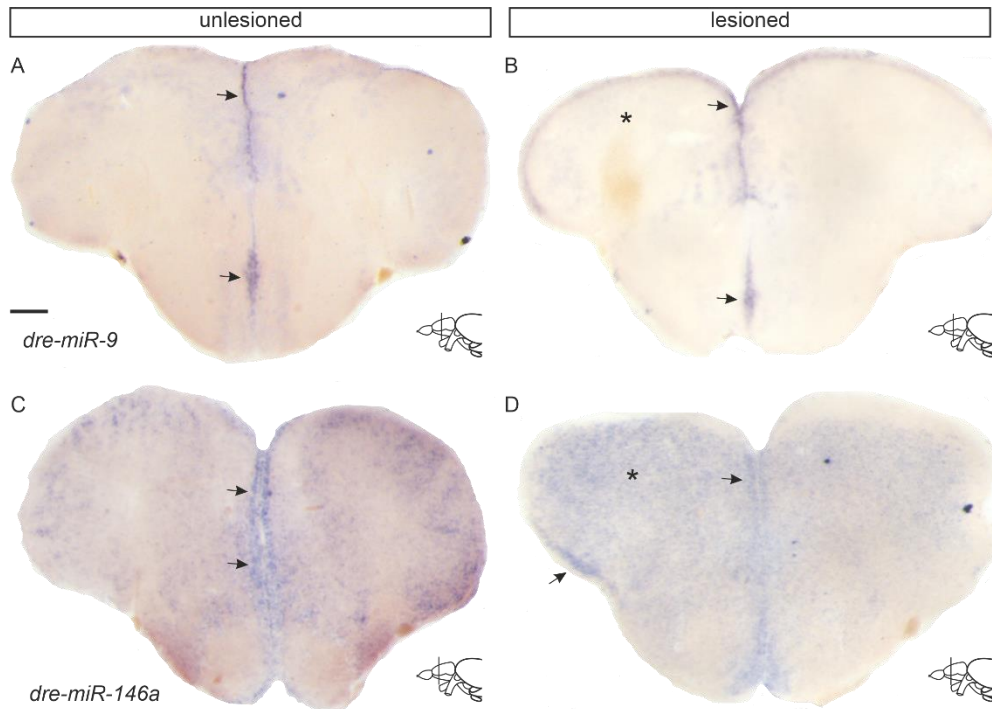


Figure 22: *dre-miR-146a* is broadly expressed in the zebrafish telencephalon. (A-B) ISH using probes against *dre-miR-9* on cross sections of unlesioned (A) and lesioned (B) WT telencephala. *dre-miR-9* was expressed in the Vz, mainly between the two hemispheres. There was no obvious upregulation of the expression level after the lesion (B). Black arrows point to areas of expression in the dorsal and ventral areas of the telencephalon. (C-D) ISH with probes against *dre-miR-146a* on cross-sections of unlesioned (C) and lesioned (D) WT telencephala. The gene is mainly expressed around the area of the Vz between the two hemispheres but not at the periphery of the dorsal telencephalon. Additional expression was detected at the periphery of the ventral telencephalon. Black arrows indicate areas of expression. Scheme in the lower right-hand corner of (A, B, C, D) indicates level of respective cross-section. The lesioned hemisphere is marked with an asterisk. Scale bar = 100 μ m

3.2.2 Visualization of pri-miRNA molecules

Unfortunately, I could not obtain LNA probes for all the miRNA candidates. Additionally, visualization of some other candidates with the LNA probes was unsuccessful. Therefore, detection of the other miRNA candidates in the zebrafish telencephalon was approached from a different angle.

During miRNA synthesis, the miRNA molecules undergo a maturation process involving several steps. The first gene product transcribed from the miRNA gene by the RNA polymerase II is called the primary miRNA (pri-miRNA) (Bartel 2004). This molecule can be hundreds to thousands of nucleotides long and is therefore significantly longer than the mature miRNA and consequently easier to detect (Bartel 2004). I cloned sequences encompassing about 200-400 bp centered around the approximate mature miRNA sequence from zebrafish gDNA into a pGEM-T Easy expression vector. From these plasmids I synthesized regular RNA ISH probes against the pri-miRNAs of all six miRNA candidates, along with a pri-miRNA probe against *dre-miR-9* to again test the functionality of the method.

These probes were consequently employed in a regular ISH on cross-sections of adult WT zebrafish telencephala (figure 23). The primary form of *dre-miR-9* was detected in the Vz but also showed additional staining outside of this area in the dorsal telencephalic area (black arrows figure 23A). Therefore, it overlaps with the previously shown expression pattern of the mature form of *dre-mir-9* (compare figure 23A with figure 22A). For the probe against *pri-miR-31*, staining could be detected in the Vz, not only between the two hemispheres but also in the periphery of the dorsal telencephalic area. However, staining was also detected outside of the Vz and in the dorsal, ventral and central nuclei of the ventral telencephalic area (black arrows figure 23B). In the case of *dre-miR-146a*, the probe against the primary form showed a staining which was visibly restricted to the Vz, although some ectopic expression was detected in the periphery of the telencephalon (black arrows figure 23C). Therefore, also in this case, the expression patterns of the primary form and the mature form overlapped but differed (compare figure 23C with figure 22C). Staining for the probe against *pri-miR-726* was identified in the Vz between the two hemispheres, as well as in the cells lining the telencephalic ventricle on the dorsal edge of the telencephalon and the very ventral area of the ventral telencephalon (black arrows figure 23D). The probes against *pri-miR-96*, *pri-miR-182* and *pri-miR-183* all displayed similar expression patterns which were centered around the area of the Vz and in the marginal zone of the dorsal telencephalon (figure 23E-G).

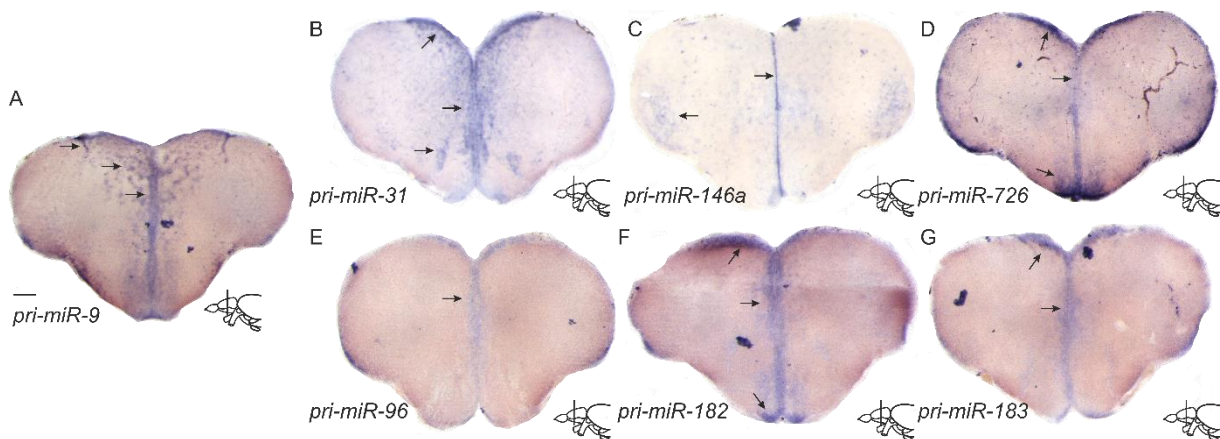


Figure 23: Primary miRNAs of all six miRNA candidates are mainly expressed in the Vz. (A-G) ISH on cross-sections of WT telencephala using probes against the primary miRNA (pri-miRNA) of *dre-miR-9* as control (A), *dre-miR-31* (B), *dre-miR-146a* (C), *dre-miR-726* (D), *dre-miR-96* (E), *dre-miR-182* (F) and *dre-miR-183* (G). The majority of the pri-miRNAs were expressed in the Vz of the telencephalon. *pri-miR-9* and *pri-miR-31* additionally displayed expression around the Vz or inside the central nuclei of the ventral telencephalon (A, B). The expression patterns of *pri-miR-96*, *pri-miR-182* and *pri-miR-183* were strikingly similar and could be detected right next to the Vz (E, F, G). Black arrows indicate areas of expression. Scheme in the lower right-hand corner of (A-G) indicates level of respective cross-section. Scale bar =100 μ m. Abbreviations: pri-miR, primary miRNA

3.2.3 Visualization of miRNA candidates in the telencephalon via individually synthesized FISH probes

Since miRNAs undergo maturation and exert their function in the mature form, the pri-miRNA detection does not undoubtedly label the site of action of individual miRNAs. Therefore, a third approach was employed to reliably detect mature miRNAs in the adult zebrafish telencephalon. This approach was developed in collaboration with organic chemists from the group of Prof. Dr. Hans-Achim Wagenknecht at the KIT and was based on individually synthesized FISH probes against each previously identified miRNA candidate.

The first generation of ssDNA FISH probes (consequently called f-FISH probes) was produced via phosphoramidite solid phase synthesis (see dissertation of Fabian Lang, 2021). For each miRNA candidate, seven complementary sequences were synthesized in which the most central thymidine was exchanged with a cU building block for the subsequent regioselective copper (I) catalytic reaction (CuAAC reaction or click reaction) which adds the fluorophore. This first generation of probes was firstly synthesized against the miRNA *dre-miR-9* (FL-13) to be able to test the method and contained a Cy5-azide as fluorophore. The probes were then utilized in a FISH on cross-sections of WT zebrafish telencephala (figure 24B). The expression pattern of the f-FISH probe against *dre-miR-9* was similar to the expression pattern of a chromogenic ISH using commercially available LNA probes on zebrafish telencephala, showing expression in the Vz of the telencephalon (compare figure 24B with figure 24A). However, the f-FISH probe resulted in a high amount of background which made it unfeasible for the detection of miRNAs. Therefore, in an effort to improve the method, a second generation of FISH probes was synthesized.

In these newly synthesized probes (consequently called l-FISH probes) four DNA nucleotides of each sequence were exchanged for LNA nucleotides which were spatially evenly distributed across the sequence. The locked conformation of the LNA nucleotides leads to increased stability of the probes. Indeed, when using the GENEGLOBE Tm Calculator from Quiagen to calculate melting temperatures of the l-FISH probes hybridized with their target miRNA, an increase of 15-20°C in comparison to the f-FISH probes was detected. Additionally, the l-FISH probes were modified with an Atto647N-azide instead of Cy5, providing a higher photo stability and higher quantum yield. The l-FISH probe against *dre-miR-9* (FL20) was again employed in a FISH experiment on cross-sections of adult WT zebrafish telencephala and after performing the experiment with different hybridization temperatures, 43°C proved to yield the most specific results (figure 24C). Expression was detected in the Vz of the telencephalon (white arrows in figure 24C) and resembled the expression pattern of the endogenous gene (figure 24A). Furthermore, it showed increased specificity and lower background compared to the f-FISH probe of the first generation (compare figure 24B with figure 24C). However, some ectopic expression was still detectable in blood vessels (figure 24C).

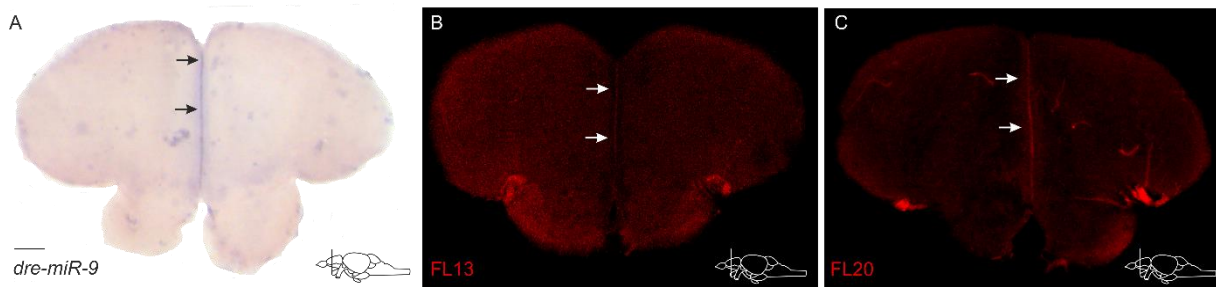


Figure 24: LNA modified I-FISH probe reliably reports expression pattern of the endogenous *dre-miR-9* gene. (A) ISH against *dre-miR-9* in cross-sections of WT telencephala using a commercially available LNA probe. (B, C) FISH on cross-sections of WT telencephala using the f-FISH probe (FL13, red) (B) or the I-FISH probe (FL20, red) (C) against *dre-miR-9*. In all three cases, expression was detected in the Vz of the telencephalon. The I-FISH probe resembled the expression pattern of the endogenous gene best and showed decreased background in comparison with the f-FISH probe. Black and white arrows indicate areas of expression. Scheme in the lower right-hand corner of (A, B, C) indicates level of respective cross-section. Scale bar = 100 μ m

After validation of the functionality of the I-FISH probes using *dre-miR-9*, I applied the I-FISH probes synthesized against *dre-miR-31* (FL21), *dre-miR-96* (FL22), *dre-miR-146a* (FL23), *dre-miR-182* (FL24), *dre-miR-183* (FL25) and *dre-miR-726* (FL26) in a FISH experiment on cross-sections of adult zebrafish telencephala (figure 25). Simultaneously the probes were used in a FISH on cross-sections of WT brains at 5 dpl (figure 25).

The FISH using the probe FL21 displayed a restricted expression pattern in the Vz of the telencephalon without as well as with telencephalic lesion (white arrows figure 25A, A'). Upregulation of expression could be detected on the margin of the telencephalic ventricle in the lesioned left hemisphere (white arrow figure 25A'). The I-FISH probe against *dre-miR-96* (FL22) reported expression in the Vz but also showed a high amount of background and ectopic expression in blood vessels (white arrows figure 25B). Additionally, no upregulation after telencephalic lesion could be detected with the probe (figure 25B'). Staining with the probe FL23 against *dre-miR-146* was visible in the Vz but was overall weak and did not show a deregulation of expression in the left lesioned hemisphere (white arrows figure 25C-C'). FL24 and FL25 both exhibited a very weak signal in the unlesioned brain but displayed a strong signal directly at the lesion site in the lesioned brain (white arrows figure 25D-E'). Additionally, the signal for FL25 was mostly detected in the Vz (white arrow figure 25E). The I-FISH probe against *dre-miR-726* (FL26) also showed staining mostly in the Vz of the telencephalon but additionally in areas outside of the Vz and in the nuclei of the dorsal and ventral telencephalic areas (white arrows figure 25F). After telencephalic lesion, there was no obvious deregulation (white arrows figure 25F'). Overall, only the probes against *dre-miR-31* (FL21), *dre-miR-182* (FL24) and *dre-miR-183* (FL25) could faithfully report an upregulation detected in the RNA sequencing experiment.

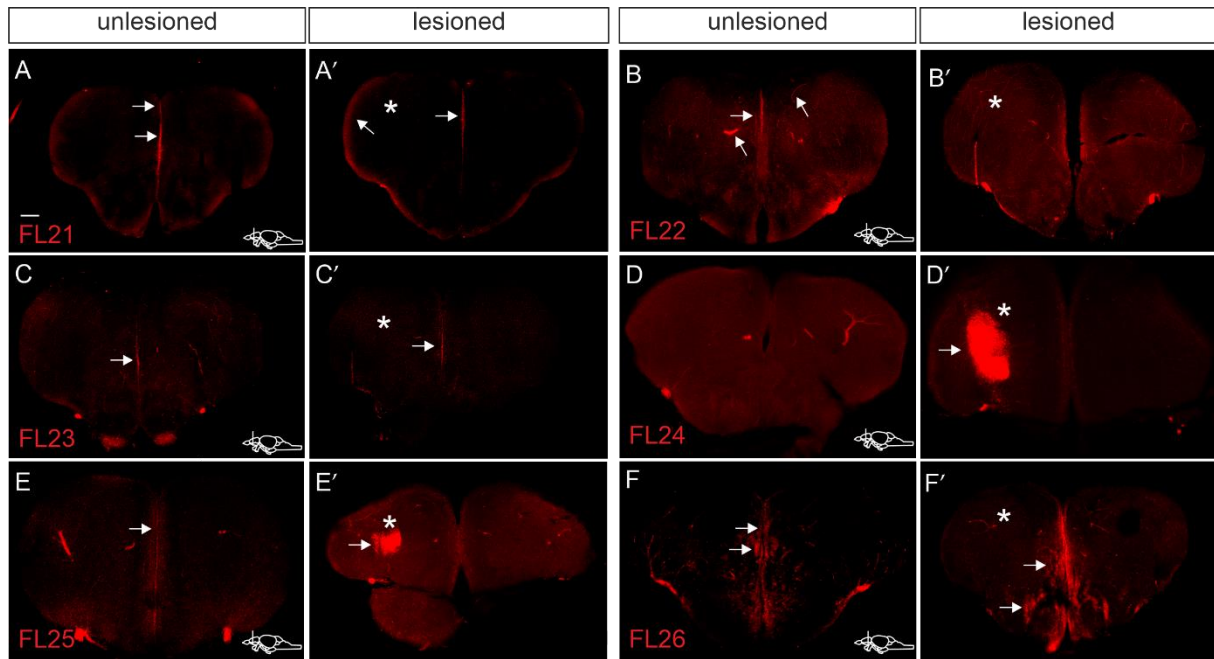


Figure 25: I-FISH probes against miRNA candidates are useful for detection of mature miRNA molecules. (A-F') FISH on telencephalic cross-sections using I-FISH probes (red) against *dre-miR-31* (A, A'), *dre-miR-96* (B, B'), *dre-miR-146a* (C, C'), *dre-miR-182* (D, D'), *dre-miR-183* (E, E') and *dre-miR-726* (F, F'). Most of the probes reported expression in the Vz (A-F') while some reported additional expression outside of the Vz (B, F). For *dre-miR-182* and *dre-miR-183* a strong signal was detected at the site of lesion after telencephalic lesion at 5 dpl (D', E'). The lesioned left hemisphere is marked with an asterisk. White arrows indicate areas where the I-FISH probe signal was perceived. Scheme in the lower right-hand corner of (A, B, C, D, E, F) indicates level of respective cross-section. Scale bar =100 μm

3.3 Visualization of key genes in the regulatory network with the help of individualized ssDNA FISH probes

In an effort to develop a method to easily visualize key genes of the GRN controlling NSC behavior in the adult zebrafish telencephalon in a time-saving and reliable manner, I again collaborated with organic chemists from the Wagenknecht group at the KIT. Together we worked on developing individualized ssDNA FISH probes (consequently called m-FISH probes) against the mRNA of different genes expressed in the zebrafish telencephalon. The design of the m-FISH probes was based on a concept involving 36 individually fluorescently labeled oligonucleotide probes that attach to one target mRNA molecule (Raj et al. 2008). This mix of 36 probes was designed in a way that it meets four basic requirements: (1) the first probe hybridizes close to the start codon of the gene (ATG). (2) The GC content of each individual probe is close to 50%. (3) At least ten nucleotides are positioned between each individual probe sequence. (4) Sequences of the mRNA which show high similarity with related genes are spared. In each individual probe, which is only 20 nt long, the most central thymidine was exchanged for a cU building block for the subsequent phosphoramidite solid phase synthesis that was already applied in the synthesis of the f- and I-FISH probes (see section 3.2.3 and dissertation of Larissa Doll, 2021) adding a Cy5-azide to each individual probe. The entire probe mix consisting of 36 probes

was synthesized against different candidate genes and applied in FISH experiments on cross-sections of WT telencephala.

3.3.1 Visualization of *sox9a* mRNA in the zebrafish telencephalon using m-FISH probes

The first set of m-FISH probes was designed against the mRNA of the gene *sox9a* (*SRY box containing transcription factor 9a*). In a previous screen for TR genes, over 1200 TRs in the zebrafish telencephalon were mapped and grouped according to their expression patterns (Diotel et al. 2015). *sox9a* was among the TRs which showed a specific and high expression in the Vz with additional weak expression in the parenchyma (Diotel et al. 2015).

In a chromogenic ISH against the mRNA of *sox9a*, I could confirm expression of the gene in the Vz, as well as the weak expression in the parenchyma, which was especially prominent in the posterior zone of the dorsal telencephalic area (Dp) (black arrows figure 26A). This ISH also served as comparison for the consequent analysis of m-FISH probes synthesized against the mRNA of *sox9a* on cross-sections of WT telencephala. The sections were counterstained with DAPI to visualize nuclei (figure 26). The signal of the m-FISH probes was mainly detected in the Vz but also outside, in the Dp (white arrows figure 26B). However, when comparing the reported expression pattern to the expression of the endogenous gene, the m-FISH probes displayed expression in a broad band of cells rather than a restricted line (white arrows figure 26C, C'). Strikingly, the localization of the DAPI staining and the signal of the m-FISH probes was highly similar (figure 26B, C').

According to the previously consulted RNA sequencing experiment comparing expression levels of genes between lesioned and unlesioned telencephalic tissue, *sox9a* is a gene which is upregulated at 5 dpl in response to telencephalic lesion (\log_2 fold change = 1.19) (Rodriguez Viales et al. 2015). This detected upregulation was also observed in an ISH on lesioned telencephalic cross-sections of adult zebrafish (figure 26D). Interestingly, the expression in the lesioned telencephalon seemed to expand and was now also detected in the Vc (black arrowhead in figure 26D). The m-FISH probes faithfully reported this upregulation in the lesioned left hemisphere of the telencephalon (white arrows figure 26E-F'). However, especially in the lesioned telencephalon it was obvious that the signal of the m-FISH probes was broader and not as restricted to the Vz as the expression pattern reported by the classical chromogenic ISH (compare figure 26D with figure 26E). The detected expression in the Vc of the telencephalon was also exhibited by the m-FISH probes in the telencephalon (white arrowhead figure 26E).

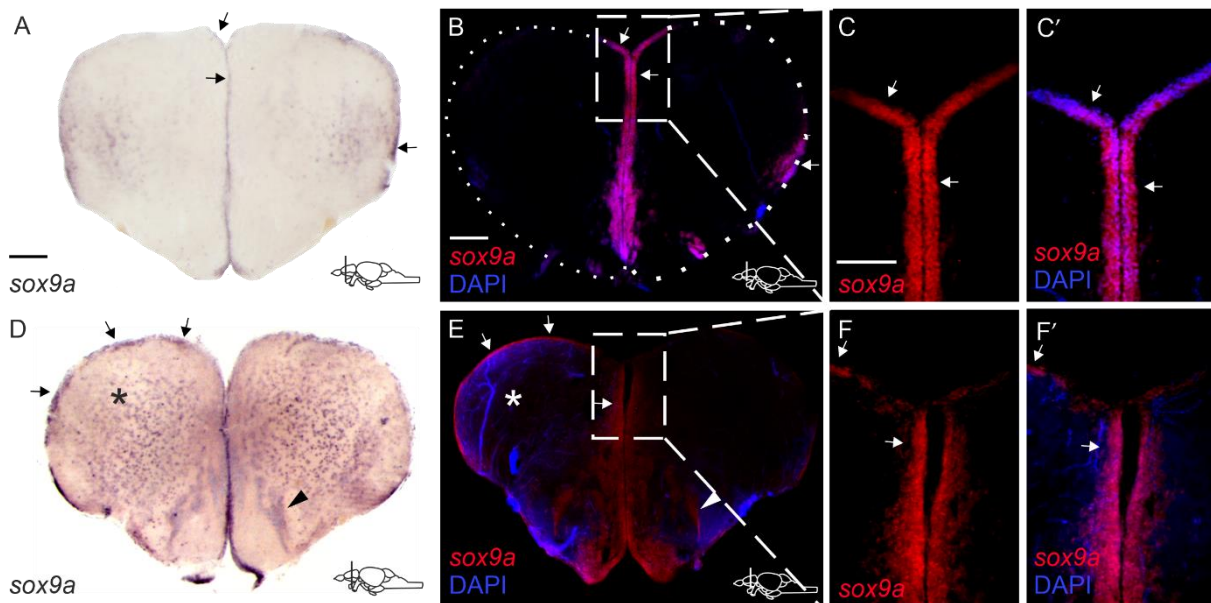


Figure 26: m-FISH probes against *sox9a* mRNA report the expression pattern of the endogenous gene and its upregulation in response to telencephalic lesion. (A, D) ISH using a DIG RNA probe against *sox9a* mRNA on cross-sections of unlesioned (A) and lesioned (D) WT telencephala. Expression was detected in the Vz of the telencephalon and in the parenchyma, especially in the Dp. (A) After lesion, *sox9a* expression was upregulated and additionally detected in the Vc (D). Black arrows indicate regions of expression. Black arrowhead points to Vc (D). (B-C', E-F') FISH using the m-FISH probes against *sox9a* mRNA (Cy5, red) on telencephalic cross-sections of WT zebrafish. Sections were counterstained with DAPI to label cell nuclei (blue). In the lesioned and in the unlesioned telencephalon, the signal from the m-FISH probes resembled the expression pattern of the endogenous gene but seemed to be detected in a broader stripe around the Vz. White boxed-in area in (B) and (E) represents area of magnification in (C-C') and (F-F') respectively. The lesioned hemisphere is indicated with an asterisk. White arrows indicate area of expression. White arrowhead in (E) points to expression in the Vc. Scheme in the lower right-hand corner of (A, B, D, E) indicates level of respective cross-section. Scale bar = 100 μm. Abbreviations: *sox9a*; *SRY box containing transcription factor 9a*

3.3.2 Co-expression studies conducted with the m-FISH probes against *sox9a*

The great advantage of having fluorescent probes available for FISH is the possibility to conduct co-expression studies. In order to decipher the function of a TR in a regulatory network controlling NSC behavior, it is important to identify their cellular location and in which cell type they are expressed. For this purpose, fluorescent probes are advantageous because they can be used in combination with Immunofluorescence (IF) or IHC experiments using antibodies against different cellular markers. Since previous experiments revealed that *sox9a* expression is restricted to the Vz of the telencephalon, I next tested the m-FISH probes against *sox9a* mRNA in combination with an antibody staining against the radial glial marker S100β (figure 27). Again, the m-FISH probes reported expression in the Vz, Vc and Dp (white arrows figure 27A). Co-localization with the signal for S100β was especially visible in the Vz between the two telencephalic hemispheres (white arrows figure 27B-B'). Taken together, the m-FISH probes are also feasible to be used in combination with IHC staining and located *sox9a* expression to RGCs in the zebrafish telencephalon.

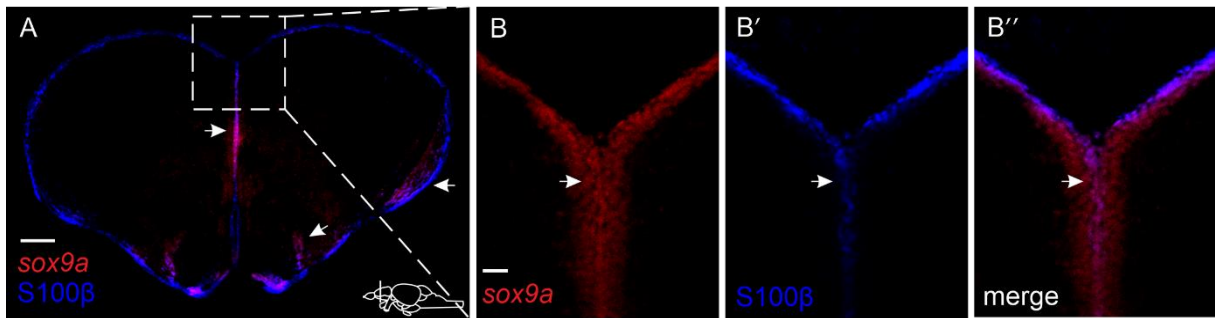


Figure 27: m-FISH probes can be used in combination with IHC to report cellular expression of *sox9a* in the adult zebrafish telencephalon. (A-B'') FISH using m-FISH probes against *sox9a* (red) in combination with IHC using an antibody against the RGC marker S100β (blue). Co-localization between the two signals was observed especially in the Vz indicating that *sox9a* is expressed in RGCs. White boxed-in area in (A) represents area of magnification in (B-B''). White arrows indicate areas where the signal of the m-FISH probes was detected. Scheme in the lower right-hand corner of (A) indicates level of cross-section. Scale bar = 100 μm in (A), 20 μm in (B, B', B'')

3.3.3 Visualization of *prdm12b* mRNA in the zebrafish telencephalon using m-FISH probes

Another gene that was identified as a TR and displayed a characteristic expression pattern in the zebrafish telencephalon was *prdm12b* (*PR domain containing 12 b*) (Diotel et al. 2015). In order to validate the functionality of the m-FISH method, I next selected this gene because it showed a characteristic expression pattern different from the one of *sox9a* (Diotel et al. 2015). m-FISH probes were synthesized against the mRNA of *prdm12b* following the same method as for *sox9a* and applied in a FISH experiment on cross-sections of the zebrafish adult telencephalon (figure 28). The signal for the m-FISH probes was detected in the Vv and Vc of the telencephalon (white arrows figure 28A-B'). This matched also the reported expression pattern for the gene *prdm12b* in the zebrafish telencephalon (Diotel et al. 2015). However, additional expression was detected in the Vz (white arrowhead figure 28A). The magnification depicts the area around the Vv and Vc as endogenous expression was reported in this area and also perceived a signal in the Vz (figure 28B, B'). The *prdm12b* m-FISH probes therefore reported an expression pattern that was broader than the expression pattern reported by classical chromogenic ISH using RNA-DIG probes (Diotel et al. 2015).

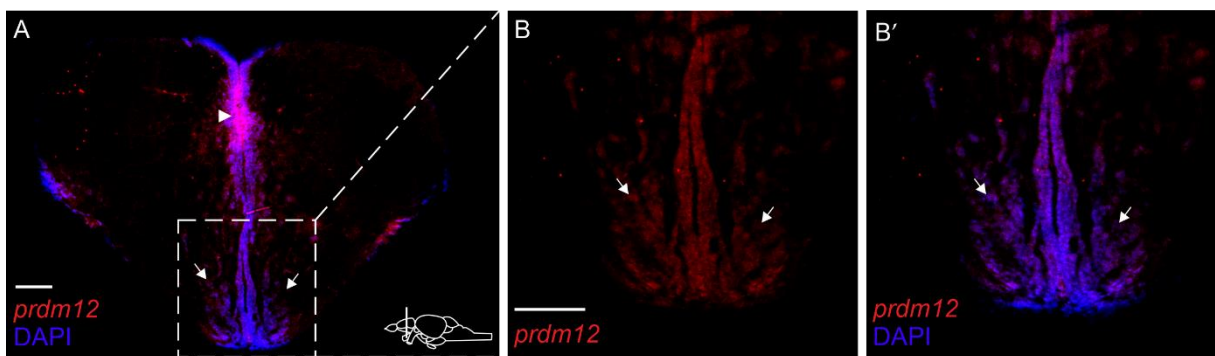


Figure 28: m-FISH probes against *prdm12b* mRNA fail to fully resemble the endogenous expression pattern of the *prdm12b* gene. (A-B') FISH using m-FISH probes (Cy5, red) against *prdm12b* mRNA on

cross-sections of the WT telencephalon counterstained with DAPI. The signal was mainly detected in the Vv, Vc and the Vz of the telencephalon. White arrows point to expression in the Vv and Vc. White arrowhead shows expression in the Vz. White boxed-in area in (A) depicts area of magnification in (B, B'). Scheme in the lower right-hand corner of (A) indicates level of respective cross-section. Scale bar = 100 μ m. Abbreviations: *prdm12b*, *PR domain containing 12b*

3.3.4 Visualization of *mdka* using m-FISH probes

Since I previously identified the specific cellular expression pattern of the gene *mdka* in the zebrafish telencephalon (see sections 3.1.2-3.1.6), I next wanted to test if the m-FISH probes are also applicable to this gene and would reliably label the specific location and the upregulation of gene expression in response to telencephalic lesion.

For that purpose, m-FISH probes against the gene *mdka* were synthesized similarly to the previously synthesized probes against *sox9a* and *prdm12b* and utilized in a FISH on cross-sections of unlesioned and lesioned (5 dpl) WT telencephala. The sections were counterstained with DAPI to visualize cell nuclei (figure 29). Without the lesion, the m-FISH probes reported *mdka* expression in the Vz of the telencephalon which matched the previously reported expression pattern (see section 3.1.2) (white arrows figure 29A, C). However, additional staining from the m-FISH probes was detected in the Vd and Vc which was also visible in a magnification of the area around the telencephalic ventricle (white arrows figure 29A, C). At 5 dpl, the signal from the m-FISH probes was more restricted to the Vz than in the unlesioned telencephalon and showed an increase in the lesioned left hemisphere (white arrow figure 29D, E). However, in the magnification it appeared that there was also some expression in the Vd (white arrow figure 29F). Additionally, in the magnification the overlap between DAPI staining and the signal from the m-FISH probes was also strikingly similar (figure 29F and F'). The expression pattern of *mdka* described by the m-FISH probes was therefore not as restricted as previously identified via classical FISH methods (see section 3.1.3) but reported the upregulation of the *mdka* expression level after telencephalic lesion.

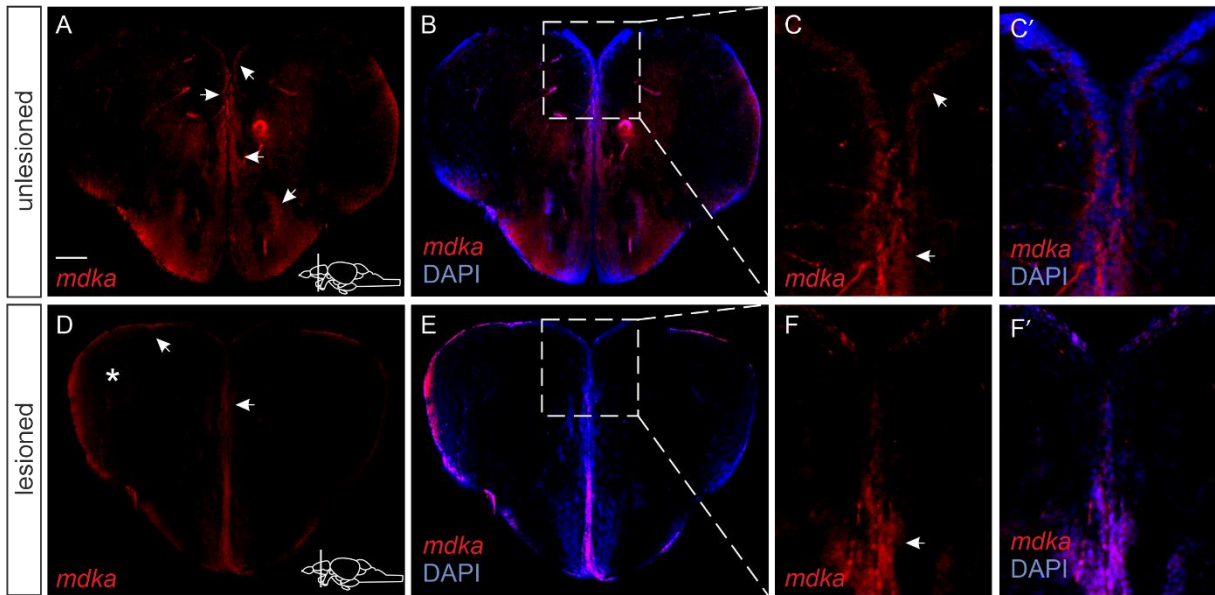


Figure 29: m-FISH probes against *mdka* mRNA report expression and upregulation of the *mdka* gene in response to lesion of the zebrafish telencephalon. (A-F') FISH using m-FISH probes against *mdka* mRNA on cross-sections of WT telencephala without (A-C') and with lesion at 5 dpl (D-F'), counterstained with DAPI. In the unlesioned telencephalon expression was reported in the Vz but also the Vd and Vc (A, C). After lesion, the signal for *mdka* mRNA was higher in the lesioned hemisphere and more restricted to the Vz (D-F'). An obvious co-localization between the m-FISH probe signal and DAPI could be observed especially in the magnification of the telencephalic ventricle in the lesioned and unlesioned telencephala (C', F'). The lesioned left hemisphere is marked with a white asterisk. White boxed-in area in (B, E) represent area of magnification in (C-C') and (F-F') respectively. White arrows point to areas where the signal from the m-FISH probes was detected. Scheme in the lower right-hand corner of (A, D) indicates level of respective cross-section. Scale bar = 100 μ m

4 Discussion

4.1 The expression of *mdka*, *mdkb* and *ptn* differ in the posterior embryo but overlap in the adult brain

When comparing the expression patterns of the three family members *mdka*, *mdkb* and *ptn* in the embryo all three mRNAs could be strongly detected in the brain regions, although in different specification (figure 10). Only *mdka* and *mdkb* were additionally observed in the neural tube (figure 10), showing their close evolutionary relationship as they are paralogues in the teleost genome (Winkler et al. 2003; Holland et al. 1994). Indeed, analysis of their phylogenetic relationship showed that *mdka* and *mdkb* emerged from a fish specific duplication which succeeded a block duplication giving rise to *midkine* and *pleiotrophin* (Winkler et al. 2003).

Interestingly, the mammalian orthologue *Mk* is also expressed in the brain and spinal cord of mouse embryos, but only detected in very low levels in adult tissue, except for high expression in the kidney (Kadomatsu et al. 1990; Sato and Kadomatsu 2012). In the adult brain, the human orthologue *MK* as well as *PTN* are only implicated in tumors (Mishima et al. 1997; Nakagawara et al. 1995). All the more interesting was the previous result of the RNA sequencing experiment showing that *mdka* is expressed in the zebrafish adult brain and even upregulated in response to injury (Gourain et al. 2021). According to the ISH of the zebrafish adult brain analysis in this thesis, *mdka*, *mdkb* and *ptn* expression was detected along the ventricular zone of the ventral and dorsal adult telencephalon (figure 11), an area which is considered to be the stem cell niche of the telencephalon because it harbors the cell bodies of RGCs, the stem cells of the telencephalon (Pellegrini et al. 2007). Since expression of all three family members was detected in this area, it is tempting to speculate that all are involved with processes controlling neurogenesis. However, the expression patterns of *mdkb* and *ptn* were broader and also detected in the different nuclei of the ventral telencephalon (figure 11). Considering the observed expression of *mdkb* and *ptn* in areas next to the Vz (figure 11), it is likely that they are also expressed by newborn neurons leaving the stem cell area to migrate to their target tissue. Overall, in the brain the expression patterns of all three family members were overlapping but distinct, an observation that was already implied by the embryo expression patterns and was also observed in other tissues like the zebrafish retina (Calinescu et al. 2009; Gramage, Li, and Hitchcock 2014). Seeing the differing expression patterns of the three family members in the zebrafish, their functions are set to also be diverse and possibly non redundant. It was already established that during development *mdka* affects somite morphology and specification of floorplate cells while *mdkb* promotes the growth of neural crest cells and plays a role during the formation of the neural plate border (Winkler et al. 2003; Winkler and Moon 2001; Liedtke and Winkler 2008). However, if the expression pattern allows to conclude

about the function, their function seems to be highly diverse from the function of *Mk* in higher vertebrates where there is no reported expression in the adult brain.

4.2 In response to telencephalic lesion *mdka* is upregulated in a delayed fashion

As previously mentioned, in an RNA sequencing experiment comparing the expression levels of genes between lesioned and unlesioned adult zebrafish telencephalic tissue at 5 dpl, *mdka* was recognized as a gene which showed a high degree of deregulation. The expression level of this gene was significantly increased in the lesioned telencephalic tissue compared to the unlesioned tissue (Gourain et al. 2021). In addition to the more restricted expression pattern in the adult zebrafish telencephalon (figure 11), this was also one reason why this work was mainly focused on the gene *mdka*, instead of its family members *mdkb* and *ptn*: they both showed no deregulation in response to telencephalic lesion. A change in expression levels in the stem cell area of the telencephalon indicates a possible involvement of the gene with reactive neurogenesis. I was able to confirm the detected upregulation in an ISH experiment conducted on zebrafish adult telencephala at 5 dpl and to quantify it in a RT-qPCR experiment (figure 14). However, when looking closely at the time course of expression the peak of expression after injury between 3 dpl and 5 dpl (figure 14) indicated a delayed response of *mdka* to the telencephalic lesion. This leads to the conclusion that *mdka* is not a gene which is involved with processes setting off immediately after the lesion, like the inflammatory response (Kyritsis et al. 2012a; Kizil, Kyritsis, et al. 2012). Rather, it implies that *mdka* is involved with mechanisms which are initiated in a delayed fashion and adopt maintenance and repair functions, including pushing the stem cells which started to proliferate in response to injury, back to quiescence. This is an important mechanism to avoid depletion of the stem cell pool. The observations reported in this thesis, including the lasting expression of *mdka* by qRGCs even after injury (figure 15) and the strong co-expression with *id1* (figure 13 and figure 15), a gene which is reportedly an important factor for maintaining stem cell quiescence, substantiate this hypothesis (Zhang et al. 2020; Zhang et al. 2021; Rodriguez Viales et al. 2015). Possibly, *mdka* is another pivotal factor for controlling stem cell behavior in the zebrafish adult telencephalon and sustaining the balance between quiescent and proliferating stem cells.

4.3 *mdka* expression is restricted to quiescent type I NSCs during constitutive and regenerative neurogenesis

In this work, I was able to show that expression of *mdka* in the adult zebrafish telencephalon is mainly detected in cells positive for the RGC marker S100 β (figure 12) which is in line with results from previously published single-cell data of the zebrafish brain (Lange et al. 2020). This was observed for constitutive, as well as regenerative neurogenesis (figure 12 and figure 15). Additionally, *mdka* expression did not co-localize with the marker for mature neurons HuC/D (figure 12). This observation

confirms previous reports in other adult tissues where *mdka* was shown to be mainly expressed by tissue specific stem cells, like the Müller glia of the adult zebrafish retina (Nagashima et al. 2020; Calinescu et al. 2009). Furthermore, *mdka* expression was restricted to non-proliferative cells, negative for the proliferation marker PCNA (figure 12 and figure 15). Taken together, this leads to the conclusion that in the adult zebrafish brain, *mdka* is expressed in non-proliferating RGCs and therefore quiescent type I stem cells. On a cellular level, this was further supported by the observation of high co-expression between the mRNAs of *mdka* and *id1*, a gene highly expressed in qRGCs and high-co-expression between the mRNA of *mdka* and cells positive for the *id1-CRM2* transgenic construct in a zebrafish transgenic line labeling qRGCs (figures 12, 13 and 15) (Rodriguez Viales et al. 2015; Zhang et al. 2020; Zhang et al. 2021). However, at least under regenerative conditions, opposing reports from studies in the zebrafish retina state that *mdka* is a gene which is expressed in activated tissue specific Müller glia (Calinescu et al. 2009). Additionally, loss of *mdka* is usually associated with decreased levels of proliferation after injury of the fin or after photoreceptor ablation in the retina (Nagashima et al. 2020; Ang et al. 2020). One explanation for this obvious contradiction could be the differing source of stem cells in the different examined tissues. For example, in the zebrafish retina, regeneration is dependent on Müller glia which first need to de-differentiate in order to re-enter the cell cycle and give rise to multipotent Müller glia progenitor cells (MPGCs) by one asymmetric division. MPGCs can consequently replace lost neurons (Raymond et al. 2006). In the zebrafish fin, osteoblast de-differentiate in order to provide progenitor cells for the repair of lesioned fin rays after injury (Sehring and Weidinger 2020). In contrast to that, the telencephalon harbors a constitutive pool of quiescent NSCs which can be recruited upon injury and by different modes of division give rise to neuroblasts, which are committed progenitors. Therefore, they do not have to undergo the additional step of de-differentiation and conversion into neuroblasts is facilitated by differing ways (Ghaddar et al. 2021). Considering the different molecular mechanisms underlying regeneration by tissue specific stem cells, *mdka* does not necessarily have to play the same role in these different processes and cells. Although since the retina, as part of the eye is derived from the brain a close relationship would be expected, small changes in the molecular context can already have a substantial impact on signaling pathways and mechanisms (Schmitt and Dowling 1994). This fact is already apparent when considering the slight differences in expression patterns between *mdka* and *mdkb* leading to diverse function in the retina (Calinescu et al. 2009). An in-depth analysis of the function of *mdka* and its gene product Mdk is therefore needed to solve this apparent contradiction.

4.4 Function of the *mdka* gene product Mdk is implicated in cell cycle regulation and proliferative pathways

Interestingly, in other organs than the brain, *mdka* function has already been investigated considering different mechanisms of action. It is for example known to act through its downstream effector *id2a* in regulating cell-cycle progression in the zebrafish retina (Luo et al. 2012; Nagashima et al. 2020). Additionally, it facilitates the formation of a fibrotic scar and promotes the repair of cardiac injury by controlling angiogenesis and extracellular matrix (ECM) components in zebrafish hearts (Grivas, González-Rajal, and de la Pompa 2021). The intriguing suggestion that in the retina there is a close relationship between cell-cycle progression and the control of stem cell proliferation by *mdka* could possibly also be transferred to analyses in the zebrafish forebrain, especially since the retina is derived from the brain (Schmitt and Dowling 1994; Luo et al. 2012; Nagashima et al. 2020).

In this work the relationship between cell-cycle kinetics and the control of NSC proliferation by *mdka* was investigated through gain-of-function and loss-of-function experiments. Overexpression of *mdka* in cells lining the telencephalic ventricle lead to a reduction in the number of proliferating cells in comparison to a control construct (figure 16). However, cerebroventricular microinjection of vivo-morpholinos into the telencephalic ventricle of adult zebrafish to test the opposite effect after blocking *mdka* did not lead to an anticipated increase in the number of proliferating cells (data not shown). Although, the possibility that simply the transfection of the vivo-morpholinos into the ventricular cells was unsuccessful should be considered since the efficiency of a morpholino knockdown is highly dependent on the expression level of the gene of interest, morpholino concentration and knockdown period (Kizil and Brand 2011; Kizil et al. 2013). Since this experiment was only conducted twice, a critical concentration or knockdown period could not be reliably determined. Usually, the efficiency rises from 12 hours after the cerebroventricular microinjection and can be up to 80% depending on the targeted gene (Kizil and Brand 2011; Kizil et al. 2013). Therefore, this experiment should be repeated in the future. Also, when comparing the number of proliferative cells in telencephalic cross-sections of *mdka* mutants (*mdka^{mi5001}*) with the number of proliferative cells in the telencephalon of WT siblings, there was no significant change in the behavior of NSCs (data not shown) (Nagashima et al. 2020).

Likewise, when employing a small molecule inhibitor for the *mdka* gene product, called inhibitor for Mdk (iMDK), there was initially a strong and obvious increase in the PCNA signal but consequent quantification of PCNA+ cells in the stem cell niche did not indicate a significant difference in comparison to telencephala treated with DMSO (figure 17) (Hao et al. 2013). Since quantification was restricted to the ventricular zone and the observed increase in fluorescent signal was mainly located in the parenchyma and in the case of lesioned telencephala, around the lesion site (figure 17), it is however still possible that overall proliferation is increased independent of or in addition to stem cell proliferation.

As a growth factor, Mk exerts its function through interaction with different receptors to activate different pathways. It interacts, among others, with anaplastic lymphoma kinase (ALK), Protein Tyrosine Phosphatase (PTP) and lipoprotein receptor related protein (LRP) which activates the PI3 kinase (PI3K)-AKT pathway (Muramatsu 2002). This pathway is implicated in cell-cycle regulation and promotes proliferation and anti-apoptotic activities (Owada et al. 1999; Dudek et al. 1997). The small molecule compound iMDK reportedly selectively inhibits the Mk mediated PI3K/AKT pathway and with this leads to increased apoptosis (Hao et al. 2013). The apparent contradiction that blocking a proliferation promoting pathway leads to more proliferation could be explained by a possible neuroprotective effect in that proliferation is increased in the zebrafish brain to replace neurons which are lost due to increased apoptosis. A neuroprotective effect of MK in rat, mouse and chick retina and in the human CNS has already been implicated in past studies (Gramage, Li, and Hitchcock 2014; Campbell et al. 2021; Muramatsu and Kadomatsu 2014; Unoki et al. 1994; Herradón and Pérez-García 2014).

In order to test whether the increase in proliferation is due to apoptosis, I conducted a TUNEL staining on unlesioned iMDK treated zebrafish telencephala (data not shown). This staining did however, not indicate an increase in the number of apoptotic cells due to iMDK treatment which implies that likely the method of uptake of iMDK over the fish' gills was unsuccessful. In this case, the observed increase of proliferating cells in the unlesioned iMDK treated telencephalon was likely due to unspecific binding of the PCNA antibody and in the lesioned iMDK treated telencephalon due to the telencephalic lesion (figure 17). As there are to date no other studies applying iMDK to zebrafish, I used a similar treatment regimen as was performed on axolotl by (Tsai, Baselga-Garriga, and Melton 2020), the only report where the drug was used in-vivo on whole animals. However, like the mammalian CNS, the zebrafish CNS possesses several barriers inhibiting the uptake of small molecules including the blood-brain-barrier (BBB) (Umans and Taylor 2012). Therefore, for further testing of the drug, other techniques like cerebroventricular microinjection should be considered to specifically target the cells lining the telencephalic ventricle and circumvent a possible blockage of drug uptake by the BBB.

Overall, overexpression of *mdka* indicated a function of the gene in regulating proliferative behavior but experiments to further substantiate this observation, so far yielded unclear results. However, upregulation in response to injury support the notion that Mdka is involved in neuroprotection in order to quickly replace neurons which are lost due to injury. Numerous reports assign a neuroprotective and also a regenerative function to midkine in multiple species and in multiple tissues but its implication in cell-cycle regulation is most accepted (Winkler and Yao 2014; Luo et al. 2012). The apparent contradiction of *mdka* mRNA being expressed in qRGCs and the suggestion that Mdka is important to regulate cell-cycle kinetics can be eradicated by the fact that Mdka is a secreted factor.

Therefore, the spatial expression of the *mdka* mRNA and the location of action of the protein do not have to overlap. Nevertheless, the mechanisms of action of Mdka remain elusive.

4.5 Combination of different computational analyses assigned four promising enhancer elements to the gene *mdka*

One key question is which factors control the specific and restricted expression of *mdka* in qRGCs during constitutive and regenerative neurogenesis. Six different putative enhancer regions, called CRMs, for the gene *mdka* could be identified using ATAC sequencing of lesioned and unlesioned adult telencephala (figure 18A). The aim of ATAC is to find possible regulatory elements through the mapping of chromatin-accessibility (Buenrostro et al. 2015). These CRMs were sought to be validated by comparative genomic approaches using the UCSC genome browser and the track hub provided by DANIO-CODE (figure 18B-C) (Baranasic et al. 2021).

Four of those putative enhancer regions proved to match with ATAC seq peaks from the DANIO-CODE track hub and also showed high conservation scores (figure 18). The region called CRM5 stood out in this analysis because it showed a full overlap with the exon 2 of the *mdka* gene which is part of the coding region (figure 18A). In order to validate the identified enhancer elements, in vivo testing in zebrafish was performed by creating transgenic lines for each putative CRM (figure 19) (Catarino and Stark 2018). The transgenic embryo carrying the CRM5 transgene best resembled expression of the endogenous *mdka* gene which can be explained by the spatial overlap of this element and exon2 (figure 18 and figure 19).

Strikingly, there is no obvious difference between the ATAC seq peaks from lesioned and unlesioned hemispheres (figure 18B-C) which would indicate an upregulation in response to injury and help to identify injury-specific elements. This is possibly due to the fact that an injury-induced upregulation would only occur in a few cells and can therefore not be detected by ATAC seq which takes all the cells in the analyzed hemisphere into account and leads therefore to a dilution of the signal.

The element CRM1 was considered special because in the ATAC seq of lesioned and unlesioned hemispheres a small peak could be observed which is why it was annotated as a CRM. However, after validation with the bioinformatics methods there was no conservation score and no overlap with any peaks from other ATAC sequencing experiments. It coincided with the coding region of another zebrafish gene, called *dgkza* indicating that CRM1 could serve as a regulatory element for this gene (figure 18B). Unfortunately, a comparison of the expression pattern of *dgkza* and the CRM1 element could not be performed because there is no record about the expression of the element in the 24 hpf embryo due to unsuccessful cloning.

The CRM6 element was identified and associated with *mdka* by Thompson et al. (2020) through ATAC sequencing of uninjured and regenerating caudal fin tissue and validated by in vivo editing of the

element in transgenic animals (Thompson et al. 2020). Since the analysis was performed on caudal fin regenerates, the absence of an ATAC peak after telencephalic lesion (figure 18C) could be due to the different mechanisms of regeneration in the two tissues (Thompson et al. 2020). Possibly, the CRM6 is a fin specific element which only reacts to injury since it also does not show up in ATAC sequencing from early developmental stages from the Skarmeta lab or unlesioned telencephalic tissue (figure 18C). In my analysis, I observed an overlap of CRM6 with the gene *tnnt3b* (figure 18C). The zebrafish gene *tnnt3b* is known to be important for the regulation of striated muscle contraction and is expressed in the somites during zebrafish development (Hsiao et al. 2003). The *Tg(mdka-CRM6-gata2a:EGFP)* transgenic line was observed to display expression in somites at 24 hpf (figure 19F). Considering this resemblance and the fact that CRM6 is about 280 kb downstream of the *mdka* gene, it is possible that CRM6 is rather a regulatory element for *tnnt3b*. However, since it did not show any co-localization with other ATAC seq peaks or a high conservation score (figure 18C), the possibility that CRM6 does not act as an enhancer should also be taken into account. A definite proof that the element can be allocated to *mdka* and serves as an enhancer cannot be presented and would need additional validation through other computational methods like conservation scores and ChIP sequencing (chromatin immunoprecipitation followed by high-throughput sequencing) targeting specific histone marks (Visel et al. 2009; Creighton et al. 2010). Admittedly, the reported long distance from the *mdka* gene is not sufficient to rule the element out as an enhancer of *mdka* since they are not always acting on the closest promoter but are known to jump neighboring promoters and regulate also more distant genes. Additionally, some enhancers have been found to regulate multiple genes which adds a layer of complexity to the identification of enhancer-gene pairs (Visel, Rubin, and Pennacchio 2009; Mohrs et al. 2001).

The more promising elements which also displayed an expression pattern in the 24 hpf embryo that was similar to the endogenous expression pattern, should be in the future investigated in the adult brain of the created transgenic lines regarding their specific cellular expression pattern and response to injury. For a better identification of which elements are closest related to *mdka*, it would be helpful to have a comparison via a transgenic line reporting the expression of *mdka*. This could be achieved by creating a knock-in line using CRISPR/Cas9 (Auer et al. 2014). Another approach to this was already started during my thesis and included the creation of an inducible *mdka* line providing the possibility to express the gene at the developmental stage and in the tissue of interest. For that purpose, I created a Gal4-driver line where the expression of Gal4 DNA binding domain (dbd) is under the regulation of a hsp70 heat-shock promoter. Furthermore, it contains a tamoxifen inducible ERT2 domain facilitating the relocation of the Gal4 protein to the nucleus, dependent on the application of tamoxifen. The UAS effector line controls expression of the *mdka* gene coupled to an EGFP reporter. So far, both constructs have been injected into zebrafish embryos and some fish were raised and identified via fin-clip (data

not shown). An outcross between those two lines can be used in the future as a reliable reporter for *mdka* expression and for comparing the expression of this reporter line to the CRM transgenic lines.

4.6 Regulation of *mdka* expression is multifaceted

Generally, regulation of a gene can occur at different levels and through different factors and regulatory systems. Thus, explicit regulation of the gene *mdka* was investigated in this work using multiple approaches.

Cell signaling pathways, pivotal for communication between and within cells facilitate their function through interaction of ligand and receptor and signaling molecules. They are important molecular mechanisms acting on target genes by regulating their transcription in a spatial and temporal manner. In the past, many signaling pathways including the BMP, Notch and Wnt pathways have been investigated for their involvement with adult neurogenesis (Diotel et al. 2020). In different studies, the Notch pathway was shown to be crucial for the control between the activated and quiescent state of neural precursors in the zebrafish (Chapouton et al. 2010; Diotel et al. 2020; Basak et al. 2012; Alunni et al. 2013; Than-Trong et al. 2018). Also, the Wnt pathway has been implicated to promote proliferation of neural precursors and just recently to be part of the cellular signature regulating the early wound healing stage after telencephalic lesion in the zebrafish (Demirci et al. 2020; Diotel et al. 2020; Urban and Guillemot 2014).

After observing a high co-expression of the genes *mdka* and *id1* in the zebrafish telencephalon (figure 13) and also a similar behavior in response to telencephalic lesion (figure 14 and figure 15) with regard to the timing of expression upregulation, the question arose if both genes are regulated by similar pathways (Rodriguez Viales et al. 2015). It is proven that the BMP pathway acts on *id1* and regulates its specific expression in the zebrafish adult telencephalon, both during constitutive and regenerative neurogenesis (Zhang et al. 2020). Furthermore, the *mdka* paralogue *mdkb* was shown to be under negative regulation by the BMP pathway (Winkler and Moon 2001). However, when the BMP pathway inhibitor DMH1 was administered to adult zebrafish via the fish water under homeostatic neurogenic conditions, no change in the expression of *mdka* could be observed (figure 20). The same was true after infliction of a telencephalic lesion (figure 20). Furthermore, when testing for *mdka* expression in telencephala of zebrafish from two heat-shock-inducible BMP transgenic lines either overexpressing *bmp2b*, a zebrafish ligand of the bmp pathway, [*Tg(hsp70:bmp2b)*] or blocking the bmp pathway through expression of the dominant-negative BMP receptor 1a mutant [*Tg(hs:dnBmpr1a)*] no change in the expression level of *mdka* could be detected (data not shown) (Chocron et al. 2007; Quillien et al. 2011). This indicates that *mdka* in contrast to its paralogue *mdkb* is not under the regulation of the BMP pathway (Winkler and Moon 2001).

Similarly, after inhibition of the Notch pathway via administration of the drug LY411575 or blocking of the Wnt/ β -catenin pathway with the drug IWR-1 under homeostatic neurogenic conditions, the expression level of *mdka* in the adult telencephalon was not found to be significantly altered (figure 21). Taken together, this shows that none of these three major signaling pathways influence *mdka* expression in the adult zebrafish telencephalon.

For regenerative neurogenesis, the inflammatory pathway is known to be a major force for inducing stem cell proliferation after brain injury in the zebrafish telencephalon (Kizil, Kyritsis, and Brand 2015; Kyritsis et al. 2012a). However, *mdka* expression levels in the adult telencephalon were not modified by Dexamethasone treatment, an inhibitor of the inflammatory response (data not shown). Likewise, sterile injection of Zymosan A did not lead to a change in *mdka* expression (data not shown). Hence, *mdka* is also independent of the inflammatory pathway under regenerative conditions.

In summary, the detailed regulation by signaling pathways of the gene *mdka* remains elusive but the investigation of putative CRMs holds the promise of identifying binding sites for TFs assigned to specific pathways. There is also evidence in the zebrafish retina that the gene *mdka* and also its paralogue *mdkb* are regulated by the circadian clock and are part of cyclical signaling episodes adding another aspect of regulation to the pool of regulatory mechanisms controlling *mdka* expression (Calinescu, Raymond, and Hitchcock 2009).

Along these lines, the identification of the basal promoter for the gene *mdka* also holds the chance of gaining more insight into *mdka* regulation. *Mk* was initially discovered as a retinoic acid (RA) responsive gene carrying a RA response element in its promoter region (Muramatsu 2014; Pedraza, Matsubara, and Muramatsu 1995). Application of exogenous RA was also reported to enhance the expression of the *mdka* paralogue *mdkb* during zebrafish development (Winkler and Moon 2001). Furthermore, the promoter of *Mk* was suggested to carry a regulatory element for hypoxia inducible factor 1 α (HIF-1 α), showing that *Mk* regulation is hypoxia dependent in mice (Reynolds et al. 2004b). The relationship between RA and *mdka* and HIF-1 α and *mdka* should be investigated deeper to decipher the regulation of the gene in addition to further experiments investigating different signaling pathways possibly influencing *mdka* expression.

On a post-transcriptional level, regulation of *mdka* could be facilitated through miRNAs. Indeed, when scanning putative targets for *dre-miR-146a*, *mdka* was recognized as a potential target through a sequence in the 3'UTR matching the seed region of *dre-miR-146a*. The regulation by miRNAs occurs on a different level as the previously discussed mechanisms: miRNAs attach to the mRNA of their targets and therefore block the translation to a protein via two different mechanisms (Bartel 2004; O'Brien et al. 2018). Hence, it is no contradiction that both RNA levels of *mdka* and *dre-miR-146a* were increased at 5 dpl in the RNA sequencing experiment although miRNAs negatively regulate their targets.

4.7 miRNAs play a pivotal role in the neurogenic regulatory network

The implication of the dynamic roles of miRNAs in the zebrafish brain has triggered a specific interest in the position of miRNAs within the GRN controlling adult neurogenesis (Lang and Shi 2012). The six miRNAs which showed the highest deregulation in response to injury in the zebrafish brain were *dre-miR-146a*, *dre-miR-31*, *dre-miR-96*, *dre-miR-182*, *dre-miR-183* and *dre-miR-726*. When analyzing potential targets of these miRNAs which also showed a downregulation after injury it became apparent that most of the miRNAs are involved in neurogenic processes targeting genes like *nrn1a* (table 14). However, *dre-miR-146a*, the gene which was upregulated the highest after telencephalic lesion, stood out after downregulated target analysis because most of the targets were rather associated with regulation of membrane repair, cytoplasm and cytoskeleton dynamics (table 14). This could be due to the fact that after lesion, neuronal pathways are not the only ones which are activated. A lesion also leads to the disruption of cells and blood vessels which need to be repaired in the process of wound healing, thereby upregulating pathways involved in membrane repair. In this case, *dre-miR-146a* could serve in controlling the translation of those genes. The observed expression pattern of *dre-miR-146a* in the zebrafish telencephalon which was not restricted to telencephalic stem cells but rather spread into the parenchyma of the telencephalon (figure 22), supports the hypothesis that *dre-miR-146a* is not solely involved in neurogenic processes in NSCs.

Nevertheless, further examination with the help of the target database TargetScanFish6.2 also identified the genes *mdka* and *s100b* as targets of *dre-miR-146a*. *s100b* gives rise to the protein S100 β which is widely accepted as a marker for radial glial cells, the stem cells of the telencephalon. When employing the pri-miRNA probe against *dre-miR-146a*, in a FISH experiment combined with IHC against S100 β on telencephalic cross-sections, I detected a high co-expression between the primary miRNA *dre-miR-146a* and the marker S100 β (data not shown), indicating that both genes are expressed in the same cell type and substantiating the finding of the computational analysis. Additionally, previous studies in the human brain indicated *miR-146a* as a regulator of early neuronal development and stem cell differentiation (Nguyen et al. 2018). Besides, *miR-146a* is the most common miRNA showing an upregulation in human neurodevelopmental disorders like autism spectrum disorder (ASD) and epilepsy (Nguyen et al. 2016; Iyer et al. 2012; Fregeac, Colleaux, and Nguyen 2016). Since miRNAs are strongly conserved within the vertebrate lineage and also the mammalian genome harbors the *miR-146a* family member, a similarity of *miR-146a* function between these two organisms is likely (Ordas et al. 2013).

Another recent study revealed that in the zebrafish telencephalon three miRNA candidates *dre-miR-31*, *dre-miR-146a* and *dre-miR-182* target genes which encode for enzymes of the cholesterol synthesis pathway. Therefore, these miRNAs play a role in regulating the dynamics of the cholesterol metabolism which is adapted after telencephalic lesion in the zebrafish telencephalon (Gourain et al. 2021).

Taken together, the results show that deciphering miRNA function is highly complex because through the shortness of their seed region, they can attach to a number of different mRNAs and therefore regulate a high number of different target genes and pathways. Conversely, one single gene can be targeted by a number of different miRNAs which is also shown in the analysis in this work (table 14). In order to gain further insight into the previously mentioned interesting relationship between *dre-miR-146a* and its reported target gene *mdka*, comprehensive methods to decipher miRNA-target relationships would be luciferase gene reporter assays and the employment of target protector morpholinos. The luciferase assay offers the chance to experimentally certify miRNA-target interactions which have been predicted via computational algorithms (Clément, Salone, and Rederstorff 2015; Jin et al. 2013). These algorithms are not always reliable and therefore further validation is needed. In the luciferase assay the predicted attachment site in the mRNA of the target gene and a mutated version of it are individually subcloned downstream of a luciferase gene and transfected together with a vector containing the specific miRNA. If there is no luciferase activity detected with the WT UTR but with the mutated version, it indicates that the miRNA can specifically bind to its target (Clément, Salone, and Rederstorff 2015; Jin et al. 2013). Target protector morpholinos are designed complementary to the miRNA binding site in the target mRNA and inhibit the interaction of the miRNA-mRNA pair which leads to a block of post-transcriptional inhibition exerted by the miRNA (Choi, Giraldez, and Schier 2007; Staton and Giraldez 2011). Both of these assays would also be applicable to test other miRNA-target interactions.

The efforts to visualize the expression of the miRNA candidates in the zebrafish adult telencephalon were not highly successful as the commercial LNA probes did not work in most cases. Therefore, ISH against the primary form of each candidate was performed and detected that all of the pri-miRNAs were mainly expressed in the ventricular zone of the telencephalon (figure 23). The expression patterns of *pri-miR-96*, *pri-miR-182* and *pri-miR-183* displayed a close resemblance (figure 23) which can be explained by the fact that they are members of one miRNA family in vertebrates and are positioned within 10 kb of each other defining them as miRNA cluster. Consequently, they are transcribed from the same genetic locus leading to high sequence similarity and also overlapping sets of target genes with similar function (Pierce et al. 2008; Woldemichael et al. 2016; Wang et al. 2016). In the zebrafish, the *mir-96/182/183* cluster is located on chromosome 4 and is encoded by a genetic region of about 1 kb (Fogerty et al. 2019). Due to the fact that I cloned about 200-300 bp for each miRNA in order to synthesize the pri-miR ISH probes from that region, the sequences of the probes are not similar but allocate to a similar genomic region. Hence, the probes report a similar expression pattern in the zebrafish telencephalon (figure 23). However, the function and role in adult neurogenesis of these miRNAs is likely overlapping as they regulate a similar set of target genes which was also observed in the RNA sequencing analysis (table 14) (Wang et al. 2016).

4.8 Development of LNA FISH probes for the detection of mature miRNA candidates in the adult zebrafish telencephalon

For the investigation of the function and role of individual miRNAs it is however more valuable to recognize the specific location of the mature miRNA as opposed to the primary form, because the pri-miRNA undergoes multiple steps of modification (Bartel 2004). For tackling the challenge of detecting mature miRNAs in the zebrafish telencephalon via easily applicable and time saving methods, I collaborated with Fabian Lang, an organic chemist from the Wagenknecht group at the KIT in the so called “FISH in fish” project.

The first set of ssDNA FISH probes (f-FISH) was quickly replaced by a more developed set of LNA (l-FISH) probes. The reason was that the f-FISH probes exhibited high fluorescent background when utilized in FISH experiments on adult zebrafish telencephala which was not the case for the LNA probes (figure 24). This was also proven in an individual experiment using a scrambled miRNA f-FISH probe which was synthesized with a random sequence that should not recognize a specific sequence in the genome. However, also this probe exhibited background staining, mainly in blood vessels, when applied to zebrafish telencephala (data not shown). This led to the conclusion that unspecific binding of the probes was high and the specificity of the probes against mature miRNAs needed to be improved. After application of l-FISH probes on cross-sections of WT telencephala the LNA probe against *dre-miR-31* was considered to have the strongest and most significant staining restricted to the ventricular zone of the telencephalon (figure 25A). Additionally, it reported an upregulation of *dre-miR-31* expression in the lesioned hemisphere at 5 dpl (figure 25A') which confirms findings from the RNA sequencing experiment. The probe against *dre-miR-146a*, the miRNA which was according to the RNA sequencing experiment deregulated the most after telencephalic lesion (table 14) failed to exhibit this deregulation but showed some weak signal in the Vz (figure 25C). The probes against *dre-miR-182* and *dre-miR-183* exhibited similar expression patterns with a strikingly high signal at the lesion site in the lesioned hemisphere (figure 25). The similarity of the signal pattern can again be explained by the clustering of these miRNAs in the genome (Woldemichael et al. 2016; Wang et al. 2016; Fogerty et al. 2019). However, the probe against the third member of this cluster, *dre-miR-96* exhibited a vastly different expression pattern (figure 25B-B'). To doubtlessly validate that the LNA probes report the correct expression patterns of miRNA candidates in the zebrafish telencephalon, a comparison to regular ISH probes would be needed. Unfortunately, ISH using commercially available LNA probes only worked in the case of *dre-miR-146a* and the positive control *dre-miR-9* (figure 22). For *dre-miR-146a* the expression patterns reported in the chromogenic ISH and the FISH using l-FISH probes were somewhat similar (compare figure 22 with figure 25) but further improvement of both methods is needed to decipher the expression of the miRNA candidates on a molecular level and allow conclusions about their specific functions during neurogenesis.

The reason why the probes lead to inconclusive results is that the target molecule is very short which can easily lead to unspecific binding of the probes. Consequently, very high hybridization and washing temperatures are needed to increase specificity of detection. Therefore, one improvement for the I-FISH probes on a technical level could be to change the conformation of the hybridization buffer. The used buffer contains 50% formamide which is a chemical used to decrease melting temperature while maintaining chromosomal structures (Zhang et al. 2015). In this case, since the LNA modified I-FISH probes are highly stable, a high hybridization and also washing temperature would be desirable to ensure stability of the attachment between probe and miRNA. Therefore, decreasing the amount of formamide in the hybridization buffer could lead to improvements of detection (Zhang et al. 2015). Furthermore, when focusing on the lesioned telencephala, it becomes obvious that the signal of the I-FISH probes was only strongly increased in three of the six cases (figure 25), which is in striking contrast to the RNA sequencing experiment reporting all of the candidates as being upregulated after telencephalic lesion as this was also the selection requirement. Additionally, only *dre-miR-31* was reported to be upregulated specifically in the ventricular zone of the telencephalon by the I-FISH probes (figure 25A') indicating involvement with NSC behavior. This difference can be explained by the fact that the RNA sequencing experiment was conducted using entire hemispheres. In this case, also cells which are not part of the telencephalic stem cell niche are taken into account and deregulation of expression in other parts of the telencephalon or at the lesion site, as in the case of *dre-miR-182* and *dre-miR-183*, is considered. In order to reliably analyze deregulation of expression levels only in the stem cell niche, FACS (fluorescence activated cell sorting) using transgenic zebrafish lines which fluorescently label NSCs would have to be employed followed by RNA sequencing (Di Giaimo, Aschenbroich, and Ninkovic 2019).

In an effort to improve the visualization I, again in collaboration with Fabian Lang, developed and tested FRET (Förster resonance energy transfer) probes. These probes are based on a three-way junction-based FRET method where two different strands, one carrying a Cy3, the other one carrying a Cy5 fluorophore, partly attach to the targeted miRNA and partly to each other. Via this attachment, the fluorophores are brought into close proximity of each other which allows FRET to take place and results in a fluorescent signal (Luo et al. 2018). A first set of probes against the miRNA *dre-miR-9* was already tested on zebrafish telencephalon sections but was so far unsuccessful (data not shown). Nevertheless, this method can be improved and further tested to allow easy and specific detection of mature miRNA molecules in the zebrafish adult telencephalon.

4.9 Individualized FISH probes against mRNAs are suitable to report expression of endogenous genes

In another segment of the “FISH in fish” project, I initially collaborated with Larissa Doll, also from the Wagenknecht group at the KIT with the aim of developing fluorescent probes which can be applied in FISH experiments against the mRNA of genes playing a key role in the regeneration of the zebrafish CNS. These m-FISH probes were based on a method where 36 individual probes were synthesized against one mRNA target and individually conjugated with a fluorophore in order to improve fluorescent detection and the signal-to-noise ratio and therefore the resolution of the resulting images (Raj et al. 2008). Since this technique demonstrated no novelty, the long-term aim of this project part was to improve the method for detection of low abundant molecules and also to use them in single molecule detection.

The first approach was with the gene *sox9a* which has been implicated as a transcription factor involved in neural regeneration and does not only show a restricted expression pattern which would help to validate the FISH method but is also reported to be upregulated after telencephalic injury (figure 26) (Scott et al. 2010; Diotel et al. 2015). After determining the correct hybridization temperature for the m-FISH probes with the help of hybridization studies, which was different from the initial report of the method, I applied the probes in several FISH experiments (Raj et al. 2008). The m-FISH probes against *sox9a* could successfully recapitulate the expression pattern of the endogenous gene in the zebrafish telencephalon, report the upregulation in response to injury and be successfully employed in a combined FISH-IHC experiment on telencephalic sections, locating *sox9a* expression to RGCs in the ventricular zone of the telencephalon (figure 26 and figure 27).

Afterwards, the chemistry part of the project was taken over by Julian Gebhard, from the Wagenknecht group. In collaboration with him I developed and applied m-FISH probes for the genes *prdm12b* which shows a distinct expression pattern in the telencephalon that is different from *sox9a*, and *mdka*, a gene whose expression pattern in the zebrafish telencephalon was extensively studied in this thesis (Diotel et al. 2015). For both cases, the resemblance of the m-FISH probes to the endogenous expression pattern was striking (figure 28 and figure 29). Additionally, in the case of *mdka*, the upregulation of expression level after telencephalic lesion was also faithfully reported by the m-FISH probes (figure 29).

However, taking all the experiments together, the probes appeared to have two main issues. Especially in the case of the *sox9a* and *prdm12b* m-FISH probes, the reported expression patterns appeared to be slightly broader and less restricted than the endogenous expression patterns of the targeted genes (figures 26 and figure 28). This observation could likely be due to the shortness of the individual probes in the m-FISH probe mix. Each of the individual sequences is only about 17 nt long which increases the chance of binding to other highly similar sequences in the genome. *sox9a* is a member of a broader

family of SRY (sex determining region Y) box transcription factors which also contains the *sox9a* paralogue *sox9b* in the teleost genome (Cresko et al. 2003). The gene *prdm12b* is also a member of a large gene family which is characterized by a conserved N-terminal PR domain. (Fog, Galli, and Lund 2012; Hohenauer and Moore 2012). This increases the likelihood that conserved or homologous sequences are present which could then be recognized by a proportion of the short m-FISH probe mix. Indeed, the expression pattern reported with the m-FISH probes against *sox9a* mRNA could likely be due to an overlap between *sox9a* and *sox9b* expression, as expression of the *sox9b* gene was detected in the medial zone of the dorsal telencephalon in an ISH experiment (data not shown). In conclusion, the recognition of sequence similarities especially poses a problem if genes are targeted which are part of broad gene family or have close homologues.

This obstacle was tried to be ruled out by next applying the method for the gene *mdka* which is a member of a smaller gene family only containing two more members in the zebrafish genome (Winkler et al. 2003; Muramatsu 2002; Matsumoto et al. 1994). Therefore, the availability of highly similar sequences is decreased. Nevertheless, despite showing a fairly restricted signal in the ventricular zone of the zebrafish telencephalon (figure 29), a striking similarity with the co-applied DAPI staining in the telencephala was observed which was also detected with the m-FISH probes against *prdm12b* (figure 28). This observation arouse suspicion that the m-FISH probes are interacting with DNA in the cell nucleus and therefore leading to unspecific fluorescent signals. Indeed, when comparing thermal stability, the ssDNA probes exhibited higher melting temperatures in probe-DNA duplexes than in probe-RNA duplexes (see dissertation of Fabian Lang, 2021).

One consideration that has to be taken into account is that the sole weakness of the m-FISH probes is not their specificity of detection but also high fluorescent background. The company molecular instruments developed probes for the recognition of molecules via FISH based on hybridization chain reaction (HCR) eliminating this problem (Dirks and Pierce 2004). They use the same basic principle of having a set of short probes which hybridize to different subsequences of the target, which is also the basis of the m-FISH probes. However, the major difference is that the HCR probes rely on a method where only a specifically bound pair of probes can be recognized by the HCR amplifier through an HCR initiator. Consequently, a fluorescent HCR amplification polymer is built, using the target bound probe pair as a starting point. Thereby, two major weaknesses are addressed: the fluorescence is increased based on only short probes which leads to reduced background and only specifically bound probe pairs can give rise to a fluorescent signal, eradicating unspecific signals (Choi et al. 2018; Schwarzkopf et al. 2021; Choi et al. 2010; Trivedi et al. 2018).

One way to improve the m-FISH probes that was already considered is to increase the length of the individual probes while simultaneously increasing the number of fluorophores per strand by having multiple fluorophore modifications. With this, the number of probes could be adapted from 36

individually labeled probes to, for example twelve longer probes with three fluorophore modifications each, increasing specificity of the probe mix while maintaining the total number of fluorophores.

Another improvement for the probes that we attempted was the development of hybridization sensitive probes based on forced intercalation (FIT) to allow the use of only very few probes for specific detection of RNA molecules (Hövelmann et al. 2014). The probes are about 20 bp long and attach to different parts of the target mRNA. They are coupled with an indole based cyanide dye which intercalates into nucleic acids. The dye molecules can emit absorbed energy when they rotate around their own central double binding but when this rotation is inhibited by intercalation, then the energy is emitted as fluorescence and can be detected. Therefore, the probes will only emit fluorescence once they are hybridized with the specific target molecule. As a first try, Julian Gebhard provided me with a set of four different probes which attach to different, not overlapping regions of the *mdka* mRNA but no specific results could be obtained so far (data not shown).

However, considering the successful employment of HCR probes from molecular instruments in FISH on different tissues and whole mount applications, a combination of improved detection and increased fluorescence should be considered for the m-FISH probes (Trivedi et al. 2018; Schwarzkopf et al. 2021). Taken together, the approach of the m-FISH probes firstly yielded promising results but technical limitations need to be decreased for doubt-free application of the method in the adult zebrafish telencephalic tissue.

5 Conclusion and future perspectives

The aim of this study was to identify key players in the GRN which regulates NSC behavior in the zebrafish adult telencephalon.

Here, I described the gene *mdka* regarding its expression pattern in the zebrafish adult brain and its expression pattern at cellular resolution in response to stab wound of the adult telencephalon. Remarkably, *mdka* expression was found to be restricted to quiescent stem cells under constitutive as well as under regenerative conditions and also to be upregulated in response to telencephalic lesion displaying a peak of expression at 5 dpl, indicating a key role of this gene in the control of stem cell behavior. This study adds *mdka* to the molecular signature of quiescent type I stem cells in the zebrafish telencephalon.

However, regulation and function of the gene was already implicated to be highly complex, a notion which was supported by findings in this work. Evidence from other organism and tissues in which Mk is clearly implicated in promoting proliferation of neural precursor cells and the fact that it serves as a ligand for ALK which induces pro-proliferative pathways in many cell types and was proven to promote cell proliferation in the zebrafish nervous system, contradict the findings from the overexpression experiment in this study (Reiff 2011; Stoica et al. 2002; Matsumoto et al. 1994; Yao et al. 2013). This experiment suggested that *mdka* confers quiescence to RGCs and should be considered misleading regarding the function of the gene. However, as already discussed most of the other observations were not made in the adult zebrafish telencephalon where different functional pathways could be active and interfering. Furthermore, *Mdka* is a pleiotropic molecule involved in a high number of different pathways and with a variety of different functions in the nervous system (Winkler and Yao 2014). Therefore, the difficulty in defining the exact function of the molecule remains (Ross-Munro et al. 2020)

In order to draw conclusions about the regulation of the gene, which helps to embed the gene in the regulatory network controlling NSC behavior and neurogenesis in the zebrafish telencephalon, the approach to decipher regulatory elements via different bioinformatics sources was promising. By extending this method and consequent testing of the identified elements for their expression in the transgenic zebrafish adult brain, as well as their response to injury, one could identify the elements which are necessary for the specific expression of *mdka* in the telencephalon under constitutive and regenerative conditions. Analysis of the putative regulatory elements opens up the possibility to identify binding sites on these elements and consequently associate regulatory pathways upstream of those binding sites and the gene *mdka*. An approach to also identify the minimal promoter for the gene which gives more conclusion about *mdka* regulation, is underway in the lab and should be extended.

The attempt to employ pri-miRNA probes to visualize expression of miRNA candidates in the zebrafish telencephalon was successful. Nevertheless, it is more valuable to visualize the mature form of a miRNA to allow conclusions about their functions. Therefore, more visual and functional assays are needed which was already approached by employing I-FISH probes against the miRNA candidates. However, this technique proved to be in need of technical improvements to reliably label the cellular location of the miRNA candidates in the adult zebrafish telencephalon.

Also, the development of individualized and easy-to-use probes against mRNAs in the zebrafish adult brain was successfully employed and reported expression of targeted mRNAs and in some cases their upregulation in response to telencephalic lesion. However, as already mentioned, the technique seems to be limited for the detection of genes with highly unique sequences which are low abundant in the zebrafish genome.

Taken together, the “FISH in fish project” gave rise to a variety of approaches and starting points to improve and develop the detection of molecules in the zebrafish adult telencephalon in the future. Most of the probes are already synthesized and ready to be used and advanced by thorough testing in the future.

In summary, this work provides insight into the spatial and temporal expression of the gene *mdka*, a gene which is possibly crucial for the maintenance of the NSC pool in the adult zebrafish telencephalon, under regenerative and homeostatic conditions. Furthermore, some insights into regulation and function of the gene are given in addition to several approaches, tools and techniques which can be used as foundation and developed further in the future in order to visualize and investigate key genes and small molecules regulating neurogenesis in the zebrafish adult brain. A thorough understanding of the interplay, regulation and function of these key factors will provide the basis for the development of drugs to battle pathological conditions including neurodegenerative diseases in humans.

6 Acknowledgements

First I would like to show my appreciation towards my professor, Uwe Strähle. Thank you for giving me the opportunity to not only complete my PhD but also my master's and my bachelor's thesis in your lab and under your supervision. Through all this time I learned to become an independent researcher and I am thankful for your help and criticism on posters, presentations, publications and ultimately this dissertation.

As well, I would like to thank Thomas Dickmeis for being my second supervisor and supporting me throughout the last years.

I would like to express my deep gratitude to Sepand for your reassurance and help through all the years. I have always valued your scientific opinion and insight on all my half-year reports, posters and especially this thesis. I am very thankful that you gave me the opportunity to contribute to a number of publications and to be a part of the MDPI special issue, both of which enabled me to develop a feeling for scientific writing and editing. I think we made a great team and were able to tackle a number of challenges throughout the years. However, you were not solely a scientific supervisor for me. Thank you for being my friend and mentor beyond the role of a supervisor and listening to my concerns when I was questioning my own work. Through all the time I greatly enjoyed our scientific and private talks and the occasional gossip we exchanged. Thank you for always being encouraging and supporting even during the most stressful times but also critical when I needed it. You gave me the courage to move forward but also taught me to think critically and to develop an idea of where my strengths and weaknesses are which helped me to figure out into which field of work I would like to go next.

A great thanks goes to the GRK2039, especially to Franzi, who has helped me a lot during the last days of the PhD. My gratitude goes also to Prof. Wagenknecht, Dr. Larissa Doll, Dr. Fabian Lang and Julian Gebhard for the insightful and interesting collaboration which gave me scientific understandings beyond the field of biology and the zebrafish brain. Thank you for making the chemistry part of the project understandable. Overall, I am thankful that I had the opportunity to be part of the GRK2039. It did not only provide me with helpful soft skills for the future but also with great experiences during all the retreats and seminar days with the other members. The scientific exchange with students from other fields and the many opportunities we were given will help me a lot in the future.

A special thanks to Tanja. With your always positive attitude and your willingness to answer all my questions you created a very positive working atmosphere in the lab. Thanks also to Anne. I always enjoyed chatting with both of you during lunchtime or at our lab gatherings about topics which were not only focused on work and often provided much needed distraction. Thank you for your scientific

and experimental help which already started when I was a bachelor's student. Furthermore, I would like to thank our postdoc Masa for always answering my questions and scientific support with cloning, imaging and a lot of other things. Overall, I had a great experience in the lab through all the years which I think is not the norm and you guys contributed a great part to the positive atmosphere.

All the best to the next generation of PhD students in our lab, Fushun, Jincan and Gökhan. I wish you the best of luck with your theses and do not forget: A PhD is hard work but I know that you can do it.

At this point I would also like to thank our students Agnes, Barbara and Sabrina. You have helped me a lot in the lab by taking over experiments. But more than that you were also fantastic company and support during the last months. I greatly enjoyed working alongside with you. You are all hard workers and I am sure you have a great career ahead of you. I wish you all the best for your future.

A special thanks goes to the girls, Amra and Miriam. You guys were my support system until the last day inside and outside of the lab and without you I would have had a lot more mental breakdowns. I am genuinely thankful that you always listened to me no matter if it was private or work problems that I needed to talk about. I would also like to mention Patrizia here. I am thankful for the joyful moments that all of us were able to share. Its not usual to have such close friends at work and I am extremely grateful for that. Amra and Patrizia, I wish you all the best in your new career paths. Miriam, believe in yourself. I am 100% confident that you will achieve a great PhD like so many before you. I hope that we will all stay in close contact in the future.

Außerdem möchte ich allen Menschen abseits vom Labor für ihre Unterstützung danken. Dazu gehört mein Freund, Dennis. Danke besonders für deine Unterstützung und Verständnis während dieser ganzen Zeit. Danke fürs Auffangen, Ablenken, Begleiten, Zuhören, Schokolade liefern, Aufmuntern und vieles Mehr.

Das gleiche gilt für meine Freunde, die immer allen meinen, auch wissenschaftlichen, Problemen zugehört haben auch wenn sie oft nichts verstanden haben. Eure kreativen Wege Ablenkung zu finden haben all die Jahre sehr dazu beigetragen, dass ich nicht komplett in meiner Arbeit versunken bin.

Zu guter Letzt möchte ich auch ganz herzlich meiner Familie für ihre Unterstützung und Beistand während des gesamten Studiums und der Zeit des Doktors danken. Ohne euch wäre ich sicher nicht so weit gekommen. Danke.

7 Literature

- Ables, J. L., N. A. Decarolis, M. A. Johnson, P. D. Rivera, Z. Gao, D. C. Cooper, F. Radtke, J. Hsieh, and A. J. Eisch. 2010. 'Notch1 is required for maintenance of the reservoir of adult hippocampal stem cells', *J Neurosci*, 30: 10484-92.
- Adolf, B., P. Chapouton, C. S. Lam, S. Topp, B. Tannhauser, U. Strahle, M. Gotz, and L. Bally-Cuif. 2006. 'Conserved and acquired features of adult neurogenesis in the zebrafish telencephalon', *Dev Biol*, 295: 278-93.
- Ahituv, Nadav, Edward M. Rubin, and Marcelo A. Nobrega. 2004. 'Exploiting human–fish genome comparisons for deciphering gene regulation', *Human Molecular Genetics*, 13: R261-R66.
- Alexandre, P., A. M. Reugels, D. Barker, E. Blanc, and J. D. Clarke. 2010. 'Neurons derive from the more apical daughter in asymmetric divisions in the zebrafish neural tube', *Nat Neurosci*, 13: 673-9.
- Altman, J. 1969. 'Autoradiographic and histological studies of postnatal neurogenesis. IV. Cell proliferation and migration in the anterior forebrain, with special reference to persisting neurogenesis in the olfactory bulb', *The Journal of comparative neurology*, 137: 433-57.
- Altman, J., and G. D. Das. 1965. 'Autoradiographic and histological evidence of postnatal hippocampal neurogenesis in rats', *The Journal of comparative neurology*, 124: 319-35.
- Alunni, A., and L. Bally-Cuif. 2016. 'A comparative view of regenerative neurogenesis in vertebrates', *Development*, 143: 741-53.
- Alunni, A., M. Krecsmarik, A. Bosco, S. Galant, L. Pan, C. B. Moens, and L. Bally-Cuif. 2013. 'Notch3 signaling gates cell cycle entry and limits neural stem cell amplification in the adult pallium', *Development*, 140: 3335-47.
- Amor, S., F. Puentes, D. Baker, and P. van der Valk. 2010. 'Inflammation in neurodegenerative diseases', *Immunology*, 129: 154-69.
- Amsterdam, A., S. Burgess, G. Golling, W. Chen, Z. Sun, K. Townsend, S. Farrington, M. Haldi, and N. Hopkins. 1999. 'A large-scale insertional mutagenesis screen in zebrafish', *Genes Dev*, 13: 2713-24.
- Amsterdam, A., and N. Hopkins. 2006. 'Mutagenesis strategies in zebrafish for identifying genes involved in development and disease', *Trends Genet*, 22: 473-8.
- Andersson, E. R., R. Sandberg, and U. Lendahl. 2011. 'Notch signaling: simplicity in design, versatility in function', *Development*, 138: 3593-612.
- Ang, Nicholas B., Alfonso Saera-Vila, Caroline Walsh, Peter F. Hitchcock, Alon Kahana, Ryan Thummel, and Mikiko Nagashima. 2020. 'Midkine-a functions as a universal regulator of proliferation during epimorphic regeneration in adult zebrafish', *PLoS One*, 15: e0232308.
- Artavanis-Tsakonas, S., K. Matsuno, and M. E. Fortini. 1995. 'Notch signaling', *Science*, 268: 225-32.
- Artavanis-Tsakonas, S., M. D. Rand, and R. J. Lake. 1999. 'Notch signaling: cell fate control and signal integration in development', *Science*, 284: 770-6.
- Auer, T. O., K. Duroure, A. De Cian, J. P. Concordet, and F. Del Bene. 2014. 'Highly efficient CRISPR/Cas9-mediated knock-in in zebrafish by homology-independent DNA repair', *Genome Res*, 24: 142-53.
- Bae, Y. K., S. Kani, T. Shimizu, K. Tanabe, H. Nojima, Y. Kimura, S. Higashijima, and M. Hibi. 2009. 'Anatomy of zebrafish cerebellum and screen for mutations affecting its development', *Dev Biol*, 330: 406-26.
- Bai, G., N. Sheng, Z. Xie, W. Bian, Y. Yokota, R. Benezra, R. Kageyama, F. Guillemot, and N. Jing. 2007. 'Id sustains Hes1 expression to inhibit precocious neurogenesis by releasing negative autoregulation of Hes1', *Dev Cell*, 13: 283-97.
- Baranasic, Damir, Matthias Hörtenhuber, Piotr Balwierz, Tobias Zehnder, Abdul Kadir Mukarram, Chirag Nepal, Csilla Varnai, Yavor Hadzhiev, Ada Jimenez-Gonzalez, Nan Li, Joseph Wragg, Fabio D'Orazio, Noelia Díaz, Benjamín Hernández-Rodríguez, Zelin Chen, Marcus Stoiber, Michaël Dong, Irene Stevens, Samuel E. Ross, Anne Eagle, Ryan Martin, Pelumi Obasaju, Sepand Rastegar, Alison C. McGarvey, Wolfgang Kopp, Emily Chambers, Dennis Wang,

- Hyejeong R. Kim, Rafael D. Acemel, Silvia Naranjo, Maciej Lapinski, Vanessa Chong, Sinnakaruppan Mathavan, Bernard Peers, Tatjana Sauka-Spengler, Martin Vingron, Piero Carninci, Uwe Ohler, Scott Allen Lacadie, Shawn Burgess, Cecilia Winata, Freek van Eeden, Juan M. Vaquerizas, José Luis Gómez-Skarmeta, Daria Onichtchouk, Ben James Brown, Ozren Bogdanovic, Monte Westerfield, Fiona C. Wardle, Carsten O. Daub, Boris Lenhard, and Ferenc Müller. 2021. 'Integrated annotation and analysis of genomic features reveal new types of functional elements and large-scale epigenetic phenomena in the developing zebrafish', *bioRxiv*: 2021.08.09.454869.
- Barbosa, J. S., R. Sanchez-Gonzalez, R. Di Giaimo, E. V. Baumgart, F. J. Theis, M. Gotz, and J. Ninkovic. 2015. 'Neurodevelopment. Live imaging of adult neural stem cell behavior in the intact and injured zebrafish brain', *Science*, 348: 789-93.
- Bartel, David P. 2004. 'MicroRNAs: Genomics, Biogenesis, Mechanism, and Function', *Cell*, 116: 281-97.
- Basak, O., C. Giachino, E. Fiorini, H. R. Macdonald, and V. Taylor. 2012. 'Neurogenic subventricular zone stem/progenitor cells are Notch1-dependent in their active but not quiescent state', *J Neurosci*, 32: 5654-66.
- Baumgart, E. V., J. S. Barbosa, L. Bally-Cuif, M. Gotz, and J. Ninkovic. 2012. 'Stab wound injury of the zebrafish telencephalon: a model for comparative analysis of reactive gliosis', *Glia*, 60: 343-57.
- Benner, E. J., D. Luciano, R. Jo, K. Abdi, P. Paez-Gonzalez, H. Sheng, D. S. Warner, C. Liu, C. Eroglu, and C. T. Kuo. 2013. 'Protective astrogenesis from the SVZ niche after injury is controlled by Notch modulator Thbs4', *Nature*, 497: 369-73.
- Bertrand, N., D. S. Castro, and F. Guillemot. 2002. 'Proneural genes and the specification of neural cell types', *Nature reviews. Neuroscience*, 3: 517-30.
- Bhattacharai, P., A. K. Thomas, M. I. Cosacak, C. Papadimitriou, V. Mashkaryan, C. Froc, S. Reinhardt, T. Kurth, A. Dahl, Y. Zhang, and C. Kizil. 2016. 'IL4/STAT6 Signaling Activates Neural Stem Cell Proliferation and Neurogenesis upon Amyloid-beta42 Aggregation in Adult Zebrafish Brain', *Cell Rep*, 17: 941-48.
- Bhattacharai, P., A. K. Thomas, M. I. Cosacak, C. Papadimitriou, V. Mashkaryan, Y. Zhang, and C. Kizil. 2017. 'Modeling Amyloid-β42 Toxicity and Neurodegeneration in Adult Zebrafish Brain', *J Vis Exp*.
- Bhattacharai, P., A. K. Thomas, Y. Zhang, and C. Kizil. 2017. 'The effects of aging on Amyloid-β42-induced neurodegeneration and regeneration in adult zebrafish brain', *Neurogenesis (Austin)*, 4: e1322666.
- Bier, E., and E. M. De Robertis. 2015. 'EMBRYO DEVELOPMENT. BMP gradients: A paradigm for morphogen-mediated developmental patterning', *Science*, 348: aaa5838.
- Bohrer, C., S. Pfurr, K. Mammadzada, S. Schildge, L. Plappert, M. Hils, L. Pous, K. S. Rauch, V. I. Dumit, D. Pfeifer, J. Dengjel, M. Kirsch, K. Schachtrup, and C. Schachtrup. 2015. 'The balance of Id3 and E47 determines neural stem/precursor cell differentiation into astrocytes', *The EMBO journal*, 34: 2804-19.
- Boldrini, M., C. A. Fulmore, A. N. Tartt, L. R. Simeon, I. Pavlova, V. Poposka, G. B. Rosoklija, A. Stankov, V. Arango, A. J. Dwork, R. Hen, and J. J. Mann. 2018. 'Human Hippocampal Neurogenesis Persists throughout Aging', *Cell Stem Cell*, 22: 589-99 e5.
- Bond, A. M., O. G. Bhalala, and J. A. Kessler. 2012. 'The dynamic role of bone morphogenetic proteins in neural stem cell fate and maturation', *Dev Neurobiol*, 72: 1068-84.
- Broglio, C., A. Gomez, E. Duran, F. M. Ocana, F. Jimenez-Moya, F. Rodriguez, and C. Salas. 2005. 'Hallmarks of a common forebrain vertebrate plan: specialized pallial areas for spatial, temporal and emotional memory in actinopterygian fish', *Brain Res Bull*, 66: 277-81.
- Buenrostro, J. D., B. Wu, H. Y. Chang, and W. J. Greenleaf. 2015. 'ATAC-seq: A Method for Assaying Chromatin Accessibility Genome-Wide', *Curr Protoc Mol Biol*, 109: 21.29.1-21.29.9.
- Burda, J. E., A. M. Bernstein, and M. V. Sofroniew. 2016. 'Astrocyte roles in traumatic brain injury', *Exp Neurol*, 275 Pt 3: 305-15.

- Burns, Kevin A., Brian L. Murphy, Steve C. Danzer, and Chia-Yi Kuan. 2009. 'Developmental and post-injury cortical gliogenesis: A Genetic fate-mapping study with Nestin CreER mice', *Glia*, 57.
- Calinescu, Anda-Alexandra, Pamela A. Raymond, and Peter F. Hitchcock. 2009. 'Midkine expression is regulated by the circadian clock in the retina of the zebrafish', *Visual neuroscience*, 26: 495-501.
- Calinescu, Anda-Alexandra, Thomas S. Vihtelic, David R. Hyde, and Peter F. Hitchcock. 2009. 'Cellular expression of midkine-a and midkine-b during retinal development and photoreceptor regeneration in zebrafish', *The Journal of comparative neurology*, 514: 1-10.
- Campbell, Warren A., Amanda Fritsch-Kelleher, Isabella Palazzo, Thanh Hoang, Seth Blackshaw, and Andy J. Fischer. 2021. 'Midkine is neuroprotective and influences glial reactivity and the formation of Müller glia-derived progenitor cells in chick and mouse retinas', *Glia*, 69: 1515-39.
- Carpentier, Pamela A., and Theo D. Palmer. 2009. 'Immune Influence on Adult Neural Stem Cell Regulation and Function', *Neuron*, 64: 79-92.
- Carron, Simone F., Dasuni S. Alwis, and Ramesh Rajan. 2016. 'Traumatic Brain Injury and Neuronal Functionality Changes in Sensory Cortex', *Frontiers in Systems Neuroscience*, 10.
- Carter, D., L. Chakalova, C. S. Osborne, Y. F. Dai, and P. Fraser. 2002. 'Long-range chromatin regulatory interactions in vivo', *Nat Genet*, 32: 623-6.
- Castor, N., and F. El Massioui. 2018. 'Traumatic brain injury and stroke: does recovery differ?', *Brain Inj*, 32: 1803-10.
- Castro, D. S., B. Martynoga, C. Parras, V. Ramesh, E. Pacary, C. Johnston, D. Drechsel, M. Lebel-Potter, L. G. Garcia, C. Hunt, D. Dolle, A. Bithell, L. Ettwiller, N. Buckley, and F. Guillemot. 2011. 'A novel function of the proneural factor *Ascl1* in progenitor proliferation identified by genome-wide characterization of its targets', *Genes Dev*, 25: 930-45.
- Catarino, R. R., and A. Stark. 2018. 'Assessing sufficiency and necessity of enhancer activities for gene expression and the mechanisms of transcription activation', *Genes Dev*, 32: 202-23.
- Cavaliere, Fabio, Monica Benito-Muñoz, and Carlos Matute. 2016. 'Organotypic Cultures as a Model to Study Adult Neurogenesis in CNS Disorders', *Stem Cells International*, 2016.
- Chambeyron, S., and W. A. Bickmore. 2004. 'Chromatin decondensation and nuclear reorganization of the *HoxB* locus upon induction of transcription', *Genes Dev*, 18: 1119-30.
- Chang, E. H., I. Adorjan, M. V. Mundim, B. Sun, M. L. Dizon, and F. G. Szele. 2016. 'Traumatic Brain Injury Activation of the Adult Subventricular Zone Neurogenic Niche', *Front Neurosci*, 10: 332.
- Chapouton, P., P. Skupien, B. Hesl, M. Coolen, J. C. Moore, R. Madelaine, E. Kremmer, T. Faus-Kessler, P. Blader, N. D. Lawson, and L. Bally-Cuif. 2010. 'Notch activity levels control the balance between quiescence and recruitment of adult neural stem cells', *J Neurosci*, 30: 7961-74.
- Chapouton, P., K. J. Webb, C. Stigloher, A. Alunni, B. Adolf, B. Hesl, S. Topp, E. Kremmer, and L. Bally-Cuif. 2011. 'Expression of hairy/enhancer of split genes in neural progenitors and neurogenesis domains of the adult zebrafish brain', *The Journal of comparative neurology*, 519: 1748-69.
- Chen, Baozhi, Michael E. Dodge, Wei Tang, Jianming Lu, Zhiqiang Ma, Chih-Wei Fan, Shuguang Wei, Wayne Hao, Jessica Kilgore, Noelle S. Williams, Michael G. Roth, James F. Amatruda, Chuo Chen, and Lawrence Lum. 2009. 'Small molecule-mediated disruption of Wnt-dependent signaling in tissue regeneration and cancer', *Nature chemical biology*, 5: 100-07.
- Chen, Z., Y. Omori, S. Koren, T. Shirokiya, T. Kuroda, A. Miyamoto, H. Wada, A. Fujiyama, A. Toyoda, S. Zhang, T. G. Wolfsberg, K. Kawakami, A. M. Phillippy, J. C. Mullikin, and S. M. Burgess. 2019. 'De novo assembly of the goldfish (*Carassius auratus*) genome and the evolution of genes after whole-genome duplication', *Sci Adv*, 5: eaav0547.
- Cheng, J. H., D. Z. Pan, Z. T. Tsai, and H. K. Tsai. 2015. 'Genome-wide analysis of enhancer RNA in gene regulation across 12 mouse tissues', *Sci Rep*, 5: 12648.
- Chocron, Sonja, Manon C. Verhoeven, Fabian Rentzsch, Matthias Hammerschmidt, and Jeroen Bakkens. 2007. 'Zebrafish *Bmp4* regulates left-right asymmetry at two distinct developmental time points', *Developmental Biology*, 305: 577-88.

- Choe, Y., S. J. Pleasure, and H. Mira. 2015. 'Control of Adult Neurogenesis by Short-Range Morphogenic-Signaling Molecules', *Cold Spring Harb Perspect Biol*, 8: a018887.
- Choi, Harry M. T., Joann Y. Chang, Le A. Trinh, Jennifer E. Padilla, Scott E. Fraser, and Niles A. Pierce. 2010. 'Programmable in situ amplification for multiplexed imaging of mRNA expression', *Nature biotechnology*, 28: 1208-12.
- Choi, Harry M. T., Maayan Schwarzkopf, Mark E. Fornace, Aneesh Acharya, Georgios Artavanis, Johannes Stegmaier, Alexandre Cunha, and Niles A. Pierce. 2018. 'Third-generation in situ hybridization chain reaction: multiplexed, quantitative, sensitive, versatile, robust', *Development*, 145.
- Choi, Wen-Yee, Antonio J. Giraldez, and Alexander F. Schier. 2007. 'Target Protectors Reveal Dampening and Balancing of Nodal Agonist and Antagonist by miR-430', *Science*, 318: 271-74.
- Clarke, J. 2009. 'Role of polarized cell divisions in zebrafish neural tube formation', *Curr Opin Neurobiol*, 19: 134-8.
- Clément, T., V. Salone, and M. Rederstorff. 2015. 'Dual luciferase gene reporter assays to study miRNA function', *Methods Mol Biol*, 1296: 187-98.
- Cohen, Sivan, Or-yam Shoshana, Einat Zelman-Toister, Nitsan Maharshak, Inbal Binsky-Ehrenreich, Maya Gordin, Inbal Hazan-Halevy, Yair Herishanu, Lev Shvidel, Michal Haran, Lin Leng, Richard J. Bucala, Sheila Harroch, and Idit Shachar. 2012. 'The Cytokine Midkine and Its Receptor RPTSn Regulate B Cell Survival in a Pathway Induced by CD74', *The Journal of Immunology*, 188: 259 - 69.
- Coolen, M., D. Thieffry, Ø Drivenes, T. S. Becker, and L. Bally-Cuif. 2012. 'miR-9 controls the timing of neurogenesis through the direct inhibition of antagonistic factors', *Dev Cell*, 22: 1052-64.
- Coolen, Marion, Shauna Katz, and Laure Bally-Cuif. 2013. 'miR-9: a versatile regulator of neurogenesis', *Frontiers in Cellular Neuroscience*, 7.
- Covacu, Ruxandra, and Lou Brundin. 2017. 'Effects of Neuroinflammation on Neural Stem Cells', *The Neuroscientist*, 23: 27 - 39.
- Cresko, William A., Yi-Lin Yan, David A. Baltrus, Angel Amores, Amy Singer, Adriana Rodríguez-Marí, and John H. Postlethwait. 2003. 'Genome duplication, subfunction partitioning, and lineage divergence: Sox9 in stickleback and zebrafish', *Developmental Dynamics*, 228: 480-89.
- Creyghton, M. P., A. W. Cheng, G. G. Welstead, T. Kooistra, B. W. Carey, E. J. Steine, J. Hanna, M. A. Lodato, G. M. Frampton, P. A. Sharp, L. A. Boyer, R. A. Young, and R. Jaenisch. 2010. 'Histone H3K27ac separates active from poised enhancers and predicts developmental state', *Proc Natl Acad Sci U S A*, 107: 21931-6.
- Dahm, Ralf, Robert Geisler, and Christiane Nüsslein-Volhard. 2006. 'Zebrafish (Danio rerio) Genome and Genetics.' in, *Reviews in Cell Biology and Molecular Medicine*.
- Dale, C Trevor. 1998. 'Signal transduction by the Wnt family of ligands', *Biochemical Journal*, 329: 209-23.
- Davidson, E. H. 2010. 'Emerging properties of animal gene regulatory networks', *Nature*, 468: 911-20.
- Davidson, Eric H. 2001. *Genomic regulatory systems: in development and evolution* (Elsevier).
- Davis, Robert Lesley, and David L Turner. 2001. 'Vertebrate hairy and Enhancer of split related proteins: transcriptional repressors regulating cellular differentiation and embryonic patterning', *Oncogene*, 20: 8342-57.
- De Santa, F., I. Barozzi, F. Mietton, S. Ghisletti, S. Polletti, B. K. Tusi, H. Muller, J. Ragoussis, C. L. Wei, and G. Natoli. 2010. 'A large fraction of extragenic RNA pol II transcription sites overlap enhancers', *PLoS Biol*, 8: e1000384.
- Demirci, Yeliz, Gokhan Cucun, Yusuf Kaan Poyraz, Suhaib Mohammed, Guillaume Heger, Irene Papatheodorou, and Gunes Ozhan. 2020. 'Comparative Transcriptome Analysis of the Regenerating Zebrafish Telencephalon Unravels a Resource With Key Pathways During Two Early Stages and Activation of Wnt/ β -Catenin Signaling at the Early Wound Healing Stage', *Frontiers in Cell and Developmental Biology*, 8.

- Dennis, C. V., L. S. Suh, M. L. Rodriguez, J. J. Kril, and G. T. Sutherland. 2016. 'Human adult neurogenesis across the ages: An immunohistochemical study', *Neuropathol Appl Neurobiol*, 42: 621-38.
- Di Giaimo, Rossella, Sven Aschenbroich, and Jovica Ninkovic. 2019. 'Fluorescence-Activated Cell Sorting-Based Isolation and Characterization of Neural Stem Cells from the Adult Zebrafish Telencephalon.' in Barbara Di Benedetto (ed.), *Astrocytes: Methods and Protocols* (Springer New York: New York, NY).
- Dimou, Leda, Christian Simon, Frank Kirchhoff, Hirohide Takebayashi, and Magdalena Götz. 2008. 'Progeny of Olig2-Expressing Progenitors in the Gray and White Matter of the Adult Mouse Cerebral Cortex', *The Journal of Neuroscience*, 28: 10434 - 42.
- Ding, M., Y. Liu, X. Liao, H. Zhan, Y. Liu, and W. Huang. 2018. 'Enhancer RNAs (eRNAs): New Insights into Gene Transcription and Disease Treatment', *J Cancer*, 9: 2334-40.
- Diotel, N., R. Rodriguez Viales, O. Armant, M. Marz, M. Ferg, S. Rastegar, and U. Strahle. 2015. 'Comprehensive expression map of transcription regulators in the adult zebrafish telencephalon reveals distinct neurogenic niches', *The Journal of comparative neurology*, 523: 1202-21.
- Diotel, N., C. Vaillant, M. M. Gueguen, S. Mironov, I. Anglade, A. Servili, E. Pellegrini, and O. Kah. 2010. 'Cxcr4 and Cxcl12 expression in radial glial cells of the brain of adult zebrafish', *The Journal of comparative neurology*, 518: 4855-76.
- Diotel, N., C. Vaillant, O. Kah, and E. Pellegrini. 2016. 'Mapping of brain lipid binding protein (Blbp) in the brain of adult zebrafish, co-expression with aromatase B and links with proliferation', *Gene Expr Patterns*, 20: 42-54.
- Diotel, Nicolas, Thierry D. Charlier, Christian Lefebvre d'Hellencourt, David Couret, Vance L. Trudeau, Joel C. Nicolau, Olivier Meilhac, Olivier Kah, and Elisabeth Pellegrini. 2018. 'Steroid Transport, Local Synthesis, and Signaling within the Brain: Roles in Neurogenesis, Neuroprotection, and Sexual Behaviors', *Frontiers in Neuroscience*, 12.
- Diotel, Nicolas, Luisa Lübke, Uwe Strähle, and Sepand Rastegar. 2020. 'Common and Distinct Features of Adult Neurogenesis and Regeneration in the Telencephalon of Zebrafish and Mammals', *Frontiers in Neuroscience*, 14: 568930-30.
- Diotel, Nicolas, Yann Le Page, Karen Mouriec, Sok-Keng Tong, Elisabeth Pellegrini, Colette Vaillant, Isabelle Anglade, François Brion, Farzad Pakdel, Bon-chu Chung, and Olivier Kah. 2010. 'Aromatase in the brain of teleost fish: Expression, regulation and putative functions', *Frontiers in Neuroendocrinology*, 31: 172-92.
- Dirks, Robert M., and Niles A. Pierce. 2004. 'Triggered amplification by hybridization chain reaction', *Proceedings of the National Academy of Sciences*, 101: 15275-78.
- Djebali, S., C. A. Davis, A. Merkel, A. Dobin, T. Lassmann, A. Mortazavi, A. Tanzer, J. Lagarde, W. Lin, F. Schlesinger, C. Xue, G. K. Marinov, J. Khatun, B. A. Williams, C. Zaleski, J. Rozowsky, M. Röder, F. Kokocinski, R. F. Abdelhamid, T. Alioto, I. Antoshechkin, M. T. Baer, N. S. Bar, P. Batut, K. Bell, I. Bell, S. Chakraborty, X. Chen, J. Chrast, J. Curado, T. Derrien, J. Drenkow, E. Dumais, J. Dumais, R. Duttagupta, E. Falconnet, M. Fastuca, K. Fejes-Toth, P. Ferreira, S. Foissac, M. J. Fullwood, H. Gao, D. Gonzalez, A. Gordon, H. Gunawardena, C. Howald, S. Jha, R. Johnson, P. Kapranov, B. King, C. Kingswood, O. J. Luo, E. Park, K. Persaud, J. B. Preall, P. Ribeca, B. Risk, D. Robyr, M. Sammeth, L. Schaffer, L. H. See, A. Shahab, J. Skancke, A. M. Suzuki, H. Takahashi, H. Tilgner, D. Trout, N. Walters, H. Wang, J. Wrobel, Y. Yu, X. Ruan, Y. Hayashizaki, J. Harrow, M. Gerstein, T. Hubbard, A. Reymond, S. E. Antonarakis, G. Hannon, M. C. Giddings, Y. Ruan, B. Wold, P. Carninci, R. Guigó, and T. R. Gingeras. 2012. 'Landscape of transcription in human cells', *Nature*, 489: 101-8.
- Doetsch, F., J. M. García-Verdugo, and A. Alvarez-Buylla. 1997. 'Cellular composition and three-dimensional organization of the subventricular germinal zone in the adult mammalian brain', *J Neurosci*, 17: 5046-61.

- Doganli, C., M. Sandoval, S. Thomas, and D. Hart. 2017. 'Assay for Transposase-Accessible Chromatin with High-Throughput Sequencing (ATAC-Seq) Protocol for Zebrafish Embryos', *Methods Mol Biol*, 1507: 59-66.
- Dong, Z., N. Yang, S. Y. Yeo, A. Chitnis, and S. Guo. 2012. 'Intralineage directional Notch signaling regulates self-renewal and differentiation of asymmetrically dividing radial glia', *Neuron*, 74: 65-78.
- Doniach, T., and T. J. Musci. 1995. 'Induction of anteroposterior neural pattern in *Xenopus*: evidence for a quantitative mechanism', *Mech Dev*, 53: 403-13.
- Doolittle, W. F. 2013. 'Is junk DNA bunk? A critique of ENCODE', *Proc Natl Acad Sci U S A*, 110: 5294-300.
- Doyon, Y., J. M. McCammon, J. C. Miller, F. Faraji, C. Ngo, G. E. Katibah, R. Amora, T. D. Hocking, L. Zhang, E. J. Rebar, P. D. Gregory, F. D. Urnov, and S. L. Amacher. 2008. 'Heritable targeted gene disruption in zebrafish using designed zinc-finger nucleases', *Nature biotechnology*, 26: 702-8.
- Driever, W, L Solnica-Krezel, AF Schier, SC Neuhauss, J Malicki, DL Stemple, DY Stainier, F Zwartkruis, S Abdelilah, and Z Rangini. 1996. 'A genetic screen for mutations affecting embryogenesis in zebrafish', *Development*, 123: 37-46.
- Dudek, H., S. Datta, Thomas Franke, Morris Birnbaum, R. J. Yao, G. Cooper, Rosalind Segal, David Kaplan, and M. Greenberg. 1997. 'Dudek H, Datta SR, Franke TF, Birnbaum MJ, Yao R, Cooper GM, Segal RA, Kaplan DR and Greenberg MERegulation of neuronal survival by the serine-threonine protein kinase Akt. *Science* 275: 661-665', *Science (New York, N.Y.)*, 275: 661-5.
- Ebert, M. S., and P. A. Sharp. 2012. 'Roles for microRNAs in conferring robustness to biological processes', *Cell*, 149: 515-24.
- Edelmann, K., L. Glashauser, S. Sprungala, B. Hesl, M. Fritschle, J. Ninkovic, L. Godinho, and P. Chapouton. 2013. 'Increased radial glia quiescence, decreased reactivation upon injury and unaltered neuroblast behavior underlie decreased neurogenesis in the aging zebrafish telencephalon', *The Journal of comparative neurology*, 521: 3099-115.
- Ekdahl, C. T., J. H. Claasen, S. Bonde, Z. Kokaia, and O. Lindvall. 2003. 'Inflammation is detrimental for neurogenesis in adult brain', *Proc Natl Acad Sci U S A*, 100: 13632-7.
- Ellwanger, D. C., F. A. Büttner, H. W. Mewes, and V. Stümpflen. 2011. 'The sufficient minimal set of miRNA seed types', *Bioinformatics*, 27: 1346-50.
- Eriksson, Peter S., Ekaterina Perfilieva, Thomas Björk-Eriksson, Ann-Marie Alborn, Claes Nordborg, Daniel A. Peterson, and Fred H. Gage. 1998. 'Neurogenesis in the adult human hippocampus', *Nature Medicine*, 4: 1313-17.
- Ernst, Jason, and Manolis Kellis. 2012. 'ChromHMM: automating chromatin-state discovery and characterization', *Nature methods*, 9: 215-16.
- . 2017. 'Chromatin-state discovery and genome annotation with ChromHMM', *Nature Protocols*, 12: 2478-92.
- Ettensohn, C. A. 2013. 'Encoding anatomy: developmental gene regulatory networks and morphogenesis', *genesis*, 51: 383-409.
- Fares, J., Z. Bou Diab, S. Nabha, and Y. Fares. 2019. 'Neurogenesis in the adult hippocampus: history, regulation, and prospective roles', *Int J Neurosci*, 129: 598-611.
- Fauq, Abdul H., Katherine Simpson, Ghulam M. Maharvi, Todd Golde, and Pritam Das. 2007. 'A multigram chemical synthesis of the gamma-secretase inhibitor LY411575 and its diastereoisomers', *Bioorganic & medicinal chemistry letters*, 17: 6392-95.
- Ferg, M., O. Armant, L. Yang, T. Dickmeis, S. Rastegar, and U. Strahle. 2014. 'Gene transcription in the zebrafish embryo: regulators and networks', *Brief Funct Genomics*, 13: 131-43.
- Fischer, A., and M. Gessler. 2007. 'Delta-Notch--and then? Protein interactions and proposed modes of repression by Hes and Hey bHLH factors', *Nucleic Acids Res*, 35: 4583-96.
- Fitch, M. T., and J. Silver. 2008. 'CNS injury, glial scars, and inflammation: Inhibitory extracellular matrices and regeneration failure', *Exp Neurol*, 209: 294-301.

- Fog, C. K., G. G. Galli, and A. H. Lund. 2012. 'PRDM proteins: important players in differentiation and disease', *Bioessays*, 34: 50-60.
- Fogerty, Joseph, Ruben Stepanyan, Lauren Cianciolo, Benjamin Tooke, and Brian Perkins. 2019. 'Genomic non-redundancy of the mir-183/96/182 cluster and its requirement for hair cell maintenance', *Scientific Reports*, 9.
- Folgueira, M., P. Bayley, P. Navratilova, T. S. Becker, S. W. Wilson, and J. D. Clarke. 2012. 'Morphogenesis underlying the development of the everted teleost telencephalon', *Neural Dev*, 7: 32.
- Fregeac, Julien, Laurence Colleaux, and Lam Son Nguyen. 2016. 'The emerging roles of MicroRNAs in autism spectrum disorders', *Neuroscience & Biobehavioral Reviews*, 71: 729-38.
- Frieden, M., H. F. Hansen, and T. Koch. 2003. 'Nuclease stability of LNA oligonucleotides and LNA-DNA chimeras', *Nucleosides Nucleotides Nucleic Acids*, 22: 1041-3.
- Frieden, Miriam, Signe M. Christensen, Nikolaj D. Mikkelsen, Christoph Rosenbohm, Charlotte A. Thue, Majken Westergaard, Henrik F. Hansen, Henrik Ørum, and Troels Koch. 2003. 'Expanding the design horizon of antisense oligonucleotides with alpha-L-LNA', *Nucleic acids research*, 31: 6365-72.
- Gaiano, N., J. S. Nye, and G. Fishell. 2000. 'Radial glial identity is promoted by Notch1 signaling in the murine forebrain', *Neuron*, 26: 395-404.
- Galgano, Michael, Gentian Toshkezi, Xuecheng Qiu, Thomas Russell, Lawrence Chin, and Li-Ru Zhao. 2017. 'Traumatic Brain Injury: Current Treatment Strategies and Future Endeavors', *Cell transplantation*, 26: 1118-30.
- Ganz, J., V. Kroehne, D. Freudenreich, A. Machate, M. Geffarth, I. Braasch, J. Kaslin, and M. Brand. 2014. 'Subdivisions of the adult zebrafish pallium based on molecular marker analysis', *F1000Res*, 3: 308.
- Gemberling, M., T. J. Bailey, D. R. Hyde, and K. D. Poss. 2013. 'The zebrafish as a model for complex tissue regeneration', *Trends Genet*, 29: 611-20.
- Ghaddar, Batoul, Luisa Lübke, David Couret, Sepand Rastegar, and Nicolas Diotel. 2021. 'Cellular Mechanisms Participating in Brain Repair of Adult Zebrafish and Mammals after Injury', *Cells*, 10: 391.
- Giraldez, A. J., R. M. Cinalli, M. E. Glasner, A. J. Enright, J. M. Thomson, S. Baskerville, S. M. Hammond, D. P. Bartel, and A. F. Schier. 2005. 'MicroRNAs regulate brain morphogenesis in zebrafish', *Science*, 308: 833-8.
- Glushakova, O. Y., D. Johnson, and R. L. Hayes. 2014. 'Delayed increases in microvascular pathology after experimental traumatic brain injury are associated with prolonged inflammation, blood-brain barrier disruption, and progressive white matter damage', *J Neurotrauma*, 31: 1180-93.
- Gourain, Victor, Olivier Armant, Luisa Lübke, Nicolas Diotel, Sepand Rastegar, and Uwe Strähle. 2021. 'Multi-Dimensional Transcriptome Analysis Reveals Modulation of Cholesterol Metabolism as Highly Integrated Response to Brain Injury', *Frontiers in Neuroscience*, 15.
- Gramage, E., and G. Herradón. 2011. 'Connecting Parkinson's disease and drug addiction: common players reveal unexpected disease connections and novel therapeutic approaches', *Current pharmaceutical design*, 17: 449-61.
- Gramage, E., J. Li, and P. Hitchcock. 2014. 'The expression and function of midkine in the vertebrate retina', *British journal of pharmacology*, 171: 913-23.
- Grandel, H., and M. Brand. 2013. 'Comparative aspects of adult neural stem cell activity in vertebrates', *Dev Genes Evol*, 223: 131-47.
- Grandel, H., J. Kaslin, J. Ganz, I. Wenzel, and M. Brand. 2006. 'Neural stem cells and neurogenesis in the adult zebrafish brain: origin, proliferation dynamics, migration and cell fate', *Dev Biol*, 295: 263-77.
- Griffiths-Jones, S. 2006. 'miRBase: the microRNA sequence database', *Methods Mol Biol*, 342: 129-38.
- Grivas, Dimitrios, Álvaro González-Rajal, and José Luis de la Pompa. 2021. 'Midkine-a regulates the formation of a fibrotic scar during zebrafish heart regeneration', *bioRxiv*: 2021.01.29.428781.

- Haffter, Pascal, Michael Granato, Michael Brand, Mary C Mullins, Matthias Hammerschmidt, Donald A Kane, Jörg Odenthal, FJ Van Eeden, Yun-Jin Jiang, and Carl-Philipp Heisenberg. 1996. 'The identification of genes with unique and essential functions in the development of the zebrafish, *Danio rerio*', *Development*, 123: 1-36.
- Hagemann, A. I., and S. Scholpp. 2012. 'The Tale of the Three Brothers - Shh, Wnt, and Fgf during Development of the Thalamus', *Front Neurosci*, 6: 76.
- Hammond, Scott M, Sabrina Boettcher, Amy A Caudy, Ryuji Kobayashi, and Gregory J Hannon. 2001. 'Argonaute2, a link between genetic and biochemical analyses of RNAi', *Science*, 293: 1146-50.
- Hampton, D. W., K. E. Rhodes, C. Zhao, R. J. M. Franklin, and J. W. Fawcett. 2004. 'The responses of oligodendrocyte precursor cells, astrocytes and microglia to a cortical stab injury, in the brain', *Neuroscience*, 127: 813-20.
- Hannon, K., E. Johnstone, L. S. Craft, S. P. Little, C. K. Smith, M. L. Heiman, and R. F. Santerre. 1993. 'Synthesis of PCR-Derived, Single-Stranded DNA Probes Suitable for in Situ Hybridization', *Analytical Biochemistry*, 212: 421-27.
- Hans, Stefan, Dorian Freudenreich, Michaela Geffarth, Jan Kaslin, Anja Machate, and Michael Brand. 2011. 'Generation of a non-leaky heat shock-inducible Cre line for conditional Cre/lox strategies in zebrafish', *Developmental Dynamics*, 240: 108-15.
- Hao, H., Y. Maeda, T. Fukazawa, T. Yamatsuji, M. Takaoka, X. H. Bao, J. Matsuoka, T. Okui, T. Shimo, N. Takigawa, Y. Tomono, M. Nakajima, I. M. Fink-Baldauf, S. Nelson, W. Seibel, R. Papoian, J. A. Whitsett, and Y. Naomoto. 2013. 'Inhibition of the growth factor MDK/midkine by a novel small molecule compound to treat non-small cell lung cancer', *PLoS One*, 8: e71093.
- Hao, J., J. N. Ho, J. A. Lewis, K. A. Karim, R. N. Daniels, P. R. Gentry, C. R. Hopkins, C. W. Lindsley, and C. C. Hong. 2010. 'In vivo structure-activity relationship study of dorsomorphin analogues identifies selective VEGF and BMP inhibitors', *ACS Chem Biol*, 5: 245-53.
- Hao, J., R. Lee, A. Chang, J. Fan, C. Labib, C. Parsa, R. Orlando, B. Andresen, and Y. Huang. 2014. 'DMH1, a small molecule inhibitor of BMP type i receptors, suppresses growth and invasion of lung cancer', *PLoS One*, 9: e90748.
- Herradón, G., and C. Pérez-García. 2014. 'Targeting midkine and pleiotrophin signalling pathways in addiction and neurodegenerative disorders: recent progress and perspectives', *British journal of pharmacology*, 171: 837-48.
- Hida, H., C. G. Jung, C. Z. Wu, H. J. Kim, Y. Kodama, T. Masuda, and H. Nishino. 2003. 'Pleiotrophin exhibits a trophic effect on survival of dopaminergic neurons in vitro', *Eur J Neurosci*, 17: 2127-34.
- Hohenauer, T., and A. W. Moore. 2012. 'The Prdm family: expanding roles in stem cells and development', *Development*, 139: 2267-82.
- Holland, Peter, Jordi GarciaFernandez, N. A. Williams, and A. Sidow. 1994. 'Gene duplications and origins of vertebrate development', *Development (Cambridge, England). Supplement*, 120: 125-33.
- Horgusluoglu, E., K. Nudelman, K. Nho, and A. J. Saykin. 2017. 'Adult neurogenesis and neurodegenerative diseases: A systems biology perspective', *Am J Med Genet B Neuropsychiatr Genet*, 174: 93-112.
- Hövelmann, Felix, Imre Gaspar, Simon Loibl, Eugeny A. Ermilov, Beate Röder, Jesper Wengel, Anne Ephrussi, and Oliver Seitz. 2014. 'Brightness through Local Constraint—LNA-Enhanced FIT Hybridization Probes for In Vivo Ribonucleotide Particle Tracking', *Angewandte Chemie International Edition*, 53: 11370-75.
- Howe, Kerstin, Matthew D. Clark, Carlos F. Torroja, James Torrance, Camille Berthelot, Matthieu Muffato, John E. Collins, Sean Humphray, Karen McLaren, Lucy Matthews, Stuart McLaren, Ian Sealy, Mario Caccamo, Carol Churcher, Carol Scott, Jeffrey C. Barrett, Romke Koch, Gerd-Jörg Rauch, Simon White, William Chow, Britt Kilian, Leonor T. Quintais, José A. Guerra-Assunção, Yi Zhou, Yong Gu, Jennifer Yen, Jan-Hinnerk Vogel, Tina Eyre, Seth Redmond, Ruby Banerjee, Jianxiang Chi, Beiyuan Fu, Elizabeth Langley, Sean F. Maguire, Gavin K. Laird, David

- Lloyd, Emma Kenyon, Sarah Donaldson, Harminder Sehra, Jeff Almeida-King, Jane Loveland, Stephen Trevanion, Matt Jones, Mike Quail, Dave Willey, Adrienne Hunt, John Burton, Sarah Sims, Kirsten McLay, Bob Plumb, Joy Davis, Chris Clee, Karen Oliver, Richard Clark, Clare Riddle, David Elliott, Glen Threadgold, Glenn Harden, Darren Ware, Sharmin Begum, Beverley Mortimore, Giselle Kerry, Paul Heath, Benjamin Phillimore, Alan Tracey, Nicole Corby, Matthew Dunn, Christopher Johnson, Jonathan Wood, Susan Clark, Sarah Pelan, Guy Griffiths, Michelle Smith, Rebecca Glithero, Philip Howden, Nicholas Barker, Christine Lloyd, Christopher Stevens, Joanna Harley, Karen Holt, Georgios Panagiotidis, Jamieson Lovell, Helen Beasley, Carl Henderson, Daria Gordon, Katherine Auger, Deborah Wright, Joanna Collins, Claire Raisen, Lauren Dyer, Kenric Leung, Lauren Robertson, Kirsty Ambridge, Daniel Leongamornlert, Sarah McGuire, Ruth Gilderthorp, Coline Griffiths, Deepa Manthravadi, Sarah Nichol, Gary Barker, Siobhan Whitehead, Michael Kay, Jacqueline Brown, Clare Murnane, Emma Gray, Matthew Humphries, Neil Sycamore, Darren Barker, David Saunders, Justene Wallis, Anne Babbage, Sian Hammond, Maryam Mashregi-Mohammadi, Lucy Barr, Sancha Martin, Paul Wray, Andrew Ellington, Nicholas Matthews, Matthew Ellwood, Rebecca Woodmansey, Graham Clark, James D. Cooper, Anthony Tromans, Darren Grafham, Carl Skuce, Richard Pandian, Robert Andrews, Elliot Harrison, Andrew Kimberley, Jane Garnett, Nigel Fosker, Rebekah Hall, Patrick Garner, Daniel Kelly, Christine Bird, Sophie Palmer, Ines Gehring, Andrea Berger, Christopher M. Dooley, Zübeyde Ersan-Ürün, Cigdem Eser, Horst Geiger, Maria Geisler, Lena Karotki, Anette Kirn, Judith Konantz, Martina Konantz, Martina Oberländer, Silke Rudolph-Geiger, Mathias Teucke, Christa Lanz, Günter Raddatz, Kazutoyo Osoegawa, Baoli Zhu, Amanda Rapp, Sara Widaa, Cordelia Langford, Fengtang Yang, Stephan C. Schuster, Nigel P. Carter, Jennifer Harrow, Zemin Ning, Javier Herrero, Steve M. J. Searle, Anton Enright, Robert Geisler, Ronald H. A. Plasterk, Charles Lee, Monte Westerfield, Pieter J. de Jong, Leonard I. Zon, John H. Postlethwait, Christiane Nüsslein-Volhard, Tim J. P. Hubbard, Hugues Roest Crollius, Jane Rogers, and Derek L. Stemple. 2013. 'The zebrafish reference genome sequence and its relationship to the human genome', *Nature*, 496: 498-503.
- Hruscha, A., P. Krawitz, A. Rechenberg, V. Heinrich, J. Hecht, C. Haass, and B. Schmid. 2013. 'Efficient CRISPR/Cas9 genome editing with low off-target effects in zebrafish', *Development*, 140: 4982-7.
- Hsiao, Chung-Der, Wei-Yuan Tsai, Long-Shyan Horng, and Huai-Jen Tsai. 2003. 'Molecular structure and developmental expression of three muscle-type troponin T genes in zebrafish', *Developmental Dynamics*, 227: 266-79.
- Huang, P., A. Xiao, M. Zhou, Z. Zhu, S. Lin, and B. Zhang. 2011. 'Heritable gene targeting in zebrafish using customized TALENs', *Nature biotechnology*, 29: 699-700.
- Huang, Shih-Min A., Yuji M. Mishina, Shanming Liu, Atwood Cheung, Frank Stegmeier, Gregory A. Michaud, Olga Charlat, Elizabeth Wiелlette, Yue Zhang, Stephanie Wiessner, Marc Hild, Xiaoying Shi, Christopher J. Wilson, Craig Mickanin, Vic Myer, Aleem Fazal, Ronald Tomlinson, Fabrizio Serluca, Wenlin Shao, Hong Cheng, Michael Shultz, Christina Rau, Markus Schirle, Judith Schlegl, Sonja Ghidelli, Stephen Fawell, Chris Lu, Daniel Curtis, Marc W. Kirschner, Christoph Lengauer, Peter M. Finan, John A. Tallarico, Tewis Bouwmeester, Jeffery A. Porter, Andreas Bauer, and Feng Cong. 2009. 'Tankyrase inhibition stabilizes axin and antagonizes Wnt signalling', *Nature*, 461: 614-20.
- Huntzinger, E., and E. Izaurralde. 2011. 'Gene silencing by microRNAs: contributions of translational repression and mRNA decay', *Nat Rev Genet*, 12: 99-110.
- Hutvagner, Gyorgy, and Phillip D Zamore. 2002. 'A microRNA in a multiple-turnover RNAi enzyme complex', *Science*, 297: 2056-60.
- Ikenaga, T., M. Yoshida, and K. Uematsu. 2005. 'Morphology and immunohistochemistry of efferent neurons of the goldfish corpus cerebelli', *The Journal of comparative neurology*, 487: 300-11.
- Ikutomo, M., H. Sakakima, F. Matsuda, and Y. Yoshida. 2014. 'Midkine-deficient mice delayed degeneration and regeneration after skeletal muscle injury', *Acta Histochem*, 116: 319-26.

- Imayoshi, I., and R. Kageyama. 2014. 'bHLH factors in self-renewal, multipotency, and fate choice of neural progenitor cells', *Neuron*, 82: 9-23.
- Iyer, A., E. Zurolo, A. Prabowo, K. Fluiters, W. G. Spliet, P. C. van Rijen, J. A. Gorter, and E. Aronica. 2012. 'MicroRNA-146a: a key regulator of astrocyte-mediated inflammatory response', *PLoS One*, 7: e44789.
- Javier, A. L., L. T. Doan, M. Luong, N. S. Reyes de Mochel, A. Sun, E. S. Monuki, and K. W. Cho. 2012. 'Bmp indicator mice reveal dynamic regulation of transcriptional response', *PLoS One*, 7: e42566.
- Jin, Y., Z. Chen, X. Liu, and X. Zhou. 2013. 'Evaluating the microRNA targeting sites by luciferase reporter gene assay', *Methods Mol Biol*, 936: 117-27.
- Jurisch-Yaksi, N., E. Yaksi, and C. Kizil. 2020. 'Radial glia in the zebrafish brain: Functional, structural, and physiological comparison with the mammalian glia', *Glia*, 68: 2451-70.
- Juven-Gershon, T., and J. T. Kadonaga. 2010. 'Regulation of gene expression via the core promoter and the basal transcriptional machinery', *Dev Biol*, 339: 225-9.
- Kadomatsu, K., M. Tomomura, and T. Muramatsu. 1988. 'cDNA cloning and sequencing of a new gene intensely expressed in early differentiation stages of embryonal carcinoma cells and in mid-gestation period of mouse embryogenesis', *Biochem Biophys Res Commun*, 151: 1312-8.
- Kadomatsu, Kenji, R P Huang, Tatsuo Sukanuma, Fusayoshi Murata, and Takashi Muramatsu. 1990. 'A retinoic acid responsive gene MK found in the teratocarcinoma system is expressed in spatially and temporally controlled manner during mouse embryogenesis', *The Journal of Cell Biology*, 110: 607 - 16.
- Kadomatsu, Kenji, Satoshi Kishida, and Shoma Tsubota. 2013. 'The heparin-binding growth factor midkine: the biological activities and candidate receptors', *J Biochem*, 153: 511-21.
- Kageyama, R., T. Ohtsuka, and T. Kobayashi. 2007. 'The Hes gene family: repressors and oscillators that orchestrate embryogenesis', *Development*, 134: 1243-51.
- Kanagaraj, Palsamy, Jessica Y. Chen, Kaia Skaggs, Yusuf Qadeer, Meghan Connors, Noah Cutler, Joshua Richmond, Vineeth Kommidi, Allison Poles, Danielle Affrunti, Curtis Powell, Daniel Goldman, and Jack M. Parent. 2022. 'Microglia Stimulate Zebrafish Brain Repair Via a Tumor Necrosis Factor- α -Initiated Inflammatory Cascade', *bioRxiv*: 2020.10.08.330662.
- Kaplan, M. S. 1985. 'Formation and turnover of neurons in young and senescent animals: an electronmicroscopic and morphometric analysis', *Ann N Y Acad Sci*, 457: 173-92.
- Kaslin, Jan, Julia Ganz, Michaela Geffarth, Heiner Grandel, Stefan Hans, and Michael Brand. 2009. 'Stem Cells in the Adult Zebrafish Cerebellum: Initiation and Maintenance of a Novel Stem Cell Niche', *The Journal of Neuroscience*, 29: 6142-53.
- Kaslin, Jan, and Pertti Panula. 2001. 'Comparative anatomy of the histaminergic and other aminergic systems in zebrafish (*Danio rerio*)', *Journal of Comparative Neurology*, 440: 342-77.
- Kawai, H., D. Kawaguchi, B. D. Kuebrich, T. Kitamoto, M. Yamaguchi, Y. Gotoh, and S. Furutachi. 2017. 'Area-Specific Regulation of Quiescent Neural Stem Cells by Notch3 in the Adult Mouse Subependymal Zone', *J Neurosci*, 37: 11867-80.
- Kawakami, Koichi. 2007. 'Tol2: a versatile gene transfer vector in vertebrates', *Genome Biology*, 8: S7.
- Kettleborough, R. N., E. M. Busch-Nentwich, S. A. Harvey, C. M. Dooley, E. de Bruijn, F. van Eeden, I. Sealy, R. J. White, C. Herd, I. J. Nijman, F. Fényes, S. Mehroke, C. Scahill, R. Gibbons, N. Wali, S. Carruthers, A. Hall, J. Yen, E. Cuppen, and D. L. Stemple. 2013. 'A systematic genome-wide analysis of zebrafish protein-coding gene function', *Nature*, 496: 494-7.
- Kikuta, Hiroshi, Mary Laplante, Pavla Navratilova, Anna Z. Komisarczuk, Pär G. Engström, David Fredman, Altuna Akalin, Mario Caccamo, Ian Sealy, Kerstin Howe, Julien Ghislain, Guillaume Pezeron, Philippe Mourrain, Staale Ellingsen, Andrew C. Oates, Christine Thisse, Bernard Thisse, Isabelle Foucher, Birgit Adolf, Andrea Geling, Boris Lenhard, and Thomas S. Becker. 2007. 'Genomic regulatory blocks encompass multiple neighboring genes and maintain conserved synteny in vertebrates', *Genome Res*, 17: 545-55.
- Kim, Tae-Kyung, Martin Hemberg, Jesse M. Gray, Allen M. Costa, Daniel M. Bear, Jing Wu, David A. Harmin, Mike Laptewicz, Kellie Barbara-Haley, Scott Kuersten, Eirene Markenscoff-

- Papadimitriou, Dietmar Kuhl, Haruhiko Bito, Paul F. Worley, Gabriel Kreiman, and Michael E. Greenberg. 2010. 'Widespread transcription at neuronal activity-regulated enhancers', *Nature*, 465: 182-87.
- Kinney, J. W., S. M. Bemiller, A. S. Murtishaw, A. M. Leisgang, A. M. Salazar, and B. T. Lamb. 2018. 'Inflammation as a central mechanism in Alzheimer's disease', *Alzheimers Dement (N Y)*, 4: 575-90.
- Kishimoto, N., C. Alfaro-Cervello, K. Shimizu, K. Asakawa, A. Urasaki, S. Nonaka, K. Kawakami, J. M. Garcia-Verdugo, and K. Sawamoto. 2011. 'Migration of neuronal precursors from the telencephalic ventricular zone into the olfactory bulb in adult zebrafish', *The Journal of comparative neurology*, 519: 3549-65.
- Kishimoto, N., K. Shimizu, and K. Sawamoto. 2012. 'Neuronal regeneration in a zebrafish model of adult brain injury', *Dis Model Mech*, 5: 200-9.
- Kizil, C., J. Kaslin, V. Kroehne, and M. Brand. 2012. 'Adult neurogenesis and brain regeneration in zebrafish', *Dev Neurobiol*, 72: 429-61.
- Kizil, C., N. Kyritsis, and M. Brand. 2015. 'Effects of inflammation on stem cells: together they strive?', *EMBO Rep*, 16: 416-26.
- Kizil, C., N. Kyritsis, S. Dudczig, V. Kroehne, D. Freudenreich, J. Kaslin, and M. Brand. 2012. 'Regenerative neurogenesis from neural progenitor cells requires injury-induced expression of Gata3', *Dev Cell*, 23: 1230-7.
- Kizil, Caghan, and Michael Brand. 2011. 'Cerebroventricular Microinjection (CVMI) into Adult Zebrafish Brain Is an Efficient Misexpression Method for Forebrain Ventricular Cells', *PLoS One*, 6: e27395.
- Kizil, Caghan, Anne Iltzsche, Jan Kaslin, and Michael Brand. 2013. 'Micromanipulation of gene expression in the adult zebrafish brain using cerebroventricular microinjection of morpholino oligonucleotides', *Journal of visualized experiments : JoVE*: e50415-e15.
- Knoth, R., I. Singec, M. Ditter, G. Pantazis, P. Capetian, R. P. Meyer, V. Horvat, B. Volk, and G. Kempermann. 2010. 'Murine features of neurogenesis in the human hippocampus across the lifespan from 0 to 100 years', *PLoS One*, 5: e8809.
- Korchynskyi, O., and P. ten Dijke. 2002. 'Identification and functional characterization of distinct critically important bone morphogenetic protein-specific response elements in the Id1 promoter', *J Biol Chem*, 277: 4883-91.
- Kornberg, R. D. 1999. 'Eukaryotic transcriptional control', *Trends Cell Biol*, 9: M46-9.
- Kozareva, D. A., J. F. Cryan, and Y. M. Nolan. 2019. 'Born this way: Hippocampal neurogenesis across the lifespan', *Aging Cell*, 18: e13007.
- Krichevsky, Anna M, Kevin S King, Christine P Donahue, Konstantin Khrapko, and Kenneth S Kosik. 2003. 'A microRNA array reveals extensive regulation of microRNAs during brain development', *Rna*, 9: 1274-81.
- Kriegstein, A. R., and M. Götz. 2003. 'Radial glia diversity: a matter of cell fate', *Glia*, 43: 37-43.
- Kroehne, V., D. Freudenreich, S. Hans, J. Kaslin, and M. Brand. 2011. 'Regeneration of the adult zebrafish brain from neurogenic radial glia-type progenitors', *Development*, 138: 4831-41.
- Krol, J., I. Loedige, and W. Filipowicz. 2010. 'The widespread regulation of microRNA biogenesis, function and decay', *Nat Rev Genet*, 11: 597-610.
- Kurreck, J., E. Wyszko, C. Gillen, and V. A. Erdmann. 2002. 'Design of antisense oligonucleotides stabilized by locked nucleic acids', *Nucleic Acids Res*, 30: 1911-8.
- Kyritsis, N., C. Kizil, S. Zocher, V. Kroehne, J. Kaslin, D. Freudenreich, A. Iltzsche, and M. Brand. 2012a. 'Acute inflammation initiates the regenerative response in the adult zebrafish brain', *Science*, 338: 1353-6.
- Kyritsis, Nikos, Caghan Kizil, Sara Zocher, Volker Kroehne, Jan Kaslin, Dorian Freudenreich, Anne Iltzsche, and Michael Brand. 2012b. 'Acute Inflammation Initiates the Regenerative Response in the Adult Zebrafish Brain', *Science*, 338: 1353-56.
- Laale, Hans W. 1977. 'The biology and use of zebrafish, *Brachydanio rerio* in fisheries research', *Journal of Fish Biology*, 10: 121-73.

- Lagos-Quintana, Mariana, Reinhard Rauhut, Winfried Lendeckel, and Thomas Tuschl. 2001. 'Identification of novel genes coding for small expressed RNAs', *Science*, 294: 853-58.
- Lam, C. S., M. Marz, and U. Strahle. 2009. 'gfap and nestin reporter lines reveal characteristics of neural progenitors in the adult zebrafish brain', *Dev Dyn*, 238: 475-86.
- Lang, Ming-Fei, and Yanhong Shi. 2012. 'Dynamic Roles of microRNAs in Neurogenesis', *Frontiers in Neuroscience*, 6.
- Lange, Christian, Fabian Rost, Anja Machate, Susanne Reinhardt, Matthias Lesche, Anke Weber, Veronika Kuscha, Andreas Dahl, Steffen Rulands, and Michael Brand. 2020. 'Single cell sequencing of radial glia progeny reveals the diversity of newborn neurons in the adult zebrafish brain', *Development*, 147: dev185595.
- Lau, Nelson C, Lee P Lim, Earl G Weinstein, and David P Bartel. 2001. 'An abundant class of tiny RNAs with probable regulatory roles in *Caenorhabditis elegans*', *Science*, 294: 858-62.
- Lee, Yoontae, Chiyong Ahn, Jinju Han, Hyoungjeong Choi, Jaekwang Kim, Jeongbin Yim, Junho Lee, Patrick Provost, Olof Rådmark, and Sunyoung Kim. 2003. 'The nuclear RNase III Drosha initiates microRNA processing', *Nature*, 425: 415-19.
- Lemus-Diaz, N., K. O. Böker, I. Rodriguez-Polo, M. Mitter, J. Preis, M. Arlt, and J. Gruber. 2017. 'Dissecting miRNA gene repression on single cell level with an advanced fluorescent reporter system', *Sci Rep*, 7: 45197.
- Lettice, L. A., S. J. Heaney, L. A. Purdie, L. Li, P. de Beer, B. A. Oostra, D. Goode, G. Elgar, R. E. Hill, and E. de Graaff. 2003. 'A long-range Shh enhancer regulates expression in the developing limb and fin and is associated with preaxial polydactyly', *Hum Mol Genet*, 12: 1725-35.
- Leucht, C., C. Stigloher, A. Wizenmann, R. Klafke, A. Folchert, and L. Bally-Cuif. 2008. 'MicroRNA-9 directs late organizer activity of the midbrain-hindbrain boundary', *Nat Neurosci*, 11: 641-8.
- Li, Q., G. Barkess, and H. Qian. 2006. 'Chromatin looping and the probability of transcription', *Trends Genet*, 22: 197-202.
- Liedtke, D., and C. Winkler. 2008. 'Midkine-b regulates cell specification at the neural plate border in zebrafish', *Dev Dyn*, 237: 62-74.
- Lieschke, Graham J., and Peter D. Currie. 2007. 'Animal models of human disease: zebrafish swim into view', *Nature Reviews Genetics*, 8: 353-67.
- Lim, D. A., A. D. Tramontin, J. M. Trevejo, D. G. Herrera, J. M. Garcia-Verdugo, and A. Alvarez-Buylla. 2000. 'Noggin antagonizes BMP signaling to create a niche for adult neurogenesis', *Neuron*, 28: 713-26.
- Lim, J., S. Yao, M. Graf, C. Winkler, and D. Yang. 2013. 'Structure-function analysis of full-length midkine reveals novel residues important for heparin binding and zebrafish embryogenesis', *Biochem J*, 451: 407-15.
- Lim, L. P., N. C. Lau, P. Garrett-Engele, A. Grimson, J. M. Schelter, J. Castle, D. P. Bartel, P. S. Linsley, and J. M. Johnson. 2005. 'Microarray analysis shows that some microRNAs downregulate large numbers of target mRNAs', *Nature*, 433: 769-73.
- Lindsey, B. W., G. E. Aitken, J. K. Tang, M. Khabooshan, A. M. Douek, C. Vandestadt, and J. Kaslin. 2019. 'Midbrain tectal stem cells display diverse regenerative capacities in zebrafish', *Sci Rep*, 9: 4420.
- Lindsey, B. W., and V. Tropepe. 2006. 'A comparative framework for understanding the biological principles of adult neurogenesis', *Prog Neurobiol*, 80: 281-307.
- Logan, Catriona Y., and Roel Nusse. 2004. 'THE WNT SIGNALING PATHWAY IN DEVELOPMENT AND DISEASE', *Annual Review of Cell and Developmental Biology*, 20: 781-810.
- Lopez-Rovira, T., E. Chaloux, J. Massague, J. L. Rosa, and F. Ventura. 2002. 'Direct binding of Smad1 and Smad4 to two distinct motifs mediates bone morphogenetic protein-specific transcriptional activation of Id1 gene', *J Biol Chem*, 277: 3176-85.
- Lumsden, A., and R. Krumlauf. 1996. 'Patterning the vertebrate neuraxis', *Science*, 274: 1109-15.
- Lund, Elsebet, Stephan Guttinger, Angelo Calado, James E Dahlberg, and Ulrike Kutay. 2004. 'Nuclear export of microRNA precursors', *Science*, 303: 95-98.

- Luo, J., R. A. Uribe, S. Hayton, A. A. Calinescu, J. M. Gross, and P. F. Hitchcock. 2012. 'Midkine-A functions upstream of Id2a to regulate cell cycle kinetics in the developing vertebrate retina', *Neural Dev*, 7: 33.
- Luo, Q., L. Liu, C. Yang, J. Yuan, H. Feng, Y. Chen, P. Zhao, Z. Yu, and Z. Jin. 2018. 'A rapid, ratiometric, enzyme-free, and sensitive single-step miRNA detection using three-way junction based FRET probes', *Nanotechnology*, 29: 114001.
- Maeda, N., K. Ichihara-Tanaka, T. Kimura, K. Kadomatsu, T. Muramatsu, and M. Noda. 1999. 'A receptor-like protein-tyrosine phosphatase PTPzeta/RPTPbeta binds a heparin-binding growth factor midkine. Involvement of arginine 78 of midkine in the high affinity binding to PTPzeta', *J Biol Chem*, 274: 12474-9.
- Magnus, Tim, Turhan Coksaygan, Thomas Korn, Haipeng Xue, Thiruma V. Arumugam, Mohamed R. Mughal, D. Mark Eckley, Sung-Chun Tang, Louis J Detolla, Mahendra S. Rao, Riccardo Cassiani-Ingoni, and Mark P. Mattson. 2007. 'Evidence that nucleocytoplasmic Olig2 translocation mediates braiŹ injur™ induced differentiation of glial precursors to astrocytes', *Journal of Neuroscience Research*, 85.
- März, M., P. Chapouton, N. Diotel, C. Vaillant, B. Hesl, M. Takamiya, C. S. Lam, O. Kah, L. Bally-Cuif, and U. Strahle. 2010. 'Heterogeneity in progenitor cell subtypes in the ventricular zone of the zebrafish adult telencephalon', *Glia*, 58: 870-88.
- März, M., R. Schmidt, S. Rastegar, and U. Strahle. 2011. 'Regenerative response following stab injury in the adult zebrafish telencephalon', *Dev Dyn*, 240: 2221-31.
- Matsui, H., and R. Takahashi. 2018. 'Parkinson's disease pathogenesis from the viewpoint of small fish models', *J Neural Transm (Vienna)*, 125: 25-33.
- Matsumoto, K., A. Wanaka, K. Takatsuji, H. Muramatsu, T. Muramatsu, and M. Tohyama. 1994. 'A novel family of heparin-binding growth factors, pleiotrophin and midkine, is expressed in the developing rat cerebral cortex', *Brain Res Dev Brain Res*, 79: 229-41.
- McLellan, A. S., T. Kealey, and K. Langlands. 2006. 'An E box in the exon 1 promoter regulates insulin-like growth factor-I expression in differentiating muscle cells', *Am J Physiol Cell Physiol*, 291: C300-7.
- Melo, C. A., J. Drost, P. J. Wijchers, H. van de Werken, E. de Wit, J. A. Oude Vrielink, R. Elkon, S. A. Melo, N. Léveillé, R. Kalluri, W. de Laat, and R. Agami. 2013. 'eRNAs are required for p53-dependent enhancer activity and gene transcription', *Mol Cell*, 49: 524-35.
- Meyer, Axel, and Manfred Schartl. 1999. 'Gene and genome duplications in vertebrates: the one-to-four (-to-eight in fish) rule and the evolution of novel gene functions', *Current Opinion in Cell Biology*, 11: 699-704.
- Miale, Irene L., and Richard L. Sidman. 1961. 'An autoradiographic analysis of histogenesis in the mouse cerebellum', *Experimental Neurology*, 4: 277-96.
- Mira, H., Z. Andreu, H. Suh, D. C. Lie, S. Jessberger, A. Consiglio, J. San Emeterio, R. Hortiguera, M. A. Marques-Torrejón, K. Nakashima, D. Colak, M. Gotz, I. Farinas, and F. H. Gage. 2010. 'Signaling through BMPRII regulates quiescence and long-term activity of neural stem cells in the adult hippocampus', *Cell Stem Cell*, 7: 78-89.
- Mishima, Kazuhiko, Akio Asai, Kenji Kadomatsu, Yasushi Ino, Kazuhiro Nomura, Yoshitaka Narita, Takashi Muramatsu, and Takaaki Kirino. 1997. 'Increased expression of midkine during the progression of human astrocytomas', *Neuroscience Letters*, 233: 29-32.
- Mithal, D. S., D. Ren, and R. J. Miller. 2013. 'CXCR4 signaling regulates radial glial morphology and cell fate during embryonic spinal cord development', *Glia*, 61: 1288-305.
- Miyazono, K., Y. Kamiya, and M. Morikawa. 2010. 'Bone morphogenetic protein receptors and signal transduction', *J Biochem*, 147: 35-51.
- Mohrs, M., C. M. Blankespoor, Z. E. Wang, G. G. Loots, V. Afzal, H. Hadeiba, K. Shinkai, E. M. Rubin, and R. M. Locksley. 2001. 'Deletion of a coordinate regulator of type 2 cytokine expression in mice', *Nat Immunol*, 2: 842-7.
- Monaco, A., M. C. Grimaldi, and I. Ferrandino. 2016. 'Neuroglial alterations in the zebrafish brain exposed to cadmium chloride', *J Appl Toxicol*, 36: 1629-38.

- Monje, M. L., H. Toda, and T. D. Palmer. 2003. 'Inflammatory blockade restores adult hippocampal neurogenesis', *Science*, 302: 1760-5.
- Mueller, Thomas, Philippe Vernier, and Mario F. Wullimann. 2004. 'The adult central nervous cholinergic system of a neurogenetic model animal, the zebrafish *Danio rerio*', *Brain Research*, 1011: 156-69.
- Mueller, Thomas, and Mario F Wullimann. 2005. "Atlas of Early Zebrafish Brain Development: A Tool for Molecular Neurogenetics." In.
- Murakawa, Y., M. Yoshihara, H. Kawaji, M. Nishikawa, H. Zayed, H. Suzuki, Consortium Fantom, and Y. Hayashizaki. 2016. 'Enhanced Identification of Transcriptional Enhancers Provides Mechanistic Insights into Diseases', *Trends Genet*, 32: 76-88.
- Muramatsu, Rieko, Chisato Takahashi, Shuzo Miyake, Harutoshi Fujimura, Hideki Mochizuki, and Toshihide Yamashita. 2012. 'Angiogenesis induced by CNS inflammation promotes neuronal remodeling through vessel-derived prostacyclin', *Nature Medicine*, 18: 1658-64.
- Muramatsu, T. 2002. 'Midkine and pleiotrophin: two related proteins involved in development, survival, inflammation and tumorigenesis', *J Biochem*, 132: 359-71.
- . 2014. 'Structure and function of midkine as the basis of its pharmacological effects', *British journal of pharmacology*, 171: 814-26.
- Muramatsu, Takashi. 2010. 'Midkine, a heparin-binding cytokine with multiple roles in development, repair and diseases', *Proceedings of the Japan Academy. Series B, Physical and biological sciences*, 86: 410-25.
- . 2011. 'Midkine: a promising molecule for drug development to treat diseases of the central nervous system', *Current pharmaceutical design*, 17: 410-23.
- Muramatsu, Takashi, and Kenji Kadomatsu. 2014. 'Midkine: an emerging target of drug development for treatment of multiple diseases', *British journal of pharmacology*, 171: 811-13.
- Nagashima, Mikiko, Travis S. D'Cruz, Antoinette E. Danku, Doneen Hesse, Christopher Sifuentes, Pamela A. Raymond, and Peter F. Hitchcock. 2020. 'Midkine- α Is Required for Cell Cycle Progression of Müller Glia during Neuronal Regeneration in the Vertebrate Retina', *The Journal of Neuroscience*, 40: 1232-47.
- Nakagawara, Akira, Jeffrey D. Milbrandt, Takashi Muramatsu, Thomas F. Deuel, H. Zhao, Avital Cnaan, and Garrett M. Brodeur. 1995. 'Differential expression of pleiotrophin and midkine in advanced neuroblastomas', *Cancer research*, 55 8: 1792-7.
- Nakahiro, T., H. Kurooka, K. Mori, K. Sano, and Y. Yokota. 2010. 'Identification of BMP-responsive elements in the mouse *Id2* gene', *Biochem Biophys Res Commun*, 399: 416-21.
- Nam, H. S., and R. Benezra. 2009. 'High levels of *Id1* expression define B1 type adult neural stem cells', *Cell Stem Cell*, 5: 515-26.
- Nasevicius, A., and S. C. Ekker. 2000. 'Effective targeted gene 'knockdown' in zebrafish', *Nat Genet*, 26: 216-20.
- Navratilova, P., D. Fredman, T. A. Hawkins, K. Turner, B. Lenhard, and T. S. Becker. 2009. 'Systematic human/zebrafish comparative identification of cis-regulatory activity around vertebrate developmental transcription factor genes', *Dev Biol*, 327: 526-40.
- Nguyen, L. S., J. Fregeac, C. Bole-Feysot, N. Cagnard, A. Iyer, J. Anink, E. Aronica, O. Alibeu, P. Nitschke, and L. Colleaux. 2018. 'Role of miR-146a in neural stem cell differentiation and neural lineage determination: relevance for neurodevelopmental disorders', *Mol Autism*, 9: 38.
- Nguyen, L. S., M. Lepleux, M. Makhoulouf, C. Martin, J. Fregeac, K. Siquier-Pernet, A. Philippe, F. Feron, B. Gepner, C. Rougeulle, Y. Humeau, and L. Colleaux. 2016. 'Profiling olfactory stem cells from living patients identifies miRNAs relevant for autism pathophysiology', *Mol Autism*, 7: 1.
- Nobrega, Marcelo A., and Len A. Pennacchio. 2004. 'Comparative genomic analysis as a tool for biological discovery', *The Journal of Physiology*, 554: 31-39.
- Noctor, S. C., A. C. Flint, T. A. Weissman, W. S. Wong, B. K. Clinton, and A. R. Kriegstein. 2002. 'Dividing precursor cells of the embryonic cortical ventricular zone have morphological and molecular characteristics of radial glia', *J Neurosci*, 22: 3161-73.

- Nolan, Patrick M, Jo Peters, Mark Strivens, Derek Rogers, Jim Hagan, Nigel Spurr, Ian C Gray, Lucie Vizor, Debra Brooker, and Elaine Whitehill. 2000. 'A systematic, genome-wide, phenotype-driven mutagenesis programme for gene function studies in the mouse', *Nature Genetics*, 25: 440-43.
- Norton, J. D. 2000. 'ID helix-loop-helix proteins in cell growth, differentiation and tumorigenesis', *J Cell Sci*, 113 (Pt 22): 3897-905.
- Nunes, M. E., T. E. Müller, M. M. Braga, B. D. Fontana, V. A. Quadros, A. Marins, C. Rodrigues, C. Menezes, D. B. Rosemberg, and V. L. Loro. 2017. 'Chronic Treatment with Paraquat Induces Brain Injury, Changes in Antioxidant Defenses System, and Modulates Behavioral Functions in Zebrafish', *Mol Neurobiol*, 54: 3925-34.
- O'Brien, Jacob, Heyam Hayder, Yara Zayed, and Chun Peng. 2018. 'Overview of MicroRNA Biogenesis, Mechanisms of Actions, and Circulation', *Frontiers in endocrinology*, 9: 402-02.
- Ochiai, Keiko, Hisako Muramatsu, Satoshi Yamamoto, Hisami Ando, and Takashi Muramatsu. 2004. 'The role of midkine and pleiotrophin in liver regeneration', *Liver International*, 24: 484-91.
- Ohgake, Shintaro, Eiji Shimizu, Kenji Hashimoto, Naoe Okamura, Kaori Koike, Hiroyuki Koizumi, Mihisa Fujisaki, Nobuhisa Kanahara, Shingo Matsuda, Chihiro Sutoh, Daisuke Matsuzawa, Hisako Muramatsu, Takashi Muramatsu, and Masaomi Iyo. 2009. 'Dopaminergic hypofunctions and prepulse inhibition deficits in mice lacking midkine', *Progress in Neuro-Psychopharmacology and Biological Psychiatry*, 33: 541-46.
- Ohtsuka, T., M. Ishibashi, G. Gradwohl, S. Nakanishi, F. Guillemot, and R. Kageyama. 1999. 'Hes1 and Hes5 as notch effectors in mammalian neuronal differentiation', *The EMBO journal*, 18: 2196-207.
- Okuda, Y., E. Ogura, H. Kondoh, and Y. Kamachi. 2010. 'B1 SOX coordinate cell specification with patterning and morphogenesis in the early zebrafish embryo', *PLoS Genet*, 6: e1000936.
- Oppenheim, R. W. 2019. 'Adult Hippocampal Neurogenesis in Mammals (and Humans): The Death of a Central Dogma in Neuroscience and its Replacement by a New Dogma', *Dev Neurobiol*, 79: 268-80.
- Ordas, Anita, Zakia Kanwal, Valesca Lindenberg, Julien Rougeot, Matyas Mink, Herman P. Spaink, and Annemarie H. Meijer. 2013. 'MicroRNA-146 function in the innate immune transcriptome response of zebrafish embryos to Salmonella typhimurium infection', *BMC genomics*, 14: 696-96.
- Owada, K., N. Sanjo, T. Kobayashi, H. Mizusawa, H. Muramatsu, T. Muramatsu, and M. Michikawa. 1999. 'Midkine inhibits caspase-dependent apoptosis via the activation of mitogen-activated protein kinase and phosphatidylinositol 3-kinase in cultured neurons', *J Neurochem*, 73: 2084-92.
- Panula, P., Y. C. Chen, M. Priyadarshini, H. Kudo, S. Semenova, M. Sundvik, and V. Sallinen. 2010. 'The comparative neuroanatomy and neurochemistry of zebrafish CNS systems of relevance to human neuropsychiatric diseases', *Neurobiol Dis*, 40: 46-57.
- Papan, C., and J. A. Campos-Ortega. 1994. 'On the formation of the neural keel and neural tube in the zebrafish *Danio (Brachydanio) rerio*', *Roux Arch Dev Biol*, 203: 178-86.
- . 1999. 'Region-specific cell clones in the developing spinal cord of the zebrafish', *Dev Genes Evol*, 209: 135-44.
- Parker, Matthew, Alistair Brock, Robert Walton, and Caroline Brennan. 2013. 'The role of zebrafish (*Danio rerio*) in dissecting the genetics and neural circuits of executive function', *Frontiers in neural circuits*, 7: 63.
- Pedraza, C., S. Matsubara, and T. Muramatsu. 1995. 'A retinoic acid-responsive element in human midkine gene', *J Biochem*, 117: 845-9.
- Pellegrini, E., K. Mouriec, I. Anglade, A. Menuet, Y. Le Page, M. M. Gueguen, M. H. Marmignon, F. Brion, F. Pakdel, and O. Kah. 2007. 'Identification of aromatase-positive radial glial cells as progenitor cells in the ventricular layer of the forebrain in zebrafish', *The Journal of comparative neurology*, 501: 150-67.

- Peter, I. S., and E. H. Davidson. 2011. 'Evolution of gene regulatory networks controlling body plan development', *Cell*, 144: 970-85.
- Pierce, M. L., M. D. Weston, B. Fritsch, H. W. Gabel, G. Ruvkun, and G. A. Soukup. 2008. 'MicroRNA-183 family conservation and ciliated neurosensory organ expression', *Evol Dev*, 10: 106-13.
- Pinto, L., and M. Gotz. 2007. 'Radial glial cell heterogeneity--the source of diverse progeny in the CNS', *Prog Neurobiol*, 83: 2-23.
- Pons-Espinal, M., E. de Luca, M. J. Marzi, R. Beckervordersandforth, A. Armirotti, F. Nicassio, K. Fabel, G. Kempermann, and D. De Pietri Tonelli. 2017. 'Synergic Functions of miRNAs Determine Neuronal Fate of Adult Neural Stem Cells', *Stem Cell Reports*, 8: 1046-61.
- Popovich, P. G., Z. Guan, V. McGaughy, L. Fisher, W. F. Hickey, and D. M. Basso. 2002. 'The neuropathological and behavioral consequences of intraspinal microglial/macrophage activation', *J Neuropathol Exp Neurol*, 61: 623-33.
- Prediger, Rui Daniel, Argelia Esperanza Rojas-Mayorquín, Aderbal S. Jr. Aguiar, Caroline Chevarin, R. Mongeau, Michel Hamon, Laurence Lanfumey, Elaine Aparecida Del Bel, Hisako Muramatsu, José Courty, and Rita Rismaž Vozari. 2010. 'Mice with genetic deletion of the heparin-binding growth factor midkine exhibit early preclinical features of Parkinson s disease', *Journal of Neural Transmission*, 118: 1215-25.
- Provost, Elayne, Jerry M. Rhee, and Steven D Leach. 2007. 'Viral 2A peptides allow expression of multiple proteins from a single ORF in transgenic zebrafish embryos', *genesis*, 45.
- Ptashne, M., and A. Gann. 1997. 'Transcriptional activation by recruitment', *Nature*, 386: 569-77.
- Qu, Q., G. Sun, W. Li, S. Yang, P. Ye, C. Zhao, R. T. Yu, F. H. Gage, R. M. Evans, and Y. Shi. 2010. 'Orphan nuclear receptor TLX activates Wnt/beta-catenin signalling to stimulate neural stem cell proliferation and self-renewal', *Nat Cell Biol*, 12: 31-40; sup pp 1-9.
- Quillien, A., B. Blanco-Sanchez, C. Halluin, J. C. Moore, N. D. Lawson, P. Blader, and E. Cau. 2011. 'BMP signaling orchestrates photoreceptor specification in the zebrafish pineal gland in collaboration with Notch', *Development*, 138: 2293-302.
- Raj, Arjun, Patrick van den Bogaard, Scott A. Rifkin, Alexander van Oudenaarden, and Sanjay Tyagi. 2008. 'Imaging individual mRNA molecules using multiple singly labeled probes', *Nature methods*, 5: 877-79.
- Rastegar, Sepand, Isabell Hess, Thomas Dickmeis, Jean Christophe Nicod, Raymond Ertzer, Yavor Hadzhiev, Wolf-Gerolf Thies, Gerd Scherer, and Uwe Strähle. 2008. 'The words of the regulatory code are arranged in a variable manner in highly conserved enhancers', *Developmental Biology*, 318: 366-77.
- Raymond, Pamela A., Linda K. Barthel, Rebecca L. Bernardos, and John J. Perkowski. 2006. 'Molecular characterization of retinal stem cells and their niches in adult zebrafish', *BMC Dev Biol*, 6: 36.
- Reiff, T., Huber, L., Kramer, M., Delattre, O., Janoueix-Lerosey, I., & Rohrer, H. 2011. 'Midkine and Alk signaling in sympathetic neuron proliferation and neuroblastoma predisposition', *Development*: 4699-708.
- Rentzsch, F., J. Bakkens, C. Kramer, and M. Hammerschmidt. 2004. 'Fgf signaling induces posterior neuroectoderm independently of Bmp signaling inhibition', *Dev Dyn*, 231: 750-7.
- Reynolds, P. R., M. L. Mucenski, T. D. Le Cras, W. C. Nichols, and J. A. Whitsett. 2004a. 'Midkine is regulated by hypoxia and causes pulmonary vascular remodeling', *J Biol Chem*, 279: 37124-32.
- Reynolds, Paul R., Michael L. Mucenski, Timothy D. Le Cras, William C. Nichols, and Jeffrey A. Whitsett. 2004b. 'Midkine Is Regulated by Hypoxia and Causes Pulmonary Vascular Remodeling*', *Journal of Biological Chemistry*, 279: 37124-32.
- Rodriguez Viales, R., N. Diotel, M. Ferg, O. Armant, J. Eich, A. Alunni, M. Marz, L. Bally-Cuif, S. Rastegar, and U. Strahle. 2015. 'The helix-loop-helix protein id1 controls stem cell proliferation during regenerative neurogenesis in the adult zebrafish telencephalon', *Stem Cells*, 33: 892-903.
- Rolls, Asya, Ravid Shechter, and Michal Schwartz. 2009. 'The bright side of the glial scar in CNS repair', *Nature Reviews Neuroscience*, 10: 235-41.

- Ross-Munro, Emily, Faith Kwa, Jenny Kreiner, Madhavi Khore, Suzanne L. Miller, Mary Tolcos, Bobbi Fleiss, and David W. Walker. 2020. 'Midkine: The Who, What, Where, and When of a Promising Neurotrophic Therapy for Perinatal Brain Injury', *Frontiers in Neurology*, 11.
- Rothenaigier, I., M. Krecsmarik, J. A. Hayes, B. Bahn, A. Lepier, G. Fortin, M. Gotz, R. Jagasia, and L. Bally-Cuif. 2011. 'Clonal analysis by distinct viral vectors identifies bona fide neural stem cells in the adult zebrafish telencephalon and characterizes their division properties and fate', *Development*, 138: 1459-69.
- Sager, Jonathan J., Qing Bai, and Edward A. Burton. 2010. 'Transgenic zebrafish models of neurodegenerative diseases', *Brain Structure and Function*, 214: 285-302.
- Sahu, M., and B. Mallick. 2018. 'Deciphering synergistic regulatory networks of microRNAs in hESCs and fibroblasts', *Int J Biol Macromol*, 113: 1279-86.
- Sakaguchi, N., H. Muramatsu, K. Ichihara-Tanaka, N. Maeda, M. Noda, T. Yamamoto, M. Michikawa, S. Ikematsu, S. Sakuma, and T. Muramatsu. 2003. 'Receptor-type protein tyrosine phosphatase zeta as a component of the signaling receptor complex for midkine-dependent survival of embryonic neurons', *Neurosci Res*, 45: 219-24.
- Sana, J., P. Faltejskova, M. Svoboda, and O. Slaby. 2012. 'Novel classes of non-coding RNAs and cancer', *J Transl Med*, 10: 103.
- Sánchez-Duffhues, G., C. Hiepen, P. Knaus, and P. Ten Dijke. 2015. 'Bone morphogenetic protein signaling in bone homeostasis', *Bone*, 80: 43-59.
- Sasai, Y. 1998. 'Identifying the missing links: genes that connect neural induction and primary neurogenesis in vertebrate embryos', *Neuron*, 21: 455-8.
- Sato, Waichi, and Kenji Kadomatsu. 2012. 'Role of Midkine in Nephrogenesis and Kidney Disease.' in Mine Ergüven, Takashi Muramatsu and Ayhan Bilir (eds.), *Midkine: From Embryogenesis to Pathogenesis and Therapy* (Springer Netherlands: Dordrecht).
- Satoh, J., H. Muramatsu, G. Moretto, T. Muramatsu, H. J. Chang, S. T. Kim, J. M. Cho, and S. U. Kim. 1993. 'Midkine that promotes survival of fetal human neurons is produced by fetal human astrocytes in culture', *Brain Res Dev Brain Res*, 75: 201-5.
- Schmidt, R., T. Beil, U. Strahle, and S. Rastegar. 2014. 'Stab wound injury of the zebrafish adult telencephalon: a method to investigate vertebrate brain neurogenesis and regeneration', *J Vis Exp*: e51753.
- Schmidt, R., U. Strahle, and S. Scholpp. 2013. 'Neurogenesis in zebrafish - from embryo to adult', *Neural Dev*, 8: 3.
- Schmitt, Ellen A., and John E. Dowling. 1994. 'Early-eye morphogenesis in the zebrafish, *Brachydanio rerio*', *Journal of Comparative Neurology*, 344: 532-42.
- Scholpp, S., O. Wolf, M. Brand, and A. Lumsden. 2006. 'Hedgehog signalling from the zona limitans intrathalamica orchestrates patterning of the zebrafish diencephalon', *Development*, 133: 855-64.
- Schwarzkopf, Maayan, Mike C. Liu, Samuel J. Schulte, Rachel Ives, N. Husain, Harry M. T. Choi, and Niles A. Pierce. 2021. 'Hybridization chain reaction enables a unified approach to multiplexed, quantitative, high-resolution immunohistochemistry and in situ hybridization', *bioRxiv*.
- Scott, C. E., S. L. Wynn, A. Sesay, C. Cruz, M. Cheung, M. V. Gomez Gaviro, S. Booth, B. Gao, K. S. Cheah, R. Lovell-Badge, and J. Briscoe. 2010. 'SOX9 induces and maintains neural stem cells', *Nat Neurosci*, 13: 1181-9.
- Sehring, Ivonne M., and Gilbert Weidinger. 2020. 'Recent advancements in understanding fin regeneration in zebrafish', *WIREs Developmental Biology*, 9: e367.
- Sheng, L., L. Wang, M. Su, X. Zhao, R. Hu, X. Yu, J. Hong, D. Liu, B. Xu, Y. Zhu, H. Wang, and F. Hong. 2016. 'Mechanism of TiO₂ nanoparticle-induced neurotoxicity in zebrafish (*Danio rerio*)', *Environ Toxicol*, 31: 163-75.
- Shi, Y., and J. Massague. 2003. 'Mechanisms of TGF-beta signaling from cell membrane to the nucleus', *Cell*, 113: 685-700.

- Shimizu, Y., Y. Ueda, and T. Ohshima. 2018. 'Wnt signaling regulates proliferation and differentiation of radial glia in regenerative processes after stab injury in the optic tectum of adult zebrafish', *Glia*, 66: 1382-94.
- Sims, Neil R., and Wai Ping Yew. 2017. 'Reactive astrogliosis in stroke: Contributions of astrocytes to recovery of neurological function', *Neurochemistry International*, 107: 88-103.
- Skaggs, K., D. Goldman, and J. M. Parent. 2014. 'Excitotoxic brain injury in adult zebrafish stimulates neurogenesis and long-distance neuronal integration', *Glia*, 62: 2061-79.
- Sofroniew, M. V. 2009. 'Molecular dissection of reactive astrogliosis and glial scar formation', *Trends Neurosci*, 32: 638-47.
- Sorrelle, N., A. T. A. Dominguez, and R. A. Brekken. 2017. 'From top to bottom: midkine and pleiotrophin as emerging players in immune regulation', *J Leukoc Biol*, 102: 277-86.
- Sorrells, S. F., M. F. Paredes, A. Cebrian-Silla, K. Sandoval, D. Qi, K. W. Kelley, D. James, S. Mayer, J. Chang, K. I. Auguste, E. F. Chang, A. J. Gutierrez, A. R. Kriegstein, G. W. Mathern, M. C. Oldham, E. J. Huang, J. M. Garcia-Verdugo, Z. Yang, and A. Alvarez-Buylla. 2018. 'Human hippocampal neurogenesis drops sharply in children to undetectable levels in adults', *Nature*, 555: 377-81.
- Spassky, Nathalie, Florian T. Merkle, Nuria Flames, Anthony D. Tramontin, Jose Manuel García-Verdugo, and Arturo Álvarez-Buylla. 2005. 'Adult Ependymal Cells Are Postmitotic and Are Derived from Radial Glial Cells during Embryogenesis', *The Journal of Neuroscience*, 25: 10 - 18.
- Spemann, H., and H. Mangold. 2001. 'Induction of embryonic primordia by implantation of organizers from a different species. 1923', *Int J Dev Biol*, 45: 13-38.
- Staton, Alison A., and Antonio J. Giraldez. 2011. 'Use of target protector morpholinos to analyze the physiological roles of specific miRNA-mRNA pairs in vivo', *Nature Protocols*, 6: 2035-49.
- Steward, M. M., A. Sridhar, and J. S. Meyer. 2013. 'Neural regeneration', *Curr Top Microbiol Immunol*, 367: 163-91.
- Stoica, G. E., A. Kuo, C. Powers, E. T. Bowden, E. B. Sale, A. T. Riegel, and A. Wellstein. 2002. 'Midkine binds to anaplastic lymphoma kinase (ALK) and acts as a growth factor for different cell types', *J Biol Chem*, 277: 35990-8.
- Strähle, Uwe, and Sepand Rastegar. 2008. 'Conserved non-coding sequences and transcriptional regulation', *Brain Research Bulletin*, 75: 225-30.
- Strand, N. S., K. K. Hoi, T. M. T. Phan, C. A. Ray, J. D. Berndt, and R. T. Moon. 2016. 'Wnt/ β -catenin signaling promotes regeneration after adult zebrafish spinal cord injury', *Biochem Biophys Res Commun*, 477: 952-56.
- Streit, A., A. J. Berliner, C. Papanayotou, A. Sirulnik, and C. D. Stern. 2000. 'Initiation of neural induction by FGF signalling before gastrulation', *Nature*, 406: 74-8.
- Streit, A., S. Sockanathan, L. Pérez, M. Rex, P. J. Scotting, P. T. Sharpe, R. Lovell-Badge, and C. D. Stern. 1997. 'Preventing the loss of competence for neural induction: HGF/SF, L5 and Sox-2', *Development*, 124: 1191-202.
- Stuart, G. W., J. V. McMurray, and M. Westerfield. 1988. 'Replication, integration and stable germ-line transmission of foreign sequences injected into early zebrafish embryos', *Development*, 103: 403-12.
- Sueda, R., and R. Kageyama. 2020. 'Regulation of active and quiescent somatic stem cells by Notch signaling', *Dev Growth Differ*, 62: 59-66.
- Svensson, Sara, Mukesh Pasupuleti, Björn Walse, Martin Malmsten, Matthias Mörgelin, Camilla Sjögren, Anders I. Olin, Mattias Collin, Artur Schmidtchen, Ruth H. Palmer, and Arne Egesten. 2010. 'Midkine and Pleiotrophin Have Bactericidal Properties', *The Journal of Biological Chemistry*, 285: 16105 - 15.
- Takke, C., and J. A. Campos-Ortega. 1999. 'her1, a zebrafish pair-rule like gene, acts downstream of notch signalling to control somite development', *Development*, 126: 3005-14.

- Takke, C., P. Dornseifer, E. v Weizsacker, and J. A. Campos-Ortega. 1999. 'her4, a zebrafish homologue of the Drosophila neurogenic gene E(spl), is a target of NOTCH signalling', *Development*, 126: 1811-21.
- Tamai, K., M. Semenov, Y. Kato, R. Spokony, C. Liu, Y. Katsuyama, F. Hess, J. P. Saint-Jeannet, and X. He. 2000. 'LDL-receptor-related proteins in Wnt signal transduction', *Nature*, 407: 530-5.
- Tatsumi, K., H. Okuda, M. Makinodan, T. Yamauchi, E. Makinodan, H. Matsuyoshi, T. Manabe, and A. Wanaka. 2010. 'Transient activation of Notch signaling in the injured adult brain', *J Chem Neuroanat*, 39: 15-9.
- Tawk, M., C. Araya, D. A. Lyons, A. M. Reugels, G. C. Girdler, P. R. Bayley, D. R. Hyde, M. Tada, and J. D. Clarke. 2007. 'A mirror-symmetric cell division that orchestrates neuroepithelial morphogenesis', *Nature*, 446: 797-800.
- Than-Trong, E., and L. Bally-Cuif. 2015. 'Radial glia and neural progenitors in the adult zebrafish central nervous system', *Glia*, 63: 1406-28.
- Than-Trong, E., S. Ortica-Gatti, S. Mella, C. Nepal, A. Alunni, and L. Bally-Cuif. 2018. 'Neural stem cell quiescence and stemness are molecularly distinct outputs of the Notch3 signalling cascade in the vertebrate adult brain', *Development*, 145.
- Thomas, M. C., and C. M. Chiang. 2006. 'The general transcription machinery and general cofactors', *Crit Rev Biochem Mol Biol*, 41: 105-78.
- Thompson, J. D., J. Ou, N. Lee, K. Shin, V. Cigliola, L. Song, G. E. Crawford, J. Kang, and K. D. Poss. 2020. 'Identification and requirements of enhancers that direct gene expression during zebrafish fin regeneration', *Development*, 147.
- Toledo, Enrique M., Marcela Colombes, and Nibaldo C. Inestrosa. 2008. 'Wnt signaling in neuroprotection and stem cell differentiation', *Progress in Neurobiology*, 86: 281-96.
- Tran, Phuong B., Ghazal Banisadr, Dongjun Ren, Anjen Chenn, and Richard J. Miller. 2007. 'Chemokine receptor expression by neural progenitor cells in neurogenic regions of mouse brain', *Journal of Comparative Neurology*, 500.
- Trivedi, Vikas, Harry M. T. Choi, Scott E. Fraser, and Niles A. Pierce. 2018. 'Multidimensional quantitative analysis of mRNA expression within intact vertebrate embryos', *Development*, 145.
- Tsai, S. L., C. Baselga-Garriga, and D. A. Melton. 2020. 'Midkine is a dual regulator of wound epidermis development and inflammation during the initiation of limb regeneration', *Elife*, 9.
- Tsutsui, J., K. Uehara, K. Kadomatsu, S. Matsubara, and T. Muramatsu. 1991. 'A new family of heparin-binding factors: strong conservation of midkine (MK) sequences between the human and the mouse', *Biochem Biophys Res Commun*, 176: 792-7.
- Tümpel, S., F. Cambroner, C. Sims, R. Krumlauf, and L. M. Wiedemann. 2008. 'A regulatory module embedded in the coding region of Hoxa2 controls expression in rhombomere 2', *Proc Natl Acad Sci U S A*, 105: 20077-82.
- Ueda, Y., Y. Shimizu, N. Shimizu, T. Ishitani, and T. Ohshima. 2018. 'Involvement of sonic hedgehog and notch signaling in regenerative neurogenesis in adult zebrafish optic tectum after stab injury', *The Journal of comparative neurology*, 526: 2360-72.
- Uehara, K., S. Matsubara, K. Kadomatsu, J. Tsutsui, and T. Muramatsu. 1992. 'Genomic structure of human midkine (MK), a retinoic acid-responsive growth/differentiation factor', *J Biochem*, 111: 563-7.
- Umans, R. A., and M. R. Taylor. 2012. 'Zebrafish as a model to study drug transporters at the blood-brain barrier', *Clinical pharmacology and therapeutics*, 92: 567-70.
- Unoki, K., N. Ohba, H. Arimura, H. Muramatsu, and T. Muramatsu. 1994. 'Rescue of photoreceptors from the damaging effects of constant light by midkine, a retinoic acid-responsive gene product', *Invest Ophthalmol Vis Sci*, 35: 4063-8.
- Urban, N., and F. Guillemot. 2014. 'Neurogenesis in the embryonic and adult brain: same regulators, different roles', *Front Cell Neurosci*, 8: 396.
- Uzman, L. Lahut. 1960. 'The histogenesis of the mouse cerebellum as studied by its tritiated thymidine uptake', *The Journal of comparative neurology*, 114: 137-59.

- van Tetering, G., and M. Vooijs. 2011. 'Proteolytic cleavage of Notch: "HIT and RUN"', *Curr Mol Med*, 11: 255-69.
- Varela-Nallar, Lorena, and Nibaldo C. Inestrosa. 2013. 'Wnt signaling in the regulation of adult hippocampal neurogenesis', *Frontiers in Cellular Neuroscience*, 7: 100-00.
- Ventura, Rachel, and James Goldman. 2007. 'Dorsal Radial Glia Generate Olfactory Bulb Interneurons in the Postnatal Murine Brain', *The Journal of neuroscience : the official journal of the Society for Neuroscience*, 27: 4297-302.
- Visel, A., M. J. Blow, Z. Li, T. Zhang, J. A. Akiyama, A. Holt, I. Plajzer-Frick, M. Shoukry, C. Wright, F. Chen, V. Afzal, B. Ren, E. M. Rubin, and L. A. Pennacchio. 2009. 'ChIP-seq accurately predicts tissue-specific activity of enhancers', *Nature*, 457: 854-8.
- Visel, A., E. M. Rubin, and L. A. Pennacchio. 2009. 'Genomic views of distant-acting enhancers', *Nature*, 461: 199-205.
- Wang, H., G. Song, H. Chuang, C. Chiu, A. Abdelmaksoud, Y. Ye, and L. Zhao. 2018. 'Portrait of glial scar in neurological diseases', *Int J Immunopathol Pharmacol*, 31: 2058738418801406.
- Wang, Jing, and Hong Cao. 2021. 'Zebrafish and Medaka: Important Animal Models for Human Neurodegenerative Diseases', *International journal of molecular sciences*, 22: 10766.
- Wang, R. N., J. Green, Z. Wang, Y. Deng, M. Qiao, M. Peabody, Q. Zhang, J. Ye, Z. Yan, S. Denduluri, O. Idowu, M. Li, C. Shen, A. Hu, R. C. Haydon, R. Kang, J. Mok, M. J. Lee, H. L. Luu, and L. L. Shi. 2014. 'Bone Morphogenetic Protein (BMP) signaling in development and human diseases', *Genes Dis*, 1: 87-105.
- Wang, Yirong, Junjie Luo, Hong Zhang, and Jian Lu. 2016. 'microRNAs in the Same Clusters Evolve to Coordinately Regulate Functionally Related Genes', *Molecular biology and evolution*, 33: 2232-47.
- Weckbach, L. T., T. Muramatsu, and B. Walzog. 2011. 'Midkine in inflammation', *ScientificWorldJournal*, 11: 2491-505.
- Wehner, D., T. M. Tsarouchas, A. Michael, C. Haase, G. Weidinger, M. M. Reimer, T. Becker, and C. G. Becker. 2017. 'Wnt signaling controls pro-regenerative Collagen XII in functional spinal cord regeneration in zebrafish', *Nature communications*, 8: 126.
- Wexler, E. M., A. Paucer, H. I. Kornblum, T. D. Palmer, and D. H. Geschwind. 2009. 'Endogenous Wnt signaling maintains neural progenitor cell potency', *Stem Cells*, 27: 1130-41.
- Whitney, Nicholas P., Tess M. Eidem, Hui Peng, Yunlong Huang, and Jialin C. Zheng. 2009. 'Inflammation mediates varying effects in neurogenesis: relevance to the pathogenesis of brain injury and neurodegenerative disorders', *J Neurochem*, 108: 1343-59.
- Wilson, S. I., A. Rydström, T. Trimborn, K. Willert, R. Nusse, T. M. Jessell, and T. Edlund. 2001. 'The status of Wnt signalling regulates neural and epidermal fates in the chick embryo', *Nature*, 411: 325-30.
- Winkler, C., and R. T. Moon. 2001. 'Zebrafish mdk2, a novel secreted midkine, participates in posterior neurogenesis', *Dev Biol*, 229: 102-18.
- Winkler, C., M. Schafer, J. Duschl, M. Scharl, and J. N. Voff. 2003. 'Functional divergence of two zebrafish midkine growth factors following fish-specific gene duplication', *Genome Res*, 13: 1067-81.
- Winkler, Christoph, and Sheng Yao. 2014. 'The midkine family of growth factors: diverse roles in nervous system formation and maintenance', *British journal of pharmacology*, 171.
- Woldemichael, Bisrat T., Ali Jawaid, Eloïse A. Kremer, Niharika Gaur, Jacek Krol, Antonin Marchais, and Isabelle M. Mansuy. 2016. 'The microRNA cluster miR-183/96/182 contributes to long-term memory in a protein phosphatase 1-dependent manner', *Nature communications*, 7: 12594-94.
- Woo, K., and S. E. Fraser. 1995. 'Order and coherence in the fate map of the zebrafish nervous system', *Development*, 121: 2595-609.
- Wullmann, M. F., B. Rupp, and H. Reichert. 1996. 'Neuroanatomy of the zebrafish brain: A topological atlas', *Birhäuser Verlag, Basel, Switzerland*: 1-144.

- Yang, Sumin, Key-Hwan Lim, Sung-Hyun Kim, and Jae-Yeol Joo. 2021. 'Molecular landscape of long noncoding RNAs in brain disorders', *Molecular Psychiatry*, 26: 1060-74.
- Yao, Sheng, Mangeng Cheng, Qian Zhang, Mariusz Wasik, Robert Kelsh, and Christoph Winkler. 2013. 'Anaplastic lymphoma kinase is required for neurogenesis in the developing central nervous system of zebrafish', *PLoS One*, 8: e63757-e57.
- Yeo, S. Y., M. Kim, H. S. Kim, T. L. Huh, and A. B. Chitnis. 2007. 'Fluorescent protein expression driven by her4 regulatory elements reveals the spatiotemporal pattern of Notch signaling in the nervous system of zebrafish embryos', *Dev Biol*, 301: 555-67.
- Yi, Rui, Yi Qin, Ian G Macara, and Bryan R Cullen. 2003. 'Exportin-5 mediates the nuclear export of pre-microRNAs and short hairpin RNAs', *Genes & development*, 17: 3011-16.
- Yiu, G., and Z. He. 2006a. 'Glial inhibition of CNS axon regeneration', *Nature reviews. Neuroscience*, 7: 617-27.
- Yiu, Glenn, and Zhigang He. 2006b. 'Glial inhibition of CNS axon regeneration', *Nature reviews. Neuroscience*, 7: 617-27.
- Zambusi, Alessandro, and Jovica Ninkovic. 2020. 'Regeneration of the central nervous system-principles from brain regeneration in adult zebrafish', *World journal of stem cells*, 12: 8-24.
- Zeng, Yan, Rui Yi, and Bryan R Cullen. 2003. 'MicroRNAs and small interfering RNAs can inhibit mRNA expression by similar mechanisms', *Proceedings of the National Academy of Sciences*, 100: 9779-84.
- Zhang, C., M. Chopp, Y. Cui, L. Wang, R. Zhang, L. Zhang, M. Lu, A. Szalad, E. Doppler, M. Hitzl, and Z. G. Zhang. 2010. 'Cerebrolysin enhances neurogenesis in the ischemic brain and improves functional outcome after stroke', *J Neurosci Res*, 88: 3275-81.
- Zhang, G., M. Ferg, L. Lubke, M. Takamiya, T. Beil, V. Gourain, N. Diotel, U. Strahle, and S. Rastegar. 2020. 'Bone morphogenetic protein signaling regulates Id1-mediated neural stem cell quiescence in the adult zebrafish brain via a phylogenetically conserved enhancer module', *Stem Cells*.
- Zhang, G., L. Lübke, F. Chen, T. Beil, M. Takamiya, N. Diotel, U. Strähle, and S. Rastegar. 2021. 'Neuron-Radial Glial Cell Communication via BMP/Id1 Signaling Is Key to Long-Term Maintenance of the Regenerative Capacity of the Adult Zebrafish Telencephalon', *Cells*, 10: 2794.
- Zhang, Jing, Huizhe Wu, Qiuchen Chen, Pengfei Zhao, Haishan Zhao, Weifan Yao, and Minjie Wei. 2015. 'A Locked Nucleic Acid Probe Based on Selective Salt-Induced Effect Detects Single Nucleotide Polymorphisms', *BioMed Research International*, 2015: 391070.
- Zhang, L., X. Yang, S. Yang, and J. Zhang. 2011. 'The Wnt/ β -catenin signaling pathway in the adult neurogenesis', *Eur J Neurosci*, 33: 1-8.
- Zhao, C., G. Sun, S. Li, and Y. Shi. 2009. 'A feedback regulatory loop involving microRNA-9 and nuclear receptor TLX in neural stem cell fate determination', *Nat Struct Mol Biol*, 16: 365-71.
- Zou, P., H. Muramatsu, T. Miyata, and T. Muramatsu. 2006. 'Midkine, a heparin-binding growth factor, is expressed in neural precursor cells and promotes their growth', *J Neurochem*, 99: 1470-9.
- Zupanc, G. K., K. Hinsch, and F. H. Gage. 2005. 'Proliferation, migration, neuronal differentiation, and long-term survival of new cells in the adult zebrafish brain', *The Journal of comparative neurology*, 488: 290-319.
- Zupanc, G. K., and R. F. Sîrbulescu. 2011. 'Adult neurogenesis and neuronal regeneration in the central nervous system of teleost fish', *Eur J Neurosci*, 34: 917-29.